SEASONAL VARIATIONS IN THE ACTIVATED SLUDGE MICROBIOME WITH RESPECT TO SEASONAL NITRIFICATION FAILURE

DISSERTATION

SUBMITTED TO THE FACULTY OF THE GRADUATE SCHOOL

OF THE UNIVERSITY OF MINNESOTA

JULIET TEGAN JOHNSTON

IN PARTIAL FULFILLMENT OF THE REQUIREMENTS

FOR THE DEGREE OF

DOCTOR OF PHILOISOPHY

DR. SEBASTIAN FELIX BEHRENS, ADVISOR

JULY 2020

Acknowledgements page

I would like to thank Dr. Sebastian Behrens for being my advisor and continually encouraged my creativity and vision through research and outreach. I want to thank Dr. Lee Penn as well as Dr. Carolyn Zeiner for being such crucial professional mentors. Without their continual guidance and support I would not have been able truly explore my passion for teaching nor find my bearings in the community. I would also like to thank my committee members Dr. Satoshi Ishii, Dr. Raymond Hozalski, and Dr. William Arnold who helped shape the direction of my research as well as explore new methodologies and techniques. Additionally, I want to thank my lab mates Gloria Thomas, Nadine Hackshaw, Zhe Du, Mariah Dormer, Aaron Paulson, Kevin Ramrattan, Jovan Popovic, Kipp Sande, Michael Brown, and Amelia McClure. You all have helped me develop so much whether it be lab techniques, teaching skills, or understanding how to become a better mentor.

I would like to thank the team at Brainerd Wastewater Treatment Facilities, especially Gregg Kropp, Kevin Kiehlbauch, and Mike Larson for helping with our sample collection. We would like to thank the University of Minnesota Genomics Center for assistance with sequencing. I would like to thank the National Science Foundation Graduate Research Fellows Program for providing me with a fellowship opportunity as well as the Legislative-Citizen Commission on Minnesota Resources for funding the project.

I want to give a huge shout-out to my Queer Science community. Especially, Dr. Lee Penn, Dr. Evan Tyler, Ryan Daley, Matilda Newton, and Deirdre Manion-Fischer who supported the first Queer Science event that snowballed into a fantastic organization and community filled with so many incredible people.

Thank you to my Gortner Cluster, Microbiome Dorks, and Civil Engineering Dungeon Crawlers, and other scientists along the way including Sarah Lucus, Lisa Fazzino, Bridget Conley, Beth Adamowicz, Morgan Estler, Kelly Wallin, Suzie Hsu, Sarah Hammerland, Emily Anderson, Qian Zhang, Ben Bonis, Eric Kees, Abhiney Jain, Michael Winikoff, Elissa Allen, Natalie Hudson-Smith, Luz Sotelo, Hector Rodriguez, Robyn Sandekian, Rachel Tenney, Emma O'Leary, Priya Hora, Sara Binahmed, Anndee Huff, Mike McCarty, and my first officemate; Rose Rutherford. You all have turned daily laborious work into such an enjoyable and communal experience. Thank you.

A HUGE thank you to my Twitter family who has made finishing up my dissertation far more pleasant during the Coronavirus Pandemic. There is too many of you to list but notable mentions include Dr. Amanda Lyn Gunn, Mo Kaze, Bevin Blake, Clara Rehmann, Isabel Ott, Justin Stewart, Dr. Maureen Berg, Anna Marie LaChance, Anika Agrawal, Joe Weaver, Nick Tooker, and Dr. Juan Pablo Ruiz Villalobos.

I want to thank my Mom, Dad, Ariel, Sonny, and Jordan who were always available to listen during the lowest periods of stress, pick me up at the lowest points of depression, and celebrate with me at the highest points of success.

Finally, I want to thank Harper, my dog. She has been alongside me the entire journey of my PhD and most of my undergraduate degree. Absolutely none of this would be possible without you, and yet you have zero clue what is going on. Get your shit together.

I love you all. Thank you so much!

Dedications page

My dissertation is dedicated to my grandma Susan Benoff who was a second mother to me growing up, my grandpa Irving Benoff, my grandfather William Johnston, and Mildred Johnston; three who passed away during my doctoral program and one who lost the ability to recognize the accomplishments I have been able to achieve.

I also want to dedicate this to our families next generation: Iris Mercer, Owen Mattson, and Francis Mattson. You are all too young to understand how aggressively I will force science upon you. I hope you love science as much as I do.

My dissertation is also dedicated to all the Queer Science participants who are developing into the next generation of badass scientists. Every one of you is fucking amazing and I am so excited to see who you become.

In loving memory to Hailey Mireles and every trans person whose lives were taken away, especially from science, simply for being themselves.

Seasonal Variations in the Activated Sludge Microbiome with Respect to Nitrification Performance

Overview Abstract

Activated sludge consists of a diverse microbial community that is used by wastewater engineers to metabolize excessive nutrients in domestic wastewater so that these excessive nutrients do not impact downstream waters. While most biological contaminant removal processes, such as carbon (measured as Biological Oxygen Demand) and phosphorous removal are performed consistently year-round, nitrification performance significantly declines in cold temperatures. The seasonal decline in nitrification performance is known as seasonal nitrification failure. To understand seasonal nitrification failure, this thesis analyzed triplicate, full-scale, sequencing batch reactors throughout several years to investigate seasonal variations in the activated sludge microbiome with respect to community composition (16S rRNA gene), the metabolically active composition (16S rRNA transcript), and expression of *amoA* (ammonia monooxygenase) which is a key-nitrification functional gene.

There were 114 OTUs (operational taxonomic units), which were consistently present in all three reactors, every week, for an entire year and together comprise 74.3% - 84.0% of the entire community. The changes in abundances of these OTUs and other seasonally present OTUs make each season's community significantly distinct from each other. The community composition was also significantly distinct from the protein-synthesis composition throughout the entire year. While the entire activated sludge community and protein-synthesis compositions fluctuated, the ammonia-oxidizing community was at a constant abundance throughout the year based on tracking known-

ammonia oxidizers and the *amoA* functional gene despite seasonal nitrification failure. While the *amoA* transcripts declined with the seasonally cold temperatures, which explain the seasonal nitrification failure's decline in activity, the known-ammonia oxidizer protein-synthesis potential measured by *Nitrosomonas* sp. 16S rRNA transcripts did not significantly decline with temperature. This suggests there are other metabolic activities performed by the known ammonia oxidizing community to maintain stable community abundance and protein synthesis potential when ammonia oxidization is no longer the most thermodynamically favorable metabolism.

This result changes the narrative that seasonal nitrification failure occurs due to declining abundances of ammonia oxidizing organisms in cold temperatures, and instead provides insight as to how *amoA* expression seasonally changes with the complex and seasonally dynamic microbial ecology of the activated sludge community. Additionally, this research provides the most comprehensive baseline of the activated sludge communities seasonal composition, protein-synthesis potential and *amoA* expression to date. Future researchers can use these results to investigate specific highlighted seasonally variant OTUs which may influent the activated sludge microbiome, as well as explore the additional roles known ammonia oxidizers play in this complex microbial system.

Thesis Contributions Page

This thesis was written by Juliet Johnston while edited and approved of by her committee comprising Dr. Sebastian Behrens, Dr. Satoshi Ishii, Dr. Raymond Hozalski, and Dr. William Arnold. The research performed throughout this thesis was performed by Juliet Johnston with notable exceptions including: assistance by numerous individuals during sampling, assistance from the University of Minnesota's Genomics Core which provided the sequencing data, and *amoA* sequence alignment which was performed by Dr. Zhe Du. Chapters 2, 4 and 5 have acknowledgments specifying those who assisted during sampling. The initial research hypothesis and ideas were a collaborative venture between Juliet Johnston, Dr. Timothy LaPara, and Dr. Sebastian Behrens. After the preliminary results from Chapter 2, the research hypotheses' and ideas were solely between Juliet Johnston and Dr. Sebastian Behrens.

Table of Contents

List of Tables

List of Figures

Appendix B

Appendix C

Chapter 1

General Introduction

Wastewater treatment plants are designed to treat influent wastewater so that the resulting effluent discharge contains minimal solids, carbon, nitrogen, and phosphorous content, in an effort to prevent downstream pollution. While solids are typically removed using physical processes, excessive nutrients are primarily removed during biological secondary treatment. Secondary treatment uses activated sludge, a diverse consortium of microbes with a prolonged growth time, to biologically metabolize these nutrients into less harmful compounds (1). These biological processes are not always performed consistently at wastewater treatment facilities which undergo significant seasonal temperature shifts (2). This is particularly noticeable with the ammonia oxidizing bacteria which lead wastewater's nitrogen cycle with ammonia oxidation which is the first major step in nitrification. Ammonia oxidizing bacteria's activity appears to be significantly hindered in cold temperature, preventing nitrification from occurring. This phenomenon is referred to as seasonal nitrification failure (3-12).

Seasonal nitrification failure has been a longstanding issue within wastewater treatment plants. Predominantly this has been studied as rate-limiting kinetics in benchtop engineering solutions, not full-scale treatment facilities. Potential solutions have explored prolonged solids retention time for longer periods of growth and bioaugmentation to introduce psychrophilic/psychrotolerant ammonia oxidizers into the activated sludge system (3-8, 10, 13-16). Unfortunately, these proposals and benchtop experiments rarely translate from the field into scale-able options for full-scale wastewater treatment facilities. The National Pollutant Discharge Elimination System permits often do not regulate

ammonia between December to April due to a lack of viable solutions (17). What is needed is an approach which focuses on what is occurring with the ammonia oxidizing community and the entire microbial community within full-scale wastewater treatment facilities. This thesis explores how the microbial community in activated sludge wastewater treatment plants fluctuate throughout the seasons.

Using a combination of molecular biology techniques including the latest in high-throughput sequencing technologies, as well as quantitative polymerase chain reaction techniques to determine copy numbers of functional genes and transcripts, how the microbial community fluctuates throughout the year in terms of abundance, activity, and growth was explored. Additionally, with a specific focus on the nitrifying biomass, a goal was to uncover trends in the ammonia oxidizing community's phylogeny and activity. This information will help future wastewater engineers to prevent seasonal nitrification failure by designing around organisms which are already present and active in wastewater treatment facilities. Below is a further outline of the Brainerd Wastewater Treatment Plant, Nitrogen Cycling at Brainerd Wastewater Treatment Plant, and the methodologies used to investigate seasonal nitrification failure at the Brainerd Wastewater Treatment Plant.

Brainerd Wastewater Treatment Plant

The Brainerd Wastewater Treatment Plant is designed for up to 6 million gallons per day (22,700 cubic meters per day) and services the cities of Brainerd and Baxter in western-central Minnesota. The treatment plant's influent wastewater is primarily domestic wastewater which services the area's population of 13,500 people. The Brainerd

Wastewater Treatment Plant underwent a significant renovation in 2010 and transformed from a conventional wastewater treatment plant into four sequencing batch reactors capable of performing enhanced biological removal of nitrogen and phosphorous.

While the treatment plant has four reactors and has the capacity for 6 million gallons per day, only three reactors actively operate at any given time with an average daily inflow closer to 2 million gallons per day. Each of these three sequencing batch reactors operates on a cycle controlled by a computer based on parameters predetermined by the chief wastewater operator. While the three active sequencing batch reactors are completely independent processes and do not mix, they receive influent wastewater from the same upstream operations and discharge to the same downstream processes.

Figure 1.1 shows a schematic of the Brainerd Wastewater Treatment Plant starting at the headworks where influent domestic wastewater is received. This wastewater passes through bar screens to remove larger solid items before a grit chamber forces smaller solid items to separate from the treatment plant process. After the grit chamber, the influent wastewater is dispersed into one of the three sequencing batch reactors for secondary treatment. Following secondary treatment, there is an equalization basin which ensures a stable effluent flow during disinfection before discharging into the Mississippi River.

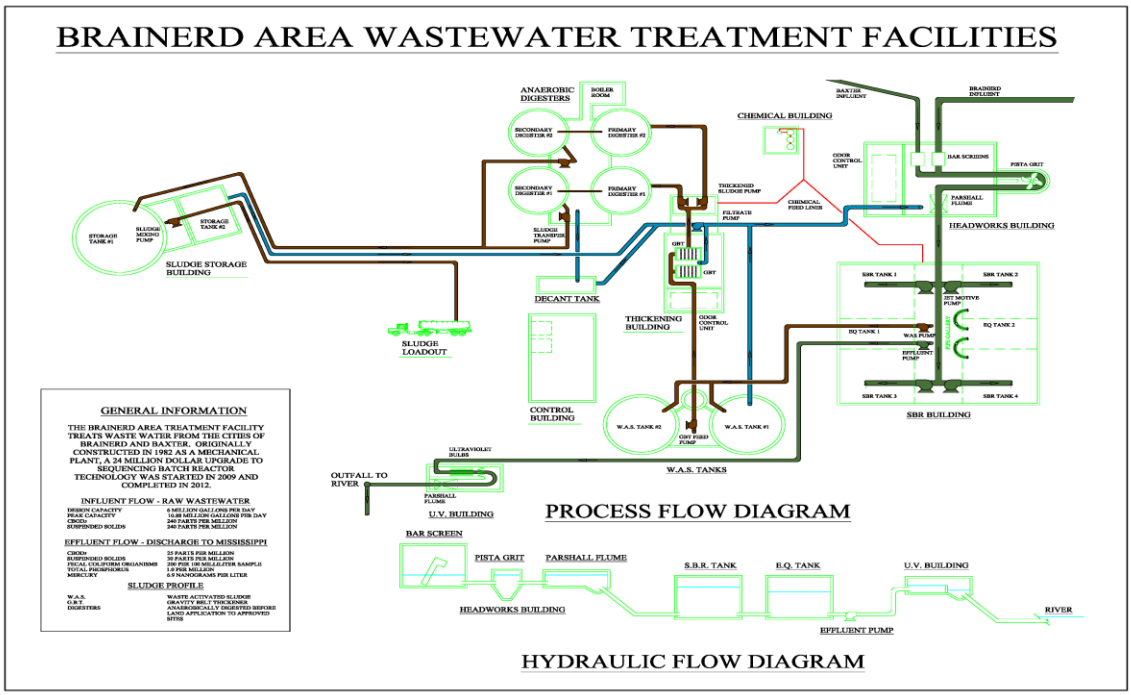

Figure 1.1 Overview of the processes performed at the Brainerd Wastewater Treatment Plant (Brainerd Public Utilities, MN). Each building is highlighted in a light green color. The top portion represents the treatment plant from a geographical overview, while the bottom portion represents the treatment plant from as hydraulic gradient with wastewater flowing downgradient for treatment. The dark green pipes indicate the influent wastewater. After secondary treatment the influent wastewater splits into a dark red piping for the treated wastewater and blue pipes for the biosolids.

Secondary treatment is the most complex stage of the operations because it relies on biological processes to remove the excessive carbon, nitrogen, and phosphorous from the influent wastewater. This diverse consortium of microbes is referred to as activated sludge, coined from founders Ardern and Lockett who recognized that recycling dense settled sludge resulted in longer growth times for microorganisms (18). The longer growth times increase the density of biomass which provides higher performance in remediating influent wastewater (8, 19-21). The typical sludge retention time at the Brainerd

Wastewater Treatment Plant is approximately 8 days to ensure growth of nitrifying biomass.

Secondary treatment is outlined in Figure 1.2 which depicts a schematic of the reactor cycle. The total reactor cycle takes approximately 6 hours. The three reactors are on an offset schedule by approximately two hours so that one reactor is always filling with influent wastewater while the other two are performing biological treatment. The first stage is *static fill* where influent wastewater flows into the reactor on the top of the activated sludge without mechanical homogenization of the influent wastewater and activated sludge. The next stage is an anoxic *mixed fill*, where the entire reactor is homogenized, carbon sources are present from the influent wastewater, but oxygen is not pumped into the reactor. The reactor is still filling with influent wastewater during this time period. *Mixed fill* is when denitrification and part of the phosphorous uptake occurs by denitrifying and phosphorous accumulating organisms occurs. Both *static fill* and *mixed fill* typically last an hour each.

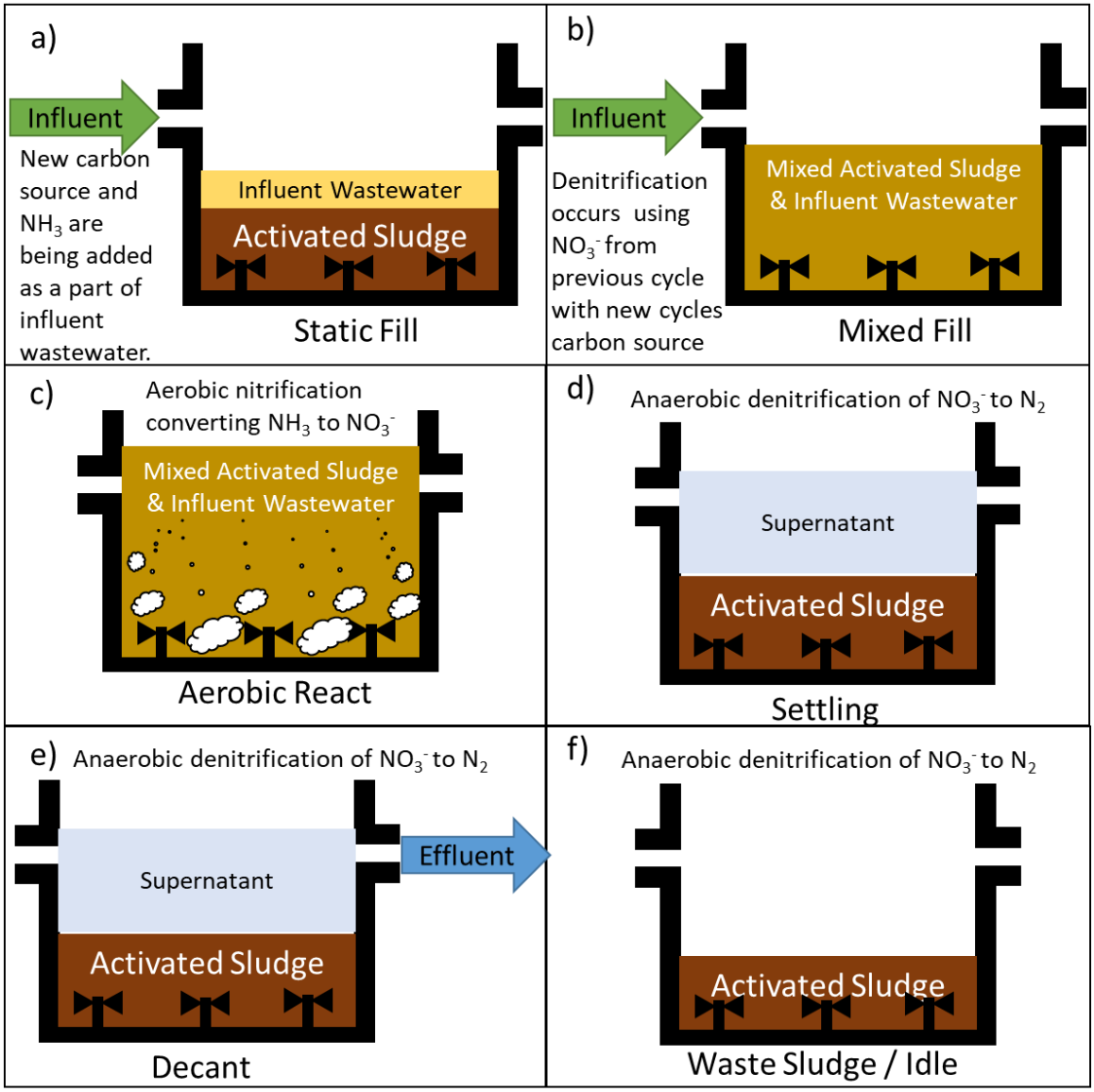

Figure 1.2 The various stages of the sequencing batch reactor cycle at Brainerd Wastewater Treatment Plant. A) depicts the *static fill* where influent wastewater is yellow, and activated sludge is dark brown. B) depicts *mixed fill* where the light brown is a homogenized mixture of influent wastewater and activated sludge. C) depicts *react* where air is pumped into the reactor to promote nitrification. D) During *settling* the supernatant and settled sludge separate so that the supernatant in blue can be *decanted* (Figure 1.2e) before some sludge is *wasted* into anaerobic digesters (Figure 1.2f).

Occasionally, during higher influent wastewater volumes, a brief *aerobic fill* occurs for 10-30 minutes. *Aerobic fill* provides oxygen to the reactor while new influent wastewater is still entering the system. For the purposes of this study, *aerobic fill* was considered negligible and incorporated into the *react* stage. During *react* the aeration system provides fine-bubbles of air into the wastewater treatment plant so that aerobic biological processes such as nitrification can occur. During the winter, there are some heaters to attempt to heat the air supplied to the reactors. The contact time between the heaters and air supply is limited. The computer system monitors the concentration of dissolved oxygen, however, will continue pumping oxygen until 3.5ppm is reached. Afterwards, the aeration system shuts off temporarily until the oxygen is consumed and the concentration of oxygen reaches 0.8ppm, and the where the aeration system turns back on. This is a technique to save on energy costs because aeration costs are typically 50% of the operational costs at most wastewater treatment facilities. *React* lasts for a minimum of 110 minutes and is typically 2-hours long.

After *react,* the mixers and aeration system completely shut down to enable activated sludge biomass to settle during the *settling* cycle. *Settling* is the final stage these studies analyze because afterwards the wastewater is no longer being treated biologically. *Settling* lasts 1-hour and is followed by a 10-45 minute *decant* period where the uppermost treated wastewater flows downstream into an equalization basin before disinfection. After *decant* there is a brief (10-20 minute) *waste sludge* where some of the activated sludge is sent to the treatment plant's anaerobic digester for further biosolids processing. There may be a period the reactors do nothing during *idle,* but typically this process restarts as influent wastewater begins to flow again.

These stages are specifically designed so that there are three distinct periods for the activated sludge microbial community. During *static fill* and *mixed fill* is the anoxic period, while *react* is the aerobic period. Finally, *settling* serves as an anaerobic period. These three periods of anoxic, aerobic, and anaerobic cycling are crucial to leveraging the nitrogen cycle through diverse organisms biologically metabolizing influent ammonia to inert dinitrogen gas.

The Nitrogen Cycle in Sequencing Batch Reactors

Domestic wastewater typically has between 25-50 mg/L of ammonia in the influent wastewater. This is predominantly organic nitrogen from urea, which breaks down into ammonia with the urease enzyme. This ammonia is removed by ammonia oxidizing microorganisms which metabolize the ammonia into nitrite using the *ammonia monooxygenase (Amo)* as well as the *hydroxylamine oxioreductase (Hao) (22, 23).* Afterwards, nitrite oxidizing bacteria metabolize the nitrite into nitrate using the *nitrite oxioreductase (Nxr)(24).* These enzymes in the presence of oxygen facilitate nitrification. Typically, nitrification is performed by two distinct organisms. There is potential, however, for some *Nitrospira* to perform both these steps. These *Nitrospira* are regarded as complete ammonia oxidizing bacteria (Comammox) (24-26).

After nitrification, the anaerobic processes of denitrification occur where the primary electron acceptor switches from oxygen to the reduced nitrogenous compounds. Initially as nitrate, the *nitrate reductase* (*Nar/Nap)* reduces the nitrate back to nitrite and later *nitrite reductase* (*Nir)* reduce nitrite to nitric oxide (27-29). Nitric oxide is further

reduced to nitrous oxide via *nitric oxide reductase (Nor).* Finally, the nitrous oxide is metabolized into dinitrogen gas with the *nitrous oxide reductase* (*Nos).* A complete breakdown of the nitrogen cycle is shown in Figure 1.3.

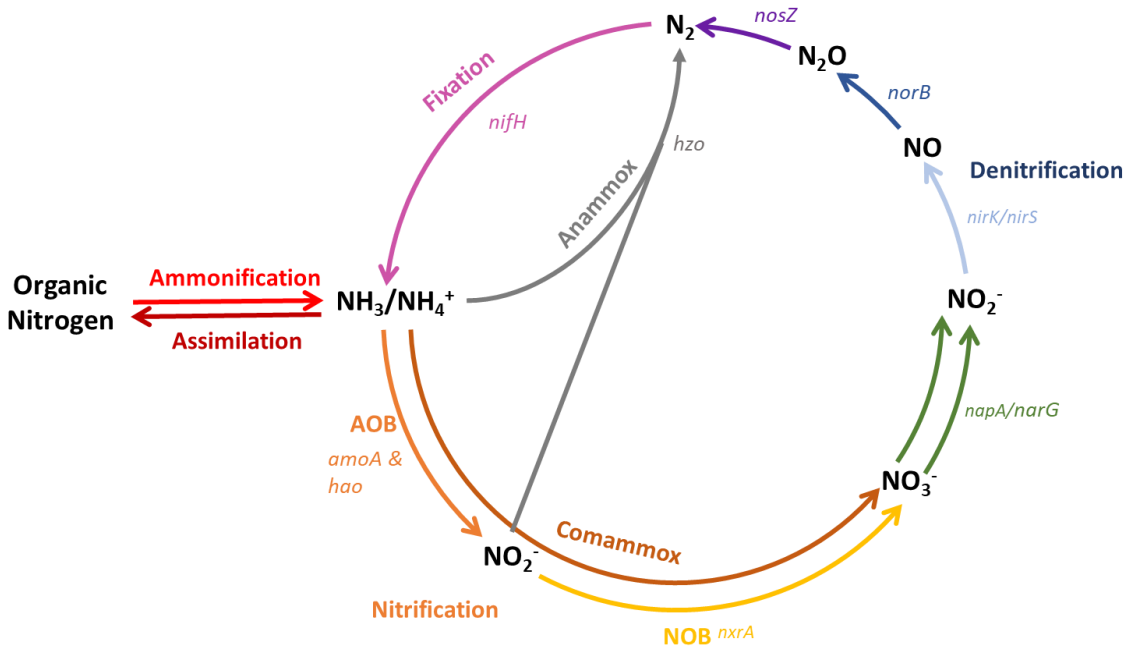

Figure 1.3 Key stages of the nitrogen cycle. Ammonification is shown in red, while assimilation is shown in dark red. Nitrification steps of ammonia oxidation and nitrite oxidation are shown in orange and yellow. Nitrate reduction is shown in green. The denitrification steps of nitrite reduction, nitric oxide reduction, and nitrous oxide reduction are shown in light blue, blue, and purple. Nitrogen fixation from nitrogen gas back to ammonia is shown in pink, while the anammox bypass from ammonia and nitrite to nitrogen gas is shown in gray.

Each step in nitrification and denitrification is critical to wastewater treatme to transfer harmful forms of nitrogenous compounds into dinitrogen gas which is inert and

comprises 78% of the atmosphere (30-32). Nitrification steps are designed to prevent excessive amounts of ammonia from being released into the environment. Ammonia is often a limiting nutrient in the environment, especially for marine waters. The excessive ammonia released from wastewater treatment plants contributes to large algal blooms growing on these excessive nutrients. The algal blooms consume most of the dissolved oxygen in these bodies of water which suffocates aerobic fish, bacteria, and plants in the water. This process is called eutrophication and can result in large hypoxic zones the size of the State of Delaware in the Gulf of Mexico resulting in over $100 million losses annually to seafood and tourism without accounting for ecosystem service losses (33-35). Preventing eutrophication has been a central tenant of wastewater treatment since the inception of activated sludge-based processes.

Performing just nitrification leaves nitrogen as nitrite and nitrate, which still contributes to eutrophication. Additionally, nitrate in excessive abundance can enter the drinking water system and contribute to blue baby syndrome. Blue baby syndrome occurs when nitrate is converted in bodies into nitrite which binds to hemoglobin in human blood preventing oxygen uptake which results in suffocation. Minimizing both ammonia, nitrite, and nitrate from effluent wastewater has become a key component of enhanced nitrogen removal.

Enhanced nitrogen removal designates wastewater treatment plants performing both nitrification and denitrification. While removing nitrite and nitrate is essential for the first steps of denitrification, the biggest challenge is ensuring nitrous oxide fully metabolizes into dinitrogen gas. Nitrous oxide is an extremely potent greenhouse gas, over 298 times as damaging as carbon dioxide based on weight-to-weight ratio (31).

While each individual nitrification and denitrification step is crucial to wastewater treatment plant performance, it begins with ammonia oxidation which is often rate-limiting based on temperature. In cold temperatures, wastewater treatment plants often struggle to meet standard effluent ammonia concentrations. This seasonal lapse in performance is called seasonal nitrification failure. The Brainerd Wastewater Treatment Facility has a significant history of not being able to meet effluent ammonia discharge limits to the point where they are no longer required to have winter permits. There has been a lack of viable, cost effective options for wastewater treatment plant operators despite growing pressure to reduce effluent nitrogen. To design for the future of year-round effective wastewater treatment plants, a thorough investigation of the activated sludge microbiome was performed, focusing on the shifts in activity of ammonia oxidizing bacteria that underperform during seasonal nitrification failure.

Methodological Approach for Investigating Seasonal Nitrification Failure of The Activated Sludge Microbiome

To comprehensively understand how the wastewater microbiome shifts during seasonal nitrification failure, this study focuses on two temporal scales. The first scale is a broader annual overview of the reactors to show gradual changes in the reactor's microbial community throughout a year. This study tracks the entire community as well as the known nitrification community as the temperature fluctuates. This study required weekly samples from the triplicate sequencing batch reactors at Brainerd Wastewater Treatment Facility to discern progressive changes in the temperature, community, and performance over time. These samples were taken while the reactors were in their aerobic

react phase and actively treating wastewater. The microbial community was tracked using next generation high throughput sequencing which provides the relative abundance of distinct phylogenetic groups of organisms. Additional analysis included quantitative polymerase chain reaction (qPCR) for specific functional genes. These genes include the 16S rRNA gene as a proxy for total biomass, ammonia monooxygenase gene (*amoA)* for both Bacteria and Archaea to determine known ammonia oxidizers, as well as *nitrite reductase* gene (*nirS* and *nirK)* and *nitrous-oxide reductase* gene (*nosZ)*, which are representative of the major denitrification pathways. Combining sequencing with qPCR provides relative community abundances to connect to absolute abundances of genes as they fluctuate throughout the year. When the nitrification performance declines during cold temperatures, we were be able to track which organisms changed in relative abundance, the shifts in the nitrification community, and if these performance shifts impacted the denitrification community whose process relies on nitrification. This shed light on how the community, specifically the known nitrifying organisms, fluctuates in abundance and performance throughout the year. This same dataset was used to build a kinetic model which predicts performance at a given time of year, based on the operational parameters such as mixed-liquor suspended solids and sludge retention time.

The second time scale will be a finer, more in-depth look at shifts in activity during the reactors' 6-hour cycles. The sequencing batch reactors continuously alternate between static filling, mixed filling, aerobic react, settling, and decanting before repeating this process throughout the year. While ammonia oxidation only occurs during the aerobic react stage, the ammonia oxidizing community only requires the presence of ammonia to begin transcribing their genes and building proteins for ammonia oxidation. Transcribing

amoA can occur rapidly within minutes when ammonia is detected by the cell. The known ammonia oxidizers as well as the activated sludge community may significantly fluctuate in activity as the sequencing batch reactors alternate between these cycle stages, and broadly throughout the seasons. To investigate the activity profiles of the activated sludge community, four sampling trips occurred at the start of each new season to provide a fingerprint that profiles these fluctuations. At the start of each season, samples were collected every 10-minutes during the static fill, mixed fill, react, and settling stages of the reactors cycle. These samples were rapidly frozen in a dry-ice and ethanol bath to preserve an exact time point. The DNA and RNA of the samples were analyzed. DNA shows the composition and functional potential of the community, and RNA will discern community members who are actively performing protein synthesis and transcribing functional genes for ammonia oxidization. Using next generation sequencing on the 16S rRNA gene and transcripts, this study can differentiate between microbes that are present, and microbes that are active in the activated sludge community. To discriminate members of the known nitrification community, additional sequencing targeted the *ammonia monooxygenase (amoA)* as a functional gene and transcript. The sequencing data provided relative abundances which can be complimented with quantitative polymerase chain reaction on the same genes for absolute abundance. This will provide a comprehensive view of the known ammonia oxidizers that are present and active during the seasons as well as the activity of the microbial community in activated sludge.

Ultimately, this study presents the most comprehensive analysis of the changes in the activated sludge microbiome to date. No previous study has observed three identical and independent reactors with the same level of temporal resolution. Additionally, no

previous study has analyzed the activity of known nitrifying organisms across the seasons using transcriptomic sequencing. This study will provide a higher resolution analysis of the known nitrifying organisms and microbial community in activated sludge. The results from this study will provide future researchers a more solidified foundation of knowledge to discern which organisms play a role, directly or indirectly, in seasonal nitrification failure.

Research Objectives and Hypotheses

Objective 1: Who is out there? Characterization and quantification of the dynamic seasonal shifts in community composition and structure of the activated sludge microbiome with special emphasis on nitrification performance.

Hypothesis 1a: The activated sludge microbiome's diversity fluctuates proportionally to the temperature with lower diversity in the winter and higher diversity in the summer.

Hypothesis 1b: The abundance of the known nitrification community will remain proportional to the nitrification performance, as nitrification performance fluctuates throughout the year.

Objective 2: Can we model them? Model the sequencing batch reactors to predict the abundance of ammonia oxidizing bacteria as well as their intended performance throughout the year.

Hypothesis 2a: The different oxygen profiles throughout the aerobic react cycle significantly impact ammonia oxidation performance.

Hypothesis 2b: The quantitative abundance of *amoA* genes to 16S rRNA genes can be used to accurately predict the nitrification performance throughout the year.

Objective 3: How active are they? Quantification of 16S rRNA transcripts as a measure of seasonal shifts in activity of microbial populations in activated sludge and measuring the seasonal dynamics of the abundance of 16S rRNA transcripts throughout a reaction cycle.

Hypothesis 3a: The microbial activity will be proportional to the water temperature, with the highest activity in the summer, and lowest in the cold winter.

Hypothesis 3b: The microbial activity will be distinctly different between the aerobic, anaerobic, and settling stages within the sequencing batch reactors.

Objective 4: When are they active? Identification of "active" taxa of the ammonia oxidizing bacteria based on high throughout amplicon sequencing of *amoA* transcripts and genes.

Hypothesis 4a: Known taxonomic groups of ammonia-oxidizers vary in their activity during different stages of a sequencing batch reactor cycle.

Hypothesis 4b: Seasonal fluctuations in activated sludge water temperatures affect the activity of known groups of ammonia-oxidizers.

Hypothesis 4c: Community structure and composition does not reflect seasonal variance in activity of individual taxa in activated sludge.

Chapter 2

Composition and Dynamics of the Activated Sludge Microbiome during Seasonal Nitrification Failure

Synopsis

Wastewater treatment plants in temperate climate zones frequently undergo seasonal nitrification failure in the winter month yet maintain removal efficiency for other contaminants. We tested the hypothesis that nitrification failure can be correlated to shifts in the nitrifying microbial community. We monitored three parallel, full-scale sequencing batch reactors over the course of a year with respect to reactor performance, microbial community composition via *16S rRNA gene* amplicon sequencing, and functional gene abundance using qPCR. All reactors demonstrated similar changes to their core microbiome, and only subtle variations among seasonal and transient taxa. We observed a decrease in species richness during the winter, with a slow recovery of the activated sludge community during spring. Despite the change in nitrification performance, ammonia monooxygenase gene abundances remained constant throughout the year, as did the relative sequence abundance of *Nitrosomonadacae*. This suggests that nitrification failure at colder temperatures might result from different reaction kinetics of nitrifying taxa, or that other organisms with strong seasonal shifts in population abundance, e.g. an uncultured lineage of *Saprospiraceae*, affect plant performance in the winter. This research is a comprehensive analysis of the seasonal microbial community dynamics in triplicate full-scale sequencing batch reactors and ultimately strengthens our basic understanding of the microbial ecology of activated sludge communities by revealing seasonal succession patterns of individual taxa that correlate with nutrient removal efficiency.

Introduction

Municipal wastewater treatment plants are designed to leverage the metabolic capabilities of microorganisms to remove excessive nutrients such as organic carbon, phosphorous, and ammonia from sewage. These diverse groups of microorganisms comprise the activated sludge microbiome which acts as the active biological component that remediates the influent wastewaters. One of the diverse microbial processes central to wastewater treatment is nitrification. Under aerobic conditions during wastewater treatment nitrifying microorganisms oxidize ammonia to nitrate. Under anaerobic conditions denitrifying bacteria can then reduce nitrate to gaseous forms of nitrogen (such as nitrous oxide and dinitrogen gas) ultimately lowering dissolved wastewater nitrogen concentrations. When untreated, elevated concentrations of ammonia, nitrite, and nitrate in rivers and streams contribute to eutrophication leading to hypoxic "dead zones" in receiving waters bodies, which constitute human and environmental health hazards. Among others these concerns have made managing the nitrogen cycle an important component of the grand challenges for environmental engineering in the 21st Century(1).

In temperate climate zones such as in many states in the Northern United States (e.g. Minnesota), wastewater treatment plants regularly experience a seasonal decrease in nitrification performance during the cold winter month. The loss in nitrification performance is often so prevalent that many local permits only require monitoring winter ammonia concentrations without any regulatory limits on effluent concentrations due to a lack of viable options for cost-effective removal of ammonia in the cold season. The discharge of elevated concentrations of ammonia (greater than 4 mg/L) with treated wastewater during the winter (water temperatures below 13°C) is referred to as 'seasonal

nitrification failure.' The State of Minnesota is working to incrementally reduce nitrogen loads to the Mississippi River by up to 40% by 2025 and even further in future years (2). In order to be able to meet these discharge milestones, concerted efforts of wastewater treatment plant operators and microbiologists will be required to further our understanding of the impacts of temperate climate zone winter conditions on the composition and activity of the activated sludge microbiome at full-scale wastewater treatment plants.

The process of nitrification is commonly carried out by separate and taxonomically diverse groups of microorganisms (3). First, ammonia-oxidizing bacteria and archaea oxidize ammonia to nitrite and then nitrite-oxidizing bacteria further oxidize nitrite to nitrate. Recently, also complete ammonia oxidizing bacteria (comammox) have been describe which are capable of oxidizing ammonia via nitrite to nitrate directly (4-7). Their role in domestic wastewater treatment, however requires further research.

Because, heating wastewater is extremely costly, wastewater operators will typically react to seasonal nitrification failure by increasing the mixed-liquor suspended solids (MLSS), prolonging sludge aeration periods, and lengthening sludge retention times (SRT). These serve as attempts to increase nitrifying biomass and prolong reaction time but have not always been successful in preventing seasonal nitrification failure. Previous studies have often revealed conflicting results when analyzing the relationship of temperature to nitrifying biomass and plant nitrogen removal performance. Unfortunately, there is a lack of studies on full-scale treatment plants in temperate climate zones that also collected yearround seasonal data, so a lot of information about nitrification performance and nitrifying biomass abundance has been derived from laboratory experiments which are often not very representative of "real-world" scenarios. For example, in several laboratory

studies using bench-scale membrane bioreactors and granular activated sludge systems no low temperature effects on the abundance of nitrifying biomass and reactor nitrification performance have been observed (8-11). This might indicate that systems operating with prolonged retention times are less affected by temperature fluctuations (9, 12). However, other laboratory studies using reactors operated similarly to full-scale sequencing batch reactors (SRBs) have reported a direct correlation between loss of nitrifying biomass and decreasing nitrogen removal efficiency (13-18). Still other laboratory studies have observed a decrease of ammonia removal efficiency at lower temperatures with no decrease in the abundance of ammonia-oxidizing bacteria, but notable fluctuations in the abundance of nitrite-oxidizing bacteria (19-21).

Only a few studies of microbial community dynamics in full-scale activated sludge systems in temperate climate zones have been performed using high-throughput microbiome analyses to compare community dynamics to ammonia removal efficiency and seasonal temperature fluctuations (6, 16, 21-27). These studies have shown that the activated sludge microbial community is shaped to some extend by both deterministic and neutral factors (21, 26-30). Shifts in wastewater treatment plant nitrification perfomrance have been also previously studied by quantifying ammonia monooxygenase (*amoA*) gene copy numbers using qPCR to monitor the seasonal dynamics of ammonia- oxidizing bacteria (AOB) (13, 15). However, nearly all current full-scale wastewater treatment plant studies have investigated continuously stirred tank reactor configurations which operate at steady-state, while information on the seasonal community dynamics in sequencing batch reactors that operate under dynamic feast-famine conditions is scarce.

Here we provide a detailed analysis of the composition and seasonal dynamics of the activated sludge microbial community in three parallel SBR of a wastewater treatment plant that almost completely loses its nitrification performance each winter. The WWTP at Brainerd Minnesota is a great sampling location to address the microbial ecology of seasonal nitrification failure because of its geographic location (Coordinates: 46°21′29″N 94°12′03″W), its continental climate with vast seasonal temperature differences (average high 26.9°C in July and average low -19.8°C in January), and because of the fact that the plant operates three parallel SBRs at any given time which allowed for replicate sampling of full-scale reactors at high temporal resolution (weekly) for over a year.

The objective of this study was to identify and quantify the abundance dynamics of core and seasonal microbial taxa in the activated sludge of three parallel, full-scale sequencing batch reactor. Shifts in abundance of microbial taxa were correlated to observed conditions of 'nitrification failure', defined as decrease in nitrification performance during winter months. We link relative sequencing abundance from high-throughput sequencing to absolute gene abundances determined by quantitative polymerase chain reaction (qPCR). Emphasis was on 'known' nitrifying microbial groups including ammonia-oxidizing bacteria, archaea and nitrite-oxidizing bacteria. We identify a 'core' community of microbial taxa that were present year-round in all three reactors, seasonal taxa that were associated with only one or multiple seasons but that were non-detectable during at least one of the four seasons, and transient taxa that were present in any of the three reactors for shorter time period but were never consistently found. We define 'abundant' microorganisms in each of these groups and correlate their occurrence and seasonal dynamics with wastewater temperature and effluent ammonia concentrations throughout

the year. This work identifies important activated sludge microorganisms that affect the nitrification performance of SRBs. Overall, this work contributes to a better understanding of the microbial community composition and dynamics of activated sludge systems in SBRs in temperate climate zones that are experience strong seasonal temperature fluctuations.

Materials and Methods

Plant and sampling

The Brainerd Wastewater Treatment Facility (WWTF) in Minnesota is a Class A facility designed to treat domestic wastewater at an average wet weather flow of 22,700 m^3/day with a carbonaceous biological oxygen demand (CBOD) influent concentration of 240 mg/L and a TSS concentration of 240 mg/L. The average observed influent ammonia concentration is 35 mg/L throughout the year, while nitrate and nitrite were not detected. The average influent flow during the study period ranged from 6,965 ± 303 m^3/day in winter 2015 to 9,577 ± 2640 m^3/day in summer 2016. The Facility has a continuous discharge to the Mississippi River.

The influent domestic wastewater is pumped into one of three parallel sequencing batch reactors (SBRs) at a time. Once a reactor has been filled aeration starts and the influent wastewater is directed into the next reactor. This process is repeated about every two hours allowing for nearly identical treatment conditions in three completely independent activated sludge reactor systems. Aeration is pulled from ambient air without prior heating. Each reactor cycle lasts approximately six hours. During each six-hour cycle reactors operational conditions switch from static filling, mixed filling, aeration, settling, decanting and waste sludge removal. The reactors are located underground and completely covered which reduces seasonal temperature variations and limits photosynthetic growth. In summer 2016, during sampling weeks 53 to 55, heavy rainfalls increased influent flow rates from 7000 m^3/day to 9500 m^3/day resulting in slightly lower sludge retention times of 4.5 days instead of 8 days during the rest of the year.

Activated sludge samples were collected for 55 consecutive weeks (July 13, 2015 to July 31, 2016) from each of the three parallel reactors in operation. The samples were always taken about one hour into the aerobic reaction cycle following reactor filling. Each reactor is connected to a sink for easy sampling. Prior to sample collection pipes were flushed for about 5 min each time. Collected wastewater samples were immediately frozen at -20°C until further processing. At week 18 the impellor of SBR 1 broke. The activated sludge of SBR 1, as well as some sludge of reactor SBR 2 and 3 were transferred into SBR 4 at this time to continue operations with three reactors. The initial startup of SBR 4 marked the only time during our year-long sampling campaign at which multiple reactor contents were blended and therefore not operated completely independent of each other. SBR 2 and 3 only donated activated sludge to SRB 4 during its initial startup. Otherwise SBR 2 and 3 were completely independent during the entire year-long experiment. Because at any given time of the year-long sampling campaign the wastewater treatment plant operated with three parallel SBRs, we decided to combine the datasets of week 1 to 17 of SBR 1 with weeks 19 to 55 of SBR 4. Because of the failure of SBR 1 during week 18 we removed the sample from the dataset. For consistency in the following data analysis we will only refer to the three parallel reactors as SBR 1, 2, and 3 with SBR 1 being the reactor that was restarted at week 18.

The plants performance data were made available to us by the wastewater facility in Brainerd, MN. Total suspended solids (TSS), pH, water temperature, biological oxygen demand (BOD), sludge volume index (SVI), mixed liquor suspended solids (MLSS), sludge blanket, ammonia and phosphorus concentrations were determined according to standard EPA methods. A summary of the plant chemical and operational parameters is

shown in Table S2.1 in the supplementary information. This includes daily temperatures, influent flow rates, and pH. Several parameters such as mixed-liquor suspended solids, BOD, and phosphorous are recorded 3 times per week. In this case we report weekly averages for that specific data in Table S2.1. The treatment plant only measured ammonia concentrations every 2-4 weeks based on their permit requirements. Due to the infrequency of ammonia testing, additional samples were collected before nitrification failure began.

Starting January 2016 (week 26) effluent wastewater samples from the reactors were collected to quantify ammonia, nitrite, and nitrate concentrations using continuous segmented flow analysis to complement the chemical data routinely monitored by the plant. Effluent samples were taken from an equalization basin that receives the supernatants of all SBRs and immediately frozen at -20°C until analysis. This means that the collected data on effluent ammonia, nitrite, and nitrate concentrations represent average values for the three operational SRBs.

Continuous Segmented Flow Analysis

Quantification of ammonia, nitrate, and nitrate concentrations in effluent wastewater were performed on a SEAL AutoAnalyzer 3 HR continuous segmented flow analyzer (Seal Analytical Inc; Mequon WI) according to standard multi-test methods as to manufacturer's instructions. In brief, effluent wastewater was diluted 1:4 with deionized water and centrifuged for 5 min at 13,000 g to collect the supernatant. Ammonia concentrations were quantified using method No. G-102-93 (with salicylate chemistry), detection range 0.25 to 25 mg/L as nitrogen. Quantification of nitrate and nitrite concentrations were performed using method No. G-109-94 with hydrazine sulfate for NO_x

measurements and without hydrazine sulfate for NO_2^- quantification, detection range 0.3 to 11 mg/L as nitrogen. NO_3^- concentrations were calculated by subtracting NO_2^- concentrations from NO_x concentrations.

16S rRNA gene amplicon sequencing

DNA was extracted from the activated sludge samples using the *FastDNA™ SPIN Kit for Soil* (MP Biomedicals; Santa Ana; CA) according to the manufacturer's instruction with the following modifications. Sludge samples were thawed on ice and thoroughly mixed before 50 µL were mixed with 450µL of 5% (v/v) sodium dodecyl sulfate lysis buffer (120 mM sodium phosphate (pH 8.0) and 5% sodium dodecyl sulfate lysis buffer). Cell lysis was performed by three consecutive freeze-thaw cycle at 20°C, thawing samples on ice in between freezing. Following cell lysis samples were incubated for 90 min at 70°C in a water bath. The following steps were carried out as to the *FastDNA™ SPIN Kit* protocol. The DNA extracts were stored at -20°C until further use.

DNA extracts were provided to the University of Minnesota Genomics Center (UMGC) for 16S rRNA gene amplicon sequencing, beginning from DNA quality assessment and quantification, barcoded amplification, PCR product purification and library preparation. Protocols for each step followed UMGC developed methods, which have been published previously by Gohl et al. (2016). Sequencing primers were those also used for the Earth Microbiome Project covering variable regions V1 through V3 on the 16S RNA gene. The choice of sequencing primers follows the recommendation of Albertsen et al. (2015) for the phylogenetic analysis of activated sludge communities (31).

Controls using PCR water for DNA extraction and PCR amplification were included to verify reagent purity and identify potential sample contamination during library construction. Sequencing of all samples and controls was performed on an Illumina MiSeq sequencing system (Illumina, San Diego, CA, USA) using the 2 x 300 bp MiSeq Reagent Kit v3 (600 cycle) (Illumina, San Diego, CA, USA). The MiSeq Reporter Software v2.5.1.3 (Illumina, San Diego, CA, USA) was used for signal processing, de-multiplexing and trimming of adapter sequences.

Microbial diversity analysis

Sequence analysis was performed using the Gopher-Pipeline of the University of Minnesota Supercomputing Institute (32). This pipeline utilizes PandaSeq to stitch primers together, QIIME, ChimeraSlayer's usearch61 method for chimera detection within QIIME. Default settings were used for quality control, primer trimming, filtering, chimera and host detection. Subsampling and rarifying samples were disabled in the pipeline. Operational taxonomic unit (OTU) picking was done outside of the Gopher-Pipeline using QIIME and the SILVA rRNA database (release 128) (33, 34). OTUs were assigned at the 97% cutoff level. Only two samples, SBR 2, week 8 and SBR 3 week 2 did not amplify and were disregarded from the dataset. DNA extraction and PCR control samples resulted in >5000 low quality sequence reads. Plotting the number of sequence reads against unique OTUs (data not shown) demonstrated that the diversity of the all controls was significantly different from all activated sludge samples.

Statistical analysis

The statistical analysis of the obtained sequence data was performed using R version 3.4.2 (35). Ordination was performed using the *vegan software* package in R while regression analysis, ANOVA and ANCOVA functions, as well as comparative t-tests were done using the *alr4* software package in R (36, 37). ANOVA was used for linear regression analysis which was performed to determine relationships over time, or temperature changes. If the null hypothesis was zero, and no linear relationship was discernable, a comparative t-test was performed to compare the statistical means for the two groups. The 95% confidence intervals for statistical mean values were calculated using R and are provided when comparing linear regressions which could disprove the null hypothesis. ANCOVA was used in specific cases to determine if multiple factors were impacted by a single response such as total biomass and temperatures effects on the ammonia oxidizing community. Constrained Correspondence Analysis (CCA) was performed using the vegan package in R, which utilizes the Chi-squared distances. The analysis was performed twice to separate variables which can be controlled by plant operators, and all environmental parameters which are uncontrollable. Temperature was used in both analyses because the parameter can potentially be controlled by plant operators, while it's also an intrinsic characteristic of the influent wastewater. All statistical values are provided in the supplementary information.

Quantitative Polymerase Chain Reaction

Quantification of 16S rRNA and functional marker genes was performed on a 7900HT Fast Real-Time PCR System with a 384-well block module (Applied Biosystems

Inc, Foster City, CA). Reactions were performed in 25 µL volumes. Each reaction mix contained 10µL of PCR Grade Water (Ambion Inc; Foster City, CA), 12.5 µL of 2X SsoFast^{TM} EvaGreen® Supermix (Bio-Rad Laboratories; Hercules, CA), 1.25 µL of 10 mg/L bovine serum albumin solution (Millipore Sigma; St. Louis, MO), 0.5 µL of forward primer (0.5 µM), 0.25 µL of reverse primer (0.5 µM), and 0.5 µL of template DNA.

Gene quantification by qPCR targeted the *16S rRNA* gene as proxy for total Bacteria, and the ammonia monooxygenase genes (*amoA)* of Bacteria and Archaea to estimate the abundance of nitrifier populations. Functional marker gene quantification to estimate population abundance of denitrifiers targeted the nitrite reductase genes *nirK* and *nirS* as well as the nitrous oxide reductase gene (*nosZ clade 1)*. Primer sequences and references are provided in Table S2.2 in the Supplementary Information. PCR cycler temperature programs for the *16S rRNA* and *amoA* gene of Bacteria comprised 40 cycles of 15 sec at 95°C and 1 min at 60°C. Both assays for the *amoA* gene of Archaea and the *nosZ* gene had 40 cycles of 15 sec at 95°C followed by 1 min at 54°C. The *nirK* and *nirS* gene qPCR assay temperature programs comprised 40 cycles of 15 sec at 98°C, 54°C for 30s, and an elongation step of 30 sec at 72°C. As standards, dilution series of linear DNA fragments (g-Blocks, IDT DNA Technologies) of the respective target genes were used. All samples, standards, and negative controls were analyzed in triplicates and amplicon specificity was confirmed by melt curve analyzes. Amplification efficiencies of the different assays ranged from 81% to 103% (average of 88%). The R^2 values of the standard curves ranged from 0.983 to 0.999 (average of 0.9926).

Data availability

Illumina sequencing reads have been deposited in the National Center for Biotechnology Sequence Read

Archive under accession number PRJNA490320.

Results

Seasonal variations in plant nitrification performance

The SBRs of the wastewater treatment facility in Brainerd Minnesota were seeded with activated sludge in September 2010. All three parallel reactors went 'online' beginning in 2011. Since the start-up of the plant, the influent wastewater temperature fluctuates seasonally from as low as 10°C in the winter to up to 20°C during the summer month. Influent wastewater temperature fluctuations are inversely correlated to effluent wastewater ammonia concentrations. With decreasing wastewater temperatures, nitrification performance declines resulting in elevated effluent water ammonia concentrations in the combined SBR's effluent stream (Figure 2.1). Figure 2.1 shows that ammonia concentrations increase at influent wastewater temperatures around 13°C and continue to rise as long as colder temperatures prevail in the winter months. The most significant increase in effluent ammonia concentration during our sampling period occurred between December 2015 (average 0.43 ± 0.42 mg/L) and January 2016 (average 4.48 ± 4.27 mg/L) ($p<0.005$). When water temperatures rise in the Spring, ammonia effluent concentrations begin to decrease again. However, recovery of complete ammonia removal takes several months, often until May or June, even after wastewater temperatures have risen again above 13°C. While permit requirements require plant operators to monitor ammonia concentrations in the wastewater effluent periodically, influent wastewater ammonia concentrations are only measured sporadically. The influent wastewater ammonia concentration at the sampled wastewater treatment plant was infrequently measured. Therefore, this study uses the average for standard domestic wastewater which typically is 35 mg/L (38) throughout the sampling year.

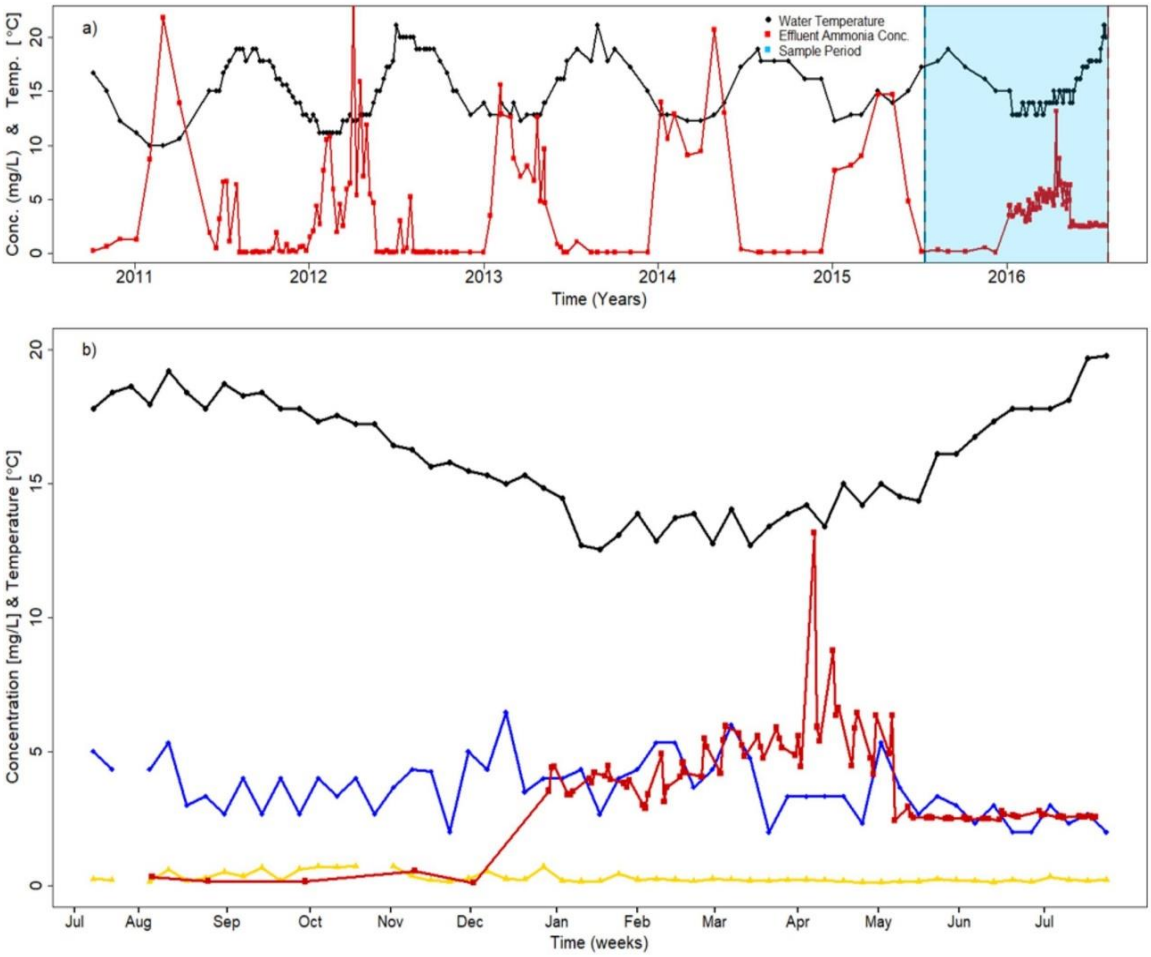

Figure 2.1. Brainerd wastewater treatment plant performance parameters from 2011 to 2016. a) Influent water temperature (black circles) and effluent ammonia concentration (red squares) for all years since plant start-up in 2011. The sampling year summer 2015 to summer 2016 is highlighted in light blue. b) Plant performance parameters for the sampling period from July 2015 to July 2016. Influent water temperature (black circles), effluent ammonia concentration (red squares), effluent biological oxygen demand (BOD) (blue diamonds), and effluent phosphate concentrations (yellow triangles). Effluent ammonia concentrations were inversely correlated to temperature. The effluent ammonia concentration between 2011 to 2015 was measured once per month by the wastewater operators at Brainerd Wastewater Treatment Facility. During seasonal nitrification failure in 2016, three samples per week were collected and analyzed by our team using

the Seal Flow AutoAnalyzer 3 HR. This causes a slight shift in the typically expected effluent concentrations during Summer 2016.

Based on the annual wastewater influent temperatures and effluent ammonia concentrations for the sampling period July 2015 to July 2016, we defined five seasons as follows: Summer (July 13th to September 22nd, 2015), Fall (September 23rd to December 20th, 2015), Winter (December 21st, 2015, to March 18th, 2016), and Spring (March 19th to June 19th, 2016). Sampling continued into Summer 2016 until July 31st, 2016.

Over the course of the 55-weeks of sampling, the influent wastewater temperature range fluctuated by 9°C with a high of 21°C in summer 2015 and a low of 12°C during the winter months. The rate of temperature decrease/increase between the cooling period (Fall and Winter month) and the warming period (Spring and Summer month) for the sampling year was ±0.043°C/day (Figure S2.1).

Effluent ammonia concentration was the only routinely monitored wastewater parameter that showed significant seasonal fluctuation ($p<0.005$), ranging from less than or equal to concentrations as low as 0.1 mg/L (method detection limit) in the Fall to 8.2 mg/L in Spring. Other parameters such as Biological Oxygen Demand (BOD_5), phosphate concentrations (P), and Total Suspended Solids (TSS) did not vary significantly with season ($p<0.74$, 0.41, and 0.20, respectively, as shown in Figure S2.1). A detailed list of average plant operational parameters for each season is provided in Table S2.1 in the supplementary information.

Seasonal community dynamics

Outcome sequencing data – general overview

The seasonal shifts in community composition in the three SBRs were analyzed using barcoded 16S rRNA gene amplicon sequencing. Sequencing resulted in 3.95 x 10^7 total reads. 92.8% of the raw reads passed the initial quality filtering. Of the remaining 3.67 x 10^7 reads 76.9% of the bases had a Q-score greater than 30. Chimera detection removed additional sequences so that in the end in 7.58 x 10^6 nonchimeric, quality-filtered reads (on average 56,000 reads per sample) were subjected to OTU clustering at the 97% cutoff level. OTU clustering resulted in 1984 unique 'species-level' OTU's for the total sequence data set. For analysis and better comparison of samples, we assumed that the read abundance, meaning the number of reads in each OTU, is corresponding to the actual abundance of the respective 16S rRNA phylotype in each activated sludge sample. However, it is important to keep in mind that the read abundance in DNA amplicon sequencing data sets is affected by DNA extraction efficiency, primer specificity, and the copy number of ribosomal RNA operons per genome and does not reflect 'real' natural abundance but is instead a commonly used estimation based on 16S rRNA genes.

Alpha diversity and reactor synchrony

We calculated the alpha diversity indices, Simpson, Shannon, and Chao1 in order to compare the local species diversity of the activated sludge communities for each of the three SBRs over the complete sampling period of 55 weeks (39-41). All three alpha diversity indices did not vary significantly with time considering the entire sampling period

(Figure S2. S2a-c). The differences in the Simpson and Shannon indices between reactors were mostly not significant ($p>0.05$) (Table S2.3). Significant differences in alpha diversity between reactors were only observed for reactors 1 and 2 as well as 2 and 4 (Table S2.3). This was most likely a consequence of the shutdown of reactor 1 at week 18 and transfer of activated sludge from reactors 1, 2 and 3 as inoculum to start up reactor 4 (in the following we refer to reactor 4 as reactor 1, see further explanations in the methods section). Reactors 2 and 3 were operated independently over the whole sampling period, however no significant differences in alpha diversity indices were observed over the entire year of sampling comparing these two reactors. The average alpha diversity indices for the three operational reactors at any given time during the sampling year were 0.97 ± 0.01, 4.53 ± 0.18, and 625 ± 87 for the Simpson, Shannon, and Chao1 indices, respectively.

While alpha diversity did not significantly vary between reactors, we observed significant differences when comparing the Simpson and Shannon indices for the different seasons. Generally, diversity was lower in the winter and higher in the summer. Including fall and spring the microbial community diversity in the reactors varied significantly each season ($p>0.05$) (Table S2.4). Exceptions were the Winter/Spring transition for Shannon and Simpson indices at class-level OTU clustering and the Summer/Fall transition for the Simpson index at genus-level OTU clustering (Table S2.4). No seasonally significant differences were observed for the Chao1 index, which fluctuated week-to-week but was consistent among the reactors (Figure S2.2c).

Definitions: core & seasonal community (one vs multiple seasons)

To study the annual shifts in the activated sludge microbial community composition and identify microbial taxa associated with seasonal shifts in wastewater temperature and effluent ammonia concentrations we group the total 1984 species-level OTUs into four categories: A 'core' community of microbial taxa that were present year-round in all three reactors, 'single season' taxa that were found during only one specific season, 'multiple season' taxa that were found during more than one season but that were absent during at least one of the four seasons, and 'transient' taxa that were present in any of the three reactors for shorter time periods (only a few weeks) but were never consistently found during an entire season or for any longer consecutive period of time.

The core community comprised 114 OTUs occurring in all three operational reactors at any time during the sampling year (Figure S2.11). This 'core' community constituted the largest fraction of the entire activated sludge community with a relative sequence abundance of 74.3% and 78.2% during the two summers 2015/16, 82.5% in winter of 2015, and 84.0% in Spring 2016 (Figure 2.2). Combining the two categories of seasonally occurring OTUs, they accounted for 15.1% and 17.6% of the activated sludge community in summers 2015/16, and only 5.3% and 6.7% in winter and spring. We identified more seasonal OTUs in the summers 2015/16 and fall (96/105 and 75 OTUs, respectively) than in the winter and spring (39 and 55 OTUs) (Figure S2.11). Transiently occurring OTUs ranged in relative sequence abundance from 6.7% to 12.3%, with relatively higher abundances in the winter than in the summer. While transiently detected OTUs made up only a relatively small fraction of the entire community in each season this

category had the highest OTU richness with numbers between 334-346 in the summer and up to 372 OTUs during the winter (Figure S2.3 in the supplementary information).

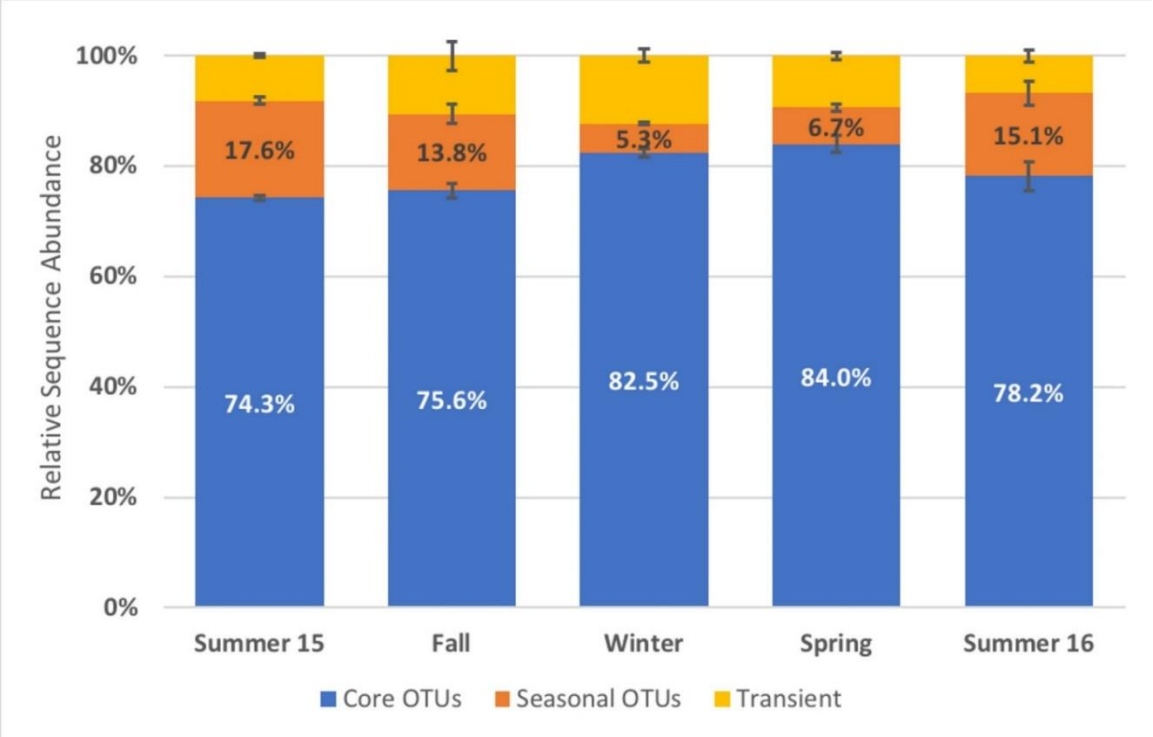

Figure 2.2. Average abundance of core, seasonal, and transient operational taxonomic units (OTUs). Core OTUs (blue) were present year-round in all three reactors. Seasonal OTUs (orange) were found during only one specific season or multiple seasons but were absent during at least one of the four seasons. Transient OTUs (yellow) were present in any of the three reactors for shorter time periods (weeks) but were never consistently found during an entire season or for any longer consecutive period of time. The relative sequence abundance of seasonal OTUs decreases during the winter and increases in the summer month.

OTUs that change with plant nitrification performance and temp

Canonical-correlation analysis (CCA) reveal that wastewater temperature was the most dominant variable affecting microbial community composition and shift throughout the year. Effluent ammonia concentration was inversely correlated to changes in wastewater temperature (Figure 2.3).

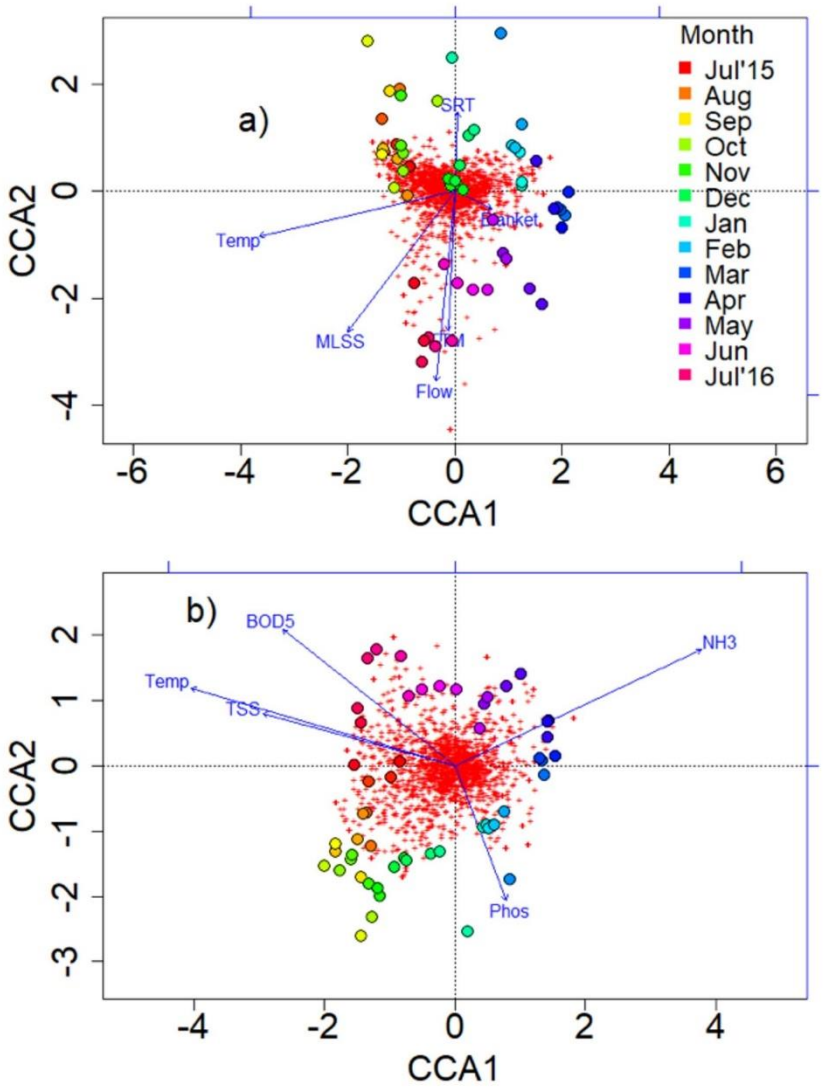

Figure 2.3. Constrained correspondence analysis (CCA) with operational and performance parameters with the activated sludge microbial community composition at the Brainerd wastewater treatment plant for July 2015 to July 2016. All classified OTUs in the complete sequence dataset are shown as red dots. The larger rainbow-colored dots represent the 55 weekly average microbial communities for the three sampled sequencing batch reactors. Parameter variable are shown as blue arrows and include temperature (Temp), mixed liquor suspended-solids (MLSS), influent flow rate as m^3/day (Flow), food-to-microbes ratio (FTM), sludge blanket levels (Blanket), sludge retention time (SRT), effluent ammonia (NH3), biological oxygen demand (BOD5), phosphorous concentration (Phos), and total suspended solids (TSS). a) The CCA including the five recorded operational parameters MLSS, Flow, FTM, Blanket, and SRT. b) CCA including the four plant performance parameters NH3, BOD5, Phos, and TSS. Temperature as potentially controllable parameter was included in both plots to emphasize its strong effect on community composition and structure.

We identified OTUs that changed in relative sequence abundance in correlation to annual fluctuations of wastewater temperature and effluent ammonia concentrations by calculating Pearson's product moment correlation coefficients (R^2) between OTU abundance and each of the two other variables. The two correlation coefficients (for water temperature and effluent ammonia concentrations) were plotted against each other for the top 95% most abundant OTUs of the activated sludge microbial community (Figure 2.4). In Figure 2.4, all OTUs with correlation coefficients of $R^2 > 0.4$ for either variable, wastewater temperature or effluent ammonia concentration, and a relative sequence abundance of > 0.1% are labeled with their specific taxa names.

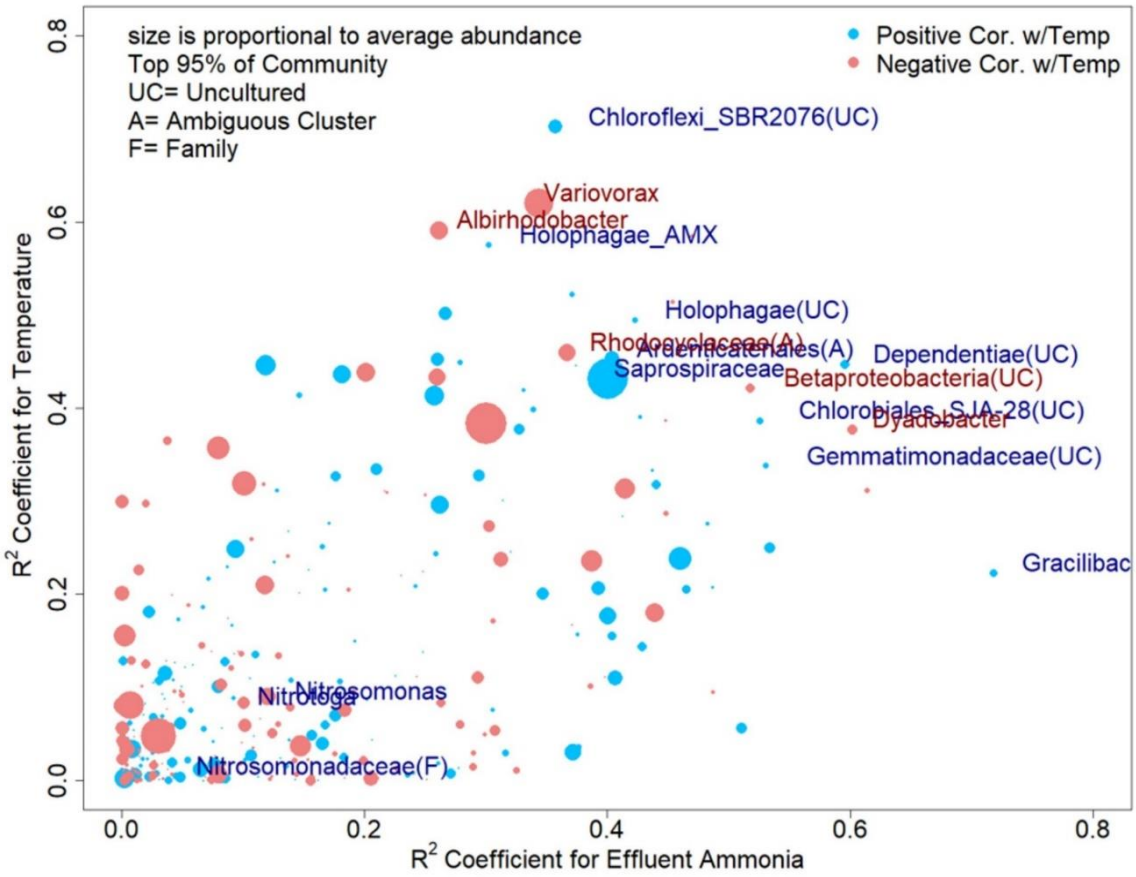

Figure 2.4. Correlation coefficients of OTUs (97% sequence similarity level) with effluent ammonia concentration and wastewater temperature for the entire sampling year. The size of the dots is proportional to the average abundance of the respective OTU. OTUs represented by blue dots have a positive correlation with temperature while OTUs represented by red dots have a negative correlation to temperature. OTUs are names by their highest taxonomic rank. OTU names are given for all OTUs with correlation coefficients of >0.4 to either wastewater temperature or effluent ammonia concentration except for OTUs classified as belonging to taxa comprising known nitrifiers in order to emphasize their weak correlation with both of these parameters. A complete list of all highlighted OTUs in this Figure 2.can be found in Table S2.5 in the supplementary information.

Among the core community OTUs, an uncultured *Saprospiraceae* (7.64% ± 2.9%), a *Comanonadaceae* (*Variovorax* (3.38 ± 2.0%)), a *Rhodocyclaceae* (0.92% ± 0.6%), and

the two uncharacterized taxa of *Chlorobi* (classified as *Chlorobiales* SJA-28 (0.14 ± 0.1%)) and *Gemmatimonadaceae* (0.12 ± 0.2%) correlated highest with the observed changes in wastewater temperature and effluent ammonia concentrations (either of the two correlation coefficients > 0.4).

Several OTUs with high correlation coefficients to wastewater temperature and effluent ammonia concentrations did not occur year-round but were instead only present for multiple consecutive seasons. Among these OTUs an uncultured *Choroflexi* SBR2076, a *Cytophagaceae* (*Dyadobacter*), and an uncultured TM6 (*Dependentiae*) occurred in two or three consecutive seasons at relative sequence abundances ranging from 0.49 ± 0.5%, 0.28 ± 0.4%, to 0.01 ± 0.0%, respectively. Another uncharacterized taxa of *Chloroflexi* further classified as *Ardenticatenales* occurred only in the fall of 2015

(single season OTU) with a relative sequence abundance of 0.57 ± 0.6% but correlation coefficients > 0.4 to wastewater temperature and effluent ammonia concentrations (R^2=0.45 and R^2=0.40, respectively). Also, some of the only transiently occurring OTUs showed strong correlation with shifts in wastewater temperature and effluent ammonia concentrations. These OTUs comprise the *Alphaproteobacteria Albirhodobacter* (0.92 ± 0.6%), an uncultured marine betaproteobacteria hot creek clone (0.22 ± 0.2%), an uncharacterized *Gracilibacteria* (0.01 ± 0.0%), and two *Acidobacteria*, *Holophagae* belonging to subgroup 7 (0.12 ± 0.2%) and subgroup 10 (0.13 ± 0.2%). Transient OTU were generally of low relative sequence abundance.

Interestingly, none of these OTUs, belonging to any taxa of known nitrifying bacteria in our activated sludge sequence data (e.g. the family *Nitrosomonadaceae*, or the genera *Nitrosomonas* and *Nitrotoga*), met these criteria, indicating that the relative

sequence abundance of known nitrifiers did not significantly change with the observed seasonal variations in water temperature and effluent ammonia concentrations (Figure 2.4). Also see the corresponding quantitative PCR results for the ammonia monooxygenase gene (*amoA*) below.

The three most abundant OTUs in each of the four arbitrary OTU groups (core, single season, multiple season, transient) are shown Figure S2.4 in the supplementary information in order to emphasize that most of the abundant OTUs in each category did not show a strong correlation ($R^2 < 0.4$) with either wastewater temperature or effluent ammonia concentration. The sum of the relative sequence abundance of the top three most abundant core OTUs averaged 20.7% ± 2.2%, while multiple season OTUs had a cumulative abundance of 1.3% ± 0.6%, and single season OTUs 0.3% ± 0.1%.

To quantify the compositional dissimilarity of the activated sludge microbial community between all 55 weekly samples of each of the three reactors, we calculated Bray-Curtis, Euclidian, and Kulczynski metrics and performed principle coordinates analysis to visualize (dis)similarities among the 16S rRNA gene amplicon data for each sample(36, 42, 43). All statistical dissimilarity matrices revealed similar results (See Figure S2. S5 to S6a-d in supplementary information) showing distinct seasonal shifts among the activated sludge communities for all three reactors. Samples collected during the winter months (blue colors) and the summer months (red colors) cluster at opposite ends of the first principle coordinate that explains most of the variation in the dataset. In Figure 2.5 the first principle coordinate for the Bray-Curtis metrics is plotted against the seasonal change in wastewater temperature emphasizing the distinct shift in microbial community composition with seasonal variation in wastewater temperatures (see also Figure S2.12 for

the portion of the total variance explained by Bray-Curtis dimensions). The fall and winter months, when wastewater temperature gradually declined, and the spring and summer months, when wastewater temperatures gradually increased again, both revealed a statistically significant ($p < 2e\text{-}16$), strong linear correlation ($R^2 > 0.81$) of microbial community dissimilarity with the seasonal trends in wastewater temperature change. Interestingly, the linear regression did not show significant differences between the slopes (Ancova $p<0.948$) of the two regression lines indicating that the rate of temperature change during fall/winter 'cool-down' and spring/summer 'warm-up' was constant. The 'cooldown' and 'warm-up' regression lines, however, had significantly different y-intercepts (Ancova $p<2.2e\text{-}16$) revealing a temperature gap of about 1.7°C between winter 'cool-down' and summer 'warm-up'. As consequence of the temperature offset between wastewater 'cool-down' starting fall 2015 and 'warm-up' beginning in spring 2016 the microbial community composition in the activated sludge of the sampled plant were significantly different from each other in summer 2015 and summer 2016 (Figure S2.10 in supplementary information).

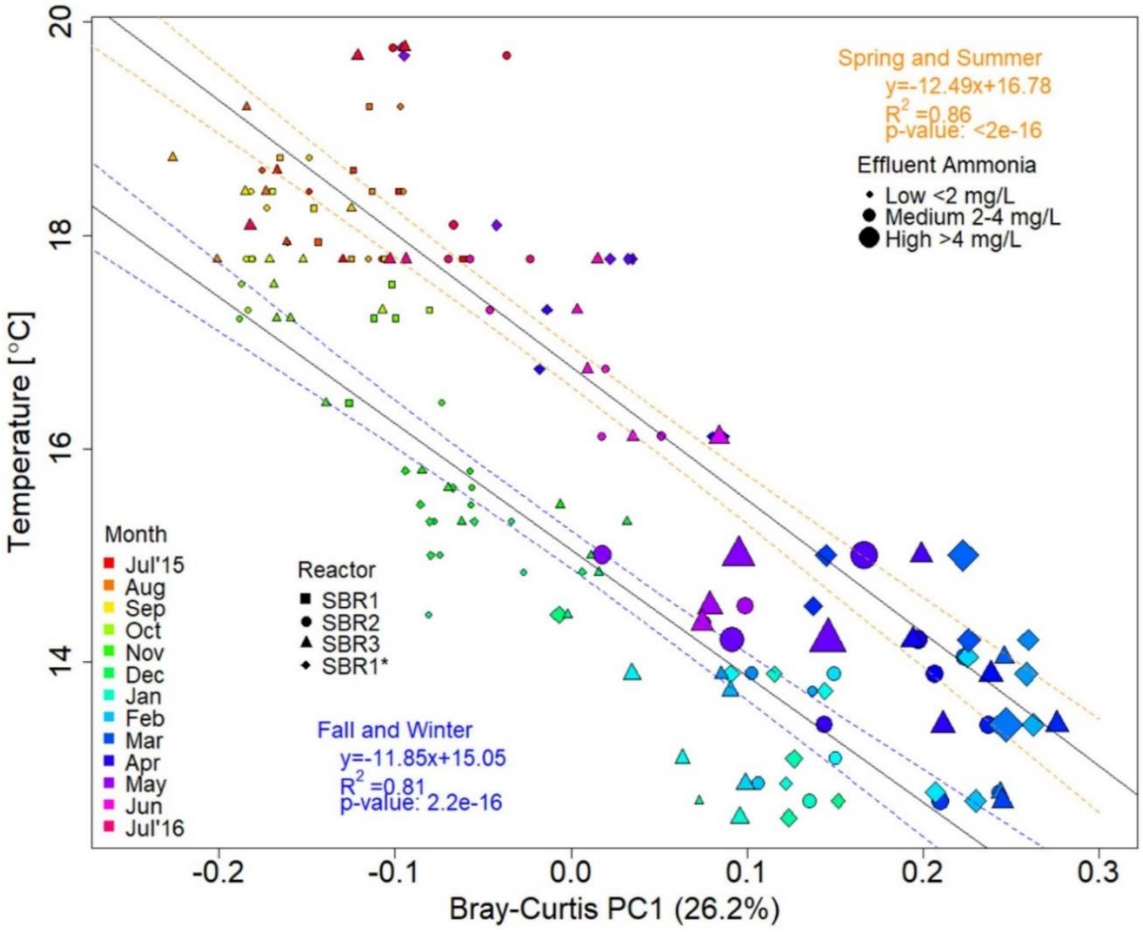

Figure 2.5. Linear regression of the first principle component (PC1) of the Bray-Curtis dissimilarity analysis with the observed fluctuation in wastewater temperature. The plot shows all 55 weekly samples of each of the three triplicate reactors (squares, circles, triangles, diamonds). Reactor 1 samples are shown before (squares) and after (diamonds) impellor failure at week 18 (November 2015). The size of each symbol denotes the effluent ammonia concentration. The rainbow-color scheme represents the sampling months with warmer summer and fall months in red/yellow colors and colder spring and winter months in blue/green colors. Linear regression lines with 95% confidence intervals for the cooling seasons (fall and winter; blue) and warming seasons (sping and summer; orange) show the strong correlation of microbial community richness with the recorded changes in wastewater temperature throughout the sampling year.

Using other matrices to quantify the compositional dissimilarity of the activated sludge microbial community showed that the temperature gap between seasonal cooling and warming periods was remarkably invariant, with 1.7°C and 1.1°C for the Kulczynski and Euclidean dissimilarity matrices, respectively (Figure S2. S6a-d, in the supplementary information).

Known functional guilds involved in N-cycling

Taxa known to comprise ammonia- and nitrite-oxidizing bacteria

We searched the activated sludge 16S rRNA gene amplicon data for taxa known to contain microorganisms capable of ammonia oxidation and nitrite oxidation. The known ammonia-oxidizing bacteria in our activated sludge samples all belonged to the family of *Nitrosomonadaceae*, comprising the genera *Nitrosomonas* and *Nitrosospina*. Only *Nitrosomonas* were detected year-round representing on average between 0.2 and 0.5% of the core community. *Nitrosospina* belonged to the category of transient OTUs because they were only detected sporadically (Figure 2.6). Interestingly, we also found anaerobic ammonia-oxidizing bacteria belonging to Candidatus *Brocadia* of the Planctomycetales in some of the samples. The *Brocadia* OTU we identified was the only known ammonia-oxidizing taxa that reveal a significant correlation to changes in wastewater temperature. While the overall sequence abundance of Candidatus *Brocadia* was relatively low (< 0.03%), the taxa increased 2.5-fold in relative sequence abundance between the months of January and July when temperatures dropped from 15°C to 12.2 °C in winter 2015/spring 2016 (Figure S2.7 in the supplemental information).

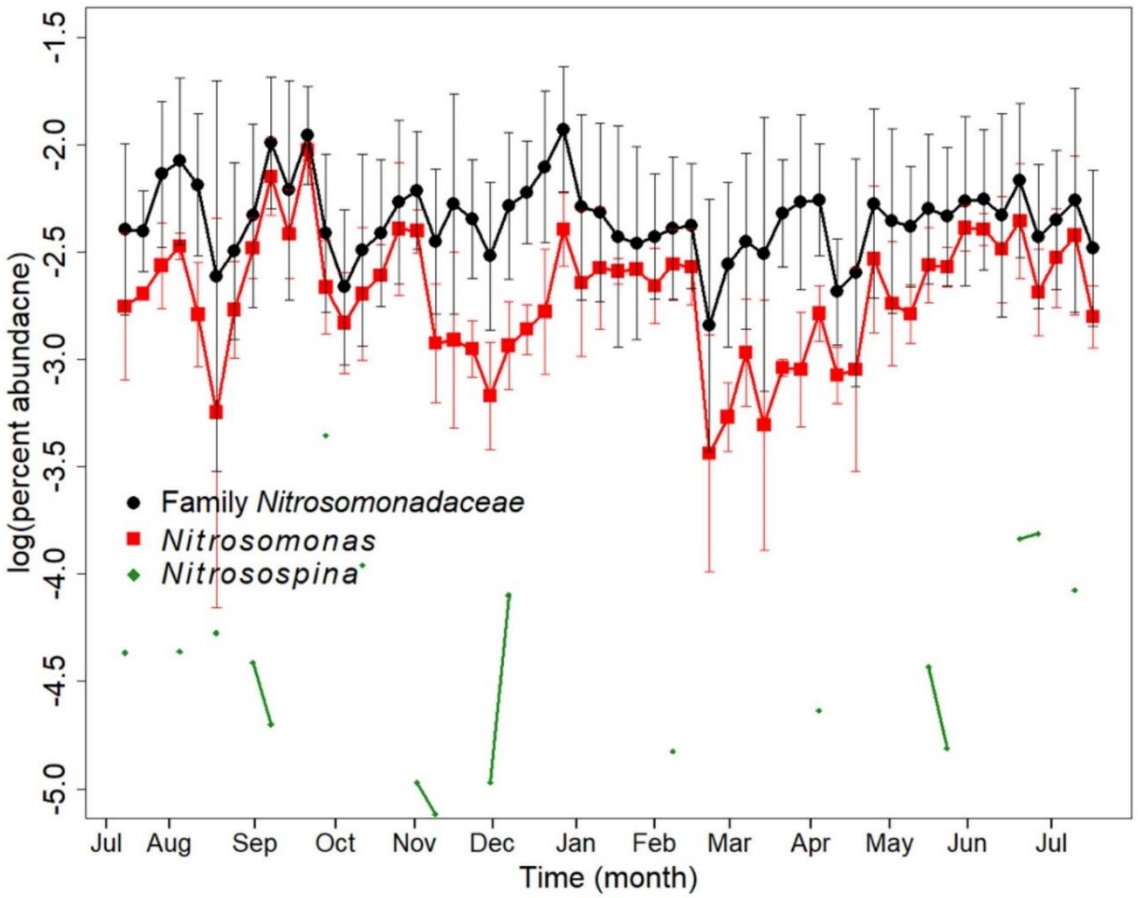

Figure 2.6. Average relative sequence abundances (three parallel reactors) of OTUs affiliated to taxa comprising known ammonia oxidizing bacteria identified in the activated sludge samples from the wastewater treatment plant at Brainerd, MN, between July 2015 and July 2016. Green *Nitrosospina* OTUs, red *Nitrosomonas* OTUs, and black sum of all *Nitrosomonadaceae* OTUs (including an ambiguous OTU cluster affiliated to this family). While *Nitrosomona*s have been detected in all samples throughout the entire year, *Nitrosopina* have only been detected sporadically in one of the three sequencing batch reactors.

Known nitrite-oxidizing bacteria belonged to *Nitrotoga*, *Nitrospira*, and *Nitrobacter*. *Nitrotoga* belonged to the core community detected throughout the entire year at a relative sequence abundance of on average >0.5%. *Nitrospira* and *Nitrobacter* have

only been identified in some of the weekly samples. Both taxa occurred sporadically and have not been detected as part of the activated sludge community over an entire season. The relative abundance of the complete nitrifying microbial community, comprising known taxa of ammonia and nitrite-oxidizing bacteria was 0.96% ± 0.37%. This relative abundance is within the lower range of typical reported abundances for nitrifier communities in activated sludge samples (21, 23, 26, 44). For example, Griffin et al (2017) report a relative abundance of *Nitrosomonas* of ~0.5%, while the relative abundances of *Nitrospira* varied between 0.75% to 2.3% in their system. However, Ju et al (2014) and Saunders et al (2016) reported a relative sequence abundance for *Nitrosomonas* of less than 1%. None of the known nitrifying functional guilds we detected in our activated sludge samples correlated significantly to either changes in wastewater temperature and effluent ammonia concentrations. Also see Figure 2.3 and description of results above.

Functional marker genes of ammonia-oxidizing bacteria and archaea

We used quantitative PCR to monitor the abundance of the 16S rRNA gene and several functional marker genes of key microbial nitrogen transformation processes in activated sludge such as ammonia oxidation, nitrite reduction, and nitrous oxide reduction. In order to quantify ammonia-oxidizing Bacteria and Archaea we used primers targeting the functional marker gene ammonia monooxygenase (*amoA*). Denitrifying bacteria were quantified by targeting the two nitrite reductase genes *nirS* and *nirK*, while microorganisms capable of nitrous oxide reduction were quantified targeting the nitrous oxide reductase gene *nosZ* clade 1. The quantitative PCR results are summarized in Figure 2.7. The synchrony of the qPCR data for reactors 2 and 3 was highly significant for all quantified

genes over the entire year. Reactor 1 was distinct from reactors 2 and 3 with respect to *nosZ* gene copy numbers (p=0.8686 and p=0.7901) and distinct from only reactor 3 for *nirK* gene copy numbers (p=0.5181), which might be due to the impellor failure of reactor 1 at week 18.

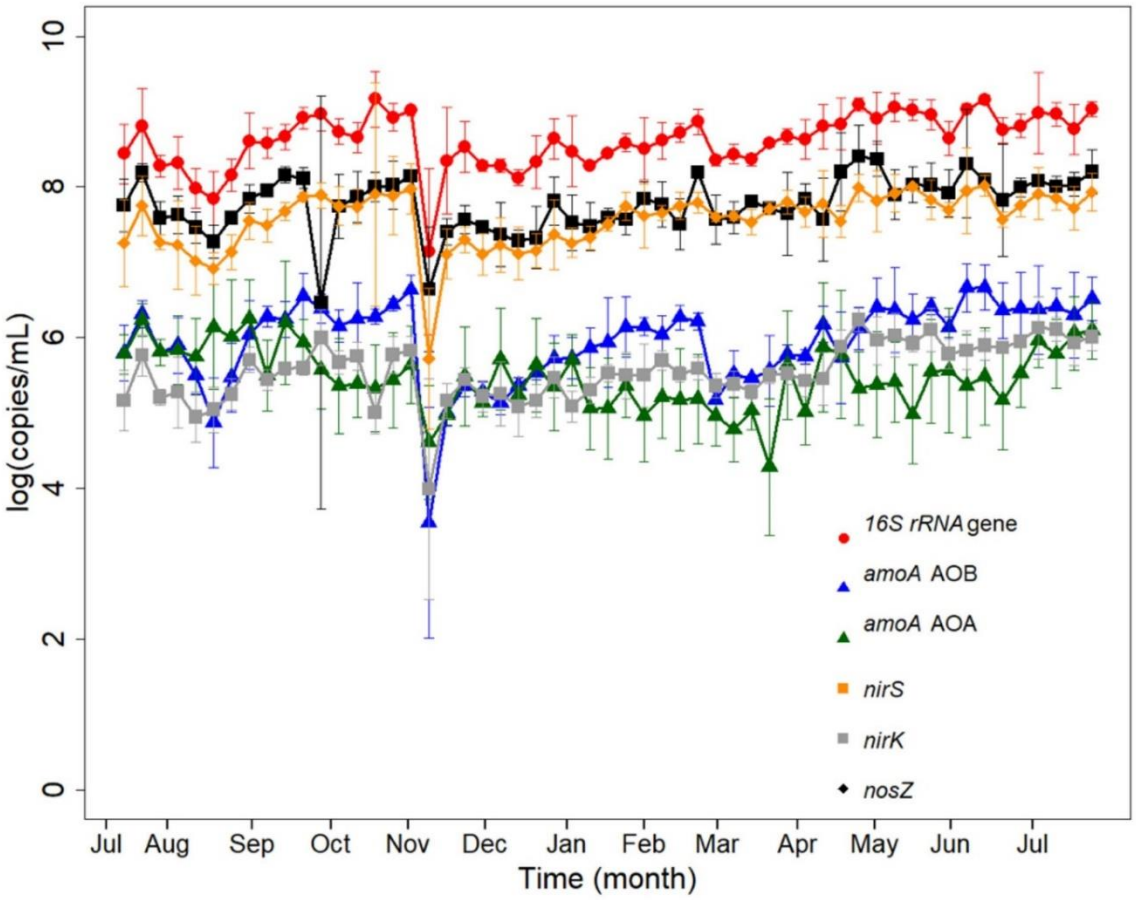

Figure 2.7. Quantitative PCR results showing the change in gene copy numbers over time for the 16S rRNA gene and process relevant functional marker genes for microbial nitrification and denitrification. Gene copy number are show as log copy number per milliliter of activated sludge. Gene copy numbers of the 16S rRNA gene (red circles), ammonia monooxygenase gene of ammonia-oxidizing bacteria (*amoA* gene of AOB; blue triangles), ammonia monooxygenase gene of ammonia-oxidizing archaea (*amoA* gene AOA; green triangles), nitrite reductase *nirS* (orange squares), nitrite reductase *nirK* (gray squares), nitrous oxide reductase *nosZ*

(black diamonds). All gene copy numbers show a significant decrease at week 18 in November 2015 when the impellor or reactor 1 broke and had to be replaced. Apart from this incidence gene copy numbers of all quantified genes were relatively stable and no statistically significant changes (Anova $p<0.05$) were identified throughout the entire year.

Over the entire year of sampling average 16S rRNA gene copy numbers were 8.62 ± 0.37 log(copies/mL). Shifts in 16S rRNA gene abundance during the year did not correlate with wastewater temperature and effluent ammonia concentrations. Overall, 16S rRNA gene copy numbers were three orders of magnitude higher than both bacterial and archaeal *amoA* gene copy numbers. Average annual *amoA* gene copy numbers were 5.94 ± 0.56 log(copies/mL) for Bacteria and 5.47 ± 0.42 log(copies/mL) for Archaea. A linear regression of bacterial *amoA* gene copy numbers with the cumulative 16S rRNA gene sequence abundance of all OTUs classified as *Nitrosomonadaceae* over the entire years resulted in a correlation coefficient of R^2 0.64 (p-value $5.21e^{-13}$) (Figure S2.9). The strong and significant correlation of both datasets confirmed that the population abundance of known ammonia-oxidizing bacteria is relatively stable throughout the year and does not change significantly when wastewater temperature dropped in the winter month.

We also tried to quantify complete ammonia oxidizing bacteria affiliated to the Nitrospira (Comammox Nitrospira) by using the recently published *amoA*-targeted qPCR primers of Pjevac et al. (45) (data not shown). In almost all activated sludge samples collected in this study, comammox Nitrospira were below our qPCR assay detection limit.

Functional marker genes of denitrifying microorganisms

The abundance of the nitrite reductase gene *nirS* was two orders of magnitude higher than the abundance of the *nirK*-type nitrite reductase. We quantified 7.57 ± 0.39 log(copies/mL) for the *nirS*-type nitrite reductase and only 5.55 ± 0.39 log(copies/mL) for the *nirK*-type nitrite reductase. Clade I-type nitrous oxide reductase gene (*nosZ*) copy numbers were 7.81 ± 0.47 log(copies/mL) (Figure 2.7). All functional genes quantified by qPCR did not show a significant change in abundance with the observed decrease in wastewater temperature and the corresponding increase in effluent ammonia concentration during the winter season.

Discussion

Reactor synchrony

At first, we compared the three parallel reactors with each other to evaluate if they are true replicates or show any significant differences with respect to composition and structure of their activated sludge communities. In this context it is important to consider that the WWTP in Brainered, MN does not have an upstream equalization basin or primary settling tank to homogenize influent wastewater. Interestingly, despite constant re-seeding of reactors with influent wastewater every 6 hours (average duration of a reactor cycle) we did not find significant differences in alpha diversity between the three reactors at any time during the year-long sampling campaign. Only on week 18, when the impellor of reactor 1 broke, differences in relative amplicon abundance and qPCR gene copy numbers became significant for reactor 1 compared to the other two reactors. While maintenance work required drastic changes in sludge volume of reactor 1 during week 18, reactor re-start by using activated sludge from the two other operational reactors established a microbial community with insignificantly different alpha diversity to the other two reactors within a week. We therefore decided to eliminate the week 18 sample of reactor 1 from the dataset and combine samples of week 1 to 17 and 19 to 55 into one continuous set of data for reactor 1. The observed similarity between the independent triplicate reactors is interesting because it means that any so slight variations in the chemical composition, physical parameters, and community composition of the influent wastewater over time, did not change the activated sludge microbial community in any of the three reactors in a way that were statistically significant. Any minor shifts in community composition between reactors resulted from transient OTUs that occurred for only a short period of time at low relative

sequence abundance before been washed out of the system again (most OTUs were singletons). The high similarity between reactors was also supported by the fact that process performance did not significantly alter between reactors at any time during the sampling year as shown in Figure 2.1b. Overall, core and shared seasonal OTUs accounted for 87.7% and 93.3% of the activated sludge communities in the three reactors. A higher similarity of the activated sludge microbial communities within different reactors of the same full-scale WWTP than between different plants has also been observed in previous studies (21).

From the perspective of an operator of a wastewater treatment plant similar to the facility in Brainerd, the similarity in community composition and structure among the three parallel reactors is an important finding because reactor failures, such as the technical problems observed in reactor 1 at week 18, will not affect the other reactors nor impair overall plant performance. The operational reactors can serve as seed banks for inoculation when maintenance or technical issues require a restart of one reactor.

Seasonal community dynamics

Activated sludge communities have been reported to be shaped by both deterministic and neutral factors (21, 26-30). At the Brainerd WWTP, temporal variation in community structure was primarily driven by changes in wastewater temperature (Figure 2.3). Also, previous studies have reported on strong seasonal effects associated with temperature on the bacterial community composition and structure in WWTP (21, 46).

Griffin and Wells (21) recently reported that the community dynamics in six full-scale reactors at four WWTPs in the Chicago area (Illinois, USA) displayed a highly

reproducible and synchronous seasonal fluctuation. They also observed that after one complete year of sampling individual reactors maintained minor but stable differences in community composition. We also found that the summer 2015 and summer 2016 microbial communities at the Brainerd WWTP in Minnesota were significantly different from each other (Figure S2.10), however, both summer sample were more similar to each other than to any of the samples from the other three seasons (winter, spring, and fall) (Figure S2.5). This suggests a seasonal community succession but continual annual drift of the activated sludge community at the Brainerd facility. How this annual community drift will affect plant functional stability and process performance on a long-term annual time scale will be an interesting topic for future studies. Based on our current data it is not possible to discern seasonal trends within one year from log term variations between consecutive years. However, seasonal community succession across multiple years has been described as a distinct characteristic of aquatic microbial communities in freshwater and marine habitats (47-49). For activated sludge systems seasonal temperature fluctuations seem to be mainly a predominant deterministic factor for the composition of communities of WWTP located in temperate climate zones, while WWTP in tropical climates with warmer, less variable average annual temperatures, continual community drift rather than seasonal succession patterns seems to drive variation in community composition (16). Interestingly, the microbiomes in WWTP located in polar regions with continuous cold climate seem to be able to maintain high performance levels in terms of organic matter and nutrient removal but these plants are usually operated at SRTs of up to 30 days (22).

Because temperature seems to be a major driver of seasonal community succession at the Brainerd WWTP, the significant differences between the summer 2015 and 2016

activated sludge communities might be explainable by the observed temperature gap between cooling and warming periods. While the rate of temperature change during cooling and warming phases was similar (±0.043°C/day) recovery of alpha and beta diversity in summer 2016 was delayed by 5.1 SRT cycles (calculation based on an annual average of 7.8 days per SRT) compared to activated sludge microbial diversity described in summer 2015. More data will be needed to evaluate if this observation is a reproducible characteristic causing annual drift of activated sludge communities in sequencing batch reactors of temperate climate WWTPs.

Co-occurrence networks can help to identify interconnections between OTUs based on their paired presence within complex communities (50). A co-occurrence analysis performed on the dataset obtained in this study did not identify any meaningful interactions between community members (data not shown) because of the high abundance of a relative low number of core OTUs with many interactions which reduced the interpretability of the obtained network. This is a known limitation of networks that are characterized by local hot spots of abundant correlations between neighboring network notes (51). Considering that variable copy number of ribosomal RNA genes can influence relative OTU abundances in sequencing libraries and the fact that metabolic functions are generally not well conserved among ribotypes, does further limit the meaningful interpretation of co-occurrence networks for the identification of putative interactions between microorganisms in the environment.

Nitrifying community

The WWTP in Brainerd repeatedly experienced a loss in nitrification performance when wastewater temperatures decreased below 13°C during the cold Minnesota winters. Despite the observed decrease in N-removal efficiency our sequencing and qPCR results showed that the abundance of known nitrifying microbial populations was rather constant throughout the entire year. As mentioned above lower temperatures reduce microbial growth rates and may wash out slow-growing nitrifiers if sludge retention times are kept constant and relatively short (annual average 7.8 days) all year long. Under this assumption we expected that the decrease in nitrification performance in the winter month might be associated with a decrease in nitrifier population abundance. However, our 16S rRNA gene amplicon sequencing and qPCR data did not reveal any significant correlation between relative OTU abundances, ammonia monooxygenase gene copy numbers and the observed seasonal fluctuations in temperature and effluent ammonia concentration. This means that the nitrifying community must maintain a growth rate higher than the inverse of the SRT in order to remain in the system. However, at the same time we observed a decrease in plant nitrification performance which means that the populations of known nitrifiers maintained their growth rates while lowering their energy generation via ammonia oxidation. Maintaining growth rates at lower rates of ammonia oxidation might be possible when organisms are metabolically versatile and flexible and can switch over to another energy metabolism or when immigration from influent sources maintain a stable population abundance. It is also conceivable that other species than the typical, known ammonia oxidizers contribute to the ammonia oxidation rates in the warmer spring and summer months but that these unknown “seasonally active” microorganisms are temperature

sensitive and are contributing less to the observed amount of ammonia removal in the winter. The fact that ammonia removal activity is never completely lost and activity is recovered in spring means that known and unknown microbial taxa capable of ammonia-oxidation must remain in the reactors year-round or are continuously immigrating with influent wastewaters.

Other studies that report on the correlation of seasonal nitrification failure with ammonia-oxidizing community dynamics based on 16S rRNA gene amplicon sequencing also observed that nitrifying populations can maintain a relatively stable abundance despite seasonal fluctuations in wastewater temperature (21). Delatolla et al. (19) quantified the biomass and rRNA content in a wastewater biofilm by fluorescence *in situ* hybridization and microscopy and did not find evidence for seasonal effects on the abundance of nitrifying microorganisms at colder temperatures (19). Conversely, Beneduce et al. (2014)(13) showed that the abundance of ammonia-oxidizing bacteria was severely affected by drastic changes in temperature, dissolved oxygen, and salinity in a wastewater treatment plant treating water from a saline thermal spa.

More data might be necessary to identify if the observed change in nitrifying activity is solely thermodynamically driven (17), or a consequence of microbial populations entering or leaving the system throughout the seasons. In Figure 2.4, we identified a couple of OTUs that showed a strong correlation in relative sequence abundance with either temperature and/or effluent ammonia concentration (also see Table S2.5 in Supplementary information). An OTU classified as uncultured *Saprospiraceae* was the second most abundant OTU in all three SBRs with an average annual abundance of 7.64% ± 2.9%. We observed a significant positive correlation with temperature as well as

a significant negative correlation with effluent ammonia concentration (Pearson R=0.69 & 0.63, p<8.1e-9 & 4.6e-5) while the relative sequence abundance of this *Saprospiraceae* OTU ranged from 12.0% during the summer down to 3.0% in the winter. We also identified a second *Saprospiraceae* OTU, classified as *Candidatus Aquirestis*, as one of the top three most abundant OTUs in the 'multiple seasons' OTU category since we detected it only in Fall of 2015 and Spring and Summer 2016 but not during the winter month. Important in this context might be that it has been shown in previous studies that with the decrease in temperatures the structure and species composition of microbial aggregates and biofilms in activated sludge can change which may directly or indirectly impact nitrification performance (19, 20). *Saprospiraceae* have been described as epiphytic rods that attach to filamentous bacteria (52). They are commonly found in flocs and aggregates of activated sludge. However, their exact role in wastewater treatment is not well understood (21, 24, 25, 53, 54). Members of the *Saprospiraceae* may be important in the breakdown of complex carbon sources. It has been suggested that their hydrolytic activity provides simple carbon substrates for other microorganisms involved in the removal of nutrients and this might even be the rate-limiting step for these processes (55, 56). However, most nitrifiers are autotrophs and do not rely on organic carbon for growth. On the other hand, Reza and Alvarez Cuenca (57) suggested that members of the family *Saprospiraceae* could also be directly involved with the nitrification processes.

It might be conceivable that a change in abundance of *Saprospiraceae* during the winter has an effect on the structural integrity of activated sludge aggregates which will alter the habitat space of nitrifier populations. This might not directly affect nitrifier population abundances but could indirectly affect nitrification efficiency if ammonia

oxidizers lose the structural support for forming close spatial associations with nitrite oxidizers in activated sludge flocs. However, in order to test this hypothesis a microscopic study will be required to visualize and quantify the involved microbial taxa and their spatial association in accordance with seasonal extremes of high and low wastewater temperatures. In this context, future studies should also evaluate the role of the ambiguous taxonomic groups affiliated with the phyla *Chlorobi* and *Chloroflexi* (Table S2.5) that we identified as core or multiple season taxa with significant correlation to wastewater temperature and effluent ammonia concentrations, for their contributions to aggregate stability and reactor nitrogen removal processes.

Conclusions

We investigated the composition and seasonal dynamics of activated sludge communities of three full-scale sequencing batch reactors of a wastewater treatment plant in a temperate climate zone, with focus on changes in community structure in response to environmental variables. We showed that:

- Temperature was the primary driver of shifts in alpha and beta community diversity
- Seasonal patterns of microbial community structure exist in highly synchronized reactors
- A set of core OTUs were highly abundant and strongly synchronized between reactors
- Individual OTUs only occurred seasonally (single season, multiple seasons) or for shorter periods of time in any of the three reactors
- Key functional groups such as ammonia oxidizing bacteria maintained stable population abundances despite decrease in plant ammonia removal performance in the winter month

To date this study is one of the most comprehensive analyzes of seasonal community dynamics in the activated sludge microbiome of SRBs in temperate climate zones that experience a periodic decrease in nitrogen removal efficiency. A more in-depth understanding of the seasonal community composition and dynamics will be beneficial for treatment plants which continually struggle to maintain efficient nitrification activities despite following typical mitigation strategies such as prolonging SRT and increasing total biomass. Future time series studies should assess the transcriptional activity of

nitrification-associated genes, in order to quantify microbial activity shifts associated with cold temperature nitrification failure so that factors controlling the abundance of nitrifying populations can be better understood. The data presented here will help to develop predictive models and new concepts to improve bioreactor design and operation condition for wastewater treatment plants in temperate climate zones so that they can achieving reliable nitrification performance at all seasons.

Acknowledgements

We would like to thank Gregg Kropp and the team at Brainerd Wastewater Treatment Facilities for sample collection and access to treatment plant performance data. We would like to thank the University of Minnesota Genomics Center for assistance with amplicon sequencing and access to the 7900HT Fast Real-Time PCR System. We would like to thank the National Science Foundation Graduate Research Fellows Program for providing Juliet Johnston with a fellowship opportunity as well as the Legislative Citizen Commission on Minnesota Resources for funding the project. Finally, thank you to Amelia McClure for helping with qPCR protocols and Deirdre Manion-Fischer for proofing.

Funding

J. Johnston was supported by the National Science Foundation Graduate Research Fellowship Program (ID: 2015191729). The research was enabled by the Legislative-Citizen Commission on Minnesota Resources (LCCMR) through a grant entitled "Wastewater Treatment Process Improvements" funded by the Environment and Natural Resources Trust Fund (ENRTF) under legal citation M.L. 2016, Chp. 186, Sec. 2, Subd. 04k.

Chapter 3

Nitritation Kinetic Model for Brainerd Wastewater Treatment Facility

Synopsis:

Wastewater treatment facilities often demonstrate significant loss in nitrification performance throughout the winter months. The understand this phenomenon, a kinetic model was created which integrated real data from Brainerd Wastewater Treatment Facility and other kinetic models. This revealed that temperature and total biomass played the most significant role in predicting the effluent ammonia concentration. While dissolved oxygen concentration may fluctuate significantly, this appeared to make no significant impact on the treatment plant performance. The incorporation of read data from high throughput sequencing and quantitative polymerase chain reaction data hinders the model due to unpredictable variations. Ultimately, using sequencing data proved to be the most accurate method of tracking the AOB community but still did not capture the actual conditions of the treatment facility.

Introduction

Kinetic models are designed to predict wastewater treatment plants operational performance based on the average chemical composition of domestic wastewater. Models such as ones developed by Gao in 2010 (1) implement the feast-famine nature of sequencing batch reactors, while common programs such as Activated Sludge Model No. 3 (2) are more representative of continuously stirred-tank reactor styles. Kinetic models are typically created to incorporate nearly every individual operational variable in wastewater treatment and every treatment plant design. However, these models all make assumptions about the microbial community based on typical activated sludge, despite numerous studies showing the microbial community strongly fluctuates with respect to temperature. These microbial community compositions are largely assumed and calculated purely mathematically, as opposed to being monitored and inputted into the model itself.

Recent advancements in molecular biology open the possibility for real-time microbial composition monitoring. This can be performed through high throughput sequencing or targeting specific organisms through functional genes. These molecular biology techniques can then be incorporated into kinetic models to provide a stronger representation of the microbial community throughout the seasons and offer a stronger ability to predict performance of treatment facilities. This study aims to connect molecular biology and kinetic models by developing a kinetic model for the Brainerd Wastewater Treatment Facility's nitrification performance using high throughput sequencing as well as quantitative polymerase chain reaction.

Methods:

Brainerd Wastewater Treatment Facility Overview: The facility consists of three sequencing batch reactors. In total, the treatment plant is designed to operate at 6 million gallons per day, but currently handles around 2 million gallons per day. Each sequencing batch reactor runs a 6-hour cycle which has several stages including "static fill", "mixed fill", "aerobic react", "settling", decant" and "idle." This model only focuses on the 2-hour "aerobic react" period. With a total of 4-cycles per day, each reactor's activated sludge community is exposed to a total of 8-hours of aerobic biological growth.

Dissolved Oxygen: Brainerd Wastewater Treatment Facility uses a computer program to control the dissolved oxygen concentration during the reaction cycle. The dissolved oxygen concentration will turn on at the start of the aerobic react cycle and continue supplying oxygen until 3.5ppm is reached. After 3.5ppm is reached the air blower will shut down and let the dissolved oxygen concentration drop until 0.75ppm where it will turn back on until either 3.5ppm is reached again, or the two-hour aerobic react cycle is finished. This frequently created three distinct trends in the aeration profile where the 3.5ppm "peak" is reached one to three times. These have been termed "single peak", "double peak", and "triple peak." Single peaks are more common during the summer months, double occurs throughout the entire year, while triple peaks most-often occur during winter. Since double peaks occur throughout the entire year, the year-long simulations were run using exclusively double peaks. Additional tests compared the average temperature extreme of 10°C and 18°C using all three profiles. An additional dissolved oxygen profile was created using a consistent 3.5ppm as comparison.

Monod Kinetics were applied to model the ammonia concentration and the dissolved oxygen concentration which were taken from sequencing batch reactors under similar operational conditions to Brainerd preforming nitritation (1). Other models such as (Activated Sludge Model No. 3) ASM3 (2) incorporate bicarbonate and nitrite concentrations as factors impacting nitritation performance. Because the pH remained relatively constant at Brainerd (influent and effluent) and the concentration of nitrite were remained low, these were removed to simplify the model.

Equation 3.1

$$\left(\frac{S_{NH3}}{K_{NH3}+S_{NH3}}\right)\left(\frac{S_{O_2}}{K_{O_2}+S_{O_2}}\right)$$

Equation 3.1 denotes the terms S for the substrate concentration of both ammonia and oxygen as well as the K "half velocity constant" which is half of the highest rate of substrate utilization for ammonia and oxygen.

Temperature: To account for the effects of temperature, a double Arrhenius equation was used as shown in Stark, 1996 (3). This was used to account improve the model at all temperature ranges and differs from common Monod models. Most Monod models replace K and K_S terms as temperature dependent. Typically, models such as ASM3 have two values for K and K_S, one value at 20°C and the other set to 10°C. These K values would be interpolated based on the provided temperature. This assumes that with increasing temperatures, the kinetics are always assumed to be increasing. This assumption is generally valid between 10-25°C but not in higher temperature ranges. Nitrification has shown to decrease in performance between 30-40°C and completely stop by 55°C. To

better model nitrification in both cold and warmer temperatures, the double Arrhenius equation was implemented as its own independent parameter. To express this component as a percentage, the peak temperature, V_{Max}, which occurs at approximately 37.25°C was divided by the given temperature value.

Equation 3.2

$$\left(\frac{A_1 e^{\frac{-E_{a1}}{RT}} - A_2 e^{\frac{-E_{a2}}{RT}}}{V_{max}(37.25°C)}\right)$$

Equation 3.2 denotes a double Arrhenius equation where each A term is the pre-exponential factor, E_a denotes the activation energy, R is the universal gas constant, T is the temperature, and V_{max} is the maximum rate of ammonia degradation based on temperature. V_{max} was used to create a unitless term that changes in percent of total possible ammonia degradation based on temperature, which could be combined with other parameters in the equation.

Biomass: Total biomass was calculated using a mass-balance for microbial growth as shown in Davis (4). It should be noted that this equation is typically derived for CSTR's, it still managed to be fitted using SBR configurations as well. This provided a total biomass approximation as mixed liquor volatile suspended solids. The parameters for yield (Y) and the decay constant (K_d) were fitted to match data supplied from Brainerd Wastewater Treatment Facility. The additional data to calculate the total biomass such as the influent BOD, effluent BOD, SRT and HRT were also provided from the wastewater facility.

The biomass for AOB was calculated in two ways, both which approximated the percent abundance of AOB within the total biomass. The first was $AOB\%_{Seq}$ which expressed the percent abundance for AOB using high-throughput sequencing data. The

number of reads which were from the family *Nitrosomonadaceae* were divided by the total number of reads in the sequencing run. Secondly was $AOB\%_{qPCR}$ which approximated the percent biomass by dividing the concentration of *amoA* gene copies/L by the concentration of *16S rRNA* gene copies/L.

Equation 3.3

$$X = \frac{\theta_c Y(S_{IN} - S)}{\theta(1 + K_d\theta_c)}$$

Equation 3.3 calculates the total biomass in the mixed liquor volative suspended solids. In this equation, θ_c represents the sludge retention time, Y is the yeild coefficient, S_{IN} is the influent BOD representing the carbon available for microbial growth, S is the effluent BOD, θ is the hydraulic retention time, and K_d is a death coefficient for microbes dying in the system.

Equation 3.4

$$X_{AOB} = X * (AOB\%_{Seq})$$

Equation 3.4 quantifies the biomass of ammonia oxidizing bacteria by taking the total biomass calculated in Equation 3.3 and multiplying this by the percent of ammonia oxidizing bacteria found in the total sequencing reads throughout the year.

Equation 3.5

$$X_{AOB} = X * (AOB\%_{qPCR})$$

Equation 3.5 quantifies the biomass of ammonia oxidizing bacteria by taking the total biomass calculated in Equation 3.3 and multiplying this by the percent of ammonia oxidizing bacteria determined by the *amoA* functional gene's total copy numbers, divided by the 16S rRNA gene total copy numbers to approximate how many ammonia oxidizing bacteria are present in the activated sludge.

Maximum Substrate Utilization Rate: The final calculation was μ_{Max} which was fitted to the model based on the effluent ammonia data supplied from Brainerd Wastewater Treatment Facility. The data was fit using only the "double peak" oxygen profile. Together with the other components created the final kinetic model as shown in Equation 6. Each variable is described below in Table 1.

Equation 3.6

$$\frac{dS_{NH3}}{dt} = -\mu_{max}\left(\frac{S_{NH3}}{K_{NH3} + S_{NH3}}\right)\left(\frac{S_{O_2}}{K_{O_2} + S_{O_2}}\right)\left(\frac{A_1 e^{\frac{-E_{a1}}{RT}} - A_2 e^{\frac{-E_{a2}}{RT}}}{V_{max}(37.25°C)}\right)(X_{AOB})$$

Equation 3.6 is a combined equation comprised of Equations 3.1-3.5. The μ_{max} term represents the maximum substrate utilization rate. This term was empirically fitted to best align with the annual data at the Brainerd Wastewater Treatment Facility. The terms for μ_{max} and X_{AOB} need to be exchanged depending whether the equation is being calculated using ammonia oxidizing bacteria biomass values derived from qPCR results or using sequencing data.

Other considerations: Ammonia oxidizing archaea (AOA) were not considered for this model yet have demonstrated to contribute to ammonia removal in wastewater treatment plants (5). AOA were present during the 2015 – 2016 sampling period but were not during the 2017 – 2018 sample period. Other models predict the AOB concentration using growth parameters (1,2,6). This was removed from the model in favor of integrating molecular techniques and real-data. Additional parameters were considered such as nitrite inhibition (2) and pH inhibition (6) but were removed since data has not shown significant

fluctuations in either at Brainerd Wastewater Treatment Facility. Finally, most models focus on continuously stirred-tank reactor, or attached growth membrane models, which were not incorporated because they do not represent the treatment facilities conditions (6).

Symbol	Definitional	Value	Units	Source
θ	Hydraulic retention time	2 hours per cycle (8 hours per day)	days	Brainerd WWTP
θ_C	Sludge retention time	Varies	days	Brainerd WWTP
Y	Yield Coefficient	0.48	mg/L biomass/ mg/L BOD	Fitted Parameter
K_d	Death Coefficient	0.15	1/days	Fitted Parameter
K_{NH3}	Half saturation constant	1.35	mg/L	Gao (2010)
K_{O2}	Half saturation constant	0.31	mg/L	Gao (2010)
S_{IN}	Influent BOD	Vaires	mg/L	Brainerd WWTP
S	Effluent BOD	Varies		Brainerd WWTP
S_{O2}	Dissolved Oxygen Conc.	Varies	mg/L	Average Profiles from Brainerd WWTP
S_{IN-NH3}	Inf. Ammonia	15	mg/L	Average for Brainerd WWTP
S_{NH3}	Ammonia Conc.	Varies	mg/L	Calculated from model
μmax_{seq}	Substrate utilization rate	-0.06967	mg-NH3/(L*min)	Derived from sequencing data
μmax_{qPCR}	Substrate utilization rate	-0.12868	mg-NH3/(L*min)	Derived from qPCR data
X	Biomass (MVLSS)	Varies	mg/L	Calculated or Given by Brainerd WWTP
$AOB\%_{Seq}$	Percent Abundance of AOB	Varies	%	(AOB reads/Total reads)
$AOB\%_{qPCR}$	Percent Abundance of AOB	Varies	%	(*amoA* copies/*16S rRNA copies)*
A_1	Pre-exponential factor	2.34E+11	mg/(kg*day)	Stark (1996)
Ea_1	Activation energy	52.9	kJ /mol	Stark (1996)
A_2	Pre-exponential factor	6.49E+11	mg/(kg*day)	Stark (1996)
Ea_2	Activation energy	55.6	kJ / mol	Stark (1996)
Vmax	Maximum rate for Arrhenius Equation	8.950038	mg/(kg*day)	Calculated from original equation

R	Universal Gas Constant	0.008134	kJ/(K*mol)	Davis (2010)

Table 3.1 highlights the variables comprising the model, typical values, units, and the source of the data.

Results:

Throughout the sampling period of 2015 – 2016, the influent wastewater temperature ranged between a high of 20°C and low of 12°C. Based on the model, this impacted the performance between 63% down to 44.5% of the maximum temperature (37.5°C). The decline into winter dropped the performance of the plant by nearly 30%. While temperature fluctuated as a steady decline into winter and rise in spring, other variables such as MLVSS significantly changed throughout the seasons, but more sporadically. The Summer average was closer to 1330 mg/L while Winter was a decline down to 965 mg/L. Other variables such as BOD_{inf}, $BOD_{eff,}$ $AOB\%_{Seq,}$ $AOB\%_{qPCR}$, θ_C, did not appear to significantly fluctuate throughout the season.

Variable Responses: The impact of each variable on the total performance of nitrification is demonstrated in Figure 1. While Brainerd's influent wastewater concentration of ammonia is typically around 35 mg/L, when mixed with activated sludge this concentration diffuses to around 15 mg/L. During the aerobic react cycle, as the ammonia concentration declines from 15 mg/L to the calculated effluent, it is in the highest region of variability from 90% down to 50% by 1.35 mg/L. This impact is shown in Figure 3.1a.

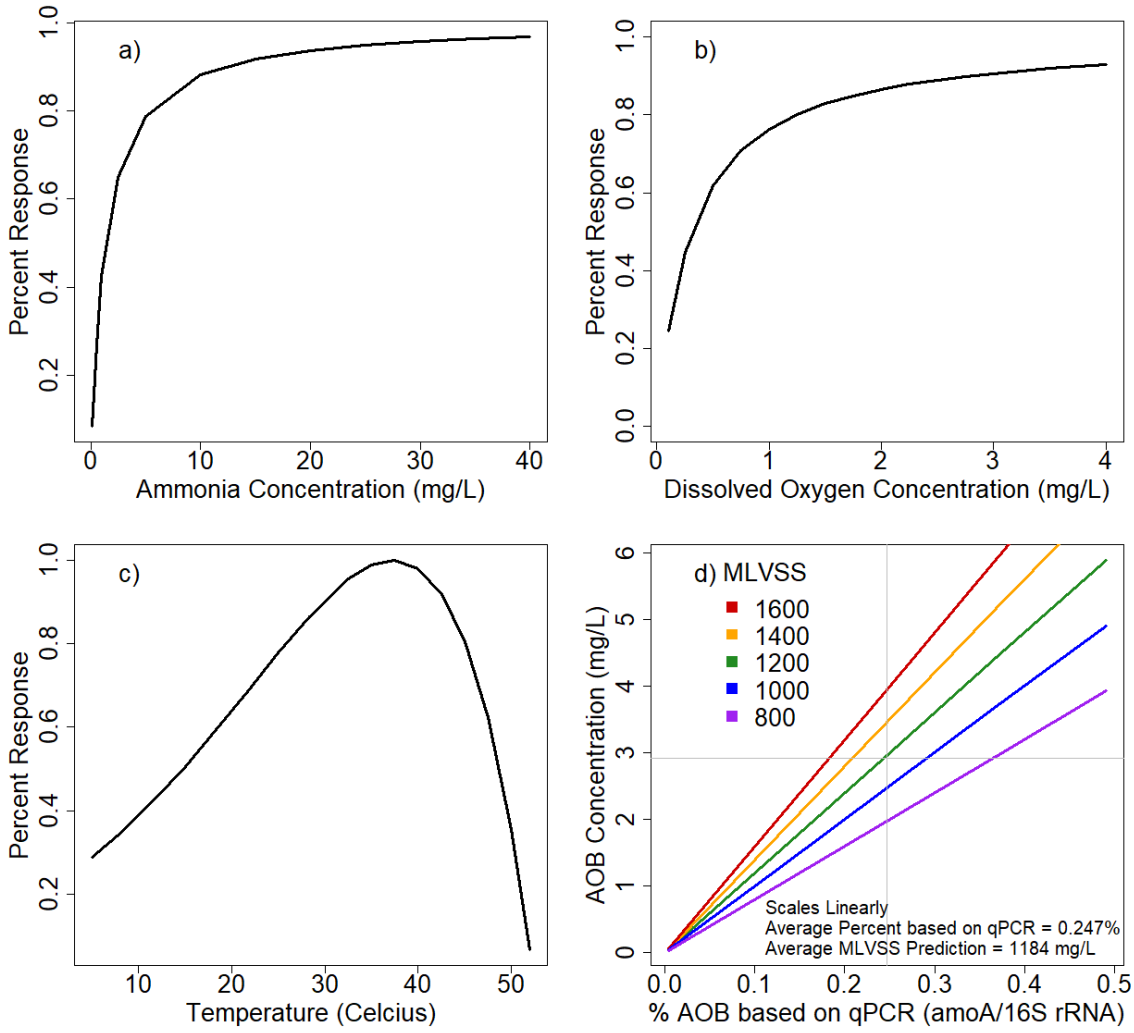

Figure 3.1(a-d) A) The impact of ammonia concentration on the model is shown as a Percent Response where the calculated rate of ammonia degradation is calculated and divided by the maximum degradation rate so that a unitless percentage can be used in the equation. As ammonia is removed from the system the performance exponentially decays. B) The dissolved oxygen concentration impacts the model as a Percent Response. C) A double-Arrhenius equation models the impact of temperature on nitrification performance. While the response is nearly linear between 10-30°C, an significant cut-off occurs after the peak at 37.25°C. D) Select MLVSS concentrations of 1600 mg/L (red), 1400 mg/L (orange), 1200 mg/L (green), 1000 mg/L (blue), and 800 mg/L (purple) are shown in reFlationship to the percentage of AOB detected in the system. The gray lines represent the average based on both MLVSS which is the biomass represented by X (horizontal) and qPCR percent abundance (vertical)

The dissolved oxygen profiles fluctuate between 0.75 mg/L up to 3.5 mg/L. This limits the impact of dissolved oxygen between 71% and 92% change in variable response as shown in Figure 3.1b. Figure 3.2a-d highlights each individual oxygen profile and the impact on dS/dT. While each dissolved oxygen profile (2a) can be shown as impacting dS/dT in Figure 3.2b, ultimately, there is not a statistically significant difference in performance across the dissolved oxygen profiles for summer conditions (2c) and winter conditions (2d). There is a significant difference shown when the dissolved oxygen concentration is held at a constant 3.5 mg/L. In summer this is minimal from ~0.4 mg/L with the profiles down to 0.07 mg/L as a constant dissolved oxygen concentration. In the winter the impact occurs from ~4.1 mg/L based on the profiles down to 3.2 mg/L with a constant dissolved oxygen concentration.

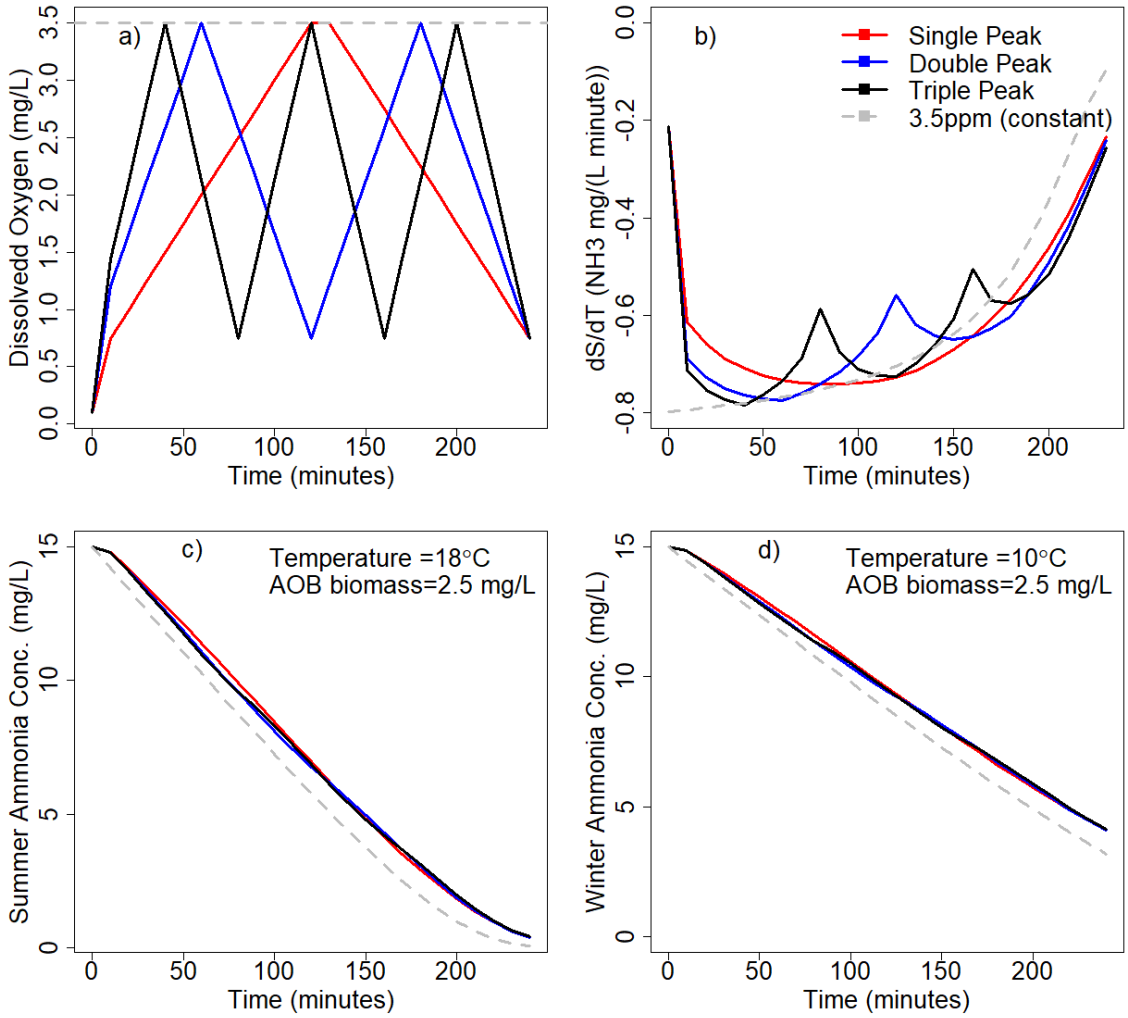

Figure 3.2 (a-d) A) The four dissolved oxygen profiles are highlighted as single peak (red), double peak (blue), triple peak (black), and a constant 3.5 mg/L (gray dash). B) Using a consistent AOB biomass (2.5mg/L) and 18°C, the change in ammonia concentration over 5 minutes is expressed as mg/(L*min). C) The dissolved oxygen profiles are tested using summer temperature conditions (18°C) and 2.5 mg-AOB/L. D) The dissolved oxygen profiles are tested using winter temperature conditions (10°C) and 2.5 mg-AOB/L.

AOB biomass was predicted using both MLVSS and a relative abundance and scaled linearly with the model's calculations as shown in Figure 3.1d. While the relative abundance for both qPCR and sequencing data were scattered (Figure 3.3a), there were no

significant correlations to temperature, MLVSS, nor effluent ammonia. Throughout the year there was no significant trend for variation in either qPCR or sequencing parameters, only a high amount of scatter. The two parameters do show similar trends in data as shown in Figure 3.3b, where they have a significant linear correlation, but with a high scatter (R^2 = 0.19). While the MLVSS was able to represent what the treatment plant recorded (Figure 3.3c), the incorporation of AOB biomass generated unpredictable trends (Figure 3.3d) and large variations in AOB biomass.

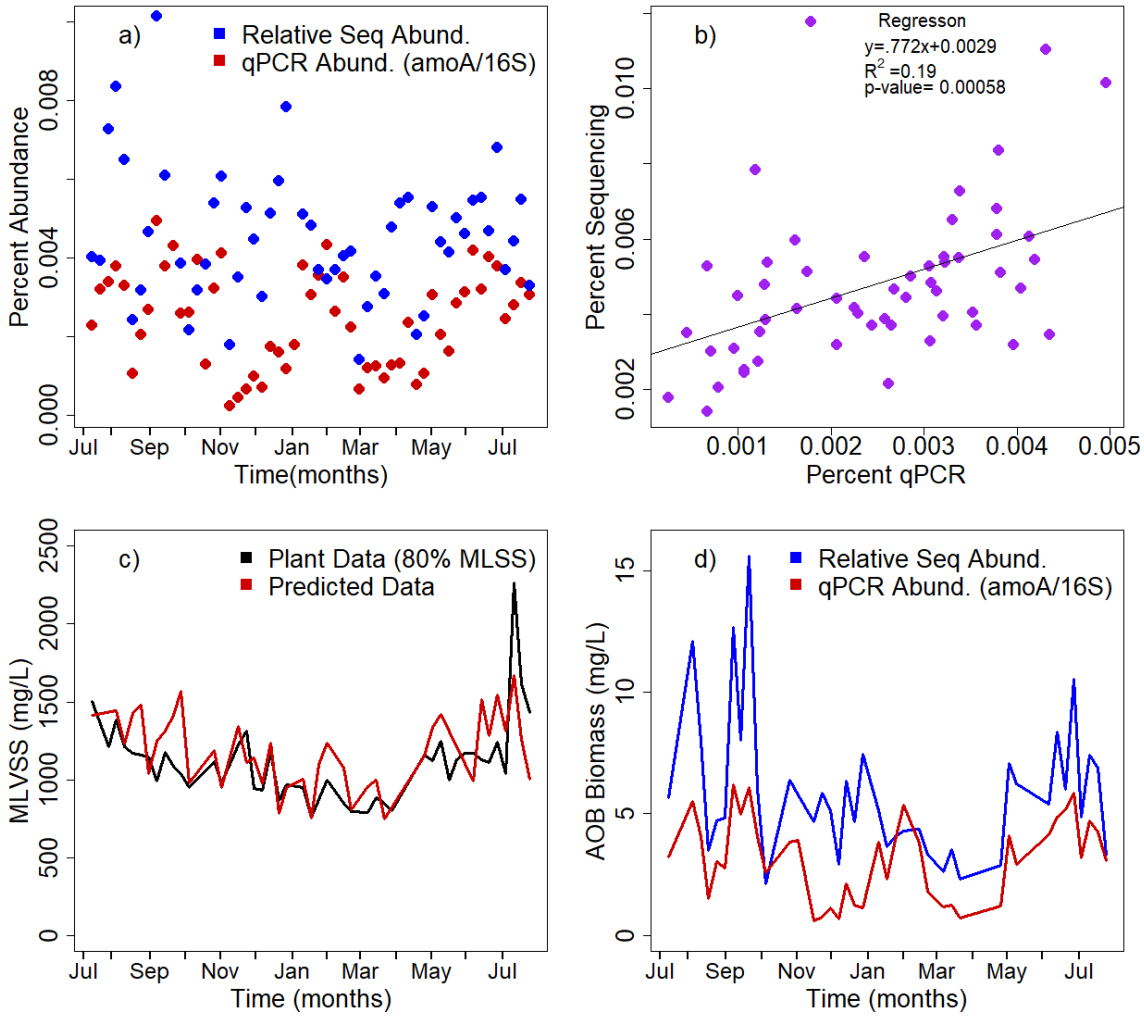

Figure 3.3 (a-d) A) The percent abundance of ammonia oxidizing bacteria both sequencing data (blue) and qPCR data (red) is shown throughout the year. While neither significantly change over time or temperature, they both experience large week-by-week fluctuations. B) The Sequencing Data and qPCR Data are statistically significantly linear ($p<0.05$) but have weak correlation $R^2= 0.19$. C) Using the recorded data from Brainerd Wastewater Treatment Plant's SRT, HRT, and BOD data, the model's MLVSS was predicted (red) and correlated similarly to the actual plant data (black). D) Combining the predicted MLVSS (Fig. 3c) with the two AOB percent abundance metrics, the final AOB concentration is determined using sequencing data (blue) and qPCR data (red).

Overall the plants performance was calculated and compared against the actual data from Brainerd Wastewater Treatment Facility as shown in Figure 3.4. Both models demonstrated the decline in performance during the winter, but also predicted several other lapses in treatment. The qPCR data predicted two majors lapses in nitrification activity in December and again in March but did not during January and February. The sequencing data only had one large lapse in performance starting in January throughout May.

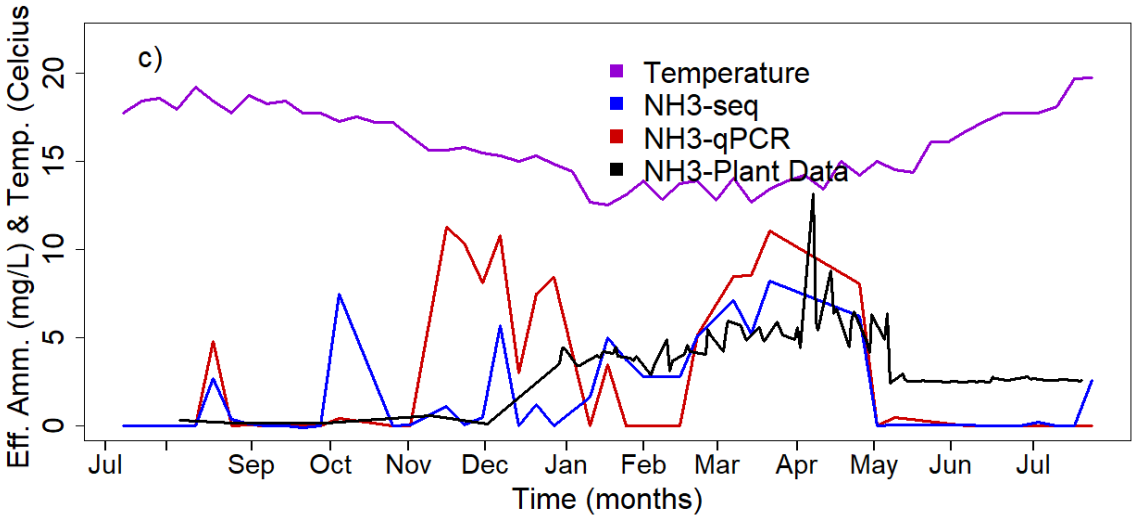

Figure 3.4 shows the trends of the predicted model, actual plant data, and temperature. The effluent ammonia concentration is predicted using sequencing data in blue, using qPCR data in red, while the actual plant data is shown in black. The temperature (purple) experiences a gradual decline from 19°C down to ~12°C in the winter before warming up again.

The necessary AOB biomass to consistently have an effluent ammonia concentration of 1 mg/L was back calculated. Using the substrate utilization rate from sequencing (μmax_{seq}), and assuming the final ammonia concentration was 1 mg/L, the biomass was predicted between 5 and 25°C. This ranged from an AOB biomass of 4.34 mg-AOB/L down to 1.61 mg-AOB/L in peak conditions. The results are shown in Figure 3.5.

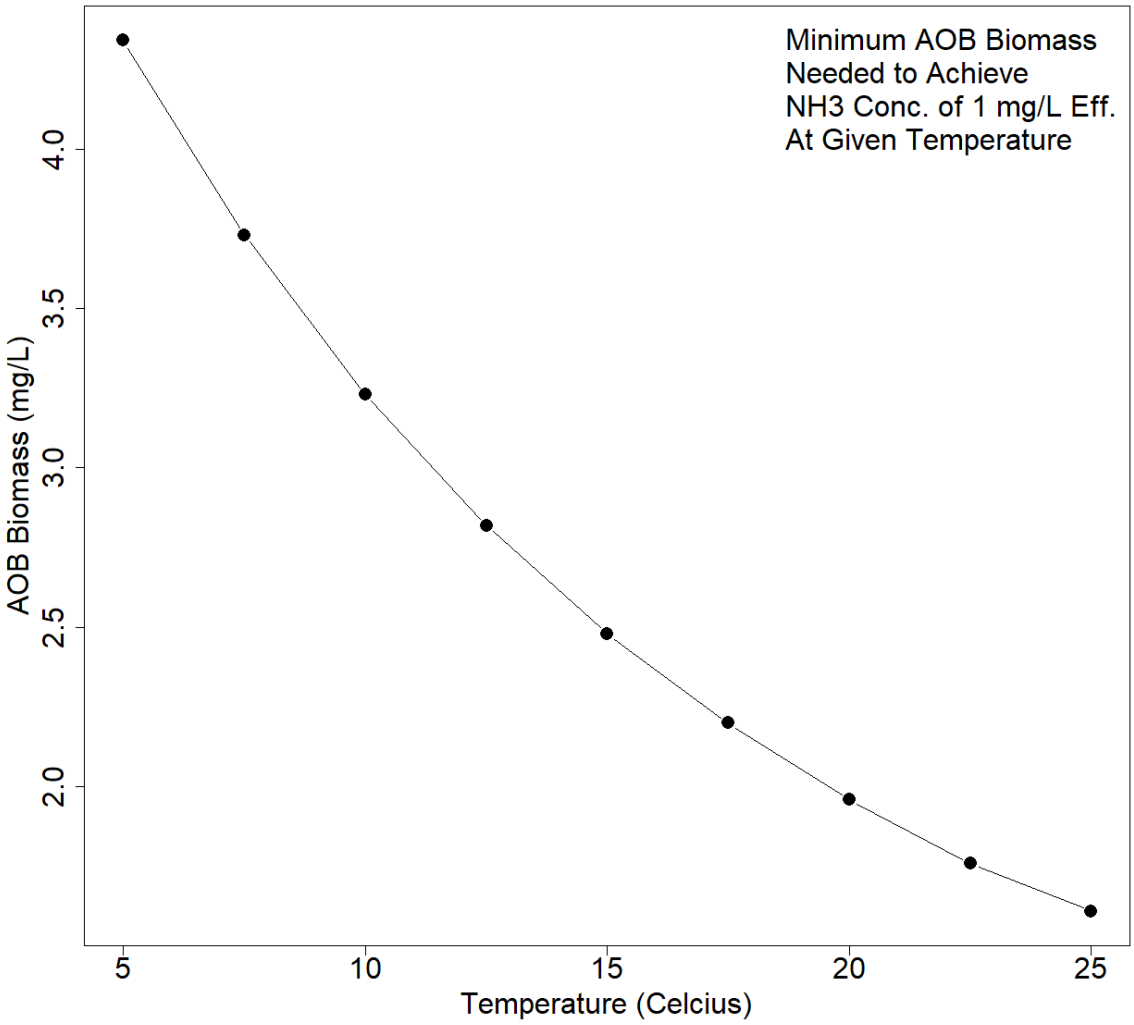

Figure 3.5 The necessary AOB biomass to achieve year-round effluent quality of 1mg/L was back calculated. As the temperature declines and nitrification becomes less kineticially feasible, more AOB biomass is necessary to achieve the same quality in higher temperatures.

Discussion:

Dissolved Oxygen Profiles: While the dissolved oxygen profiles do vary, ultimately there is little effect on the nitrification activity. Each profile; single double, and triple peak, performs almost identically throughout the different seasons. Future models for these sequencing batch reactors might not need to incorporate dissolved oxygen as a significant factor and can account for other variables which ultimately increase value to the precision of the model. There remains potential that these dissolved oxygen profiles impact heterotrophic growth, and change the MLVSS, but this is not accounted for in this model.

Biomass Prediction: While total biomass expressed as MLVSS was able to be predicted with similar trends to the actual data from Brainerd, the inclusion of both sequencing data and qPCR data ultimately hinders the model. The qPCR data is exceptionally problematic since small changes in either *amoA* or *16S rRNA* concentrations create major precessions in the model. There is potential that the qPCR primers are too specific and are not fully capturing the diversity of ammonia oxidizing bacteria in the wastewater treatment plant. This could explain the high variability of nitrification performance this predictor demonstrates. Similarly, the sequencing data only targets known ammonia oxidizing bacteria. Other bacteria may be contributing to ammonia oxidation which were not included in the model causing unpredictable shifts in performance. Ultimately, the concentration of MLVSS might be a stronger predictor for nitrification performance than incorporating new scientific tools to account for AOB biomass.

Substrate Concentration: Using the same amount of biomass (2.5 mg-AOB/L) at two temperatures (18°C & 10°C) the time to achieve an effluent ammonia quality of 1

mg/L was calculated. The model predicted approximately 107 minutes at 18°C and 165 minutes at 10°C. Since the current total aerobic reaction time is only 120 minutes, the operators would need to continue aerating for an additional 45 minutes to continue the same effluent ammonia quality. Presently, the treatment plant does have some allocated idle time after the previous reaction cycle decants. This could be an opportunity to increase the aerobic reaction period an additional 30 minutes. Having a reaction time of 150 minutes would achieve approximately 1.9 mg/L effluent ammonia. This is still a significant decrease in ammonia from the predicted 4.3 mg/L at the current 120 minute aerobic react.

Ideal AOB Biomass: The lowest temperature Brainerd Wastewater Treatment Facility typically experiences are 10°C. To maintain consistent removal (1mg/L of ammonia), Figure 3.5 suggests at least 3.23 mg-AOB/L. However, the wastewater operators previously ran higher MLVSS activated sludge systems (MLSS > 2,500 mg/L) and still experienced seasonal issues. After years of operation, they've experienced less seasonal nitrification failure by lowering MLVSS in the winter, which is against conventional logic and the model's predictions. There may be other variables which effect nitrification that have not previously been recorded.

Conclusion:

Creating a model helps predict the impact of various factors in the wastewater treatment plant. Ultimately, the unique dissolved oxygen profiles did not significantly impact the effluent ammonia concentration. Temperature, total biomass (MLVSS) appear to be the two largest model predictors for effluent ammonia concentration. Integrating additional datasets such as sequencing data and qPCR created heightened complexity which ultimately hindered the model's ability to accurately predict the effluent ammonia concentration. Finally, there is an opportunity for the treatment plant to increase the aerobic reaction time or maintain a consistent 3.5ppm of dissolved oxygen for increased removal efficiency.

Chapter 4

Seasonal Activity and Community Composition Shifts in Full-Scale Activated Sludge Sequencing Batch Reactors

Importance

Sequencing batch reactors are a common design for wastewater treatment plants, particularly in smaller municipalities due to their low footprint and ease of operations. However, like most treatment plants in temperate/continental climates, the microbial community involved in water treatment is highly seasonal and their biological processes can be sensitive to cold temperatures. The seasonality of these microbial communities has been explored primarily in conventional treatment plants, but not in sequencing batch reactors. Furthermore, most studies often only address "which organisms are present?". However, the activated sludge microbial community is very diverse that it is often hard to discern which organisms are "active" and which organisms are simply "present". In this study we are applying additional sequencing techniques to also address "which organisms are active?" and "which organisms are growing?" By addressing these three questions, we gain new insights into seasonal microbial populations dynamics and activity patterns affecting wastewater treatment.

Synopsis

Activated sludge is comprised of diverse microorganisms which remediate wastewater. Previous research has characterized activated sludge using 16S rRNA gene amplicon sequencing which can helps to address questions about the relative abundance of microorganisms, regardless of cells being active, inactive, or dead. In this study we use 16S rRNA amplicon transcript sequencing in order to characterize "active" populations (via protein synthesis potential) and gain a deeper understanding of microbial activity patterns within activated sludge. Seasonal abundances of individual populations in activated sludge change over time, yet a persistent group of core organisms remains throughout the year which are traditionally classified on presence or absence without monitoring their activity or growth. The goal of this study was to further our understanding of how the activated sludge microbiome changes between seasons with respect to population abundance, activity, and growth. Triplicate sequencing batch reactors were sampled in 10-minute intervals throughout reaction cycles during all four seasons. We quantified the gene and transcript copy numbers of 16S rRNA amplicons using real-time PCR and sequenced the products to reveal community abundance and activity changes. We observed significantly different compositions when comparing 16S rRNA genes and transcripts for every season. Further investigation revealed 108 OTUs with stable abundance, activity, and growth throughout the year. Non-proliferating OTUs were commonly human-health related, while OTUs that showed seasonal abundance changes have previously been identified as being associated with floc formation and bulking. We observed significant differences in 16S rRNA transcript copy numbers, particularly at lower temperatures which lasted until the activated sludge community had acclimated to

warmer water temperatures again. Ultimately, this study provides an in-depth seasonal analysis of the activated sludge microbiome and is one of the first investigations into the seasonal dynamics of microbial activity variations based on quantifying and sequencing 16S rRNA transcripts.

Introduction

The activated sludge process is a biological nutrient removal process in wastewater treatment plants (WWTP) relying on taxonomically and metabolically diverse microbial consortia of which the majority of microorganisms have yet-to-be cultured and are carrying out unknown functions(1). Understanding seasonal dynamics and activity of individual microbes in this complex community is paramount to future sustainable nutrient management and economic wastewater treatment(2). Activated sludge is dependent on specific core microorganisms to obtain desired process outcomes. The activated sludge microbiome has been extensively studied(3-13) and facilitated development of an ecosystem-specific reference database(14). However, activated sludge is dependent on physiological activity of specific microbial functional groups, hence it is essential to combine information on microbiome taxonomy and classification with phenotypic information on the physiological state of identified microbial populations.

16S rRNA gene amplicon sequencing is the standard method for identification, characterization of the diversity, composition, and dynamics of microbial communities. However, most sequencing studies are based on amplifying rRNA genes from environmental DNA extracts. Environmental DNA extracts contain DNA from active cells, inactive but viable cells, dormant cells, as well as extracellular DNA from degraded or lysed cells. Therefore, analyses based on environmental DNA presents a one-sided view of the community structure lacking information on the metabolic state of microbial populations(15). In contrast environmental RNA provides a more immediate view on microbial activities because RNA has a rapid turnover rate within cells(16) and a shorter half-life than DNA(17). Thus, sequencing reverse transcripts (cDNA) of 16S rRNA is more

representative of the 'active' fraction of the total microbial community(18). The number of sequencing tags of a specific taxon in an RNA-based 16S rRNA library relative to DNA-based 16S rRNA gene library can be used as a measure of potential activity. Therefore, parallel sequencing and comparison of 16S rRNA amplicon libraries based on RNA and DNA can help to: 1) reveal shifts in activity patterns among rare and abundant taxa; 2) identify populations in the activated sludge community changing their physiological state during different SBR cycles; and allow new insights into seasonal variations in physiological states of core members of the activated sludge community.

This approach has been used in previous studies of microbiomes in soils and lakes and provided the basis for generating and testing hypotheses on the complex interplay of microbial community structure and activity(19-24). While ribosomal RNA as measure of microbial activity has limitations(18), ribosomal RNA is a critical component required for protein synthesis. The ratio of 16S rRNA transcripts and 16S rRNA gene amplicons of a specific taxa can therefore serve as proxy of potential for *de novo* protein synthesis.

Previous studies have reported the activated sludge core community (4-11) mostly based on the abundance and occurrence frequency of OTUs. Griffin et al., reported on a core microbial community of 134 OTUs across six wastewater treatment plants in the Midwest of the United States. The core community they observed was also highly synchronous by season(7). Saunders et al. analyzed the microbial community composition of 13 wastewater treatment plants in Denmark. They identified 63 core genus-level OTUs, and found numerous OTUs in the influent wastewater which seemed to continuously seed the activated sludge microbial community (10). Interestingly Saunders et al. reported that *Nitrotoga* were the dominant nitrite-oxidizing bacterial taxa in their analyzed systems,

while many other published studies on the activated sludge microbial community hypothesized that the *Nitrospira* is a ubiquitous taxa of nitrite-oxidizing bacteria across global wastewater treatment plants (4). A study by the Global Water Microbial Consortium notes 28 core OTUs which were prevalent in most wastewater treatment plants across the world and considered core OTUs to be prevalent in over 80% of the wastewater treatment facilities worldwide. While speculations on the existence of a global core activated sludge microbiome are intriguing it also raise questions as to why there are consistent deviations from the global activated sludge microbiome consensus (3, 4, 10) and what causes these alterations in microbial community assembly..

For the WWTP under investigation in this study we have also previously reported on the core community by sequencing and comparing the occurrence and abundance of 16S rRNA gene amplicons from three parallel sequencing batch reactors (SBR) sampled weekly over a year(3). This study focused on OTUs which correlated to both season temperature variations and nitrification performance which drastically declined during cold temperatures despite annual stability in abundance amongst the ammonia oxidizing community. We reported 114 OTUs which were consistently present in the SBRs and classified these OTUs as the core microbiome. While all these previous studies have expanded our understanding of the diversity of activated sludge, many of the identified taxa are not known or have not been characterized with respect to metabolic function and physiological role in wastewater treatment. This issue is discussed in the Microbial Database for Activated Sludge (MiDAS) field guide which specializes in curation of microorganisms performing important functions in WWTPs(14). We therefore decided to evaluate if 16S rRNA transcript sequencing alongside routine DNA-based 16S rRNA gene

amplicon sequencing and absolute quantification of microbial biomass by quantitative PCR can inform and guide the identification of process-relevant 'key players' in diverse activated sludge 'core' microbiomes. Here we report how this approach helped us to identify core OTUs not only present, but also active and proliferating in the dynamic environment of SBRs.

In order to expand the 'core' microbiome definition with these new criteria, we set out to analyze how the activated sludge microbiome fluctuates across seasons and reactor cycles. Seasonal data have the potential to reveal compositional changes influenced by plant operational and environmental parameters such as seasonal temperature changes. Using full-scale SBRs enables observations across hydraulic residence times which are only observable by batch and plug-flow reactors, but not in continuously-stirred tank reactors(25). Throughout seasons and reactor cycles we sequenced the 16S rRNA gene as marker gene for composition and 16S rRNA transcripts which serve as a proxy for the protein synthesis potential(18). Additionally, the 16S rRNA transcript copy numbers were quantified using reverse transcription quantitative PCR at different reactor cycles to discern overall variations in protein synthesis potential. Our data provides insight into the activity and composition of the activated sludge community between seasons and helps to identify seasonal variations in activity profiles among taxa. This study presents a comprehensive analysis of the activated sludge microbiome comparing three parallel full-scale SBRs. We are describing activated sludge community shifts comparing inflow and different reactor cycles based on 16S rRNA gene and 16S rRNA transcript amplicon sequencing. Further we performed our analysis on a WWTP in a continental climate which undergoes strong seasonal temperature variations (3). This allowed us to compare samples collected during

the four seasons with respect to community shifts and plant performance parameters. By combining DNA and RNA amplicon sequencing and quantitative (RT-)qPCR, we gain insights into the assembly and seasonal shifts of the activated sludge community. We outline new criteria for analyzing activated sludge ‘core’ microbiomes, comprising presence, activity, and growth. Our approach can further inform researchers on the importance and role of many yet-to-be-cultured and uncharacterized taxa in activated sludge.

Materials and Methods

Wastewater Treatment Plant

Brainerd Wastewater Treatment Facility has three full-scale SBRs averaging six-hour long cycles. Typically, one hour of static filling (SF), one hour of mixed fill (MF), 2 hours of aerobic react cycle, one hour of settling, and one final hour for decanting, wasting excess activated sludge, and sitting idle. The final hour for decanting, wasting sludge, and idle was not sampled. The program is set to fill the reactor up to a third influent wastewater, and two thirds activated sludge before beginning the reaction cycle. Additional details of the plant configuration and standard operations are described in Johnston, 2019(3).

Sample Collection

Sample trip occurred within 10-days at the start of each season (July 1st, 2017, October 3^{rd,} 2017, December 27th, 2017, and March 27th, 2018). Samples were collected every 10-minutes from each SBR cycle. The SBRs are equipped with a faucet which draws from an individual reactor. These faucets were used to collect samples from the reactors. The faucets were drawn for at least 30-seconds to ensure a fresh sample not idle in the pipes.

Five minutes prior to settling, we collected 20 liters of activated sludge in a carboy to simulate the settling occurring in the reactor. From the carboy, samples were collected from the settled sludge at the bottom using the carboy's spigot valve, while grab samples were collected from the top half to represent decanted wastewater.

Sample aliquots in 2ml microcentrifuge tubes were rapidly frozen to approximately -72°C in a bath of dry ice and ethanol. No RNA stabilization solutions were used since

preliminary testing determined them to be less consistent than rapid freezing (data not shown). Samples were stored in -80°C and thawed prior to nucleic acid extractions or chemical analysis.

The transcriptional response for 16S rRNA were quantified at every time interval. The 16S rRNA gene quantities were only quantified at select times. These time points represent the midpoint for Static Fill (30min), Mixed Fill (80min), the beginning of React (140min), the ending of React (220min), and the midpoint time for the decanted and settled sludge during Settling (270min). These six time points, for the triplicate reactors, across the seasons, were used for 16S rRNA amplicon sequencing analysis to compare the 16S rRNA transcript and the 16S rRNA gene abundances. These time points will be abbreviated as SF (Static Fill), MF (Mixed Fill), R1 (React 140 minutes), R2 (React 220 minutes), SS (settled sludge), and DW (decanted water) troughout the remaining manuscript.

Nucleic Acid Extraction and Reverse Transcription

Frozen samples were centrifuged for 5 minutes at 13 000 g to thaw, then resuspended and transferred into lysis buffer for either DNA or RNA extraction. Cells were disrupted using the FastPrep-24 5G Homogenizer (Santa Ana, CA) for 40 seconds at 6m/s. The DNA extractions were performed using 50µL of homogenized sample and followed the protocol for the MP BIO FastDNA™ Spin Kit for Soil (Santa Ana, CA).

RNA extractions were performed using 250µL of sample following the protocol for Quick-RNA Fecal/Soil Microbe Microprep Kit by Zymo Research (Irvine, CA). During the final step to elute RNA from the filter, 50µL of DNAse/RNAse Free water was used to create aliquots of the extracted RNA. After RNA extraction, DNA was removed using the

TURBO DNA-*free*™ Kit from Invitrogen (Carlsbad, CA). The incubation of the DNase enzyme was increased from 30 to 40 minutes before inactivation to ensure removal of residual DNA. Finally, reverse transcription was performed using PrimeScript RT-PCR Kit from Takara (Kusatsu, Japan). The incubation step was increased from 15 to 20 minutes before inactivation to ensure reverse transcription completed. During protocol development, each step was confirmed using qPCR/RT-qPCR for two functional genes (16S rRNA and *amoA*) as well as DNA and RNA high sensitivity fluorometric assays on a Qubit 4 Fluorometer by Invitrogen (Carlsbad, CA) as shown in the supplemental (Figures S4.1-S4.3).

qPCR and RT-qPCR

Quantification was performed on a Bio-Rad CFX Connect Real-Time PCR Instrument (Hercules, CA). Each reaction contained 10µL of PCR Grade Water (Ambion Inc; Foster City, CA), 12.5µL of 2X SsoFastTM EvaGreen® Supermix (Bio-Rad Laboratories; Hercules, CA), 1.25µL of 10mg/L bovine serum albumin solution (Millipore Sigma; St. Louis, MO), 0.5µL of forward primer (0.5µM), 0.25µL of reverse primer (0.5µM), and 0.5µL of template (c)DNA. The primer set used targeted the 16S rRNA genes/transcript (V3 region 338-F CCTACGGGAGGCAGCAG and 518-R ATTACCGCGGCTGCTGG(26)) served as proxy for total biomass and protein synthesis capability. For statistical analysis, when a value fell below the detection limit after repetitive attempts, a value of half the detection limit was used(27). The average amplification standard had an efficiency of 92.9% ± 6.9% and R^2 coefficient of 0.968 ± 0.041.

Sequencing and Data Analysis

Sequencing was performed by the University of Minnesota's Genomic Core using V1-V3 primers for 16S rRNA based under conditions in Johnston 2019(3, 28). Sequencing analysis was performed using DADA2 in RStudio(29, 30). Default settings were used unless noted with *truncLen=c(290,270)* to remove low quality ends. Reads under 200 base-pairs were removed (*minLen=c(200,200))*. Additional settings were *maxMismatch=1* and *minOverlap=20*, which forces merges only ≥20 overlapping base-pairs with 1 mismatching base-pair. The distribution of sample reads is shown in Figure S4.4.

Operational taxonomic units (OTU) referenced SILVA rRNA SSU 132(31) at the 97% cutoff. DADA2 classified 1 002 genus-level. The average sample finished with 44 601 ± 18 580 merged reads. Seven samples poorly amplified, with a total of less than 1 000 reads and were removed from the dataset (Table S4.1).

Statistical Analysis

Statistical analysis and graphing was performed using RStudio version 3.6.0(29). Bray-Curtis dissimilarity was performed using the *vegan* package to calculate the distances and percent variance explained(32, 33). Adonis tests were used to determine the significance of ordination clusters. ANOVA and regression analysis were used to determine the relationship between transcript abundances over time. Student T-Tests were used to determine significant differences across gene/transcript quantifications.

Consistent Core Microbiome Requirements

The three criteria we developed are to determine the most stable organisms in abundance, activity, and growth. 1) Abundant OTUs are detectible each season (using an average of R1 and R2 for the three SBRs) and did not vary in relative 16S rRNA gene

sequence abundance more than 1-log across all seasons. 2) Active OTUs are detectible each season (using an average of R1 and R2 for the three SBRs) and did not vary in 16S rRNA transcript relative abundance more than 1-log across all seasons. These 1-log cutoffs were selected because microbial growth and diversity is log-normally distributed where meaningful changes occur over logarithmic increments (34). Additionally, we are using these 1-log cutoffs since previous works that focus on OTUs have shown that OTUs significantly correlate the temperature by following a similar frequency to temperature's seasonal sine-wave pattern, regardless of the amplitude of the actual temperature change. This study focuses on the variations in large changes in amplitude of seasonal OTUs by selecting a 1-log cutoff to be applied to log-transformed data(35, 36). 3) Growing OTUs measured a >1-log increase in absolute abundance when comparing the influent wastewater to the activated sludge community (using an average of R1 and R2 for the three SBRs). The absolute abundance was calculated by multiplying the relative 16S rRNA gene sequence abundance bythe total 16S rRNA gene copy number obtained by qPCR for each of the sampled sequencing batch reactior cycle phases. A more detailed equation and explanation can be found in the supplemental materials (Equation S1).

Data availability

Sequences are available from the NCBI Sequence Read Archive with accession number PRJNA591266.

Results:

Plant Performance

Data records provided by Brainerd Wastewater Treatment Facility were used to tabulate average plant operational parameters and performance metrics during a 30-day period around each of the four sampling dates (Table 4.1). Temperatures, and volumetric flow rates were measured daily (n=30 per month) whereas other parameters were measured three times per week (n=12 per month). Both influent water temperature, and air temperature were statically different across seasons. The influent and effluent wastewater volume in fall was significantly higher than other seasons, likely due to tourism in the area. The chemical composition of the influent wastewater remained highly similar and did not significantly change for most parameters over the seasons. An exception were the effluent ammonia and total suspended solids concentrations. Total suspended solids appear to have higher concentrations in the summer and fall. However these data points seemed to be largely driven by outlier datapoints of very high concentrations measured just once per month (612 mg/L in summer and 1073 mg/L in fall). We decided to not remove these datapoints since they are public records recorded by the wastewater operators. Suspended solid concentrations peaked always after our sampling days and were unlikely to impact our results. Effluent ammonia was only measured once per month, and therefore statistical inferences could not be made. We have previously shown detailed annual changes in effluent ammonia, which is known to be significantly impacted during cold temperatures in what is referred to as seasonal nitrification failure(3).

	Summer '17	Fall '17	Winter '17	Spring '18
Sample Date	July 1st, 2017	October 3rd, 2017	December 27th, 2017	March 27th, 2018
Inf. Water Temp. (°C)	17.53 ± 0.51	15.93 ± 0.91	13.89 ± 0.90	11.56 ± 0.58
Air Temp. Range (°C)	13.3 to 27.8	11.7 to 16.1	-33.9 to -20.6	-18.8 to -8.1
Influent (m^3/day)	9 774 ± 318	12 911 ± 1 591	9 956 ± 409	9 410 ± 364
Effluent (m^3/day)	8 910 ± 455	12 547 ± 1 818	9 138 ± 591	8 638 ± 409
Inf. BOD5 (mg/L)	175 ± 52	167 ± 64	139 ± 48	164 ± 29
Eff. BOD5 (mg/L)	2.00 ± 0.00	1.23 ± 0.60	1.33 ± 0.49	1.75 ± 0.27
Inf. TSS (mg/L)	338 ± 138	378 ± 261	169 ± 52	263 ± 47
Eff. TSS (mg/L)	2.83 ± 1.34	2.85 ± 2.41	1.92 ± 0.67	2.92 ± 1.38
Inf. Phos. (mg/L)	4.87 ± 0.44	3.58 ± 0.67	5.08 ± 0.30	5.51 ± 0.47
Eff. Phos (mg/L)	0.20 ± 0.06	0.33 ± 0.23	0.15 ± 0.06	0.18 ± 0.02
Eff. NH3 (mg/L)*	0.10	0.10	4.12	9.43
MLSS (mg/L)	1 378 ± 166	1 335 ± 152	1 165 ± 219	1 092 ± 167

*Values only recorded once per month. Date closest to sampling trip was used.

Table 4.1 features seasonal operational conditions and performance metrics for the sample trips taken throughout 2017-2018. The data presented is an average of a 30-day window around the sample period. The influent water and air temperatures, and flowrates, had periods of statistically significant differences compared to other seasons. Other than effluent ammonia, typical effluent operational performance metrics for biological oxygen demand, phosphorous, and total suspended solids did not statistically vary throughout the seasons.

Quantification of 16S rRNA Transcript and 16S rRNA Gene Abundance during Reactor Cycles

We quantified 16S rRNA transcript abundances during the reactor cycle at 10-minute intervals at all four seasons (Figure 4.1). The average 16S rRNA transcript abundances (log(transcripts/mL)) during the SF was 11.4±0.5 in summer, 13.4±1 in fall, 11.7±1 in winter and 11.9±0.5 in spring. When the influent wastewater and activated sludge were mixed during MF, the 16S rRNA transcript abundances (log(transcripts/mL)) reached 12.3±0.7 in summer, 13.8±0.3 in fall, 12.5±0.9 in winter, and 12.5±0.4 in spring. The mixing led to statistically significant increases in 16S rRNA transcript abundances in

summer, winter, and spring (all $p<0.05$) while transcript abundance in fall remained constant ($p=0.12$). During the 2-hour long aerobic react cycle (R1&R2) the average 16S rRNA transcript abundances (log(transcripts/mL)) were 11.9±0.9 in summer, 13.7±0.5 in fall, 11.5±0.9 in winter, and 12.9±0.4 in spring. At the onset of aeration, the samples collected in winter experienced a statistically significant decline in 16S rRNA transcript abundance ($p<4.5e-5$). During the aerobic react cycle, 16S rRNA transcript abundances in the summer were significantly lower than in spring ($p<1.8e-5$), but higher than in the winter ($p<0.025$). During settling, the bottom sludge (SS) averaged 16S rRNA transcript abundances (log(transcripts/mL)) of 13.2±0.5 in summer, 14.5±0.4 in fall, 13.1±1.0 in winter, and 12.9±0.3 in spring. In the supernatant water we quantified 16S rRNA transcript abundances (log(transcripts/mL)) of 11.1±1.1 in summer, 12.3±0.8 in fall, 11.3±0.8 in winter, and 10.9±0.8 in spring.

The 16S rRNA gene abundance did not show any statistically significant seasonal differences when comparing different reactor cycles. The average 16S rRNA gene abundances ranged from 8.6±0.2 log(genes/mL) during SF to an average of 9.6±0.42 log(genes/mL) during MF, R1, and R2.

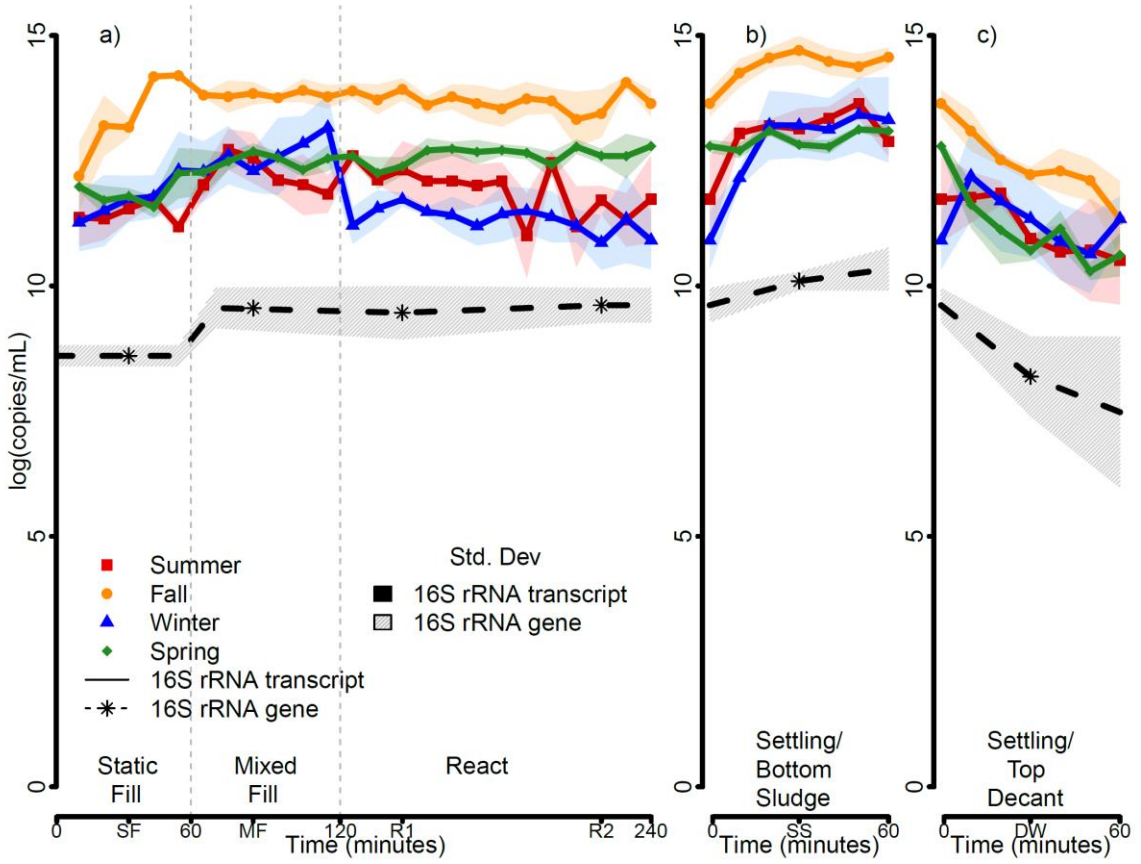

Figure 4.1 The activity of the influent wastewater and activated sludge community is shown for each season and throughout the reactor cycle in 10-minute intervals. Figure 4.1a shows the SF, MF, R1 and R2 cycles, while Figure 4.1b&c timepoints occur simultaneously, as the activated sludge settles (SS) to the bottom(6b) and decants (DW) from the top (6c) of the reactor. The quantitative abundance of 16S rRNA transcript (solid lines) are shown by season (summer in red squares, fall in orange circles, winter blue triangles, and spring green diamonds). The solid hatch represents the standard deviation for the 16S rRNA transcript. The dashed line and dashed gray hatch represent and average abundance of 16S rRNA genes throughout the year, which do not significantly change with respect to seasons. The transcript abundances in the fall are continuously significantly higher transcript copy numbers for 16S rRNA, while the other seasons remain relatively comparable at different stages. Each season experiences a significant increase in transcripts once the activated sludge is mixed with the influent wastewater, followed typically by a period of stabilization throughout the reaction cycle. Winter experienced a significant decrease in 16S rRNA transcripts at the onset of aeration. Settling causes an increased concentration of activity in the thick bottom settled sludge while the decant significantly declines before moving on in the treatment process.

Beta Diversity Analysis

In Figure 4.2a, PC1 (x-axis) represents 38.2% of the total variance explained and separates the inflow community (SF) from activated sludge samples. PC2 (y-axis) represents 17.3% of the total variance explained and separates 16S rRNA gene sequences and 16S rRNA transcripts. Within PC2, we also observed separation of the seasons within the activated sludge compositions. The 16S rRNA gene and 16S rRNA transcript compositions were most different comparing fall and spring. The activated sludge 16S rRNA transcript community composition in winter and summer overlapped, however their season's 16S rRNA gene community compositions did not.

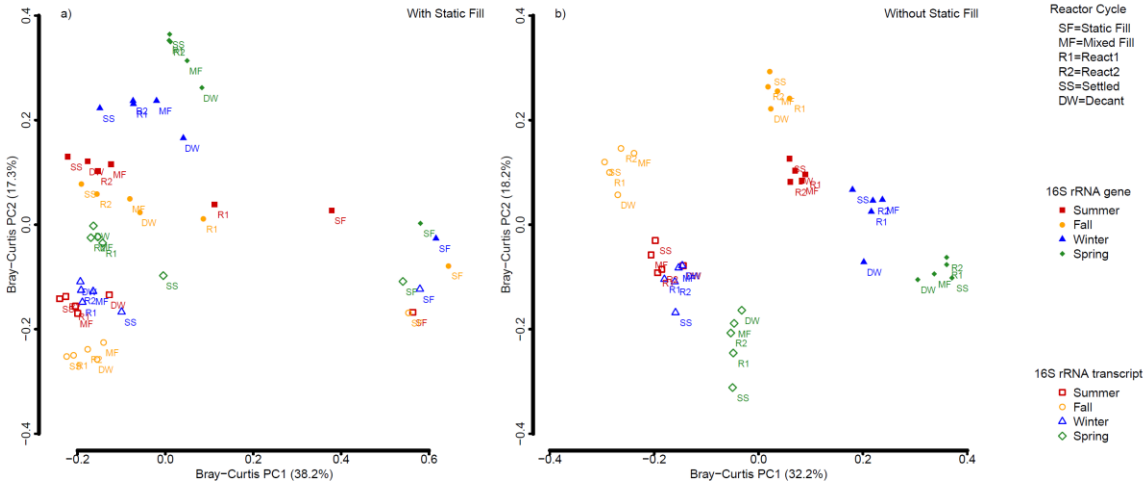

Figure 4.2 Principle coordinates analysis was used to compare trends in reactor cycles, the community composition and expression, as well as seasonal trends. Figure 4.2a highlights the difference between the influent wastewater and the activated sludge community. Figure 4.2b removes the static fill to represent the distinct separation of 16S rRNA genes and 16S rRNA transcripts in the activated sludge over the x-axis, while the seasons are separated on the y-axis. The 16S rRNA gene is represented by the closed shapes, while the 16S rRNA transcript is denoted by the open shapes. Summer

is represented by red squares, fall by orange diamonds, winter by blue triangles, and spring by green diamonds. The acronyms correlate to the six reactor cycles sequenced in the study.

We removed SF data and recalculated dissimilarity to emphasize differences within the activated sludge composition throughout reactor cycles (Figure 4.2b). PC1 (x-axis) represents 32.2% of the total variance explained and separates the 16S rRNA gene communities from the 16S rRNA transcripts. PC2 (y-axis) represents 18.2% of the total variance explained and shows separation of communities by season. The activated sludge 16S rRNA transcript compositions from winter and summer overlapped, however their 16S rRNA gene community composition did not. Additional dissimilarity analysis was performed to separate the 16S rRNA genes from the transcripts in order to determine if further trends in separation across specific reactor cycles would become apparent (Figure S4.5). In Figure S4.5a, PC2 (y-axis) showed a slight separation of the DW samples from the other reactor cycle's 16S rRNA gene compositions.

Seasonal Shifts of 16S rRNA Gene and Transcript Community Composition

Figure 4.3 compares the log-ratio of the relative abundance of individual OTU's between seasons based on 16S rRNA genes (x-axis) and 16S rRNA transcripts (y-axis). OTU distribution along the x-axis denotes log-fold change in relative abundance of 16S rRNA genes between seasons. Distribution along the y-axis indicates log-fold change in relative 16S rRNA transcripts abundance of induvial OTUs when comparing activated sludge samples from different seasons. OTUs having higher 16S rRNA gene abundance in a seasonal comparison are more intensely colored towards the respective season color. The

size of each OTU is proportional to the average 16S rRNA gene abundance between the two compared seasons. OTUs outside of the dash-lined box in the center of each plot change more than 1-log in relative abundance between the two seasons, while less than 1-log changes are within the dash-lined box.

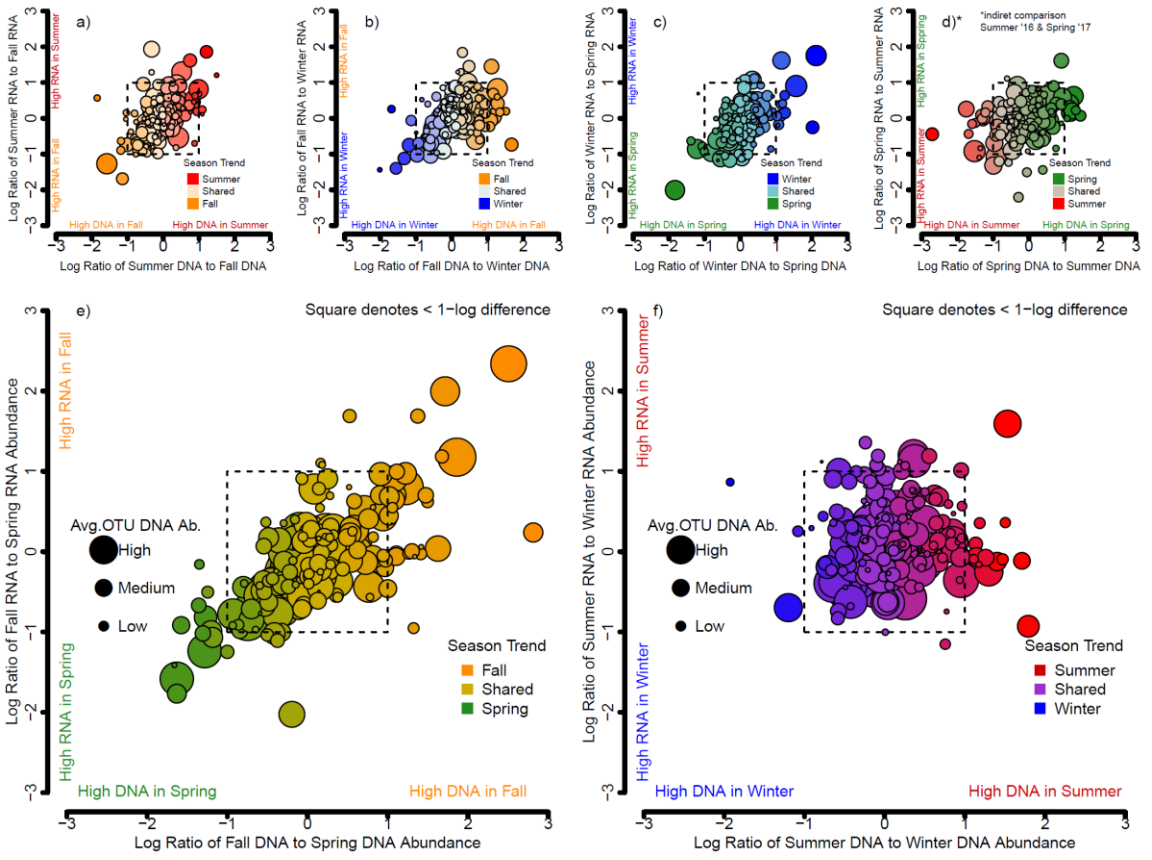

Figure 4.3 Each plot compares two seasons ratio of 16S rRNA gene composition as well as the 16S rRNA transcription composition to discern how much variation occurs between successive seasons (Figure 4.3a-d) and 6-month intervals (Figure 4.3e&f). Each circle represents an OTU plotted with the average DNA percent abundance representing their size. Both axes represent a logarithmic ratio for the OTUs percent abundance based on 16S rRNA gene (x-axis) and 16S rRNA transcript (y-axis). The ratios compare seasonal trends with summer (red), fall (orange), winter (blue), and spring (green). The intensity of the color scales proportionally with the OTUs higher abundance season. If an OTU is always within <1-log change based on the16S rRNA gene, it is at a constant abundance. If an OTU is always within <1-log change based

on the 16S rRNA transcript, it is at a constant activity. There are 119 OTUs which meet both criteria for every plot (Figure 4.3a-f) and are within the dashed square.

Figures 4.3a-d show successive seasonal comparisons, while Figures 4.3e&f shows 6-month intervals, to emphasize seasonal variations. Successional seasons (Figure 4.3a-d) on average share 92.5%±2.8% of the same 16S rRNA gene composition, and 97.9±0.6% 16S rRNA transcript composition. Therefore, 7.5±2.8% of the 16S rRNA gene communities are unique to each season. Only 2.1%±0.6% of the 16S rRNA transcript composition were unique comparing successive seasons. On average 79.3%±5.1% of the 16S rRNA gene composition and 82.7%±7.3% of the 16S rRNA transcript composition did not change more than 1-log between successive seasons.

When comparing compositions in fall to spring (Figure 4.3e) both communities share 87.4% 16S rRNA gene compositions and differ 12.6% each. However, only 63.2% and 68.6% of the 16S rRNA gene composition remains at similar abundances (<1-log), while 24.2% and 18.9% significantly change between fall and spring. The 16S rRNA transcript compositions are 94.9% and 96.7% similar in fall and spring, with 5.1% and 3.3% unique compositional changes. Despite the similar taxonomic compositions, 41.4% of fall and 19.5% of spring 16S rRNA transcript composition significantly change between seasons, leaving 53.5% and 77.1% of the composition at similar percent abundances.

Summer and winter (Figure 4.3f), appear more similar with 95.5% and 95.0% overlapping 16S rRNA gene composition, and 80.7% and 84.0% 16S rRNA gene compositions at similar levels of percent abundances. Therefore only 4.5% and 5.0% is unique to each season, and 14.8% and 11.0% significantly change between summer to

winter. There is less variation among 16S rRNA transcripts with 97.9% and 98.3% shared transcript compositions, and 85.2% and 90.6% shared composition at similar percent abundances. Summer and winter samples only had 2.1% and 1.7% unique 16S rRNA transcripts, and 12.7% and 7.7% significant variation in relative transcript abundance.

We observed linearity of OTU 16S rRNA gene and transcript abundances comparing fall and spring samples ($p<<0.05$, $R^2=45.8\%$). Summer and winter do not significantly correlate 16S rRNA genes to transcripts ($p>0.95$). All four successional seasons (Figure 4.3a-d) had statistically significant correlations between 16S rRNA genes and transcripts ($p<<0.05$), with low R^2 values averaging 20.7±7.5%.

119 OTUs did not change more than 1-log in gene or transcript abundance throughout the year. These 119 OTUs comprise the following percent abundances based on 16S rRNA gene composition per season: 69.6% in summer, 59.0% in fall, 75.7% in winter, and 63.6% in spring. These 119 OTUs comprise the following percent abundances based on 16S rRNA transcript composition: 63.5% in summer, 49.1% in fall, 70.4% in winter, and 73.3% in spring. The top five most abundant OTUs from these 119 OTUs are also listed in Figure 4.5. Additional seasonally unique, and significantly changing OTUs per season are listed in Supplemental Tables S4.2 and S4.3.

Comparison of Influent Wastewater Community and Activated Sludge

To differentiate OTUs growing in activated sludge from OTUs passing through with influent wastewater, the absolute abundance of each OTU in the SF community was compared to the average absolute abundance during the reaction cycle (R1 and R2) using

a mass-balance of each OTU (Equation S4.1). Figure 4.4 compares absolute abundances of OTUs in the SF community to the combined reaction cycle (R1 and R2). OTUs increasing greater than 1-log from the SF community are OTUs which grow and recycle in activated sludge. OTUs with less than 1-log difference in abundance do not significantly grow and will wash out. In Figure 4.4, OTUs are represented by dots, and those OTUs within the shaded region do not significantly grow.

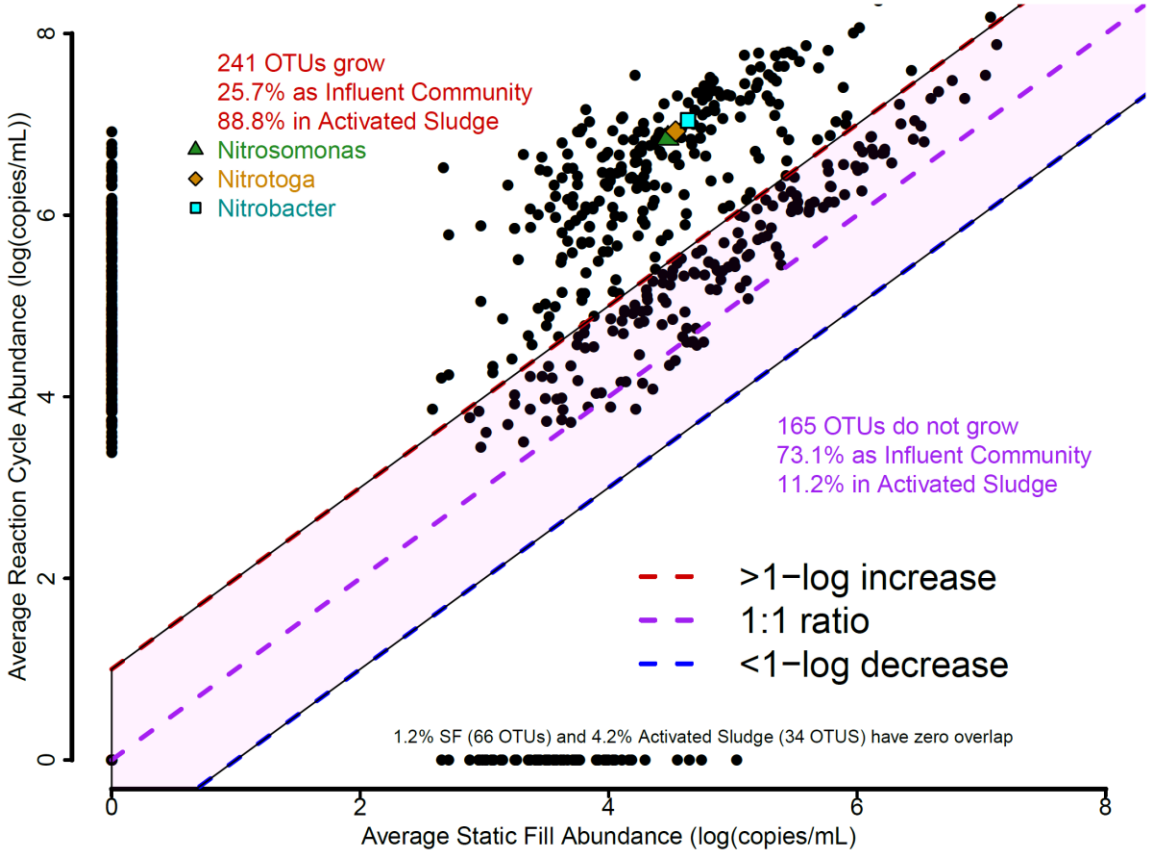

Figure 4.4 A mass balance was performed on each OTU to discern which organisms are significantly growing and proliferating in activated sludge or passing through the system. The 16S rRNA gene relative abundance from sequencing is multiplied by the quantitative total abundance of 16S rRNA gene copies via qPCR to yield an absolute abundance of each OTU. Each dot represents a unique OTU which appeared in both SF and during the react cycle. The x-axis is the abundance during SF, while the y-axis is the average abundance throughout the year during R1, and R2. Nitrifying

organisms are denoted in green triangles (*Nitrosomonas*), orange diamonds (*Nitrotoga*) and cyan squares (*Nitrobacter*). The red line denotes the cutoff for OTUs which are greater than 1-log difference, the purple line denotes exactly 1-to-1 ratio, and the blue line is a less than 1-log decrease cutoff. Anything falling between these bounds (purple shaded region) is considered at similar abundances entering the system and leaving the system at a nearly 1-to-1 ratio. Above this shaded region, are OTUs which grew in abundance and are propagated in activated sludge.

506 OTUs were assessed in Figure 4.4, but only 406 overlap between the reactor cycles. Of the 406 overlapping OTUs, 165 OTUs are in the shaded region which comprises 73.1% of the SF community. Although influent wastewater makes up on average a third of the reactor volume, these 165 OTUs constitute 11.2% of activated sludge. The region above the shaded area represents OTUs in the reactor which are growing in activated sludge. These 275 OTUs grow to represent 88.8% of the activated sludge community but are 25.7% of the influent wastewater community.

100 OTUs do not overlap between SF and the react cycles due to low sequencing reads. 66 of these OTUs are in the SF community comprising 1.2%. The remaining 34 OTUs were unique to activated sludge representing 4.2% of the total activated sludge community.

The Consistent Core Microbiome

We found 108 OTUs meeting our three criteria for "core microbiome." Figure 4.5 highlights 179 OTUs which exhibited consistent abundance (<1-log annually), and 172 OTUs with consistent protein synthesis activity (<1-log annually). 119 OTUs exhibit both consistent 16S rRNA gene and transcript abundances. Of the 275 OTUs which were

growing in activated sludge (Figure 4.4), 108 had constant abundance and activity, meeting all three criteria for our "core microbiome": Growth, Abundance, and Activity. According to our 16S rRNA gene analysis, these OTUs comprise 58.7% of the activated sludge composition in summer, 51.5% in fall, 70.8% in winter, and 59.6% in spring. The same OTUs represent 60.2%, 46.9%, 66.5%, and 70.5% of the summer, fall, winter and spring 16S rRNA transcript abundance, respectively. The top five OTUs of the consistent "core microbiome" are listed in Figure 4.5 with their average annual relative abundance. Additionally, the top three OTUs fulfilling one or two criteria are listed in Figure 4.5 with their respective average annual relative abundances.

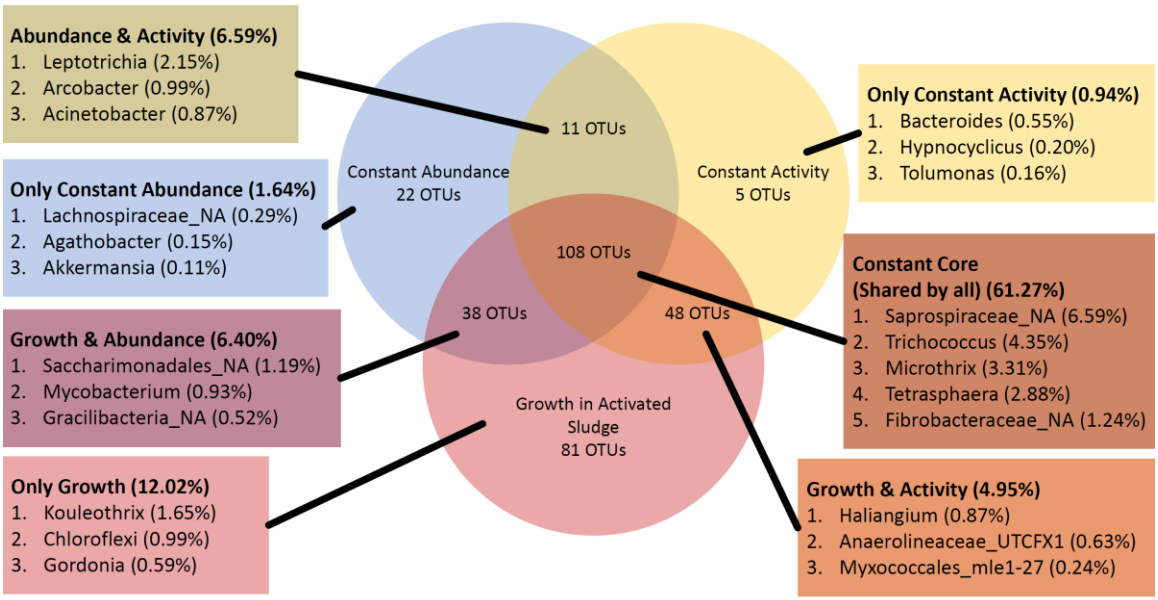

Figure 4.5 is a Triple Venn Diagram representing the intersections of the three criteria for the consistent core microbiome. The three criteria were constant abundance in blue(<1-log change in relative abundance throughout the year based on 16S rRNA genes shown in Figure 4.3), constant activity in yellow (<1-log change in relative abundance throughout the year based on 16S rRNA transcript shown in Figure 4.3), and in activated sludge in red (>1-log change

in absolute abundance compared to influent wastewater as shown in Figure 4.4). The top three OTUs based on relative abundance averaged across seasons and during the reaction cycle (average of R1 & R2) is listed for OTUs which meet one or two criteria, while the top five OTUs which met all three criteria are listed. There are a total of 179 constant abundance OTUs, 172 constant activity OTUs, and 275 proliferating OTUs. 108 OTUs met all three criteria as the consistent core microbiome.

Interestingly, 29.2% to 48.5% of the activated sludge microbiome composition based on 16S rRNA genes varies significantly in abundance or growth throughout the year. Accordingly, 29.5% to 53.1% of the 16S rRNA transcript composition of the activated sludge microbiome varies significantly in abundance.

Figure 4.6 highlights the top 50 most abundant OTUs according to our 16S rRNA gene amplicon sequencing results of samples collected during the react cycle. For the majority of OTUs, relative 16S rRNA gene abundances were proportional to the 16S rRNA transcript abundances with less than 1-log fold differences. While proportional, 16S rRNA transcripts copy numbers were generally higher than 16S rRNA gene copy numbers. The 50 OTUs listed in Figure 4.6 comprise 56.7±6.8% of the 16S rRNA gene community, yet they make up 67.5±3.5% of the community based on 16S rRNA transcript sequencing. However, of the 50 most abundant OTUs, 10 OTUs had at least one season with more than a 1-log difference between gene and transcript copy numbers, while 5 OTUs showed higher than 1-log differences between gene and transcript copy numbers over multiple seasons. *Leptotrichia* was notably far less "active" in terms of 16S rRNA transcript abundance than the 16S rRNA gene abundance would have suggested (2.1% relative 16S rRNA gene abundance compared to 0.1% relative 16S rRNA transcript abundance composition).

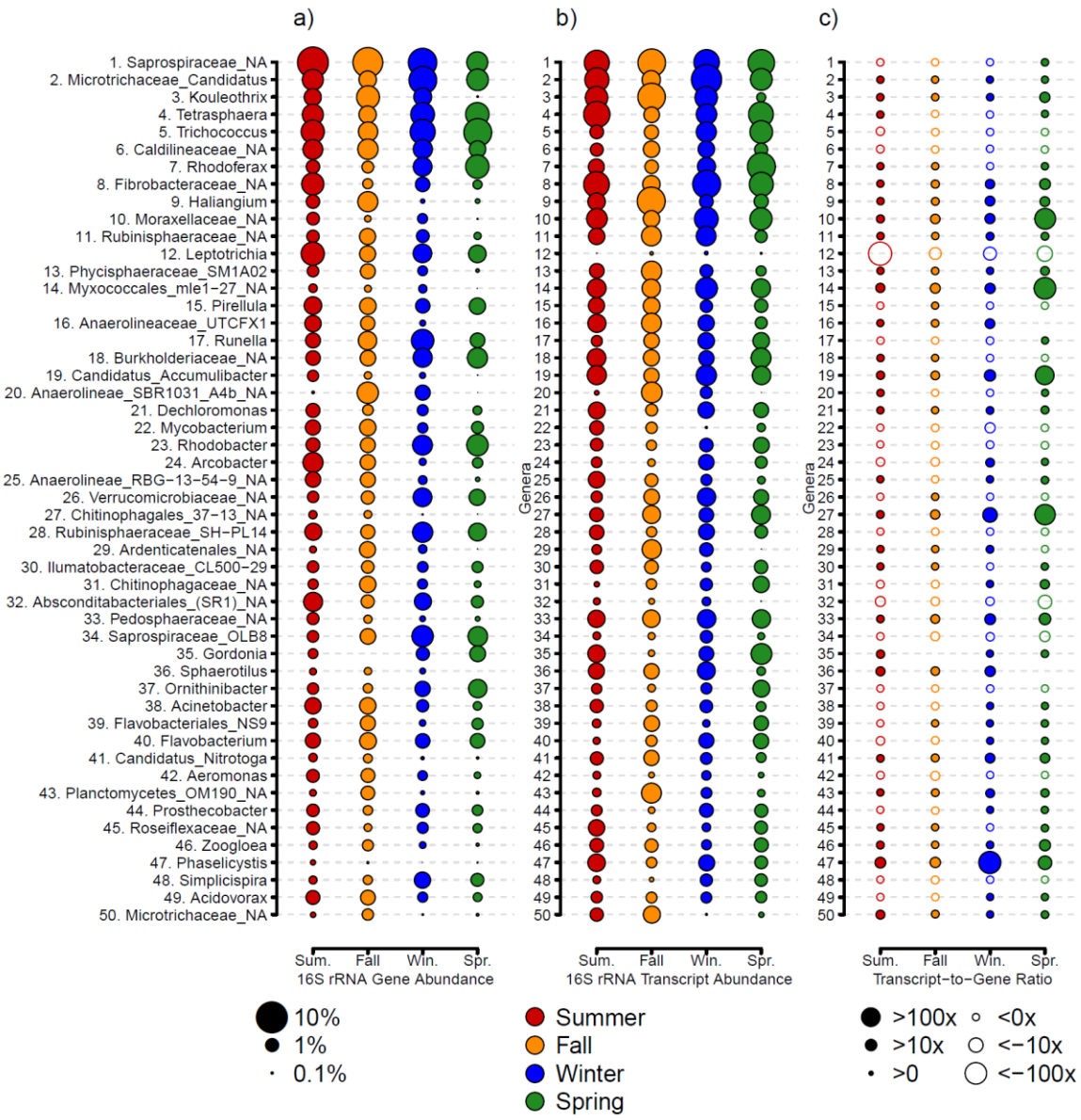

Figure 4.6. Relative abundances of the top 50 OTUs during the react cycle (average of R1 and R2) for all four seasons. Each season is color coded with summer in red, fall in orange, winter in blue, and spring in green. The size of each circle is proportional to the relative sequence abundance. Figure 4.6a shows relative 16S rRNA gene sequence abundance and Figure 4.6b shows relative 16S rRNA transcript abundances. Figure 4.6c shows the ratio of transcripts-to-genes. Higher transcript relative abundances are indicated by solid circles, while higher gene abundances are indicated by open circles.

Among the top 50 OTUs were several OTUs which declined in 16S rRNA gene abundance during winter or spring but maintained stable 16S rRNA transcript abundances and therefore had a high transcript-to-gene ratio. These OTUs include several uncharacterized organisms from *Moraxellaceae*, *Myxococcales*, Candidatus *Accumulibacter*, *Chitinophagales*, and *Phaselicystis.* While Candidatus *Accumulibacter* is a known phosphate accumulating organism, the rest of these have yet unknown roles in wastewater treatment facilities (14, 37).

Discussion

In this study we investigated the response of the activated sludge microbiome in three full-scale SBRs of a WWTP previously described to experience seasonal variations in composition and seasonal nitrification failure. We sampled inflow wastewater and activated sludge and applied high-throughput 16S rRNA transcript sequencing alongside RT-qPCR to break down the complex composition of the activated sludge microbiome into taxonomic groups of microorganisms not only abundant residents of a reactor 'core' community but metabolically active and growing during a full reactor cycle.

Activated sludge systems are designed to recycle settled solids so microorganisms have longer generation times. 16S rRNA gene amplicon sequencing based on activated sludge DNA extracts will pick up inactive and dormant species and extracellular DNA. 16S rRNA transcript sequencing in conjunction with 16S rRNA gene sequencing has the potential to reveal OTUs which maintain a detectable amount of ribosomal RNA indicating their metabolic capacity for instant de novo protein biosynthesis. Considering only our 16S rRNA gene sequence data, we would have identified 179 OTUs as activated sludge core microbiome members based on the relative abundance. By also sequencing 16S rRNA transcripts we were able to extend the core microbiome definition to include 119 OTUs not only consistently abundant but also active in the sense that they cell contained detectable amounts of ribosomal RNA as indicator for their preparedness to synthesize new proteins.

Quantitative-PCR revealed total 16S rRNA transcript copy numbers were about 2-3 order of magnitude higher than 16S rRNA gene copy numbers (Figure 4.1). This was expected as most cells maintain thousands to ten thousand of ribosomes when they are metabolically active. In Fall, 16S rRNA transcript copy numbers were significantly higher

during all reactor cycles compared to Winter, Spring, and Summer. While 16S rRNA transcript copy numbers in Spring and Summer were not significantly different from each other they were greater than 16S rRNA transcript copy numbers in the winter during the react cycle. As a consequence of aeration with cold air during the winter, we observed a decrease in 16S rRNA transcript copy numbers by up to 2 orders of magnitude. This indicates that the activated sludge microbiome reacts with a decrease in protein synthesis potential due to the exposure to cold air during aeration and the consequential drop in water temperature. We observed this phenomenon when quantifying 16S rRNA transcripts, not 16S rRNA gene copy numbers which serve as proxy for total cell counts. The observed decrease in protein synthesis potential in the activated sludge community did not affect total cell biomass.

The activated sludge composition did not significantly change throughout reactor cycles yet the was significantly different from the microbial community in the influent wastewater (SF)(Figure 4.2A). By calculating absolute abundances, we found 25.7% of the influent wastewater OTUs replicate and grow to comprise 88.8% of activated sludge yet 73.1% of influent passes washes out as 11.2% of the activated sludge composition.

Seasonal Shifts in the Activated Sludge Microbiome

Based on Bray-Curtis dissimilarity, the activated sludge composition varied most when comparing 16S rRNA gene with 16S rRNA transcript composition (32.2% variance explained), emphasizing the value of considering to sequence 16S rRNA transcript in addition to 16S rRNA genes(18). The seasons during which activated sludge samples were collected were the second most differentiating principle component describing activated sludge composition, with a total of 18.2% of explained total variance. Fall and spring

samples had the most distinct compositions (Figure 4.2b). Summer and winter composition were statistically more similar based on Bray-Curtis dissimilarity for 16S rRNA transcripts (Figure 4.2b).

The sampling dates in fall and spring succeeded the longest periods of continually warm and continually cold weather conditions. While fall and spring compositions appeared to be distinct (Figure 4.2b), 16S rRNA transcript copy numbers during fall and spring were relatively stable and slightly higher than compared to the reactor's samples in summer and winter. The transient weather conditions leading into summer and winter resulted in a more similar composition between these two seasons but the lower 16S rRNA transcript copy numbers during mixed fill and react cycles demonstrated a lower protein synthesis potential as the activated sludge microbial tries to acclimate to changing temperatures. Temperature is continually demonstrated to be a significant driving factor affecting activated sludge community compositions(4, 7), however, by including quantification of 16S rRNA transcript copy numbers we demonstrated how microbial community activity is also impacted by seasonal temperatures. The decrease in transcript copy numbers at the onset of aeration in winter demonstrate this phenomenon because the sampled wastewater treatment plant experienced a sudden cold front the day before sampling. Air temperatures decreased from -8°C to -20°C during the day and from -18°C to -33°C during the night. Cold-shock and recovery have been observed in lab-scale, but we show this phenomena affecting a full-scale WWTP(38, 39). As global climate changes the likelihood of more drastic weather impacted shifts in temperature will rise, emphasizing why it is important to better understand the boundaries of resilience of activated sludge microbial community activities to ensure stable process performance in the future(40).

Based on Bray-Curtis dissimilarity, activated sludge composition varied prominently with seasons yet shifts between reactor cycles were less pronounced. As expected, the DW had the most dissimilar composition but not significantly. 16S rRNA transcript composition was expected to show more variation across reactor cycles since ribosomal RNA has a shorter half-life than genomic DNA(41). Because generation times of most microorganism are longer than the average duration of an complete cycle (SRT>>HRT(25)) composition did not change significantly once the influent wastewater mixed with activated sludge.

Activated sludge microbial community resilience and plant performance stability are continuously been impacted by the influent wastewater. In this study we observed the largest community dissimilarity (38.2%, Figure 4.2a) between the influent wastewater sampled during SF and the activated sludge microbial community. While the activated sludge community composition showed slight seasonal variations, we observed little variation throughout the whole year in the influent wastewater chemical and composition. This has also been observed by Newton et al. previously(5). Since Ibarelez et al. showed influent wastewater impacts activated sludge microbial community structure, we used a mass balance approach to determine which OTUs were growing (or not) in our SBRs. Individual OTU growth rates were calculated similarly to Saunders et al.(10) but using 16S rRNA gene copy numbers for total biomass.

Among the OTUs, which were not growing during the react cycles of the reactors we identified primarily human-health related bacterial taxa. These included taxa such as *Leptotrichia* (2.1%±1.0%) which is found as part of the oral and intestinal human microflora(42), *Arcobacter* (1.0%±0.9%), a taxa comprising enteropathogenic

bacteria(43), and *Acinetobacter* (0.9%%±0.5%), containing species related to human infections(44). These OTUs have also been observed in influent and effluent wastewater by Numberger et al(45), based on relative sequence abundance. Using a mass-balance approach to approximate absolute OTU abundances we found human health-related OTUs, while present, were not growing in the activated sludge reactors. One exception was *Mycobacterium* (0.9%±0.0%), known to comprise species causing tuberculosis and leprosy. *Mycobacterium* OTUs were present and growing in the SBR, however *Mycobacterium* was less active during the winter because we observed a lower protein synthesis potential(46).

The parallel sequencing of DNA and RNA in conjunction with 16S rRNA gene and transcript copy number quantification enable us to categorize the identified OTUs in the activated sludge samples in several different categories based on their abundance, activity and growth in the system. OTUs which were identified as "growing" but fluctuated in abundance and activity by more than 1-log comprised members of the taxa *Kouleothrix* (1.7%±1.6%), uncultured OTUs belonging to the phylum *Chloroflexi* (1.0%±1.3%), and *Gordonia* (0.6%±0.5%). *Kouleothrix* have been described to be associated with sludge bulking(47), while members of the diverse phylum *Chloroflexi* include microorganisms capable of degrading halogenated hydrocarbons as well as filamentous microorganisms are part of activated sludge flocs(48). Members of the taxa *Gordonia* have been described to be capable of degrading various xenobiotic compounds(49). Other floc forming organisms of the genus *Zoogloea* fluctuated in abundance throughout the seasons, but within a lower range. *Zoogloea* is regarded as a ubiquitous taxa among wastewater treatment plants, with relative sequence abundance of typically around 0.89% (4). However, we observed the

highest relative 16S rRNA gene abundance of *Zoogloea* in the fall at 0.56% and the lowest in the spring at 0.1%. Interestingly, based on relative 16S rRNA transcript abundances, *Zoogloea* comprised 1.77% in the fall and 0.55% in the winter. These observed changes in abundance and activity of floc-forming microbial taxa in activated sludge may contribute to seasonal variations in in plant process performances by impacting activated sludge aggregate structure and stability.

Forty-eight OTUs identified as "growing" in the batch reactors which made up an average of 4.95% of the bulk activated sludge community also had a high protein synthesis potential but fluctuated in abundance by more than 1-log between seasons. The most abundant among these identified OTUs was *Haliangium* (0.87%±1.2%). *Haliangium* are detected in Carrousel oxidation ditch systems and might be involved in denitrification(50, 51). We do not know much about denitrifiers in SBRs but since the WWTP undergoes seasonal nitrification failure, the abundance of denitrifiers might be affected. It is noteworthy, that among the top 50 OTUs in Figure 4.6, only *Nitrotoga,* a nitrite oxidizing bacterium is present, while *Nitrosomonas* which is the predominant ammonia oxidizer is far lower in abundance at 0.20%±0.20.

One objective of this study was to identify OTUs which belong to the activated sludge 'core' microbiome in the sampled treatment plant. A total of 108 OTUs met our three criteria for abundance, activity, and growth. Most of these OTUs are typical members of activated sludge microbial communities such as *Tetrasphaera* (2.9%±1.3%)(52), which is a known phosphate accumulating microorganism, and *Saprospiraceae* (6.6%±3.5%), filamentous bacteria with a so far unknown role in activated sludge(50). *Saprospiraceae* was the highest abundance OTU with a stable 16S rRNA gene and transcript abundance

throughout the year, while our previous study noted it as the second most abundant OTU(3). Interestingly, some of the most ubiquitous OTUs recently identified by a survey of the Global Water Microbiome Consortium were not present in our SBRs (4). For example, we didn't find evidence for the presence of the recently isolated organism *Casimicrobium huifangae* that might play a role in phosphate removal and nitrate reduction. Our activated sludge communities also did not contain any members of the genus *Nitrospira(53).* While the Global Water Microbiome Consortium reported on the ubiquitous presence of *Nitrospira* in a global survey of WWTPs(4), the most abundant known nitrite-oxidizers in the SBR samples in this study were *Nitrotoga* (0.2%±0.2%) and *Nitrobacter* (0.3%±0.2%)(54). However, the global assessment of activated sludge bacterial communities mostly featured conventional continuously stirred tank reactor configurations. *Nitrosomonas* (0.2%±0.2%) was the most abundant known ammonia oxidizer in our system. All three known nitrifying taxa present in the sampled treatment plant in this study, *Nitrosomonas*, *Nitrotoga*, and *Nitrobacter*, met our three criteria for consistent core OTUs (Figure 4.4), based on consistent abundance, growth, and protein synthesis potential, despite seasonal nitrification failure(3). All three known nitrifiers remaining active and continuing to grow despite the seasonal nitrification failure raises the question if these species are metabolically more flexible than known and capable of switching when wastewater temperatures decrease.

Activated sludge presents one of the most diverse and dynamic engineered microbial ecosystems. This study presents a detailed analysis of the influent wastewater and activated sludge microbiome during the stages of a reactor cycle. By quantifying and sequencing the 16S rRNA genes and transcripts, we identify bacterial taxonomic groups

based on their changes in abundance, protein synthesis potential, and their continued growth in SBRs. This study improves our understanding of the microbial ecology of activated sludge and emphasizes the need to move from describing activated sludge compositions by relative sequence abundances to an absolute quantitative assessment incorporating activity of individual core taxa, if we want to better understand their role in community functions and resilience to perturbation in the future.

Acknowledgements

We would like to thank the team at Brainerd Wastewater Treatment Facilities for sample collection and access to treatment plant performance data. We would like to thank the University of Minnesota Genomics Center for assistance with amplicon sequencing. We would like to thank Laurel Hunt, Deirdre Manion-Fischer, and Michael Brown for assistance on sampling trips. We would like to thank the National Science Foundation Graduate Research Fellows Program for providing Juliet Johnston with a fellowship opportunity as well as the Legislative-Citizen Commission on Minnesota Resources for funding the project. J. Johnston was supported by the National Science Foundation Graduate Research Fellowship Program (ID: 2015191729). The research was enabled by the Legislative-Citizen Commission on Minnesota Resources (LCCMR) through a grant entitled "Wastewater Treatment Process Improvements" funded by the Environment and Natural Resources Trust Fund (ENRTF) under legal citation M.L. 2016, Chp. 186, Sec. 2, Subd. 04 k.

Chapter 5

Seasonal Variations in the Ammonia Oxidizing Community in Triplicate Full-Scale Sequencing Batch Reactors

Synopsis

Ammonia oxidizing bacteria play an important role in activated sludge microbial communities by oxidizing ammonia from influent wastewater to prevent eutrophication from excessive nitrogenous compounds. However, ammonia oxidizing bacteria are sensitive to cold temperatures causing 'seasonal nitrification failure' where nitrification performance declines. To understand why seasonal nitrification is prevalent, we sampled triplicate full-scale sequencing batch reactors each season for ammonia monooxygenase (*amoA)* gene and transcript quantification as well as high-throughput sequencing during the reactor cycle. The *amoA* transcript copy numbers fluctuated throughout the seasons with similar seasonal trends as temperature indicating there is less *amoA* activity resulting in nitrification failure. While *amoA* activity shifts were expected, this seasonal pattern was not observed in *Nitrosomonas* spp. 16S rRNA transcript quantification, which stabilized during peak nitrification failure. The stability of *Nitrosomonas* spp. 16S rRNA transcripts indicates the community may remain active using other metabolic pathways which requires their stable protein synthesis potential. Additionally, we observed *Nitrosospira* briensis having a higher *amoA* transcript-to-gene ratio than any other *amoA* ASV cluster. This suggests the activated sludge process does not select for the most active ammonia oxidizing bacteria and can be further optimized for ammonia oxidizing bacteria already within the system.

Introduction

Wastewater treatment plants leverage ammonia oxidizing bacteria with nitrite oxidizing bacteria during aerobic treatment to perform nitrification, the biological oxidation of ammonia. Ammonia is common byproduct of urea which is in domestic wastewater at concentrations between 25-50 mg/L (1). The ammonia is first metabolized into nitrite by the ammonia oxidizing bacteria, then into nitrate by the nitrite oxidizing bacteria. This process is known as nitrification and it is essentially to meeting water quality standards determined by the National Pollutant Discharge Elimination System permits (2). These permits require a minimum of monthly testing for effluent ammonia concentrations, but often only have achievable water quality standards during the summer and fall months. There is often a gap in permitted levels of effluent ammonia concentrations in temperate and continental climates because wastewater treatment plants often cannot meet these standards during the colder seasons due to seasonal nitrification failure (3). Seasonal nitrification failure occurs when the temperatures drop during the colder seasons and the biological process of nitrification is severely hindered (4). This hinderance is particularly noticeable at the initial ammonia oxidation step which creates rate-limiting issues for the nitrite oxidizing bacteria downstream denitrification biological processes. Seasonal nitrification failure is so prevalent, that despite it being the largest annual release of ammonia from domestic wastewater treatment plants, it goes unregulated due to a lack of affordable treatment options such as heating operations or chemical treatment. Environmental engineers are working to prevent this due to the environmental degradation caused as a result of eutrophication in bodies of water receiving effluent wastewater (2). This study aims to explore how the ammonia oxidizing community's transcriptional

expression fluctuates throughout the seasons in order to determine baselines for which ammonia oxidizing bacteria are most impacted by temperature in a full-scale triplicate sequencing batch reactor (SBR) wastewater treatment plant.

Cold temperature nitrification has been explored in numerous lab-scale investigations which typically suggest longer solid retention times and attached growth on membranes to increase nitrifying organisms biomass, and that in synthetic and bioaugmented microbial community's high-performance cold temperature nitrification is possible (5-12). While this wisdom has been known to wastewater operators for years, it rarely makes significant impacts on nitrification performance when scaled-up into full-scale wastewater treatment plants likely as a result of the real-life complexity and diversity in activated sludge systems. The treatment plant in this study has had a significant history of trying different operational parameters to strengthen cold weather nitrification performance to no avail. The inability for benchtop reactors to scale appropriately to full-scale wastewater treatment plants presents a gap in knowledge where we need to better understand the ammonia oxidizing community's phylogeny and activity in full-scale wastewater treatment plants and determine transcriptional activity baselines so that an appropriate assessment can be performed when scaling-up benchtop experiments.

We have previously characterized the broader microbial community composition at the Brainerd Wastewater Treatment Facility and demonstrated that the ammonia oxidizing community's abundance does not significantly change throughout the seasons despite seasonal nitrification failure (13). Additionally, we have shown that the dominant nitrite oxidizers are *Nitrotoga,* and *Nitrobacter* as opposed to *Nitrospira* which has potential to perform both ammonia oxidation and nitrite oxidation. The niche branch of

Nitrospira performing both steps are referred to as Comammox bacteria (complete ammonia oxidizing bacteria) and have a unique ammonia monooxygenase gene (14, 15). However, due to lack of *Nitrospira's* presence, this study will focus on the traditional *amoA* functional gene for ammonia monooxygenase.

To understand how the ammonia oxidizing community is changing in activity, the 16S rRNA transcripts and *amoA* transcripts will be sequenced and quantified. Transcripts have a relatively short lifespan when compared to DNA and therefore are more reflective of microbial communities' activity. The 16S rRNA transcripts are reflective of the overall cellular activity because these rRNA transcripts are a critical component required for protein synthesis. 16S rRNA transcripts can therefore serve as a proxy for *de novo* protein synthesis (16). The fraction of total 16S rRNA transcripts which are known ammonia oxidizers will be characterized by sequencing the reverse transcripts cDNA via 16S rRNA amplicon sequencing. This will ultimately discern *how active is the ammonia oxidizing cells* whereas *amoA* transcript quantification will discern *how active is the ammonia oxidizing metabolic function?*

The *amoA* transcript quantification serves as a proxy for activity for the ammonia monooxygenase metabolic pathways, and by additionally sequencing these transcripts we can gain a high resolution of the phylogeny of active ammonia oxidizers. While 16S rRNA gene amplicon sequencing of specific regions (V1-V3 for activated sludge (17)) is the standard for total bacterial communities, it often lacks strain specific information for common ammonia oxidizing bacteria. Sequencing the *amoA* functional gene provides far more taxonomic resolution and insight into the specific phylogeny of active ammonia oxidizers (18, 19). By sequencing the *amoA* transcripts we can discern how active

commonly culturable *Nitrosomonas* europaea and *Nitrosomonas* eutropha are from less commonly studied *Nitrosomonas* briensis or potentially unculturable forms of ammonia oxidizers (20).

This study will investigate the nitrification community's abundance, cellular activity, and metabolic activity throughout seasons and the reactor cycles in triplicate full-scale SBR activated sludge system. We will be sequencing and quantifying 16S rRNA and *amoA* genes and transcripts to discern detailed changes in the ammonia oxidizing community's composition, protein synthesis potential, and metabolic activity. Because we have previously observed constant abundance of ammonia oxidizing bacteria, we hypothesize cellular activity also remains relatively constant throughout the seasons, while the ammonia oxidizing metabolic pathway fluctuates. Additionally, by investigating strain specific changes in the *amoA* phylogeny we hope to discern which ammonia oxidizers are the most active populations throughout cold temperatures so that engineers can design processes which select for organisms which can proliferate in full-scale treatment plants and bridge the gap between benchtop and full-scale investigations.

Methods:

Complete methods have been previously described in Johnston 2020 (21) which includes: sample collection, DNA and RNA extraction, qPCR and RT-qPCR, 16S rRNA gene and transcript sequencing analysis, and statistical analysis. In brief the previous methods include:

Sample trips occurred within 10-days at the start of each season (July 1st, 2017, October 3^{rd,} 2017, December 27th, 2017, and March 27th, 2018). Samples were collected every 10-minutes from each SBR cycle throughout the cycles Static Fill (SF), Mixed Filled (MF), Aerobic React (R1 at the onset of aeration, and R2 just prior to the end of aeration), and concurrent timepoints of Settled Sludge (SS) and Decanted Water (DW) from the bottom and top portion of the reactor.

Sample aliquots in 2ml microcentrifuge tubes were rapidly frozen to approximately -72°C in a bath of dry ice and ethanol and preserved in -80°C until downstream processing. DNA was extracted using MP BIO FastDNA™ Spin Kit for Soil (Santa Ana, CA). RNA extractions were performed using Quick-RNA Fecal/Soil Microbe Microprep Kit by Zymo Research (Irvine, CA). From these RNA extracts, residual DNA was digested using TURBO DNA-*free*™ Kit from Invitrogen (Carlsbad, CA) followed by reverse transcription using PrimeScript RT-PCR Kit from Takara (Kusatsu, Japan). All DNA and cDNA products were quantified on a Bio-Rad CFX Connect Real-Time PCR Instrument (Hercules, CA) with an average amplification standard efficiency of 92.9% ± 6.9% and R^2 coefficient of 0.968 ± 0.041.

16S rRNA sequences were performed using V1-V3 primers at the University of Minnesota's Genomics Core (22) and were analyzed using DADA2 (23) in RStudio (24) referencing the SILVA rRNA SSU 132 database (25). Statistical analysis was performed using the *vegan (26)* and *alr4 (27)* packages in RStudio.

Primers and Sequencing Analysis

The primers used for *amoA* gene and transcript quantification of ammonia oxidizing bacteria are amoA-1Fmod (5'-3' CTGGGGTTTCTACTGGTGGTC) and GenAOBR (5'-3' GCAGTGATCATCCAGTTGCG) published by Meinhardt et al in 2015 (28). Additionally, we used GenAOAF (5'-3' ATAGAGCCTCAAGTAGGAAAGTTCTA) and GenAOAR (5'-3' CCAAGCGGCCATCCAGCTGTATGTCC) primers for ammonia oxidizing archaea but this data was not significant for this study (28). For sequencing analysis, the amoA-1Fmod primer was still used, however, the reverse primer amoA-2R (5'-3' CCCCTCKGSAAAGCCTTCTTC) (18) was used to significantly increase the region size to approximately 490 base-pairs for a more detailed genomic resolution of variations in the *amoA* phylogeny. These primers were fitted with the Nextera primer adapters for Illumina MiSeq sequencing at the University of Minnesota's Genomics Core. Since we assume lower species richness in *amoA* sequencing results, these samples were on a "stowaway" MiSeq lane with other samples which provides a minimum of 1,000,000 reads, but overall, less depth than a full Mi-Seq lane. The *amoA* gene samples had a total of 4,597,063 raw reads and the *amoA* transcripts totaled 3,647,505 raw reads.

Demultiplexed raw sequences were imported to Quantitative Insights Into Microbial Ecology 2 (QIIME 2 version 2019.1; https://qiime2.org/) for initial processing and quality control (29). DADA2 plugin was applied to trim the low quality regions of

forward and reverse reads at 290 and 260 bp (23), respectively, and the primers were removed simultaneously. The chimera removal and sequence dereplication were further performed by DADA2 with default settings. The amplicon sequence variants (ASVs) generated from DADA2 were directly used for sequence alignment and masking by align-to-tree-mafft-fastree pipeline in q2-phylogeny plugin, to remove the gaps and highly variable regions. Then the phylogenetic trees was built by FastTree program (30). The *amoA* gene samples averaged 16,978±6763 merged pairs per sample and the *amoA* transcript samples averaged 13,106±7431 merged pairs per sample (please see Supplemental Figure 5.1 for distribution). According to the ASVs summary from DADA2, the sequence libraries of *amoA* gene and transcripts were rarefied to a sampling depth of 5000 and 2000 sequences, respectively, for alpha and beta diversity estimation.

A custom *amoA* reference database was created for taxonomic analysis. High-quality *amoA* sequences with score above 430, HMM coverage higher than 80%, and size larger than 200 amino acids, were downloaded from FunGene database (http://fungene.cme.msu.edu/) (31). The unique taxonomy annotation was adopted from NCBI database through Entrez using a custom Perl script. The *amoA* sequences were trimmed to extract the reference reads for our *amoA primers*. A Naïve Bayes classifier was then trained using the reference reads and taxonomic annotation in q2-feature-classifier plugin, for taxonomic classification.

Segmented Flow Injection Analyzer

Ammonia and nitrate were quantified using a SEAL AutoAnalyzer 3HR continuous segmented flow analyzer (Seal Analytical Inc; Mequon, WI). This methodology uses the

manufactures instructions (No. G-102-93 for ammonia, and No. G-109-94 for nitrate) and is further described in Johnston 2019 (5).

Data availability

16S rRNA amplicon sequences are available from the NCBI Sequence Read Archive with accession number PRJNA591266. The *amoA* amplicon sequences are available from the NCBI Sequence Read Archive with accession number PRJNA605150.

Results:

Seasonally Changing Plant Parameters and Performance

Historical data records (2010 to 2018) provided by Brainerd Wastewater Treatment Facility were used to plot average annual influent water temperature (blue) and effluent ammonia concentrations (red) (Figure 5.1). Other plant operational parameters and performance metrics for the sampling period can be found in Table S1, but do not significantly change throughout the year. Influent water temperature and effluent ammonia concentrations revealed an inverse relationship, with lower temperatures in winter and spring correlating with raising ammonia concentrations in the plant effluent. At the Brainerd Wastewater Treatment Facility and other wastewater treatment plants in continental climate zones this annual decrease in plant ammonia removal performance is commonly referred to as cold temperature nitrification failure. Ammonia concentrations in the effluent during the four sampling events in summer, fall and, winter of 2017, and spring of 2018 are included as datapoints in Figure 5.1. The average effluent ammonia concentrations reported by the Brainerd Wastewater Treatment Plant during the sampling events ranged from 1.59±0.43 mg/L in the summer, 0.31±0.26 in the fall, 5.63±4.02mg/L in the winter, to 6.62±4.88mg/L in the spring of 2018. Except for the sampling event in fall 2017, effluent ammonia concentrations were always within the standard deviation of the annual average effluent ammonia concentrations recorded from 2010-2018.

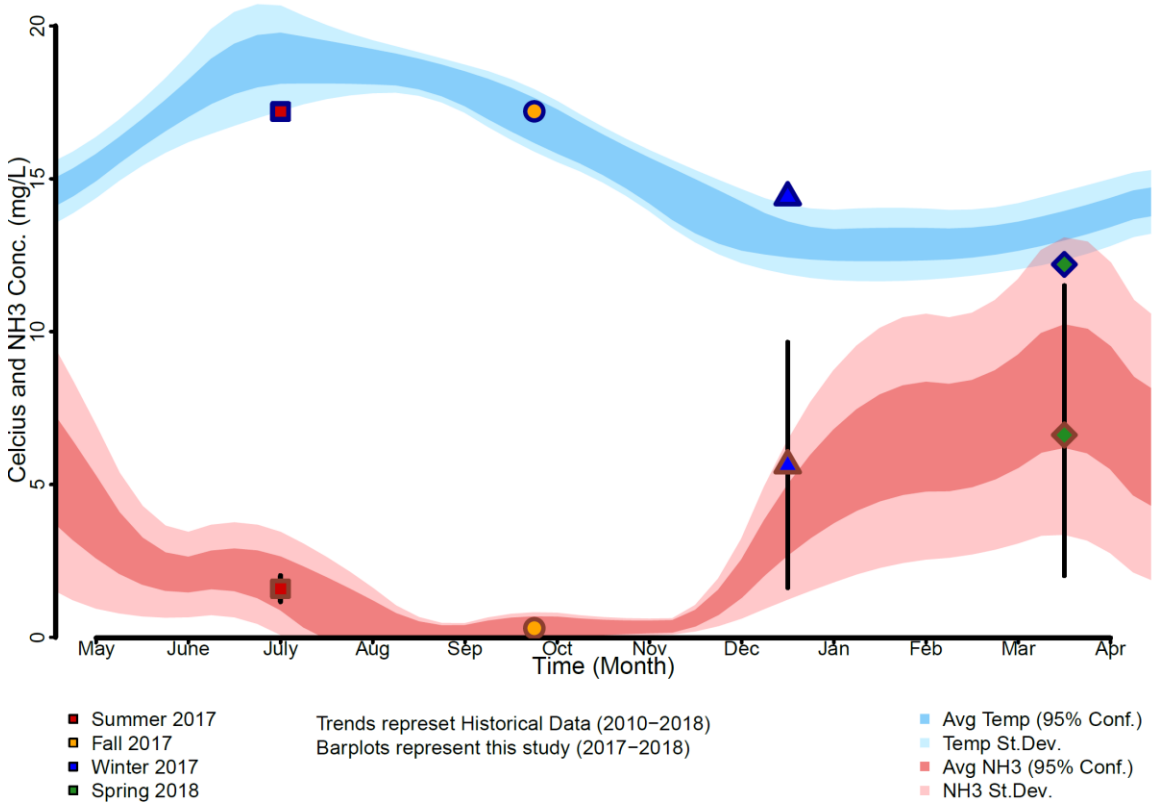

Figure 5.1 The seasonal trends from 2010 to 2018 of effluent wastewater ammonia concentration is denoted in shades of red with the average (95% CI) in dark red, and the standard deviation in light red. In dark blue is the average (95% CI) influent wastewater temperature, with the standard deviation in light blue. The data points are the influent water temperature and effluent wastewater concentration from this study's four sampling periods with summer in red squares, fall in orange circles, winter in blue triangles, and spring in green diamonds.

Figure 5.2 shows how the influent ammonia is biologically oxidized throughout the reactor cycle. During SF, there is an average of 25mg/L±14mg/L of ammonia with high variations depending on the time of day filled. Once the reactors mix influent wastewater with activated sludge during MF, the average drops to 9.0mg/L±2.7mg/L for summer, fall

and winter which were not statistically distinct. The ammonia concentration in spring does significantly decline between SF and MF, but only to 20mg/L±9mg/L which was significantly higher than other seasons. After the aerobic react cycle where ammonia oxidation occurs, the ammonia concentration was down to 0.5mg/L in summer, 2.3mg/L in fall, 5.8mg/L in winter, and 14.6mg/L in spring. The anaerobic settling cycle was measured as the bottom settled sludge (Figure 5.2b) and the decanted water (Figure 5.2c), but this did not result in statistically significant further removal of ammonia for any season.

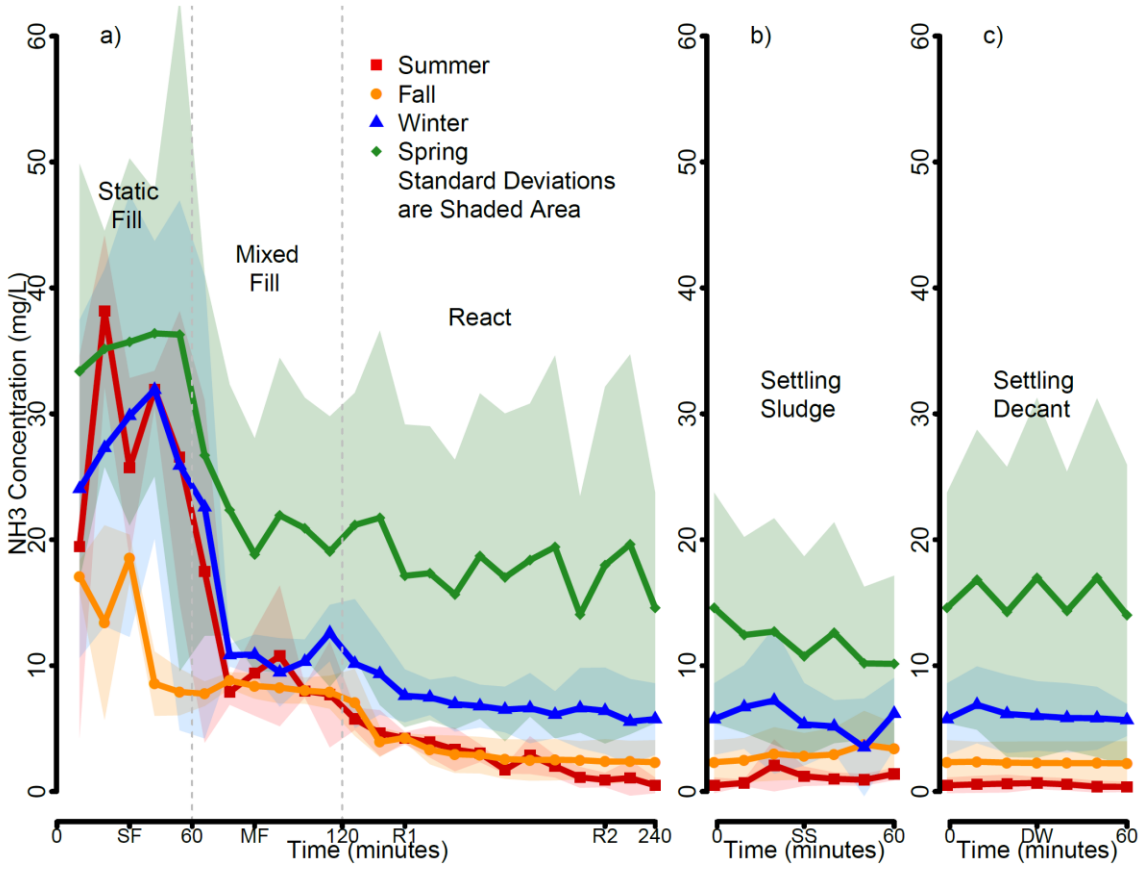

Figure 5.2 The average ammonia concentration (mg/L) per season (summer in red squares, fall in orange circles, winter in blue triangles, spring in green diamonds) throughout the reactor cycle is reported with the standard deviations shown in the shaded area. Figure 5.2a shows starts with the static fill, where large

variations in influent ammonia occur due to the fill time from fluctuations in diurnal loading. Mixed fill tends to level off as activated sludge is mixed with influent wastewater, before the aerobic react cycle where ammonia oxidation typically occurs. Figure 5.2b&c occur simultaneously as anaerobic settling occurs showing the dense settled activated sludge in Figure 5.2b while the decanted effluent wastewater is shown in Figure 5.2b. The is no statistical difference between summer and fall during react and settling, while winter and spring are significantly higher and distinct from each other. Seasonal nitrification failure impacts spring the most, with poor performance and high variations among triplicate reactors due to diurnal loading. Individual reactors performances are shown in Supplemental Figure S5.5.

Seasonal variation in nitrifier gene and transcript abundances

The *amoA* transcript copies numbers were quantified at 10-minute intervals throughout the reactor cycle and are shown in Figure 5.3. The SF was highly variable for all seasons, with an average of 6.1±1.7 log(copies/mL). The highest abundance of amoA transcript copies occurs in the fall with an average of 9.4±0.5 log(copies/mL) throughout MF, R1, and R2 which were significantly higher than all other seasons. The *amoA* transcript copies in summer and winter were not statistically different (p=0.09) and averaged 8.1±0.9 log(copies/mL) in the summer and 7.7±1.5 log(copies/mL) in the winter. The copies numbers for winter and spring not significantly different (p=0.08), but spring is significantly different from summer (p=6.3e-6) with an average abundance of 7.3±0.8 log(copies/mL).

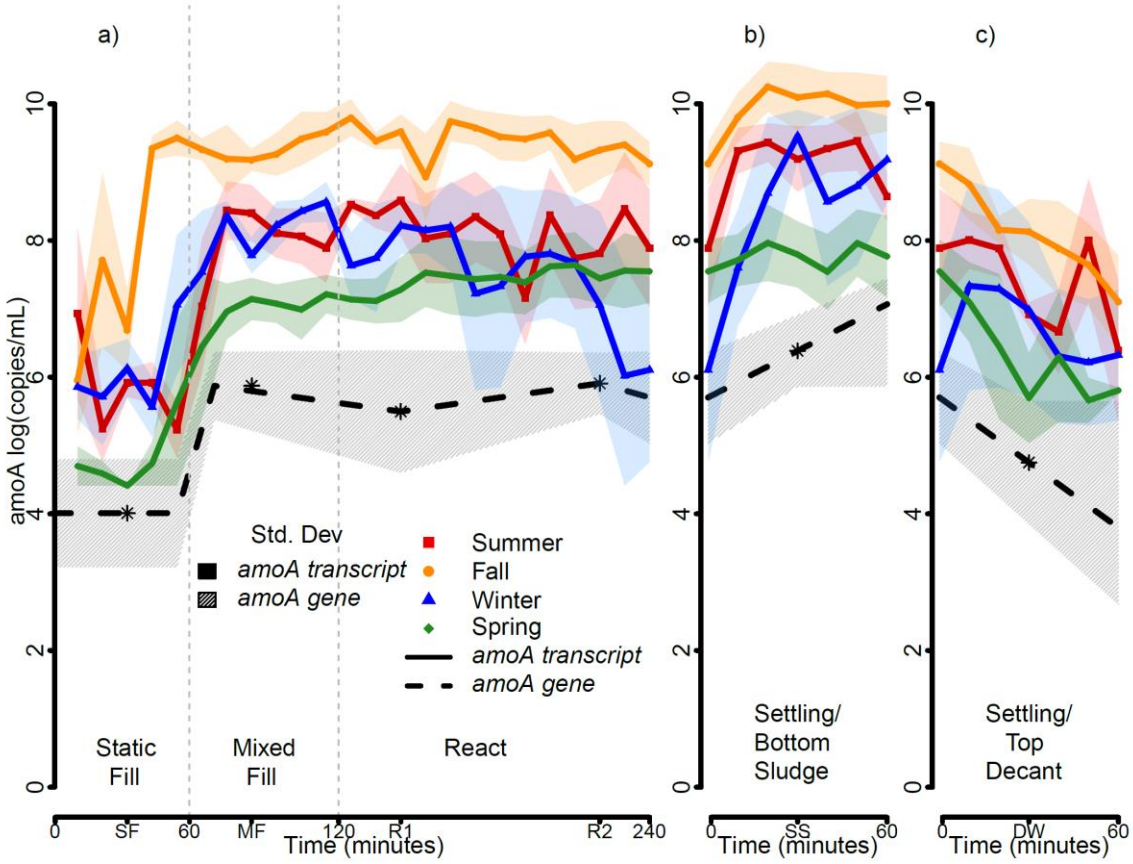

Figure 5.3 The *amoA* transcript activity and *amoA* gene abundance is shown for each season and throughout the reactor cycle in 10-minute intervals. Figure 5.6a shows the SF, MF, R1 and R2 cycles, while Figure 5.6b&c timepoints occur simultaneously, as the activated sludge settles (SS) to the bottom(6b) and decants (DW) from the top (6c) of the reactor. The quantitative abundance of *amoA* transcripts (solid lines) are shown by season (summer in red squares, fall in orange circles, winter blue triangles, and spring green diamonds). The solid hatch represents the standard deviation for the *amoA* transcript. The dashed line and dashed gray hatch represent and average abundance of *amoA* genes throughout the year, which do not significantly change with respect to seasons. The transcript abundances in the fall are continuously significantly higher transcript copy numbers for *amoA* while summer and winter remain relatively comparable at different stages. The transcript abundances in spring are significantly smaller during MF, R1, and SS. Each season experiences a significant increase in transcripts once the activated sludge is mixed with the influent wastewater, followed typically by a period of stabilization throughout the reaction cycle. Settling causes an increased concentration

of activity in the thick bottom settled sludge while the decant significantly declines before moving on in the treatment process.

During settling, the *amoA* transcript copy numbers significantly increased as the dense activated sludge settled to the bottom of the reactor. Each season averaged *amoA* transcript copy numbers log(copies/mL) of 9.2±0.6 in summer, 10.0±0.6 in fall, 8.7±1.5 in winter, and 7.8±0.8 in spring. The decanted water similarly saw a significant decrease in *amoA* transcripts as most of the floccular sludge settled removing the suspended solids. The decanted water averaged *amoA* transcript copy numbers log(copies/mL) of 7.3±1.2 in summer, 8.0±1.0 in fall, 7.7±1.8 in winter, and 6.2±1.1 in spring.

Quantification of *amoA* gene copy numbers did not reveal statistically significant seasonal variations throughout reactor cycles SF, MF, R1, and R2 for the four seasons and were therefore averaged together in the black dashed line and hatch for standard deviation as shown in Figure 5.3. The average SF *amoA* gene abundance was 4.0±0.8 log(copies/mL). The average *amoA* gene abundance throughout MF, R1, and R2 was 5.8±0.7 log(copies/mL). The SS increased concentration up to 6.4±0.5 log(copies/mL) while the DW decreased down to 4.8±0.9 log(copies/mL).

In order to gain further insights into the seasonal differences in ammonia oxidizer activity during aerobic react cycle (R1 and R2), we used results from *amoA* transcript RT-qPCR (Figure 5.3) and a quantitative abundance of *Nitrosomonas* spp. OTUs obtained by 16S rRNA amplicon sequencing obtained from our previous work (21). In Figure 5.4a we correlate the relative abundance of *Nitrosomonas* spp. 16S rRNA transcripts multiplied by total 16S rRNA transcripts per mL with *amoA* transcripts copy numbers obtained by RT-

qPCR. The Tukey box and whisker graphs at the bottom and right edge of Figure 5.4 show the differences in the range of each season's *amoA* transcript and *Nitrosomonas* spp. 16S rRNA transcript abundances.

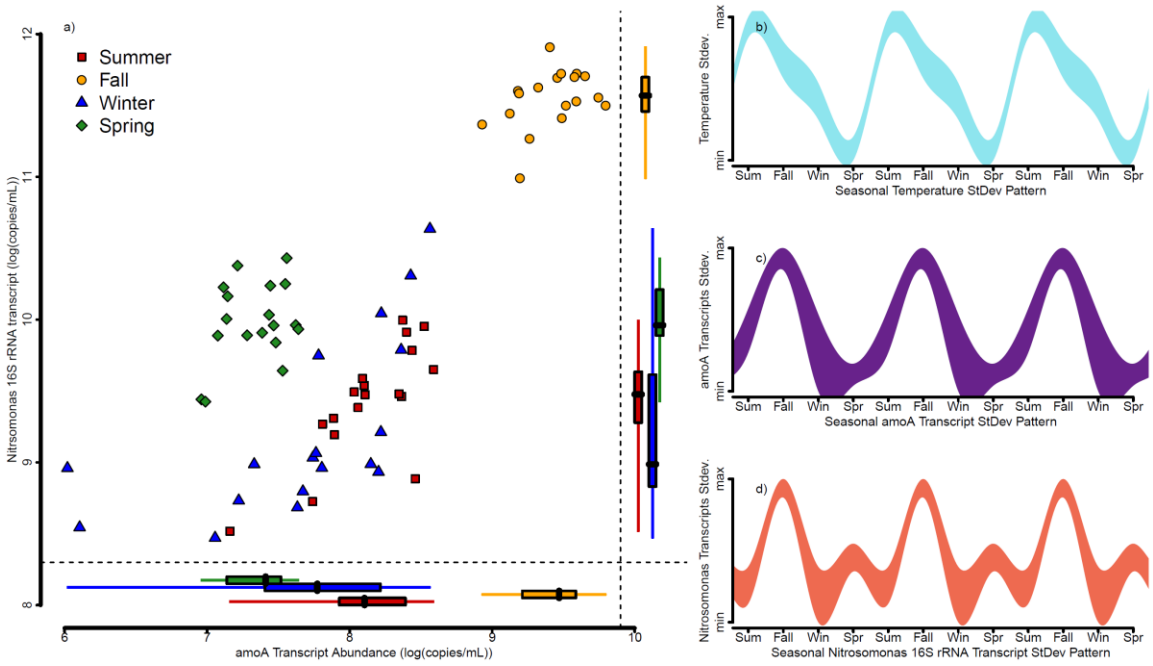

Figure 5.4 The correlation between the *amoA* transcript abundance (x-axis) with the absolute abundance of the uncultured *Nitrosomonas* spp. transcripts (y-axis) is plotted by season in Figure 5.4a. Summer is the red squares, fall is the orange circles, winter is the blue triangles, and spring is the green diamonds. Additionally, Tukey box-and-whisker plots of the data is shown with the extremes, the 25% and 75% interquartile ranges, and the median value. Figure 5.4b&c&d use the standard deviations for temperature, *amoA* transcripts, and uncultured *Nitrosomonas* spp. transcripts extrapolated into seasonal sine-wave trends to demonstrate how temperature and *amoA* activity move together, while uncultured *Nitrosomonas* spp. transcripts have a unique stability during the spring.

The *amoA* transcript abundances were the highest in the fall (9.4±0.2 log(transcripts/mL)) followed by summer (8.1±0.4 log(transcripts/mL)) then winter (7.7±0.7 log(transcripts/mL)) with the lowest in the spring (7.3±0.2 log(transcripts/mL)). Winter and spring did not show statistically different average transcript abundances ($p>0.065$). The seasonal trend of *amoA* transcript abundance followed the reactor water temperature seasonal profiles as shown in Figure 5.4c. However, *Nitrosomonas* spp. 16S rRNA transcript abundance profiles did not follow the same seasonal trend as shown in Figure 5.4d. *Nitrosomonas* spp. 16S rRNA transcript were highest in the fall (11.5±0.2 log(transcripts/mL)), followed by spring (10.0±0.3 log(transcripts/mL)), summer (9.4±0.4 log(transcripts/mL)), and winter (9.2±0.6 log(transcripts/mL)). Winter and summer were statistically similar ($p>0.246$) while the other seasons were statistically distinct ($p<0.05$). While Figure 5.1 demonstrates the sine-cosine relationship between temperature and effluent ammonia concentration, Figure 5.4b&c demonstrate the sine-sine wave relationship between temperature and *amoA* transcripts using the standard deviation of the data collected. However, *Nitrosomonas* spp. 16S rRNA transcripts do not appear to distinctly follow either of these trends.

Ammonia Monooxygenase Sequencing Results

Sequencing the *amoA* gene and transcript revealed phylogenetic shifts in the ammonia oxidizing community throughout the reactor cycle. Using the Faith Phylogenetic Diversity Index (32), the SF of influent wastewater consistently had higher phylogenetic diversity than the other reactor cycles (Supplemental Figure S5.3). The average relative abundance throughout the year, for each reactor cycle is shown in Figure 5.5. Five clusters

of ASV's averaged a relative abundance greater than 1% each throughout the year. These five clusters of ASVs cumulatively totaled >97.6% of the ammonia oxidizing bacteria based on *amoA* gene relative abundance and >98.6% based on *amoA* transcript relative abundance. The SF, primarily domestic wastewater, had two predominant ammonia oxidizers based on *amoA* gene amplicon sequencing with relative abundances of 43.75%±8.23% for *Nitrosococcus* sp. and 32.48%±12.18% for uncultured *Nitrosomonas* sp. The SF *amoA* transcript relative abundances throughout the year were 59.30%±4.11% for uncultured *Nitrosomonas* sp. and 26.22%±5.92% for *Nitrosococcus* sp. Once activated sludge is mixed with influent wastewater, the average for uncultured *Nitrosomonas* sp. during MF, R1, and R2 is 66.61%±7.4% based on *amoA* genes and 86.56%±9.42% based on *amoA* transcripts. The *Nitosococcus* sp. dropped significantly in relative abundance to 20.66%±4.25% based on *amoA* genes and 9.34%±6.76% based on *amoA* transcripts. These major trends were common across individual seasons histograms, as shown in Supplemental Figure S5.2.

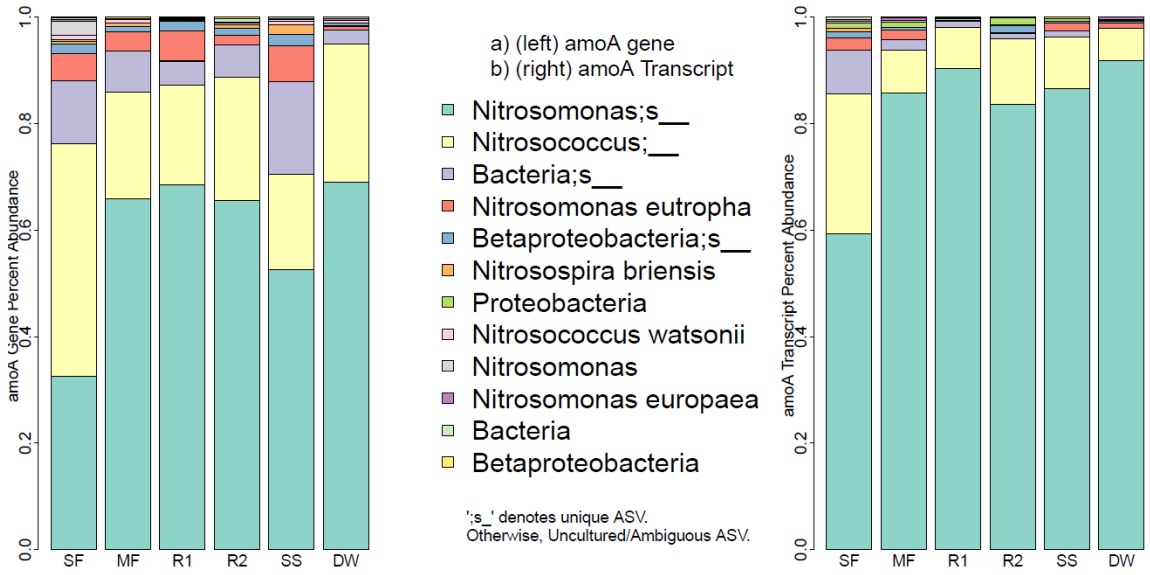

Figure 5.5 The average relative abundance from the three SBRs across all four seasons of ASVs based on taxonomic assignment from *amoA* genes and *amoA* transcripts are shown above. The average of ASVs based on *amoA* gene amplicon sequencing are shown on the left in Figure 5.5a, while the *amoA* transcript amplicon sequencing results are shown in Figure 5.5b. Overall, an uncultured species of *Nitrosomonas* sp. dominated the activated sludge system, while *Nitrosococcus* sp. dominated the influent wastewater during SF. A breakdown of the triplicate reactors in each season is shown in Supplemental Figure S5.2.

To understand how active each ASV cluster is on a cell-by-cell basis, Figure 5.6 plots the relative abundance of each ASV on the x-axis, with a log-transformed *amoA* relative abundance of transcripts-to-genes ration on the y-axis. Several data points (notably the lowest abundance ASVs) are not depicted due to insufficient reads in each season. The largest group of uncultured *Nitrosomonas* sp. present in the system, only had slightly more transcript-to-genes (+30%±12%, whereas *Nitrosospira* briensis had over a ten-fold increase in transcripts-to-genes (1651%±345%). Uncultured *Nitrosomonas* sp. did average 66.61%±5.20% of the overall *amoA* composition and certainly performs the largest

percentage of ammonia oxidizing occurring, on a cell-to-cell basis *Nitrosospira* briensis (0.05%±0.04%) appears to be far more active.

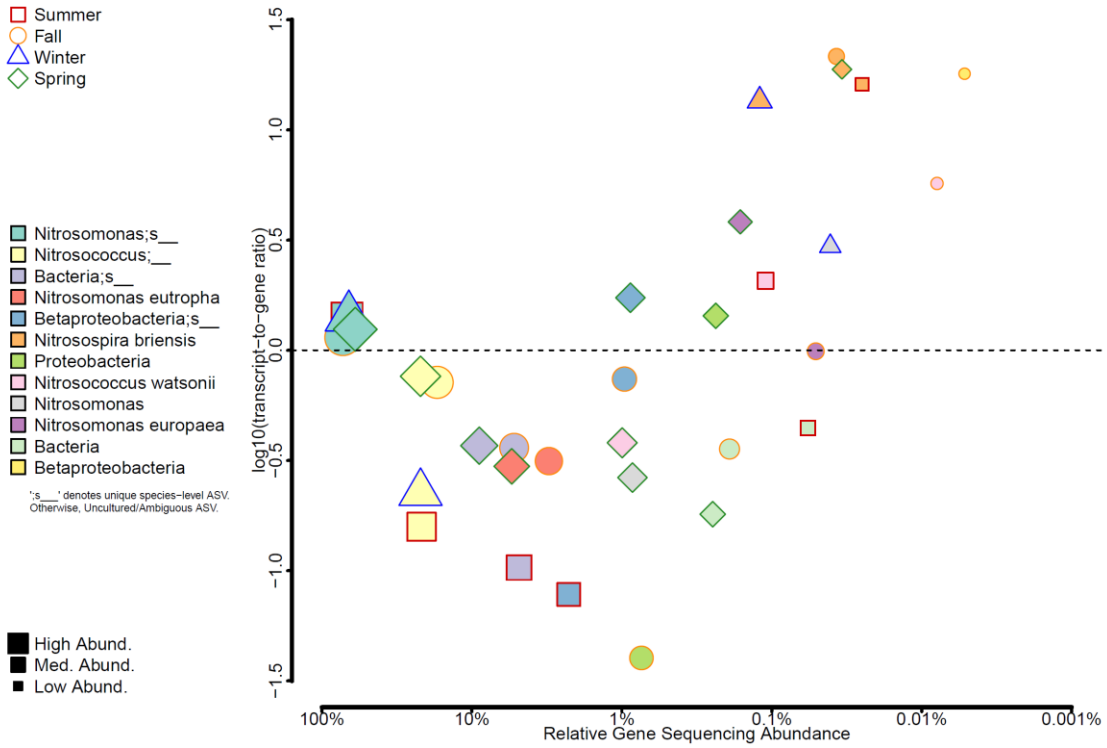

Figure 5.6 The ratio of *amoA* transcripts-to-genes is shown in the plot above with the log(relative abundance) of *amoA* genes across the x-axis, and the log(ratio of transcripts-to-genes) across the y-axis. Each color denotes a unique *amoA* ASV, where the size is proportional to the relative abundance of *amoA* genes. The shape and outline color of each ASV changes with respect to season with red squares in the summer, orange circles in the fall, blue triangles in the winter, and green diamonds in the spring. The higher abundance ASVs have a 1:1 transcript-to-gene ratio, while there is less *amoA* activity in the mid-abundance ASVs. ASVs with the lowest relative abundance of *amoA* genes tended to be the most active with respect to *amoA* transcript activity.

Ammonia Oxidizing Archaea.

Beyond typical ammonia oxidizing bacteria, we quantified *amoA* genes and transcripts for ammonia oxidizing archaea. The average concentration of ammonia oxidizing archaea *amoA* genes in the activated sludge were 3.5±0.5 log(copies/mL). Nearly 80% of the initial archaea *amoA* transcripts were below the detection limit before determined to be insignificant to plant operations. A summary of the ammonia oxidizing archaea *amoA* genes is shown in Supplemental Figure S5.4.

Discussion

Seasonal Nitrification Failure

Seasonal nitrification failure did occur during the sampling year with the average ammonia concentration in the DW rising to 6.2±2.8mg/L in winter and 10.1±7.0 in spring. The ammonia concentration had large standard deviations in spring, likely due to different initial concentrations in each reactor during the filling processes (SF and MF). For each sample trip, the start times for filling a reactor were at approximately 10am, 12pm, and 2pm. Whichever reactor starts filling closest to 10am typically reported a lower concentration of ammonia in the influent wastewater. This is a result of the differences in the diurnal volumetric flows coming into the treatment plant, where early mornings have an increased use of showers and running water which creates a peak volume of influent wastewater but lowers the concentration of ammonia (33). This creates different initial concentrations of ammonia in the reactors, while the actual degradation rate throughout the three reactors in spring is not statistically significant as shown in Supplemental Figure S5.5.

The full-scale sequencing batch reactors in this study, typically perform simultaneous nitrification, denitrification, and phosphorous removal. Similar lab-scale reactors have sustained nitrification, denitrification, and phosphorous removal at temperatures as low as 10°C but have prolonger aeration periods of 4-hours (34). Aeration already accounts for approximately 44% of the operational costs at wastewater treatment facilities, making doubling the period of aeration likely infeasible for most municipalities (35).

Seasonal dynamics of nitrifier abundance and activity

Our results show based on DNA extractions, *amoA* gene copy numbers were stable throughout the year. We observed 5.8±0.7 log(copies/mL) of *amoA* genes, while similar studies have shown between 5.5 and 7.5 log(copies/mL) of *amoA* genes for ammonia oxidizing bacteria in several municipal and industrial wastewater treatment facilities (13, 36, 37). On the RNA level however, we observed a strong correlation of *amoA* transcript copy numbers with temperature. According to the observed trends in wastewater temperature and nitrification performance (Figure 5.1), *amoA* transcript abundance was highest in the fall following a prolonged period of warm summer temperatures (Figure 5.3). The *amoA* transcript abundance was lowest in the spring after month of cold winter temperatures (Figure 5.2). This is consistent with previously reported observations of the seasonal dynamics in cell (38) and transcript (39-41) abundance among nitrifying populations and likely explains why wastewater treatment plants experience seasonal nitrification failure. Interesting to us was that we observed in this study that the 16S rRNA transcript abundance of *Nitrosomonas* spp. did not decrease with decreasing wastewater temperatures. While we quantified the highest abundance of *Nitrosomonas* spp. 16S rRNA transcripts in the fall, the second highest transcript abundances were recorded in spring. This means that *Nitrosomonas* spp. increased their average protein synthesis potential in the spring to a level higher than the observed average protein synthesis potentials quantified for winter and summer (Figure 5.7). This suggests that *Nitrosomonas* spp. are capable of maintaining and increasing their ribosome numbers at low wastewater temperatures, once the temperature stabilizes. If an increase in ribosome counts is indicative of cell metabolic activity and growth, then it appears that the observed increase in protein synthesis potential

in *Nitrosomonas* spp. during the spring is not associated with ammonia oxidation since ammonia concentrations in the effluent are highest during in spring. Also, *Nitrosomonas* spp. cells abundance (16S rRNA gene copy numbers) does not decrease in spring either raising the question of how Nitrosomonas spp. maintains cell growth based on an energy metabolism other than ammonia oxidation.

In order to maintain a constant abundance level in an SBR, cell growth is required in order to avoid washout and a decrease in population abundance. If the growth of *Nitrosomonas* spp. during the cold season is not associated with a measurable extent of ammonia oxidization it might indicate that *Nitrosomonas* spp. are capable of surviving on a minimal amount of energy from ammonia oxidation or switching to an energy metabolism other than ammonia oxidation at lower temperatures in order to be able to continue to grow and maintain a stable population size. Previous studies have demonstrated that *Nitrosomonas europaea* has both nitrite reductase and nitric oxide reductase (42) and several species have urease (20), but whether or not these are predominantly used by *Nitrosomonas* in activated sludge hasn't been explored. These pathways are all linked to the nitrogen cycle. Instead of predominantly performing ammonia oxidation, perhaps performing multiple steps of the nitrogen cycle as the reactors alternate between aerobic and anaerobic cycles is sufficient for sustained growth. Additionally, all ammonia oxidizing bacteria can fix carbon via the Calvin Cycle and several have specialized carboxysomes for carbon fixation (43-45). While *Nitrospira* comammox organisms are not present in our system, recent analysis has shown they have metabolic diversity possibly due to selective environmental pressures such as oxygen availability(46). These additional sources of energy in *Nitrosomonas,* urease activity, denitrification genes, and carbon

fixation needs to be further analyzed to determine if this community has transcriptional changes in these pathways across seasonal temperature fluctuations.

We also previously observed that general bacterial 16S rRNA transcript copy numbers significantly declined in the winter once reactors start to get aerated with cold ambient air after a sudden cold shock (21). During this cold shock, this study shows the abundance *of amoA* transcript copy numbers only slowly declined in response to the onset of aeration in the winter. This suggests that while the overall protein synthesis potential of the activated sludge microbial community has immediate responses, transcription of *amoA* genes progressively declines and is less impaired by a decline in reactor water temperature. While we observed a correlation between the seasonal abundance of *amoA* transcripts and reactor nitrification performance, the decrease in community 16S rRNA transcripts at onset of aeration during winter indicates a general decline in microbial activity in the activated sludge during cold season reaction cycles. This suggests that the decrease in ammonia removal at colder temperatures is not solely associated with the abundance and activity of uncultured *Nitrosomonas* spp. but also associated with the activity of other activated sludge community members that might directly or indirectly affect ammonia removal from wastewater. While we expected to quantify differences in *amoA* transcript copy numbers, switching from the mainly anoxic mixed fill reactor to the react cycles with active sludge aeration, the rather consistent *amoA* transcript copy numbers transitioning from mixed fill to aeration might be due to the previously reported finding that *amoA* expression is controlled and regulated by the presence and concentration of ammonium, not oxygen (47). There appeared to be significant declines during DW, and increases during SS, which

is most likely a result of the settling process removing concentrated nitrifying flocs from DW, and settling them into the bulking activated sludge in SS.

Phylogeny of amoA Sequences

Overall, we observed little seasonal variation in *amoA* phylogeny, and no significant differences between the triplicate sequencing batch reactors ammonia oxidizing community. The lack of seasonal variations in ammonia oxidizer populations has been previously reported in 12 wastewater treatment plants near Tokyo (48), however, these treatment plants are in a subtropical climate where their reported air temperatures varied between 14°C to 31°C whereas we observed air temperatures between -34°C to 28°C. The vast majority of sequences from the SF influent wastewater as well as in the activated sludge community come from uncultured strains of *Nitrosomonas* and *Nitrosococcus.* In fact, only 4 ASV clusters were cultured species accounting for 3.5%±2.8% of the *amoA* gene relative abundances, and only 1.6%±1.3% of the *amoA* transcript relative abundances. This is reflective of "The Great Plate Counting Anomaly (49)," where the majority of available reference genes is dependent on the few cultured organisms. Our results show similar trends of predominantly unknown *Nitrosomonas* species to Wang et al 2010 (50) who performed T-RFLP fingerprinting over various wastewater treatment plants. However, they did not report any *Nitrosococcus* despite our study using the same forward primers and only slight variations in reverse primers. Additionally, neither of our previous 16S rRNA amplicon sequencing datasets (13) detected *Nitrosococcus* which might be a limitation in the 16S rRNA primer selection (17). Alternatively, this might be a cluster

from *Nitrosomonas* europaea Nm50, which has an extremely similar *amoA* amplicon, potentially from horizontal gene transfer (51).

Transcript Expression

We determined the ratio of relative abundances of *amoA* transcripts to *amoA* genes as a normalization of the cellular activity for each ASV cluster. The Faiths phylogenetic diversity index (Supplemental Figure S5.3) indicated that there is less diversity of organisms expressing *amoA* transcripts than there were with the functional gene, making most ASV clusters have low transcript-to-gene ratios. The vast majority of transcripts and ammonia oxidation occurring might belong to an uncultured group of *Nitrosomonas* sp, but their ratio of transcripts-to-genes was only slightly greater than one-to-one at 1.3±0.1 transcripts/genes. The most active ASV per *amoA* gene, across all four seasons was *Nitrosospira* briensis which averaged 17.5±3.5 transcripts/genes. *Nitrosospira* briensis's resilience has been demonstrated before in ammonia starvation experiments where the *amoA* transcription rate slowly depleted over a week without significant changes to biomass (52). *Nitrosospira* briensis was first isolated by Helene Winogradsky, and is typically found in freshwater ecosystems, agricultural fields, and meadows (53, 54). It is currently unclear why this organism appears to have such a high activity per cell yet remain at such low abundances in activated sludge. There might be competition or significant environmental pressures which minimize cellular growth (55). Unfortunately, few studies have focused on *Nitrosospira* briensis in engineered systems. Further research should explore how to leverage what appears to be a particularly active species of ammonia oxidizers, throughout seasonal variations, to mitigate seasonal nitrification failure.

Conclusions

This study is the first major investigation into the seasonal dynamics of ammonia monooxygenase transcript expression in full-scale activated sludge sequencing batch reactors. Throughout this study we have demonstrated: 1) there are strong seasonal patterns to the *amoA* transcript expression likely resulting in seasonal nitrification failure. 2) the lack of seasonal fluctuations in *amoA* gene abundance and uncultured *Nitrosomonas* spp. 16S rRNA transcripts suggest stable cellular functions such as protein synthesis potential and open the potential for other metabolic functions for energy. 3) There are clusters of ammonia oxidizers such as *Nitrosospira* briensis which have higher transcript expressions than other organisms that could be leveraged for more effective nitrification performance in wastewater treatment facilities. Understanding how the phylogeny and expression of *amoA* transcripts varies provides a basis to reevaluate how nitrification is handled presently in most wastewater treatment plants, and design around the most active nitrifiers to prevent seasonal nitrification failure.

Acknowledgements

We would like to thank the team at Brainerd Wastewater Treatment Facilities for sample collection and access to treatment plant performance data. Additional thanks to Laurel Hunt, Deirdre Manion-Fischer and Michael Brown for their assistance during sampling trips. We would like to thank the University of Minnesota Genomics Center for assistance with amplicon sequencing. We would like to thank the National Science Foundation Graduate Research Fellows Program for providing Juliet Johnston with a fellowship opportunity as well as the Legislative-Citizen Commission on Minnesota Resources for funding the project. J. Johnston was supported by the National Science Foundation Graduate Research Fellowship Program (ID: 2015191729). The research was enabled by the Legislative-Citizen Commission on Minnesota Resources (LCCMR) through a grant entitled "Wastewater Treatment Process Improvements" funded by the Environment and Natural Resources Trust Fund (ENRTF) under legal citation M.L. 2016, Chp. 186, Sec. 2, Subd. 04 k.

Chapter 6

Conclusions

Summary of Conclusions

This thesis is a culmination of three major publications centering around seasonal fluctuations in the activated sludge microbiome and an exploration into the kinetic activity of the ammonia oxidizing community in sequencing batch reactors. Throughout this complete body of works, six major conclusions were drawn and are summarized below.

There exists a replicable core community and seasonal community in activated sludge sequencing batch reactors. Chapter 1 presents 114 OTUs which were found in the triplicate sequencing batch reactors at every week for an entire year. These OTUs varied between 74.3% of the activated sludge composition in the warmer seasons where there is overall more diversity, up to 82.5% of the activated sludge composition in the colder months when diversity and species richness is significantly lower. Chapter 3 explored a very similar subset of 108 OTUs which met three criteria for constant abundance, constant protein synthesis potential, and constant growth which fluctuates between 63.2% up to 84.0% of the community composition based on 16S rRNA genes, and 53.5% to 90.6% based on 16S rRNA transcripts.

While Chapter 1 and Chapter 3 present different definitions of the core microbiome focusing on either persistent presence or the three criteria, they both reveal that in completely independent sequencing batch reactors with negligible differences in influent wastewater and operational parameters exists highly similar and synchronous activated sludge systems. This concept of a core wastewater treatment plant has been explored before, but these comparisons are across different treatment plants and geographies. Most

conventional wastewater treatment plants have only one reactor which offers only technical replication to be processed. Replicable core microbiomes in such a complex and dynamic full-scale system provides significant insight into the assembly of the activated sludge microbial community composition.

Core OTUs such as *Mitrothrix* and *Tetrasphaera* are common to numerous activated sludge systems, OTUs like *Saprospiraceae* do experience significant seasonality with higher abundances in the summer and declines in the winter which might change the floccular formation of activated sludge. Knowing which organisms are expected to be present and at which abundance throughout the seasons enables us to quickly assess variations when non-ideal operations occur. Even recognizing that organisms such as *Nitrosomonas* and *Nitrotoga* are core OTUs despite unstable performance reveals there may be other OTUs and attributing factors to seasonal nitrification than simply loss in metabolic activity. Our inclusion of 16S rRNA transcript sequencing and quantification enables researchers to have a baseline understanding of how the activity of these organisms fluctuates throughout the season and if there are significant periods of growth and proliferation or inactivity throughout the year.

These replicable core microbiomes also conversely apply to organisms which were transient or not growing in the activated sludge system. The activated sludge community composition is so rich and diverse that it is potentially difficult to assess which organisms are insignificant or negligible during operations. By analyzing which OTUs were not present across all three reactors and understanding what percentage of influent wastewater OTUs do not grow, we are able to presume these OTUs are not likely candidates for causing disruptions in operational performance.

Ultimately, our characterization of the core microbiome, and Chapter 3's core criteria which included 16S rRNA transcript composition and activity, we are able to more accurately define how the activated sludge microbiome assembles and generate stronger hypotheses of what to expect in further research.

Temperature is the driving factor for the changes in the activated sludge community composition, protein synthesis potential, given stable operational parameters. Previous studies have shown that the type of influent wastewater and the sludge retention time are the two most important factors when determining the activated sludge community composition. In our study, the influent wastewater was consistently domestic wastewater, which is a steady, homogenous chemical composition. Additionally, the sludge retention time made the most significant impacts when increased between 4-6 days up to 7-10 days since numerous organisms such as nitrifying bacteria rely on prolonged sludge retention times. After 7-10 days, distinctions between conventional activated sludge (SRT 7 -10 days) and membrane bioreactors (infinitely long SRT) do not appear to have significant compositional distinctions and synchronize with temperature.

Since the Brainerd Wastewater Treatment Plant consistently maintained sludge retention times longer than 7 days and the predominantly handles domestic wastewater, temperature was the driving factor in community composition. This has been previously shown in conventional treatment plants, and membrane bioreactors, but our results in Chapter 1 defined that temperature predicted the community composition in triplicate reactors. Additionally, the few annual studies grab samples only once a month or twice a year, while the vast majority of activated sludge community composition studies only

sample once per year. Our weekly sampling provides a high-resolution and steady shift in how the activated sludge microbiome changes throughout the year. We were able to show that the exact same temperature, does not fully indicate the same community composition. Instead, knowing both temperature and whether the temperature was increasing in the spring to summer seasons or decreasing in the fall to winter seasons made a significant impact what the activated sludge community composition dynamics.

This was followed-up in Chapter 3 which was able to identify OTUs that were in various growth or decline stages by using 16S rRNA transcript amplicon sequencing to identify OTUs fluctuating in protein synthesis potential. Ultimately, this calls upon future researchers to include more specific information about when their samples were taken, and how active their community composition was at the time. It is insufficient to merely state which temperature a sample was collected at; sample collection requires an understanding of seasonality to accurately determine the activated sludge community compositions stage in growth. The combined results in Chapter 1 and Chapter 3 signify that given stable influent and sludge retention time, temperature with the season are the biggest factors in understanding the activated sludge community composition dynamics.

Variations in the dissolved oxygen profiles do not significantly impact the performance of nitrification. The Brainerd Wastewater Treatment Plant largely operates on a computer-controlled system, with specific dissolved oxygen parameters to minimize the expensive costs of aeration during secondary treatment. The system is designed to diffuse air until a maximum of 3.5ppm is reached. The air blowers will shut off until a lower limit of 0.75ppm occurs. This causes several peaks to occur during the 2-hour

aeration, specifically we observed seasonal trends where warmer months had multiple peaks (up to three), and colder months only peaked once during the reaction cycle. Since oxygen levels are known to impact the ammonia oxidizing community when set to a constant dissolved oxygen concentration, we set out to model the unique oxygen profiles observed at the Brainerd Wastewater Treatment Plant and determine their impact.

Chapter 2 highlights how regardless of one, two, or three peaks in the dissolved oxygen profile, there is no observable difference in the expected performance of the ammonia oxidizing community. The impacts of these peaks were negligible as the cumulative sum of oxygen supplied to a reactor was statistically identical. Further analysis may be necessary to understand if these profiles are significantly impacting the heterotrophic bacterial community, especially since Chapter 3 revealed significant changes in the 16S rRNA transcript copy numbers while experiencing a winter cold-shock during aeration, but currently the consistent BOD_5 performance strongly suggests this too is negligible. This data validates that temperature is still the major driving factor in ammonia oxidation and community composition as opposed to shifts in the oxygen profiles. Possibly the two variables, temperature and dissolved oxygen, are inextricably interlinked and need further investigations to discern why these oxygen profiles shift throughout the year. For now, understanding that the dissolved oxygen profiles were not the primary cause of seasonal nitrification failure compelled us to further uncover shifts in the ammonia oxidizing community's phylogeny and transcriptional activity.

Ammonia oxidizing bacteria can maintain stable population abundances, stable protein synthesis potential, yet have variations in *ammonia monooxygenase*

transcriptional activity suggesting an alternative metabolic function. Chapter 1 analyzed the abundance of the ammonia oxidizing community throughout the entire year by two metrics. The first, quantifying the relative abundance of known ammonia oxidizing bacteria from 16S rRNA gene amplicon sequencing revealed consistent abundances between 0.2% and 0.5% of the overall activated sludge composition. The second was a quantification of the *ammonia monooxygenase* functional gene which maintained a stable 5.94±0.56 log(copies/mL) throughout the year. These values were replicated in Chapter 3 which similar levels of relative abundance, gene copy numbers, and using a mass-balance approach of 16S rRNA gene quantification, determined similar levels of absolute abundance in the activated sludge system.

Chapter 3 additionally showed stable protein synthesis potential for known ammonia oxidizing bacteria based on 16S rRNA transcript amplicon sequencing. While there were changes using a mass-balance 16S rRNA transcript approach, the observed changes in sequencing abundance did not align with the temperature changes nor the performance during seasonal nitrification. The only observed changes which correlated to temperature and seasonal nitrification failure was quantifying the *ammonia monooxygenase* transcript via reverse-transcript quantitative polymerase chain reaction. Having stable abundances and protein synthesis potential and observed growth via 16S rRNA gene mass-balance suggests the known ammonia oxidizing bacteria are continually growing and thriving in activated sludge. However, since the anticipated *ammonia monooxygenase* transcript activity significantly changes, this ultimately suggests that there is potential for a shift in metabolic activity for ammonia oxidizing bacteria. There are

several potential pathways indicated by complete genomes of known ammonia oxidizers which future research should explore.

There is a selective growth and proliferation for *Nitrosomonas* species over other known ammonia oxidizing bacteria in sequencing batch reactors. Influent domestic wastewater entering the Brainerd Wastewater Treatment Plant had two predominant ammonia oxidizers based on *amoA* gene amplicon sequencing with relative abundances of 43.75%±8.23% for *Nitrosococcus* sp. and 32.48%±12.18% for *Nitrosomonas* sp. Despite *Nitrosococcus* sp. being slightly more abundant, *Nitrosomonas* sp. dominates influent domestic wastewater in terms of protein synthesis potential measured via *amoA* transcript amplicon sequencing. The *amoA* transcript relative abundances throughout the year were 59.30%±4.11% for *Nitrosomonas* sp. and 26.22%±5.92% for *Nitrosococcus* sp. This becomes evident during the activated sludge process since *Nitrosomonas* sp. is the only OTU to experience significant growth, as shown in Chapter 4 comprising well over 60% of the *amoA* gene composition and over 80% of the *amoA* transcript composition. *Nitrosomonas* sp. appears to be growing and proliferating in domestic wastewater based on the high *amoA* transcript copy numbers, which leads to its continual growth in activated sludge. Most lab based kinetic studies focus on culturable *Nitrosomonas* eutropha, watsonii, and europaea but there is a specific uncultured species that is the most prolific in domestic wastewater treatment processes.

The activated sludge system is not optimized for the most active known ammonia oxidizing organisms present in the system such as *Nitrosospira* briensis. Chapter 4 explores the taxonomy of the abundant ammonia oxidizers based on *amoA* gene amplicon sequencing and the active ammonia oxidizers based on *amoA* transcript amplicon sequencing. When comparing the ratio of relative abundance of *amoA* transcripts-to-genes, the largest group of *Nitrosomonas* sp. present in the system, only had slightly more transcript-to-genes (+30±12%, whereas *Nitrosospira* briensis had over a ten-fold increase in transcripts-to-genes (1651%±345%). *Nitrosomonas* sp. did average 66.61%±5.20% of the overall *amoA* composition and certainly performs the largest percentage of ammonia oxidizing occurring, on a cell-to-cell basis *Nitrosospira* briensis (0.05%±0.04%) appears to be far more active.

This suggests ammonia oxidization performance in wastewater treatment plants have the potential to be more efficient if redesigned around the proliferation of *Nitrosopira* briensis instead of *Nitrosomonas* sp. Further investigations need to explore how the surrounding microbial ecology selects for *Nitrosomonas* over other known ammonia oxidizing bacteria. Despite not being the most active and efficient, *Nitrosomonas* might be the most competitive based on the specific engineering conditions and surrounding microbial ecology.

Future Studies

This thesis presents many new questions and avenues for future researchers to consider. Several of the most significant are outlined below:

Role of *Saprospiraceae* in Activated Sludge Wastewater Treatment Plants

An uncultured *Saprospiraceae* OTU has been identified throughout this study as a core organism in activated sludge and is typically between 1-5% of abundance throughout all activated sludge wastewater treatment studies. This organism additionally has a strong correlation to both temperature and effluent ammonia concentration. While whole genome sequencing studies of *Saprospiraceae* do not indicate nitrogen cycling genes, it is specifically noted that this organism is on the outside of floc structures around the aerobic nitrifying bacteria populations. Further investigations need to study whether the absence or presence of *Saprospiraceae* in activated sludge plays an indirect role in the activity of nitrifying bacteria, and floccular structure.

Temperature Dependent Single-Cell Transcriptomics of Ammonia Oxidizing Bacteria

Nitrosomonas is typically regarded as an ammonia oxidizer despite having numerous functional genes for other functions such as urease enzymes, and denitrification genes. Using single-cell transcriptomics to isolate *Nitrosomonas* at various temperatures, we can discern the activity of each pathway. This will help determine if at low temperatures, *Nitrosomonas* can still maintain basic cellular functions without relying primarily on energy from ammonia oxidation.

Competition in Ammonia Oxidizing Bacteria and Nitrite Oxidizing Bacteria

Nitrification is performed by numerous organisms, with unique sets of genes and rates of gene expression. There is a lot of variation within available functional genes in microbes commonly occurring in wastewater treatment plants between ammonia oxidizers *Nitrosomonas* and *Nitrosospira*, and nitrite oxidizers *Nitrospira*, *Nitrobacter*, and *Nitrotoga*. This becomes more complex with the inclusion of comammox (complete ammonia oxidizing) and anammox (anaerobic ammonia oxidation) bacteria. There is a significant amount of competition for incoming urea and ammonia. Our lab will explore different combinations of organisms to understand how the expression of various functional genes shift based on synergistic and competitive relationships

	Nitrosomonas	***Nitrosococcus***	***Nitrospira***	***Nitrospira (CMX)***	***Nitrotoga***	***Nitrobacter***	***AMX***
Gene	**Ammonia Oxidizer**	**Ammonia Oxidizer**	**Nitrite Oxidizer**	**Ammonia & Nitrite Oxidizer**	**Nitrite Oxidizer**	**Nitrite Oxidizer**	**Shortcut Ammonia Oxidizer**
Urease	Varies	Yes	Yes	Yes	-	Yes	Yes
amo	Yes	Yes	-	Yes	-	-	Yes
hao	Yes	Yes	-	Yes	-	-	Varies
nxr+nas	-	-	Yes	Yes	Yes	Yes	Yes
nir	Yes	-	Yes	Yes	Yes	Yes	Similar?

Table 6.1 shows the distribution of genes available to common genera of ammonia oxidizing and nitrite oxidizing bacteria. Typically, research has focused on interactions of just ammonia oxidation and nitrite oxidation, leaving uncertainty to how these organisms compete for energy using *urease* and *nir* functions

within floc structures. With the addition of recently discovered comammox (CMX) bacteria and advances in molecular techniques, there is a critical need for a reevaluation of competition and cooperation.

Comprehensive List of References

Chapter 1 Introduction References

1. Daims H, Taylor MW, Wagner M. Wastewater treatment: a model system for microbial ecology. Trends Biotechnol. 2006;24(11):483-9.
2. Beneduce L, Spano G, Lamacchia F, Bellucci M, Consiglio F, Head IM. Correlation of seasonal nitrification failure and ammonia-oxidizing community dynamics in a wastewater treatment plant treating water from a saline thermal spa. Ann Microbiol. 2014;64(4):1671-82.
3. Alawi M, Off S, Kaya M, Spieck E. Temperature influences the population structure of nitrite-oxidizing bacteria in activated sludge. Environ Microbiol Rep. 2009;1(3):184-90.
4. Di Trapani D, Christensson M, Torregrossa M, Viviani G, Ødegaard H. Performance of a hybrid activated sludge/biofilm process for wastewater treatment in a cold climate region: Influence of operating conditions. Biochemical Engineering Journal. 2013;77:214-9.
5. Ducey TF, Vanotti MB, Shriner AD, Szogi AA, Ellison AQ. Characterization of a microbial community capable of nitrification at cold temperature. Bioresour Technol. 2010;101(2):491-500.
6. Gonzalez-Martinez A, Munoz-Palazon B, Rodriguez-Sanchez A, Maza-Marquez P, Mikola A, Gonzalez-Lopez J, et al. Start-up and operation of an aerobic granular sludge system under low working temperature inoculated with cold-adapted activated sludge from Finland. Bioresour Technol. 2017;239:180-9.

7. Gonzalez-Martinez A, Sihvonen M, Munoz-Palazon B, Rodriguez-Sanchez A, Mikola A, Vahala R. Microbial ecology of full-scale wastewater treatment systems in the Polar Arctic Circle: Archaea, Bacteria and Fungi. Sci Rep. 2018;8(1):2208.
8. Head MA, Oleszkiewicz JA. Bioaugmentation for nitrification at cold temperatures. Water Res. 2004;38(3):523-30.
9. Hendrickx TL, Kampman C, Zeeman G, Temmink H, Hu Z, Kartal B, et al. High specific activity for anammox bacteria enriched from activated sludge at 10 degrees C. Bioresour Technol. 2014;163:214-21.
10. Hoang V, Delatolla R, Laflamme E, Gadbois A. An Investigation of Moving Bed Biofilm Reactor Nitrification during Long-Term Exposure to Cold Temperatures. Water Environ Res. 2014;86(1):36-42.
11. Niu C, Wu J, Ling H, Wang L. Cold-Shock Resistance of Activated Sludge Microorganisms Strengthened by a Static Magnetic Field. Pol J Environ Stud. 2019;28(3):1847-55.
12. Smith DW, Hrudey SE, International Association on Water Pollution Research. Conference : Toronto O. Design of water and wastewater services for cold climate communities : proceedings of a post-conference seminar held on 28th and 29th June 1980, in Edmonton, Canada in conjunction with the 10th IAWPR Conference held in Toronto, Canada. Oxford ; New York: Oxford ; New York : Pergamon; 1981.
13. Delatolla. Effects of Long Exposure to Low Temperatures on Nitrifying Biofilm and Biomass in Wastewater Treatment. Water Environ Res. 2012;84(4).

14. Dueholm MS, Marques IG, Karst SM, D'Imperio S, Tale VP, Lewis D, et al. Survival and activity of individual bioaugmentation strains. Bioresour Technol. 2015;186:192-9.
15. Leu S-Y, Stenstrom MK. Bioaugmentation to Improve Nitrification in Activated Sludge Treatment. Water Environ Res. 2010;82(6):524-35.
16. Tang HL, Chen H. Nitrification at full-scale municipal wastewater treatment plants: Evaluation of inhibition and bioaugmentation of nitrifiers. Bioresour Technol. 2015;190:76-81.
17. MPCA. Minnesota NPDES Wastewater Permit Nitrogen Monitoring Implementation Plan. Minnesota: Minnesota Pollution Control Agency; 2014.
18. Ardern E, Lockett WT. Experiments on the oxidation of sewage without the aid of filters. Journal of the Society of Chemical Industry. 1914;33(10):523-39.
19. Chen Y, Lan S, Wang L, Dong S, Zhou H, Tan Z, et al. A review: Driving factors and regulation strategies of microbial community structure and dynamics in wastewater treatment systems. Chemosphere. 2017;174:173-82.
20. Huang Z, Gedalanga PB, Asvapathanagul P, Olson BH. Influence of physicochemical and operational parameters on Nitrobacter and Nitrospira communities in an aerobic activated sludge bioreactor. Water Res. 2010;44(15):4351-8.
21. Siripong S, Rittmann BE. Diversity study of nitrifying bacteria in full-scale municipal wastewater treatment plants. Water Res. 2007;41(5):1110-20.

22. Hink L, Gubry-Rangin C, Nicol GW, Prosser JI. The consequences of niche and physiological differentiation of archaeal and bacterial ammonia oxidisers for nitrous oxide emissions. ISME J. 2018;12(4):1084-93.
23. Soliman M, Eldyasti A. Ammonia-Oxidizing Bacteria (AOB): opportunities and applications—a review. Reviews in Environmental Science and Bio/Technology. 2018;17(2):285-321.
24. Daims H, Lucker S, Wagner M. A New Perspective on Microbes Formerly Known as Nitrite-Oxidizing Bacteria. Trends Microbiol. 2016;24(9):699-712.
25. Daims H, Lebedeva EV, Pjevac P, Han P, Herbold C, Albertsen M, et al. Complete nitrification by Nitrospira bacteria. Nature. 2015;528(7583):504-9.
26. van Kessel MA, Speth DR, Albertsen M, Nielsen PH, Op den Camp HJ, Kartal B, et al. Complete nitrification by a single microorganism. Nature. 2015;528(7583):555-9.
27. Alzate Marin JC, Caravelli AH, Zaritzky NE. Nitrification and aerobic denitrification in anoxic-aerobic sequencing batch reactor. Bioresour Technol. 2016;200:380-7.
28. He Q, Zhou J, Song Q, Zhang W, Wang H, Liu L. Elucidation of microbial characterization of aerobic granules in a sequencing batch reactor performing simultaneous nitrification, denitrification and phosphorus removal at varying carbon to phosphorus ratios. Bioresour Technol. 2017;241:127-33.
29. Osaka T, Ebie Y, Tsuneda S, Inamori Y. Identification of the bacterial community involved in methane-dependent denitrification in activated sludge using DNA stable-isotope probing. FEMS Microbiol Ecol. 2008;64(3):494-506.

30. Harter J, Krause HM, Schuettler S, Ruser R, Fromme M, Scholten T, et al. Linking N2O emissions from biochar-amended soil to the structure and function of the N-cycling microbial community. ISME J. 2014;8(3):660-74.
31. Parravicini V, Svardal K, Krampe J. Greenhouse Gas Emissions from Wastewater Treatment Plants. Energy Procedia. 2016;97:246-53.
32. Todt D, Dörsch P. Mechanism leading to N2O production in wastewater treating biofilm systems. Reviews in Environmental Science and Bio/Technology. 2016;15(3):355-78.
33. Kennicutt MC. Water Quality of the Gulf of Mexico. In: Ward CH, editor. Habitats and Biota of the Gulf of Mexico: Before the Deepwater Horizon Oil Spill: Volume 1: Water Quality, Sediments, Sediment Contaminants, Oil and Gas Seeps, Coastal Habitats, Offshore Plankton and Benthos, and Shellfish. New York, NY: Springer New York; 2017. p. 55-164.
34. Laurent A, Fennel K, Ko DS, Lehrter J. Climate Change Projected to Exacerbate Impacts of Coastal Eutrophication in the Northern Gulf of Mexico. Journal of Geophysical Research: Oceans. 2018;123(5):3408-26.
35. Lewis WM, Wurtsbaugh WA, Paerl HW. Rationale for Control of Anthropogenic Nitrogen and Phosphorus to Reduce Eutrophication of Inland Waters. Environ Sci Technol. 2011;45(24):10300-5.

Chapter 2 References

1. Engineering NAo, National Academies of Sciences E, Medicine. Environmental Engineering for the 21st Century: Addressing Grand Challenges. Washington, DC: The National Academies Press; 2018. 120 p.
2. MPCA. Minnesota NPDES Wastewater Permit Nitrogen Monitoring Implementation Plan. Minnesota: Minnesota Pollution Control Agency; 2014.
3. Kuyper MMM. A fight for scraps of ammonia. Nautre News & Views. 2017;549:162.
4. Daims H, Lebedeva EV, Pjevac P, Han P, Herbold C, Albertsen M, et al. Complete nitrification by Nitrospira bacteria. Nature. 2015;528(7583):504-9.
5. van Kessel MA, Speth DR, Albertsen M, Nielsen PH, Op den Camp HJ, Kartal B, et al. Complete nitrification by a single microorganism. Nature. 2015;528(7583):555-9.
6. Gonzalez-Martinez A, Rodriguez-Sanchez A, van Loosdrecht MCM, Gonzalez-Lopez J, Vahala R. Detection of comammox bacteria in full-scale wastewater treatment bioreactors using tag-454pyrosequencing. Environ Sci Pollut Res. 2016;23(24):25501-11.
7. Chao Y, Mao Y, Yu K, Zhang T. Novel nitrifiers and comammox in a full-scale hybrid biofilm and activated sludge reactor revealed by metagenomic approach. Appl Microbiol Biot. 2016;100(18):8225-37.
8. Yuan Q, Oleszkiewicz JA. Low temperature biological phosphorus removal and partial nitrification in a pilot sequencing batch reactor system. Water Science & Technology. 2011;63(12).

9. Gonzalez-Martinez A, Munoz-Palazon B, Rodriguez-Sanchez A, Maza-Marquez P, Mikola A, Gonzalez-Lopez J, et al. Start-up and operation of an aerobic granular sludge system under low working temperature inoculated with cold-adapted activated sludge from Finland. Bioresour Technol. 2017;239:180-9.
10. Wang Y, Zhang Z, Qiu L, Guo Y, Wang X, Xiong X, et al. Effect of temperature downshifts on biological nitrogen removal and community structure of a lab-scale aerobic denitrification process. Biochemical Engineering Journal. 2015;101:200-8.
11. Kosonen H, Heinonen M, Mikola A, Haimi H, Mulas M, Corona F, et al. Nitrous Oxide Production at a Fully Covered Wastewater Treatment Plant: Results of a Long-Term Online Monitoring Campaign. Environ Sci Technol. 2016;50(11):5547-54.
12. Di Trapani D, Christensson M, Torregrossa M, Viviani G, Ødegaard H. Performance of a hybrid activated sludge/biofilm process for wastewater treatment in a cold climate region: Influence of operating conditions. Biochemical Engineering Journal. 2013;77:214-9.
13. Beneduce L, Spano G, Lamacchia F, Bellucci M, Consiglio F, Head IM. Correlation of seasonal nitrification failure and ammonia-oxidizing community dynamics in a wastewater treatment plant treating water from a saline thermal spa. Ann Microbiol. 2014;64(4):1671-82.
14. Guo J, Zhang L, Chen W, Ma F, Liu H, Tian Y. The regulation and control strategies of a sequencing batch reactor for simultaneous nitrification and denitrification at different temperatures. Bioresour Technol. 2013;133:59-67.

15. Yu H, Meng W, Song Y, Tian Z. Understanding bacterial communities of partial nitritation and nitratation reactors at ambient and low temperature. Chemical Engineering Journal. 2018;337:755-63.
16. Ju F, Guo F, Ye L, Xia Y, Zhang T. Metagenomic analysis on seasonal microbial variations of activated sludge from a full-scale wastewater treatment plant over 4 years. Env Microbiol Rep. 2014;6(1):80-9.
17. Zhang S, Wang Y, He W, Wu M, Xing M, Yang J, et al. Impacts of temperature and nitrifying community on nitrification kinetics in a moving-bed biofilm reactor treating polluted raw water. Chemical Engineering Journal. 2014;236:242-50.
18. Gnida A, Wiszniowski J, Felis E, Sikora J, Surmacz-Górska J, Miksch K. The effect of temperature on the efficiency of industrial wastewater nitrification and its (geno)toxicity. Archives of Environmental Protection. 2016;42(1):27-34.
19. Delatolla. Effects of Long Exposure to Low Temperatures on Nitrifying Biofilm and Biomass in Wastewater Treatment. Water Environ Res. 2012;84(4).
20. Hoang V, Delatolla R, Laflamme E, Gadbois A. An Investigation of Moving Bed Biofilm Reactor Nitrification during Long-Term Exposure to Cold Temperatures. Water Environ Res. 2014;86(1):36-42.
21. Griffin JS, Wells GF. Regional synchrony in full-scale activated sludge bioreactors due to deterministic microbial community assembly. ISME J. 2017;11(2):500-11.
22. Gonzalez-Martinez A, Sihvonen M, Munoz-Palazon B, Rodriguez-Sanchez A, Mikola A, Vahala R. Microbial ecology of full-scale wastewater treatment systems in the Polar Arctic Circle: Archaea, Bacteria and Fungi. Sci Rep. 2018;8(1):2208.

23. Ju F, Zhang T. Bacterial assembly and temporal dynamics in activated sludge of a full-scale municipal wastewater treatment plant. ISME J. 2015;9(3):683-95.
24. Muszyński A, Tabernacka A, Miłobędzka A. Long-term dynamics of the microbial community in a full-scale wastewater treatment plant. International Biodeterioration & Biodegradation. 2015;100:44-51.
25. Gao P, Xu W, Sontag P, Li X, Xue G, Liu T, et al. Correlating microbial community compositions with environmental factors in activated sludge from four full-scale municipal wastewater treatment plants in Shanghai, China. Appl Microbiol Biotechnol. 2016;100(10):466373.
26. Saunders AM, Albertsen M, Vollertsen J, Nielsen PH. The activated sludge ecosystem contains a core community of abundant organisms. ISME J. 2016;10(1):11-20.
27. Valentin-Vargas A, Toro-Labrador G, Massol-Deya AA. Bacterial community dynamics in fullscale activated sludge bioreactors: operational and ecological factors driving community assembly and performance. Plos One. 2012;7(8):e42524.
28. Ofiteru ID, Lunn M, Curtis TP, Wells GF, Criddle CS, Francis CA, et al. Combined niche and neutral effects in a microbial wastewater treatment community. Proc Natl Acad Sci U S A. 2010;107(35):15345-50.
29. Ayarza JM, Erijman L. Balance of neutral and deterministic components in the dynamics of activated sludge floc assembly. Microb Ecol. 2011;61(3):486-95.
30. Meerburg FA, Vlaeminck SE, Roume H, Seuntjens D, Pieper DH, Jauregui R, et al. High-rate activated sludge communities have a distinctly different structure

compared to low-rate sludge communities, and are less sensitive towards environmental and operational variables. Water Res. 2016;100:137-45.

31. Albertsen M, Karst SM, Ziegler AS, Kirkegaard RH, Nielsen PH. Back to Basics--The Influence of DNA Extraction and Primer Choice on Phylogenetic Analysis of Activated Sludge Communities. Plos One. 2015;10(7):e0132783.
32. Garbe J. Gopher-Pipelines: University of Minnesota; 2017 [Available from: https://bitbucket.org/jgarbe/gopher-pipelines.
33. Yilmaz P, Parfrey LW, Yarza P, Gerken J, Pruesse E, Quast C, et al. The SILVA and "All-species Living Tree Project (LTP)" taxonomic frameworks. Nucleic Acids Res. 2014;42(Database issue):D643-8.
34. J Gregory Caporaso JK, Jesse Stombaugh, Kyle Bittinger, Frederic D Bushman, Elizabeth K Costello, Noah Fierer, Antonio Gonzalez Peña, Julia K Goodrich, Jeffrey I Gordon, Gavin A Huttley, Scott T Kelley, Dan Knights, Jeremy E Koenig, Ruth E Ley, Catherine A Lozupone, Daniel McDonald, Brian D Muegge, Meg Pirrung, Jens Reeder, Joel R Sevinsky, Peter J Turnbaugh, William A Walters, Jeremy Widmann, Tanya Yatsunenko, Jesse Zaneveld & Rob Knight. QIIME allows analysis of high-throughput community sequencing data. Nature Methods. 2010(7).
35. RStudio-Team. RStudio: Integrated Development for R. RStudio Incorporated; 2015.
36. Jari Oksanen FGB, Michael Friendly, Roeland Kindt, Pierre Legendre, Dan McGlinn, Peter R. Minchin, R. B. O'Hara, Gavin L. Simpson, Peter, Solymos

MHHS, Eduard Szoecs and Helene Wagner. Ecology Package. R Package Version 24-4: vegan: Community; 2017.

37. Weisberg S. Applied Linear Regression. Fourth Edition ed. Hooken NJ: Wiley; 2014.
38. Davis ML. Water and Wastewater Engineering: Design Principles and Practice. Professional ed: McGraw-Hill Education; 2010.
39. Shannon W. The Mathematical Theory of Communication. Urbana, USA: University of Illinois Press; 1949.
40. Simpson E. Measurement of Diversity. Nature. 1949;163(688):163.
41. Hughes JB, Hellmann JJ, Ricketts TH, Bohannan BJM. Counting the Uncountable: Statistical Approaches to Estimating Microbial Diversity. Appl Environ Microbiol. 2001;67(10):4399-406.
42. Roger Bray TC. An Ordination of the Upland Forest Communitiies of Southern Wisconsin. Ecological Monographs. 1957;27(4):325-49.
43. Danielsson P-E. Euclidean Disance Mapping. Computer Graphics and Image Processing. 1980;14:227.
44. Coyotzi S, Pratscher J, Murrell JC, Neufeld JD. Targeted metagenomics of active microbial populations with stable-isotope probing. Curr Opin Biotechnol. 2016;41:1-8.
45. Pjevac P, Schauberger C, Poghosyan L, Herbold CW, van Kessel MAHJ, Daebeler A, et al. AmoA-Targeted Polymerase Chain Reaction Primers for the Specific Detection and Quantification of Comammox Nitrospira in the Environment. Frontiers in Microbiology. 2017;8.

46. Flowers JJ, Cadkin TA, McMahon KD. Seasonal bacterial community dynamics in a full-scale enhanced biological phosphorus removal plant. Water Res. 2013;47(19):7019-31.
47. Fuhrman JA, Hewson I, Schwalbach MS, Steele JA, Brown MV, Naeem S. Annually reoccurring bacterial communities are predictable from ocean conditions. Proc Natl Acad Sci U S A. 2006;103(35):13104-9.
48. Ashley Shade, Angela D. Kent, Stuart E. Jones, Ryan J. Newton, Eric W. Triplett, Katherine D. McMahon. Interannual Dyanmics and Phenology of Bacterial Communities in a Eutrophic Lake. Limnology and Oceanography. 2007;52(2):487-94.
49. Shade A, Caporaso JG, Handelsman J, Knight R, Fierer N. A meta-analysis of changes in bacterial and archaeal communities with time. ISME J. 2013;7(8):1493-506.
50. Faust K, Raes J. Microbial interactions: from networks to models. Nat Rev Microbiol. 2012;10(8):538-50.
51. Berry D, Widder S. Deciphering microbial interactions and detecting keystone species with cooccurrence networks. Front Microbiol. 2014;5:219.
52. Xia Y, Kong Y, Thomsen TR, Halkjaer Nielsen P. Identification and ecophysiological characterization of epiphytic protein-hydrolyzing saprospiraceae ("Candidatus Epiflobacter" spp.) in activated sludge. Appl Environ Microbiol. 2008;74(7):2229-38.
53. Guo J, Ni BJ, Han X, Chen X, Bond P, Peng Y, et al. Unraveling microbial structure and diversity of activated sludge in a full-scale simultaneous nitrogen and

phosphorus removal plant using metagenomic sequencing. Enzyme Microb Technol. 2017;102:16-25.

54. Guo Y, Peng Y, Wang B, Li B, Zhao M. Achieving simultaneous nitrogen removal of low C/N wastewater and external sludge reutilization in a sequencing batch reactor. Chemical Engineering Journal. 2016;306:925-32.
55. E. Morgenroth, R. Kommedal, Harremoes P. Processes and modeling of hydrolysis of particulate organic matter in aerobic wastewater treatment- a review. Water Science & Technology. 2002;45(6):45-50.
56. Nielsen PH, Mielczarek AT, Kragelund C, Nielsen JL, Saunders AM, Kong Y, et al. A conceptual ecosystem model of microbial communities in enhanced biological phosphorus removal plants. Water Res. 2010;44(17):5070-88
57. Reza M, Alvarez Cuenca M. Nitrification and denitrifying phosphorus removal in an upright 854 continuous flow reactor. Water Sci Technol. 2016;73(9):2093-100.

Chapter 3 References

1. Gao, D.; Peng, Y.; Wu, W.; Kinetic Model for Biologic Nitrogen Removal Using Shortcut Nitrification-Denitrification Processes in Sequencing Batch Reactor. *Environ. Sci. Technol.;* 2010, 44, 5015-5021
2. Gujer, W.; Henze, M.; Mino, T.; van Loosdrecht, M. Activated sludge model No. 3. *Water Sci.Technol.* 1999, *39*, 183–193.
3. Stark, J. Modeling the temperature response of Nitrification. *Biogeochemistry.* 1996, 35, 433 – 445
4. Davis, M.L. *Water and Wastewater Engineering: Design Principles and Practice*, Edn. Professional. (McGraw-Hill Education, 2010).
5. Martens-Habbena W.; Stahl, D., Nitrogen metabolism and kinetics of ammonia-oxidizing archaea. *Methods Enzymol.* 2011, 496, 465 – 487
6. Soliman, M.; Eldyasti, A.; Ammonia-Oxidizing Bacteria: Opportunities and applications- a review. *Environ. Sci. Biotechnol.* 2018, 17, 285 - 321

Chapter 4 References

1. Daims H, Taylor MW, Wagner M. Wastewater treatment: a model system for microbial ecology. Trends Biotechnol. 2006;24(11):483-9.
2. Ofiteru ID, Lunn M, Curtis TP, Wells GF, Criddle CS, Francis CA, et al. Combined niche and neutral effects in a microbial wastewater treatment community. Proc Natl Acad Sci U S A. 2010;107(35):15345-50.
3. Johnston J, LaPara T, Behrens S. Composition and Dynamics of the Activated Sludge Microbiome during Seasonal Nitrification Failure. Sci Rep. 2019;9(1):4565.
4. Wu L, Ning D, Zhang B, Li Y, Zhang P, Shan X, et al. Global diversity and biogeography of bacterial communities in wastewater treatment plants. Nature Microbiology. 2019;4(7):1183-95.
5. Newton RJ, McLellan SL, Dila DK, Vineis JH, Morrison HG, Eren AM, et al. Sewage Reflects the Microbiomes of Human Populations. mBio. 2015;6.
6. Yasong C, Junling L, Zheng Z, Huiping C, Yuke P, Lin X. Nitrogen removal and responses of bacterial communities in activated sludge under different operational manipulations. Water Sci Technol. 2019;79(4):607-18.
7. Griffin JS, Wells GF. Regional synchrony in full-scale activated sludge bioreactors due to deterministic microbial community assembly. ISME J. 2017;11(2):500-11.
8. Cao CY, Lou IC, Huang C, Lee MY. Metagenomic sequencing of activated sludge filamentous bacteria community using the Ion Torrent platform. Desalin Water Treat. 2016;57(5):2175-83.

9. Gao P, Xu W, Sontag P, Li X, Xue G, Liu T, et al. Correlating microbial community compositions with environmental factors in activated sludge from four full-scale municipal wastewater treatment plants in Shanghai, China. Appl Microbiol Biotechnol. 2016;100(10):4663-73.
10. Saunders AM, Albertsen M, Vollertsen J, Nielsen PH. The activated sludge ecosystem contains a core community of abundant organisms. ISME J. 2016;10(1):11-20.
11. Ju F, Guo F, Ye L, Xia Y, Zhang T. Metagenomic analysis on seasonal microbial variations of activated sludge from a full-scale wastewater treatment plant over 4 years. Env Microbiol Rep. 2014;6(1):80-9.
12. Jiang XT, Guo F, Zhang T. Population Dynamics of Bulking and Foaming Bacteria in a Full-scale Wastewater Treatment Plant over Five Years. Sci Rep. 2016;6:24180.
13. Ju F, Zhang T. Bacterial assembly and temporal dynamics in activated sludge of a full-scale municipal wastewater treatment plant. ISME J. 2015;9(3):683-95.
14. McIlroy SJ, Saunders AM, Albertsen M, Nierychlo M, McIlroy B, Hansen AA, et al. MiDAS: the field guide to the microbes of activated sludge. Database (Oxford). 2015;2015.
15. Gentile G, Giuliano L Fau - D'Auria G, D'Auria G Fau - Smedile F, Smedile F Fau - Azzaro M, Azzaro M Fau - De Domenico M, De Domenico M Fau - Yakimov MM, et al. Study of bacterial communities in Antarctic coastal waters by a combination of 16S rRNA and 16S rDNA sequencing. (1462-2912).

16. Deutscher MP. Degradation of RNA in bacteria: comparison of mRNA and stable RNA. (1362-4962).
17. Novitsky JA, Karl DM. Characterization of microbial activity in the surface layers of a coastal sub-tropical sediment. Marine Ecology Progress Series. 1986;28(1/2):49-55.
18. Blazewicz SJ, Barnard RL, Daly RA, Firestone MK. Evaluating rRNA as an indicator of microbial activity in environmental communities: limitations and uses. The ISME journal. 2013;7(11):2061-8.
19. Campbell BJ, Yu L Fau - Heidelberg JF, Heidelberg Jf Fau - Kirchman DL, Kirchman DL. Activity of abundant and rare bacteria in a coastal ocean. (1091-6490).
20. Gaidos E, Rusch A Fau - Ilardo M, Ilardo M. Ribosomal tag pyrosequencing of DNA and RNA from benthic coral reef microbiota: community spatial structure, rare members and nitrogen-cycling guilds. (1462-2920).
21. Hunt DE, Lin Y, Church MJ, Karl DM, Tringe SG, Izzo LK, et al. Relationship between Abundance and Specific Activity of Bacterioplankton in Open Ocean Surface Waters. Appl Environ Microbiol. 2013;79(1):177.
22. Jones SE, Lennon JT. Dormancy contributes to the maintenance of microbial diversity. Proceedings of the National Academy of Sciences. 2010;107(13):5881.
23. Lanzen A, Jorgensen Sl Fau - Bengtsson MM, Bengtsson Mm Fau - Jonassen I, Jonassen I Fau - Ovreas L, Ovreas L Fau - Urich T, Urich T. Exploring the composition and diversity of microbial communities at the Jan Mayen hydrothermal vent field using RNA and DNA. (1574-694).

24. Weigold P, Ruecker A, Loesekann-Behrens T, Kappler A, Behrens S. Ribosomal Tag Pyrosequencing of DNA and RNA Reveals “Rare” Taxa with High Protein Synthesis Potential in the Sediment of a Hypersaline Lake in Western Australia. Geomicrobiology Journal. 2016;33(5):426-40.
25. Davis ML. Water and Wastewater Engineering: Design Principles and Practice. Professional ed: McGraw-Hill Education; 2010.
26. Ulrich Nubel FG-P, Gerard Muyzer. PCR Primers To Amplify 16S rRNA Genes from Cyanobacteria. Appl Environ Microbiol. 1997;63(8).
27. Cohen MA, Ryan PB. Observations Less than the Analytical Limit of Detection: A New Approach. Japca. 1989;39(3):328-9.
28. Gohl DM, Vangay P, Garbe J, MacLean A, Hauge A, Becker A, et al. Systematic improvement of amplicon marker gene methods for increased accuracy in microbiome studies. Nat Biotechnol. 2016;34(9):942-9.
29. RStudio-Team. RStudio: Integrated Development for R. RStudio Incorporated; 2015.
30. Callahan BJ, McMurdie PJ, Rosen MJ, Han AW, Johnson AJA, Holmes SP. DADA2: High-resolution sample inference from Illumina amplicon data. Nature Methods. 2016;13:581.
31. Yilmaz P, Parfrey LW, Yarza P, Gerken J, Pruesse E, Quast C, et al. The SILVA and "All-species Living Tree Project (LTP)" taxonomic frameworks. Nucleic Acids Res. 2014;42(Database issue):D643-8.
32. Jari Oksanen FGB, Michael Friendly, Roeland Kindt, Pierre Legendre, Dan McGlinn, Peter R. Minchin, R. B. O'Hara, Gavin L. Simpson, Peter, Solymos

MHHS, Eduard Szoecs and Helene Wagner. Ecology Package. R Package Version 24-4: vegan: Community; 2017.

33. Roger Bray TC. An Ordination of the Upland Forest Communitiies of Southern Wisconsin. Ecological Monographs. 1957;27(4):325-49.
34. Head MA, Oleszkiewicz JA. Bioaugmentation for nitrification at cold temperatures. Water Res. 2004;38(3):523-30.
35. Gao WJ, Qu X, Leung KT, Liao BQ. Influence of temperature and temperature shock on sludge properties, cake layer structure, and membrane fouling in a submerged anaerobic membrane bioreactor. Journal of Membrane Science. 2012;421-422:131-44.
36. Niu C, Wu J, Ling H, Wang L. Cold-Shock Resistance of Activated Sludge Microorganisms Strengthened by a Static Magnetic Field. Pol J Environ Stud. 2019;28(3):1847-55.
37. Garcia MJ, Nuñez MC, Cox RA. Measurement of the Rates of Synthesis of Three Components of Ribosomes of Mycobacterium fortuitum: A Theoretical Approach to qRT-PCR Experimentation. PLOS ONE. 2010;5(7):e11575.
38. Couturier MR, Slechta ES, Goulston C, Fisher MA, Hanson KE. Leptotrichia Bacteremia in Patients Receiving High-Dose Chemotherapy. Journal of Clinical Microbiology. 2012;50(4):1228.
39. Collado L, Figueras MJ. Taxonomy, epidemiology, and clinical relevance of the genus Arcobacter. Clin Microbiol Rev. 2011;24(1):174-92.

40. Wong D, Nielsen TB, Bonomo RA, Pantapalangkoor P, Luna B, Spellberg B. Clinical and Pathophysiological Overview of Acinetobacter Infections: a Century of Challenges. Clin Microbiol Rev. 2017;30(1):409.
41. Numberger D, Ganzert L, Zoccarato L, Mühldorfer K, Sauer S, Grossart H-P, et al. Characterization of bacterial communities in wastewater with enhanced taxonomic resolution by full-length 16S rRNA sequencing. Sci Rep. 2019;9(1):9673.
42. Forbes BA, Hall GS, Miller MB, Novak SM, Rowlinson M-C, Salfinger M, et al. Practice Guidelines for Clinical Microbiology Laboratories: Mycobacteria. Clin Microbiol Rev. 2018;31(2):e00038-17.
43. Nittami T, Shoji T, Koshiba Y, Noguchi M, Oshiki M, Kuroda M, et al. Investigation of prospective factors that control Kouleothrix (Type 1851) filamentous bacterial abundance and their correlation with sludge settleability in full-scale wastewater treatment plants. Process Safety and Environmental Protection. 2019;124:137-42.
44. Speirs LBM, Rice DTF, Petrovski S, Seviour RJ. The Phylogeny, Biodiversity, and Ecology of the Chloroflexi in Activated Sludge. Frontiers in Microbiology. 2019;10:2015.
45. Arenskötter M, Bröker D, Steinbüchel A. Biology of the metabolically diverse genus Gordonia. Appl Environ Microbiol. 2004;70(6):3195-204.
46. Xia Y, Kong Y, Thomsen TR, Halkjaer Nielsen P. Identification and ecophysiological characterization of epiphytic protein-hydrolyzing saprospiraceae

("Candidatus Epiflobacter" spp.) in activated sludge. Appl Environ Microbiol. 2008;74(7):2229-38.

47. McIlroy SJ, Starnawska A, Starnawski P, Saunders AM, Nierychlo M, Nielsen PH, et al. Identification of active denitrifiers in full-scale nutrient removal wastewater treatment systems. Environmental Microbiology. 2016;18(1):50-64.
48. Gunther S, Trutnau M, Kleinsteuber S, Hause G, Bley T, Roske I, et al. Dynamics of polyphosphate-accumulating bacteria in wastewater treatment plant microbial communities detected via DAPI (4',6'-diamidino-2-phenylindole) and tetracycline labeling. Appl Environ Microbiol. 2009;75(7):2111-21.
49. Daims H, Lebedeva EV, Pjevac P, Han P, Herbold C, Albertsen M, et al. Complete nitrification by Nitrospira bacteria. Nature. 2015;528(7583):504-9.

Chapter 5 References

1. Butler D, Friedler E, Gatt K. Characterising the quantity and quality of domestic wastewater inflows. Water Sci Technol. 1995;31(7):13-24.

2. Engineering NAo, National Academies of Sciences E, Medicine. Environmental Engineering for the 21st Century: Addressing Grand Challenges. Washington, DC: The National Academies Press; 2018. 120 p.

3. MPCA. Minnesota NPDES Wastewater Permit Nitrogen Monitoring Implementation Plan. Minnesota: Minnesota Pollution Control Agency; 2014.

4. Tang HL, Chen H. Nitrification at full-scale municipal wastewater treatment plants: Evaluation of inhibition and bioaugmentation of nitrifiers. Bioresour Technol. 2015;190:76-81.

5. Alawi M, Off S, Kaya M, Spieck E. Temperature influences the population structure of nitrite-oxidizing bacteria in activated sludge. Environ Microbiol Rep. 2009;1(3):184-90.

6. Ducey TF, Vanotti MB, Shriner AD, Szogi AA, Ellison AQ. Characterization of a microbial community capable of nitrification at cold temperature. Bioresour Technol. 2010;101(2):491-500.

7. Di Trapani D, Christensson M, Torregrossa M, Viviani G, Ødegaard H. Performance of a hybrid activated sludge/biofilm process for wastewater treatment in a cold climate region: Influence of operating conditions. Biochemical Engineering Journal. 2013;77:214-9.

8. Gonzalez-Martinez A, Munoz-Palazon B, Rodriguez-Sanchez A, Maza-Marquez P, Mikola A, Gonzalez-Lopez J, et al. Start-up and operation of an aerobic granular

sludge system under low working temperature inoculated with cold-adapted activated sludge from Finland. Bioresour Technol. 2017;239:180-9.

9. Head MA, Oleszkiewicz JA. Bioaugmentation for nitrification at cold temperatures. Water Res. 2004;38(3):523-30.

10. Hoang V, Delatolla R, Laflamme E, Gadbois A. An Investigation of Moving Bed Biofilm Reactor Nitrification during Long-Term Exposure to Cold Temperatures. Water Environ Res. 2014;86(1):36-42.

11. Delatolla. Effects of Long Exposure to Low Temperatures on Nitrifying Biofilm and Biomass in Wastewater Treatment. Water Environ Res. 2012;84(4).

12. He S, Ding L, Pan Y, Hu H, Ye L, Ren H. Nitrogen loading effects on nitrification and denitrification with functional gene quantity/transcription analysis in biochar packed reactors at 5 °C. Sci Rep. 2018;8(1):9844.

13. Johnston J, LaPara T, Behrens S. Composition and Dynamics of the Activated Sludge Microbiome during Seasonal Nitrification Failure. Sci Rep. 2019;9(1):4565.

14. Daims H, Lebedeva EV, Pjevac P, Han P, Herbold C, Albertsen M, et al. Complete nitrification by Nitrospira bacteria. Nature. 2015;528(7583):504-9.

15. Pjevac P, Schauberger C, Poghosyan L, Herbold CW, van Kessel MAHJ, Daebeler A, et al. AmoA-Targeted Polymerase Chain Reaction Primers for the Specific Detection and Quantification of Comammox Nitrospira in the Environment. Frontiers in Microbiology. 2017;8.

16. Blazewicz SJ, Barnard RL, Daly RA, Firestone MK. Evaluating rRNA as an indicator of microbial activity in environmental communities: limitations and uses. The ISME journal. 2013;7(11):2061-8.

17. Albertsen M, Karst SM, Ziegler AS, Kirkegaard RH, Nielsen PH. Back to Basics--The Influence of DNA Extraction and Primer Choice on Phylogenetic Analysis of Activated Sludge Communities. Plos One. 2015;10(7):e0132783.

18. Rotthauwe JH, Witzel KP, Liesack W. The ammonia monooxygenase structural gene amoA as a functional marker: molecular fine-scale analysis of natural ammonia-oxidizing populations. Appl Environ Microbiol. 1997;63(12):4704-12.

19. Purkhold U, Pommerening-Roser A Fau - Juretschko S, Juretschko S Fau - Schmid MC, Schmid Mc Fau - Koops HP, Koops Hp Fau - Wagner M, Wagner M. Phylogeny of all recognized species of ammonia oxidizers based on comparative 16S rRNA and amoA sequence analysis: implications for molecular diversity surveys. (0099-2240 (Print)).

20. Soliman M, Eldyasti A. Ammonia-Oxidizing Bacteria (AOB): opportunities and applications—a review. Reviews in Environmental Science and Bio/Technology. 2018;17(2):285-321.

21. Johnston JB, Sebastian. Seasonal Activity and Community Composition Shifts in Full-Scale Activated Sludge Sequencing Batch Reactors. Applied and Environmental Microbiology 2020.

22. Gohl DM, Vangay P, Garbe J, MacLean A, Hauge A, Becker A, et al. Systematic improvement of amplicon marker gene methods for increased accuracy in microbiome studies. Nat Biotechnol. 2016;34(9):942-9.

23. Callahan BJ, McMurdie PJ, Rosen MJ, Han AW, Johnson AJA, Holmes SP. DADA2: High-resolution sample inference from Illumina amplicon data. Nature Methods. 2016;13:581.

24. RStudio-Team. RStudio: Integrated Development for R. RStudio Incorporated; 2015.

25. Yilmaz P, Parfrey LW, Yarza P, Gerken J, Pruesse E, Quast C, et al. The SILVA and "All-species Living Tree Project (LTP)" taxonomic frameworks. Nucleic Acids Res. 2014;42(Database issue):D643-8.

26. Jari Oksanen FGB, Michael Friendly, Roeland Kindt, Pierre Legendre, Dan McGlinn, Peter R. Minchin, R. B. O'Hara, Gavin L. Simpson, Peter, Solymos MHHS, Eduard Szoecs and Helene Wagner. Ecology Package. R Package Version 24-4: vegan: Community; 2017.

27. Weisberg S. Applied Linear Regression. Fourth Edition ed. Hooken NJ: Wiley; 2014.

28. Meinhardt KA, Bertagnolli A, Pannu MW, Strand SE, Brown SL, Stahl DA. Evaluation of revised polymerase chain reaction primers for more inclusive quantification of ammonia-oxidizing archaea and bacteria. Environ Microbiol Rep. 2015;7(2):354-63.

29. Bolyen E, Rideout JR, Dillon MR, Bokulich NA, Abnet CC, Al-Ghalith GA, et al. Reproducible, interactive, scalable and extensible microbiome data science using QIIME 2 (vol 37, pg 852, 2019). Nat Biotechnol. 2019;37(9):1091-.

30. Price MN, Dehal PS, Arkin AP. FastTree 2-Approximately Maximum-Likelihood Trees for Large Alignments. Plos One. 2010;5(3).

31. Fish JA, Chai BL, Wang Q, Sun YN, Brown CT, Tiedje JM, et al. FunGene: the functional gene pipeline and repository. Frontiers in Microbiology. 2013;4.

32. Faith DP. Conservation evaluation and phylogenetic diversity. Biological Conservation. 1992;61(1):1-10.

33. Ip SY, Kolarik LO, Pilkington NH, Raper WGC, Swinton EA. Physicochemical treatment of an Australian municipal wastewater. Water Res. 1977;11(2):173-80.

34. Li C, Liu S, Ma T, Zheng M, Ni J. Simultaneous nitrification, denitrification and phosphorus removal in a sequencing batch reactor (SBR) under low temperature. Chemosphere. 2019;229:132-41.

35. Sid S, Volant A, Lesage G, Heran M. Cost minimization in a full-scale conventional wastewater treatment plant: associated costs of biological energy consumption versus sludge production. Water Science and Technology. 2017;76(9):2473-81.

36. Limpiyakorn T, Kurisu F Fau - Yagi O, Yagi O. Quantification of ammonia-oxidizing bacteria populations in full-scale sewage activated sludge systems and assessment of system variables affecting their performance. (0273-1223 (Print)).

37. Limpiyakorn T, Sonthiphand P, Rongsayamanont C, Polprasert C. Abundance of amoA genes of ammonia-oxidizing archaea and bacteria in activated sludge of full-scale wastewater treatment plants. Bioresource Technol. 2011;102(4):3694-701.

38. Datta T, Racz L Fau - Kotay SM, Kotay Sm Fau - Goel R, Goel R. Seasonal variations of nitrifying community in trickling filter-solids contact (TF/SC) activated sludge systems. (1873-2976 (Electronic)).

39. Ebie Y, Miura H, Noda N, Matsumura M, Tsuneda S, Hirata A, et al. Detection and quantification of expression of amoA by competitive reverse transcription-PCR. Water Sci Technol. 2002;46(1-2):281-8.

40. Yasong C, Junling L, Zheng Z, Huiping C, Yuke P, Lin X. Nitrogen removal and responses of bacterial communities in activated sludge under different operational manipulations. Water Sci Technol. 2019;79(4):607-18.

41. Araki N, Yamaguchi T, Yamazaki S, Harada H. Quantification of amoA gene abundance and their amoA mRNA levels in activated sludge by real-time PCR. Water Sci Technol. 2004;50(8):1-8.

42. Kozlowski JA, Price J, Stein LY. Revision of N2O-Producing Pathways in the Ammonia-Oxidizing

Bacterium Nitrosomonas europaea ATCC 19718. Appl Environ Microbiol. 2014;80(16):4930.

43. Rae BD, Long BM, Badger MR, Price GD. Functions, compositions, and evolution of the two types of carboxysomes: polyhedral microcompartments that facilitate CO2 fixation in cyanobacteria and some proteobacteria. Microbiol Mol Biol Rev. 2013;77(3):357-79.

44. Marin B, Nowack ECM, Glöckner G, Melkonian M. The ancestor of the Paulinella chromatophore obtained a carboxysomal operon by horizontal gene transfer from a Nitrococcus-like gamma-proteobacterium. BMC Evol Biol. 2007;7:85-.

45. Bollmann A, Sedlacek Cj Fau - Norton J, Norton J Fau - Laanbroek HJ, Laanbroek Hj Fau - Suwa Y, Suwa Y Fau - Stein LY, Stein Ly Fau - Klotz MG, et al. Complete genome sequence of Nitrosomonas sp. Is79, an ammonia oxidizing bacterium adapted to low ammonium concentrations. Standards in Genmic Sciences. 2013(1944-3277 (Print)).

46. Yang Y, Daims H, Liu Y, Herbold CW, Pjevac P, Lin J-G, et al. Activity and Metabolic Versatility of Complete Ammonia Oxidizers in Full-Scale Wastewater Treatment Systems. mBio. 2020;11(2):e03175-19.

47. A. Sayavedra-Soto L, G. Hommes N, A. Russell S, Arp D. Sayavedra-Soto LA, Hommes NG, Russel SA, Arp DJ.. Induction of ammonia monooxygenase and hydroxylamine reductase mRNAs by ammonium in Nitrosomonas europaea. Mol Microbiol 20: 541-5481996. 541-8 p.

48. Limpiyakorn T, Shinohara Y, Kurisu F, Yagi O. Communities of ammonia-oxidizing bacteria in activated sludge of various sewage treatment plants in Tokyo. FEMS Microbiol Ecol. 2005;54(2):205-17.

49. Staley Jt Fau - Konopka A, Konopka A. Measurement of in situ activities of nonphotosynthetic microorganisms in aquatic and terrestrial habitats. (0066-4227 (Print)).

50. Wang X, Wen X, Criddle C, Wells G, Zhang J, Zhao Y. Community analysis of ammonia-oxidizing bacteria in activated sludge of eight wastewater treatment systems. Journal of Environmental Sciences. 2010;22(4):627-34.

51. Juretschko S, Timmermann G, Schmid M, Schleifer K-H, Pommerening-Röser A, Koops H-P, et al. Combined molecular and conventional analyses of nitrifying bacterium diversity in activated sludge: Nitrosococcus mobilis and Nitrospira-like bacteria as dominant populations. Appl Environ Microbiol. 1998;64(8):3042.

52. Bollmann A, Schmidt I, Saunders AM, Nicolaisen MH. Influence of Starvation on Potential Ammonia-Oxidizing Activity and amoA mRNA Levels of Nitrosospira briensis. Appl Environ Microbiol. 2005;71(3):1276.

53. Winogradsky S, Winogradsky H. Études sur la microbiologie du sol. VII. Nouvelles recherches sur les organismes de la nitrification. Ann Inst Pasteur (Paris). 1933;50:350-432.

54. Rice MC, Norton JM, Valois F, Bollmann A, Bottomley PJ, Klotz MG, et al. Complete genome of Nitrosospira briensis C-128, an ammonia-oxidizing bacterium from agricultural soil. Stand Genomic Sci. 2016;11:46-.

55. Costa E, Perez J, Kreft JU. Why is metabolic labour divided in nitrification? Trends Microbiol. 2006;14(5):213-9.

Appendix A Supplemental References

1. Alawi, M., Off, S., Kaya, M., & Spieck, E. (2009). Temperature influences the population structure of nitrite-oxidizing bacteria in activated sludge. *Environ Microbiol Rep, 1*(3), 184-190.
2. 2. Gerda Harms, A. C. L., Heve M. Dionisi, Igrid R. Gregory, Victoria M. Garrett, Shawn A. Hawkins, Kevin G. Robinson, Gary S. Sayler. (2003). Real-Time PCR Quantification of Nitrifying Bacteria in a Municipal Wastewater Treatment Plant. *Environmental Science & Technology, 37*, 343-351.
3. 3. Gesche Braker, A. F., Karl-Paul Witzel. (1998). Development of PCR Primer Systems for Amplification of Nitrite Reductase Genes (nirK and nirS) To Detect Denitrifying Bacteria in Environmental Samples. *Applied and Environmental Microbiology, 64*(10).
4. Harter, J., El-Hadidi, M., Huson, D. H., Kappler, A., & Behrens, S. (2017). Soil biochar amendment affects the diversity of nosZ transcripts: Implications for N2O formation. *Scientific Reports, 7*(1), 3338.
5. Hendrickx, T. L., Kampman, C., Zeeman, G., Temmink, H., Hu, Z., Kartal, B., & Buisman, C. J. (2014). High specific activity for anammox bacteria enriched from activated sludge at 10 degrees C. *Bioresour Technol, 163*, 214-221.
6. Meinhardt, K. A., Bertagnolli, A., Pannu, M. W., Strand, S. E., Brown, S. L., & Stahl, D. A. (2015). Evaluation of revised polymerase chain reaction primers for more inclusive quantification of ammonia-oxidizing archaea and bacteria. *Environ Microbiol Rep, 7*(2), 354-363.

7. Pjevac, P., Schauberger, C., Poghosyan, L., Herbold, C. W., van Kessel, M. A. H. J., Daebeler, A., . . . Daims, H. (2017). AmoA-Targeted Polymerase Chain Reaction Primers for the Specific Detection and Quantification of Comammox Nitrospira in the Environment. *Frontiers in Microbiology*, *8*.

8. Throback, I. N., Enwall, K., Jarvis, A., & Hallin, S. (2004). Reassessing PCR primers targeting nirS, nirK and nosZ genes for community surveys of denitrifying bacteria with DGGE. *FEMS Microbiol Ecol*, *49*(3), 401-417.

9. Ulrich Nubel, F. G.-P., Gerard Muyzer. (1997). PCR Primers To Amplify 16S rRNA Genes from Cyanobacteria. *Applied and Environmental Microbiology*, *63*(8).

Appendix A

Supplementary Information for Chapter 2

Composition and Dynamics of the Activated Sludge Microbiome during Seasonal Nitrification Failure

Table S2.1. Physical and chemical parameters of influent and effluent wastewater at the Brainerd wastewater treatment plant throughout the sampling year from July 2015 to July 2016.

	Temp [°C]	TSS [mg/L] (inf.)	TSS [mg/L] (eff.)	pH (inf.)	pH (eff.)	PO_4^{2-} [mg/L] (inf.)	PO_4^{2-} [mg/L] (eff.)	BOD_5 [mg/L] (inf.)	BOD_5 [mg/L] (eff.)	NH_3 [mg-N/L] (eff.)	Total Inflow (m^3/day)	F/M Ratio	SRT (days)	MLSS (mg/L)	Sludge Blanket (meters)	SVI ml/g
Summer '15	18.35 ± 0.77	411 ± 86	6.1 ± 2.8	7.49 ± 0.23	7.32 ± 0.10	4.92 ± 1.0	0.36 ± 0.2	248 ± 53	3.85 ± 2.2	0.24 ± 0.12	7,306 ± 303	0.0839 ± 0.025	8.28 ± 3.02	1531 ± 394	1.80 ± 0.25	120 ± 14
Fall '15	16.52 ± 1.03	374 ± 105	3.9 ± 1.6	7.49 ± 0.35	7.39 ± 0.13	5.32 ± 1.3	0.44 ± 0.3	236 ± 71	3.96 ± 2.6	0.27 ± 0.24	7,154 ± 379	0.0836 ± 0.027	8.39 ± 2.22	1308 ± 339	1.93 ± 0.44	131 ± 21
Winter '15-16	13.60 ± 0.97	306 ± 62	5.1 ± 1.9	7.52 ± 0.38	7.32 ± 0.11	5.22 ± 0.9	0.25 ± 0.2	193 ± 53	4.22 ± 2.1	4.20 ± 0.79	6,965 ± 303	0.0861 ± 0.025	7.64 ± 1.42	1086 ± 126	1.96 ± 0.28	139 ± 17
Spring '16	14.95 ± 1.28	319 ± 69	4.6 ± 1.9	7.43 ± 0.21	7.28 ± 0.13	4.82 ± 1.0	0.18 ± 0.1	216 ± 61	3.17 ± 1.4	4.54 ± 2.20	7,836 ± 530	0.0814 ± 0.022	8.56 ± 2.03	1303 ± 200	1.78 ± 0.23	96 ± 12
Summer '16	18.48 ± 1.02	454 ± 134	3.4 ± 1.4	7.37 ± 0.17	7.23 ± 0.10	3.99 ± 0.8	0.22 ± 0.1	312 ± 74	2.33 ± 0.84	2.60 ± 0.08	9,577 ± 2650	0.1215 ± 0.019	5.56 ± 1.37	1960 ± 702	1.98 ± 0.29	89 ± 21

Table S2.2. Primer sequences used for quantitative PCR.

Target Gene	Forward Primer Sequence (5'- 3')	Reverse Primer Sequence (5'-3')	Reference
***16S rRNA gene* (V3 region)**	**338-F** CCTACGGGAGGCAGCAG	**518-R** ATTACCGCGGCTGCTGG	(Nübel & Muyzer, 1997)
***amoA* (Bacteria)**	**550-F** TCAGTAGCYGACTACACMGG	**745-R** CTTTAACATAGTAGAAAGCG	(Harms et al. 2003)
***amoA* (Archaea)**	**GenAOA-F** ATAGAGCCTCAAGTAGGAAAGTTCTA	**GenAOA-R** CCAAGCGGCCATCCAGCT GTATGTCC	(Meinhardt et al. 2015)
nirK	**nirK876c** ATYGGCGGVCAYGGCGA	**nirK1040** GCCTCGATCAGRTTRTGG	(Braker et al. 1998)
nirS	**nirSCd3aF** AACGYSAAGGARACSGG	**nirSR3cd** GASTTCGGRTGSGTCTTSAYGAA	(Throback et al. 2004)
nosZ Clade 1	**nosZ2F** CGCRACGGCAASAAGGTSMSSGT	**nosZ2R** CAKRTGCAKSGCRTGGCAGAA	(Harter et al. 2017)
amoA clade A (Comammox)	***comaA-244F*** *TAYAAYTGGGTSAAYTA*	***comA-659R*** *ARATCATSGTGCTRTG*	(Pjevac et al., 2017; Throback et al., 2004)
amoA clade B (Comammox)	***comaA-244F*** *TAYTTCTGGACRTTYTA*	***comA-659R*** *ARATCCARACDGTGTG*	(Pjevac et al., 2017; Throback et al., 2004)

Table S2.3. P-values of a pairwise comparison of a linear regression of Shannon, Simpson, and Chao1 diversity indices for the activated sludge microbial communities in the sequencing batch reactors of the sampled WWTP. P-values > 0.05 indicate that the diversity indices for the reactor pairs are not significantly different, rejecting the null hypothesis that the slope is zero.

Shannon Genus Level				
	SBR 1	SBR 2	SBR 3	SBR 1*
SBR 1	x	1.40E-01	2.54E-01	x
SBR 2	1.40E-01	x	7.67E-01	1.31E-03
SBR 3	2.54E-01	7.67E-01	x	2.28E-01
SBR 1*	x	1.31E-03	2.28E-01	x

Shannon Class Level				
	SBR 1	SBR 2	SBR 3	SBR 1*
SBR 1	x	2.24E-02	1.41E-01	x
SBR 2	2.24E-02	x	9.26E-01	1.75E-01
SBR 3	1.41E-01	9.26E-01	x	8.31E-01
SBR 1*	x	1.75E-01	8.31E-01	x

Simpson Genus Level				
	SBR 1	SBR 2	SBR 3	SBR 1*
SBR 1	x	8.70E-02	2.69E-01	x
SBR 2	8.70E-02	x	1.15E-01	2.03E-03
SBR 3	2.69E-01	1.15E-01	x	5.12E-01
SBR 1*	x	2.03E-03	5.12E-01	x

Simpson Class Level				
	SBR 1	SBR 2	SBR 3	SBR 1*
SBR 1	x	1.37E-01	5.14E-01	x
SBR 2	1.37E-01	x	9.46E-01	6.02E-01
SBR 3	5.14E-01	9.46E-01	x	9.38E-01
SBR 1*	x	6.02E-01	9.38E-01	x

Chao1 Genus Level				
	SBR 1	SBR 2	SBR 3	SBR 1*
SBR 1	x	2.78E-02	3.32E-01	x
SBR 2	2.78E-02	x	6.56E-02	8.77E-01
SBR 3	3.32E-01	6.56E-02	x	5.62E-01
SBR 1*	x	8.77E-01	5.62E-01	x

Table S2.4 P-values of a t-test comparing the means of Shannon, Simpson, and Chao1 diversity indices for the activated sludge microbial communities in the sequencing batch reactors of the sampled WWTP for the four seasons. P-values < 0.05 indicate that the diversity indices for the respective season are significantly different for the respective reactor pair. Almost every season in all reactors had significantly different alpha diversities.

Shannon Genus Level				
	Summer	Fall	Winter	Spring
Summer	x	1.59E-02	1.20E-11	7.71E-16
Fall	1.59E-02	x	1.15E-02	8.39E-05
Winter	1.20E-11	1.15E-02	x	1.52E-02
Spring	7.71E-16	8.39E-05	1.52E-02	x

Shannon Class Level				
	Summer	Fall	Winter	Spring
Summer	x	2.94E-03	1.83E-18	1.02E-17
Fall	2.94E-03	x	3.44E-10	9.48E-10
Winter	1.83E-18	3.44E-10	x	7.69E-01
Spring	1.02E-17	9.48E-10	7.69E-01	x

Simpson Genus Level				
	Summer	Fall	Winter	Spring
Summer	x	1.90E-01	3.44E-07	6.24E-12
Fall	1.90E-01	x	4.05E-05	6.55E-10
Winter	3.44E-07	4.05E-05	x	1.53E-03
Spring	6.24E-12	6.55E-10	1.53E-03	x

Simpson Class Level				
	Summer	Fall	Winter	Spring
Summer	x	2.74E-03	1.09E-17	7.62E-13
Fall	2.74E-03	x	2.44E-08	8.45E-07
Winter	1.09E-17	2.44E-08	x	9.08E-01
Spring	7.62E-13	8.45E-07	9.08E-01	x

Chao1 Genus Level				
	Summer	Fall	Winter	Spring
Summer	x	1.74E-01	4.65E-02	4.05E-01
Fall	1.74E-01	x	9.29E-01	4.33E-01
Winter	4.65E-02	9.29E-01	x	2.27E-01
Spring	4.05E-01	4.33E-01	2.27E-01	x

Table S2.5. OTUs with relative sequence abundance > 0.1% and Pearson's product moment correlation coefficients $R^2 > 0.4$ for either of the variables wastewater temperature or effluent ammonia concentration. OTU classification at the 97% sequence similarity cut-off (species-level). The last column to the right shows if the respective taxa belongs to the OTU category core, single season, multiple season, or transient.

OTU	R^2 Temperature	R^2 Effluent Ammonia	Average % Abundance	Season category
*Bacteroidetes_Sphingobacteriia_Sphingobacteriales_Saprospiraceae*_uncultured	0.432	0.400	7.64% ± 2.92%	Core
Proteobacteria_Betaproteobacteria_Burkholderiales_Comamonadaceae_Variovorax	0.620	0.344	3.38% ± 2.08%	Core
Proteobacteria_Alphaproteobacteria_Rhodobacterales_Rhodobacteraceae_Albirhodobacter	0.591	0.261	0.92% ± 0.56%	Transient
*Proteobacteria_Betaproteobacteria_Rhodocyclales Rhodocyclaceae*_ambiguous_taxa	0.460	0.367	0.78% ± 0.49%	Core
*Chloroflexi_Ardenticatenia_Ardenticatenales*_ambiguous_taxa	0.454	0.404	0.57% ± 0.58%	Single Season Fall
*Chloroflexi*_SBR2076_uncultured bacterium	0.702	0.357	0.49% ± 0.47%	Multiple Season (Sum/Fall/Win)
Bacteroidetes_Cytophagia_Cytophagales_Cytophagaceae _Dyadobacter	0.377	0.602	0.28% ± 0.39%	Multiple Season (Spr/Sum)
TM6 (*Dependentiae*)_uncultured bacterium	0.447	0.596	0.01% ± 0.01%	Multiple Season (Sum/Fall)
Proteobacteria _Betaproteobacteria _Hot Creek 32_	0.422	0.518	0.22% ± 0.21%	Transient

_uncultured marine bacterium				
*Gracilibacteria*_ambiguous_taxa	0.223	0.718	0.01% ± 0.02%	Transient
*Chlorobi_Chlorobia_Chlorobiales*_SJA-28_uncultured bacterium	0.387	0.525	0.14% ± 0.14%	Core
*Acidobacteria_Holophagae*_Subgroup 10_ABS-19_bacterium enrichment culture clone	0.576	0.302	0.13% ± 0.17%	Transient
*Gemmatimonadetes_Gemmatimonadetes_Gemmatimonadales_Gemmatimonadaceae*_uncultured	0.338	0.530	0.12% ± 0.18%	Core
*Acidobacteria_Holophagae*_Subgroup 7_uncultured soil bacterium	0.495	0.423	0.12% ± 0.18%	Transient
OTU affiliated to taxa of known nitrifying bacteria				
Proteobacteria_Betaproteobacteria_Nitrosomonadales_Nitrosomonadaceae_Nitrosomonas	0.127	0.085	0.24% ± 0.19%	Core
Proteobacteria_Betaproteobacteria_Nitrosomonadales_Nitrosomonadaceae	0.038	0.005	0.48% ± 0.26%	Core
*Proteobacteria_Betaproteobacteria_Nitrosomonadales_Gallionellaceae*_Candidatus *Nitrotoga*	0.101	0.079	0.47% ± 0.30%	Core

Table S2.6. Using the quantitative PCR data to compare reactors these p-values were used determine a linear relationship between each SBRs' gene abundance with an Anova test. Cells are highlighted in red when $p<0.05$. This was complimented with a Students t-test since most reactors did not change significantly throughout the year.

16S rRNA	SBR 1	SBR 2	SBR 3	SBR 1*
SBR 1	x	3.49E-03	2.53E-02	n/a
SBR 2	3.49E-03	x	1.65E-06	2.13E-03
SBR 3	2.53E-02	1.65E-06	x	3.03E-05
SBR 1*	n/a	2.13E-03	3.03E-05	x

nosZ	SBR 1	SBR 2	SBR 3	SBR 1*
SBR 1	x	8.69E-01	7.90E-01	n/a
SBR 2	8.69E-01	x	2.77E-02	1.58E-01
SBR 3	7.90E-01	2.77E-02	x	1.78E-02
SBR 1*	n/a	1.58E-01	1.78E-02	x

AOB	SBR 1	SBR 2	SBR 3	SBR 1*
SBR 1	x	1.23E-03	1.35E-03	n/a
SBR 2	1.23E-03	x	1.41E-07	9.30E-05
SBR 3	1.35E-03	1.41E-07	x	1.00E-10
SBR 1*	n/a	9.30E-05	1.00E-10	x

AOA	SBR 1	SBR 2	SBR 3	SBR 1*
SBR 1	x	1.23E-03	1.35E-03	n/a
SBR 2	1.23E-03	x	1.41E-07	9.30E-05
SBR 3	1.35E-03	1.41E-07	x	1.00E-10
SBR 1*	n/a	9.30E-05	1.00E-10	x

nirK	SBR 1	SBR 2	SBR 3	SBR 1*
SBR 1	x	1.06E-02	5.18E-01	n/a
SBR 2	1.06E-02	x	3.60E-02	1.16E-04
SBR 3	5.18E-01	3.60E-02	x	4.26E-10
SBR 1*	n/a	1.16E-04	4.26E-10	x

nirS	SBR 1	SBR 2	SBR 3	SBR 1*
SBR 1	x	3.42E-03	2.31E-02	n/a
SBR 2	3.42E-03	x	5.01E-05	1.08E-04
SBR 3	2.31E-02	5.01E-05	x	2.87E-07
SBR 1*	n/a	1.08E-04	2.87E-07	x

Table S2.7. Using the quantitative PCR data to compare reactors a Student's t-test was performed to compare the means of the average gene abundance between reactors. Red cells highlight p <0.05. The average gene abundance throughout the year is not statistically different between reactors with a few exceptions when comparisons are made with SBR 1 and SBR 1* which were not operational throughout the entire year.

16S rRNA	SBR 1	SBR 2	SBR 3	SBR 1*
SBR 1	x	3.92E-01	2.23E-01	7.48E-01
SBR 2	3.92E-01	x	5.55E-01	5.16E-01
SBR 3	2.23E-01	5.55E-01	x	2.77E-01
SBR 1*	7.48E-01	5.16E-01	2.77E-01	x

nosZ	SBR 1	SBR 2	SBR 3	SBR 1*
SBR 1	x	3.53E-01	5.02E-01	7.38E-01
SBR 2	3.53E-01	x	4.56E-01	1.35E-01
SBR 3	5.02E-01	4.56E-01	x	3.48E-01
SBR 1*	7.38E-01	1.35E-01	3.48E-01	x

AOB	SBR 1	SBR 2	SBR 3	SBR 1*
SBR 1	x	3.67E-02	2.77E-01	4.32E-03
SBR 2	3.67E-02	x	3.78E-01	2.24E-01
SBR 3	2.77E-01	3.78E-01	x	6.68E-02
SBR 1*	4.32E-03	2.24E-01	6.68E-02	x

AOA	SBR 1	SBR 2	SBR 3	SBR 1*
SBR 1	x	1.72E-02	6.96E-01	6.53E-04
SBR 2	1.72E-02	x	6.66E-02	1.44E-01
SBR 3	6.96E-01	6.66E-02	x	3.41E-03
SBR 1*	6.53E-04	1.44E-01	3.41E-03	x

nirK	SBR 1	SBR 2	SBR 3	SBR 1*
SBR 1	x	6.79E-01	9.41E-01	5.71E-01
SBR 2	6.79E-01	x	7.30E-01	2.76E-01
SBR 3	9.41E-01	7.30E-01	x	5.09E-01
SBR 1*	5.71E-01	2.76E-01	5.09E-01	x

nirS	SBR 1	SBR 2	SBR 3	SBR 1*
SBR 1	x	4.10E-01	5.28E-01	7.83E-01
SBR 2	4.10E-01	x	9.65E-01	2.46E-01
SBR 3	5.28E-01	9.65E-01	x	3.69E-01
SBR 1*	7.83E-01	2.46E-01	3.69E-01	x

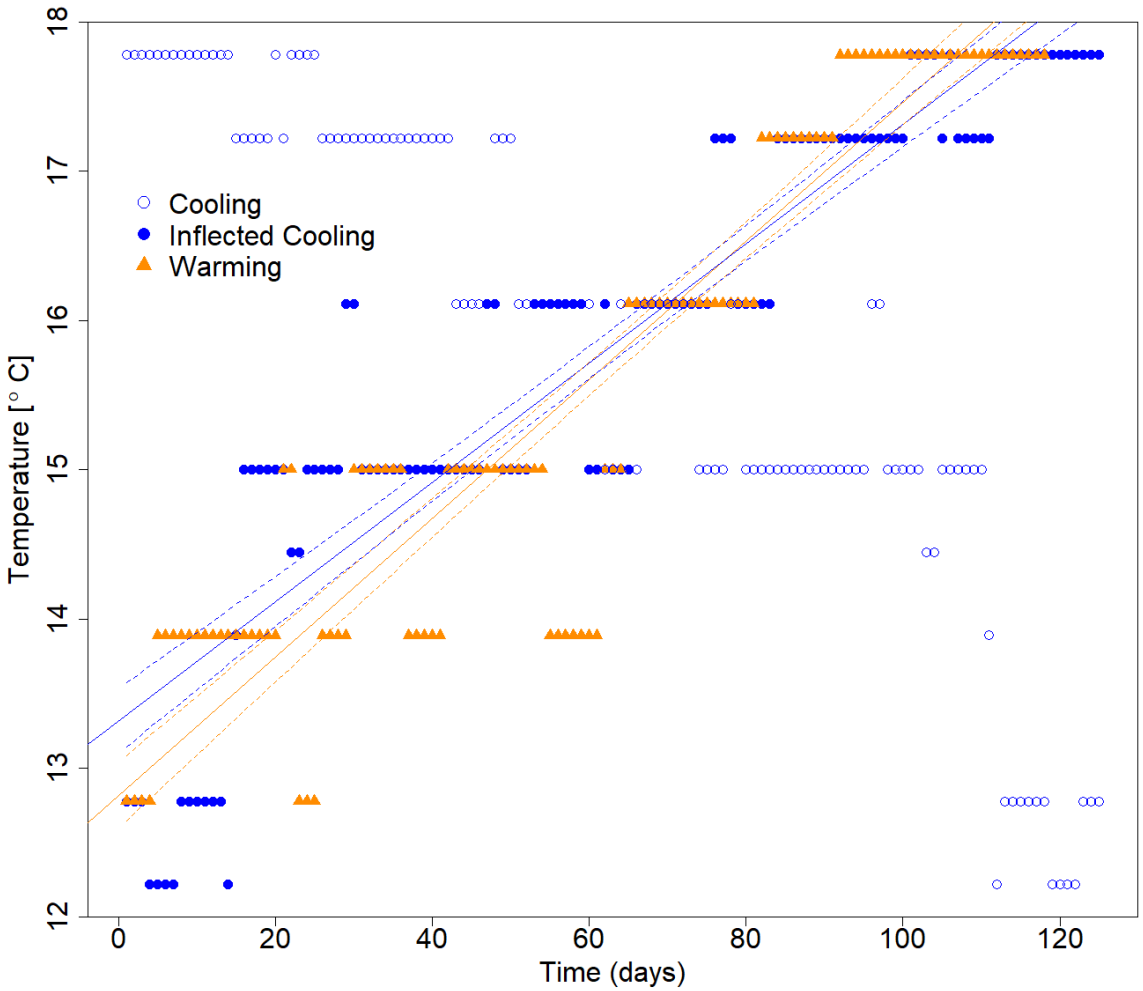

Figure S2.1. This plot denotes the temperature regression between Fall and Winter against Spring and Summer. The blue outlined circles show the original Fall and Winter data whereas the blue filled circles are inflected over the x-axis to show the flipped alignment alongside the orange triangle Spring and Summer data points. The slopes are not statistically different with the average rate of change as approximately ±0.043°C/day. The solids lines denote the linear regression while the dashed lines denote the 95% confidence interval for the average.

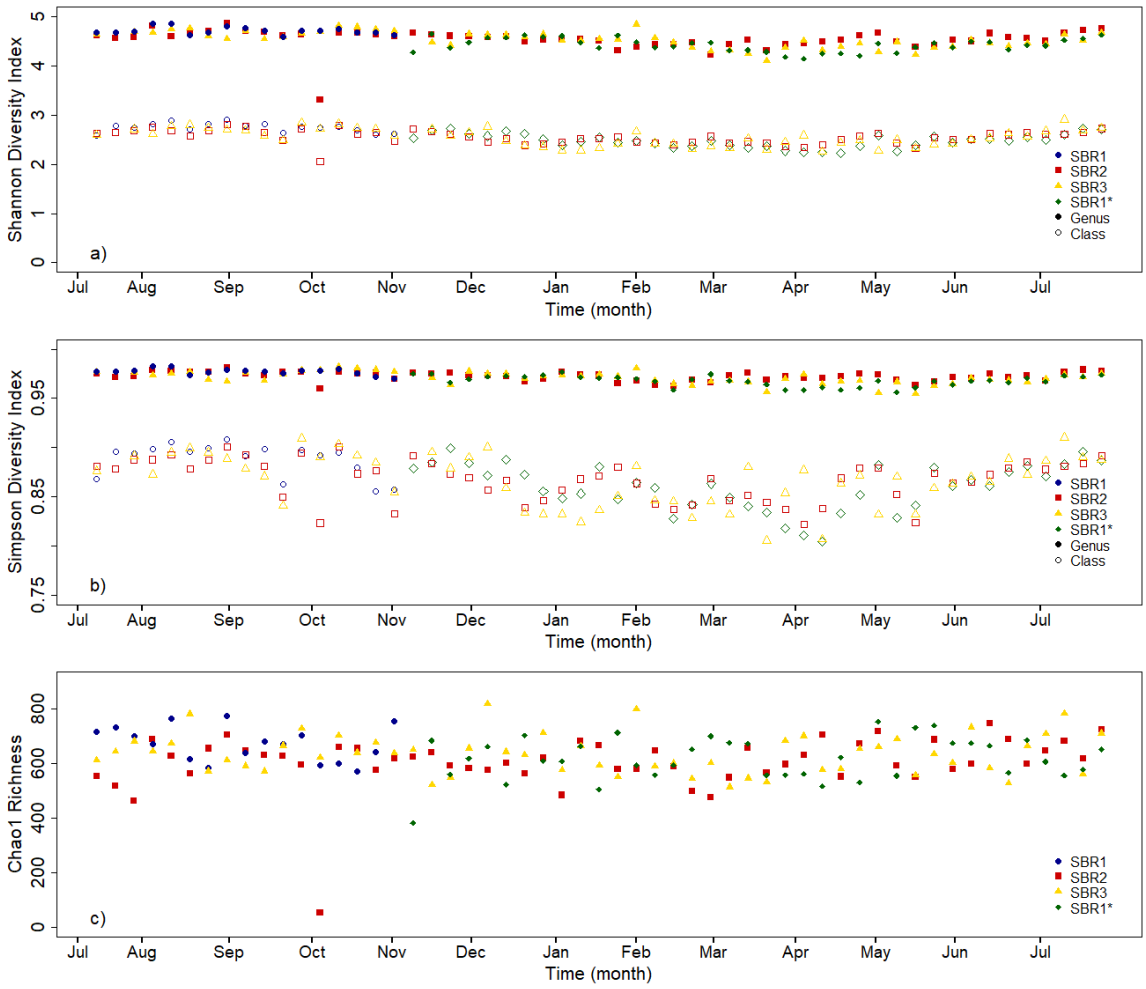

Figure S2.2. Different alpha diversity metrics were performed across the different reactors through a) Shannon Diversity b) Simpson Diversity, and c) Chao1 Richness. Each sequencing batch reactor is shown individually as blue circles for SBR1, red squares for SBR2, yellow triangles for SBR3, and green diamonds for SBR1*. Simpson and Shannon diversity were calculated at two levels, genus level (solid shapes) and class level (outlined shapes).

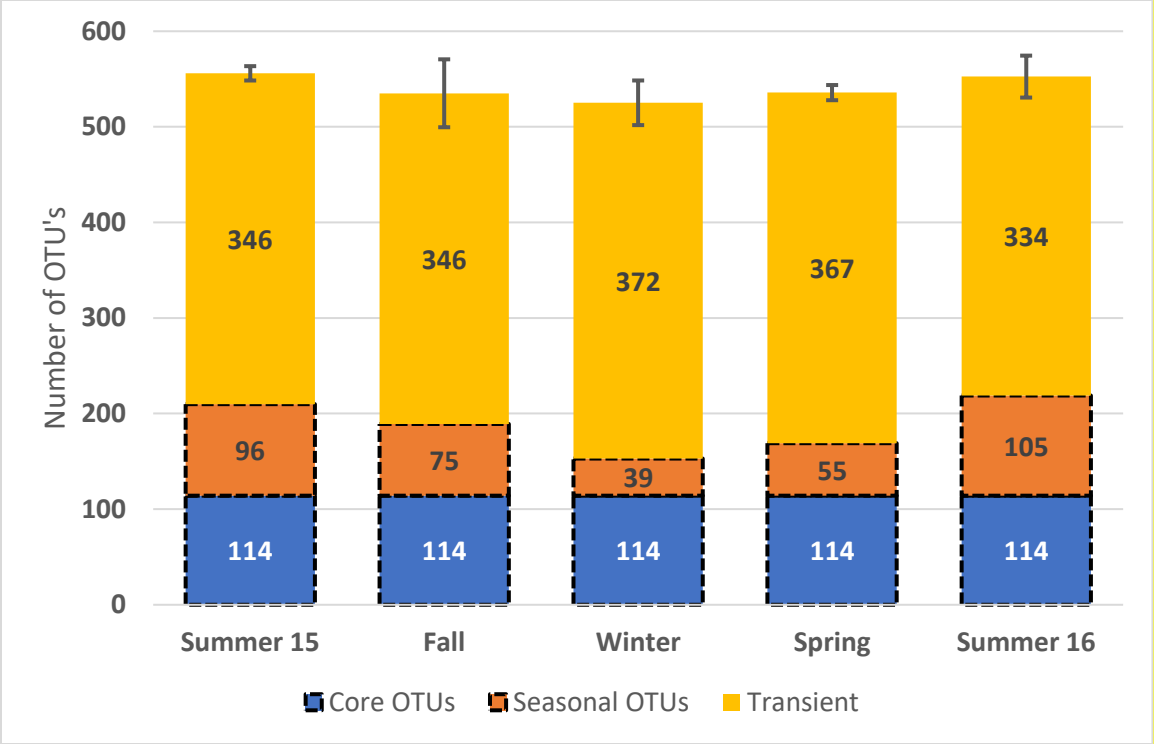

Figure S2.3. The average number of genus level OTUs in the core community (blue), seasonal community (both multiple and single season are in orange), and transient community (yellow) for each season. The black dashed line is exact values shared by all reactors while transient is an average between the reactors. The core community stays constant throughout the year, the transient community also remains consistent, while the seasonal OTUs decrease the richness of the reactors in the winter.

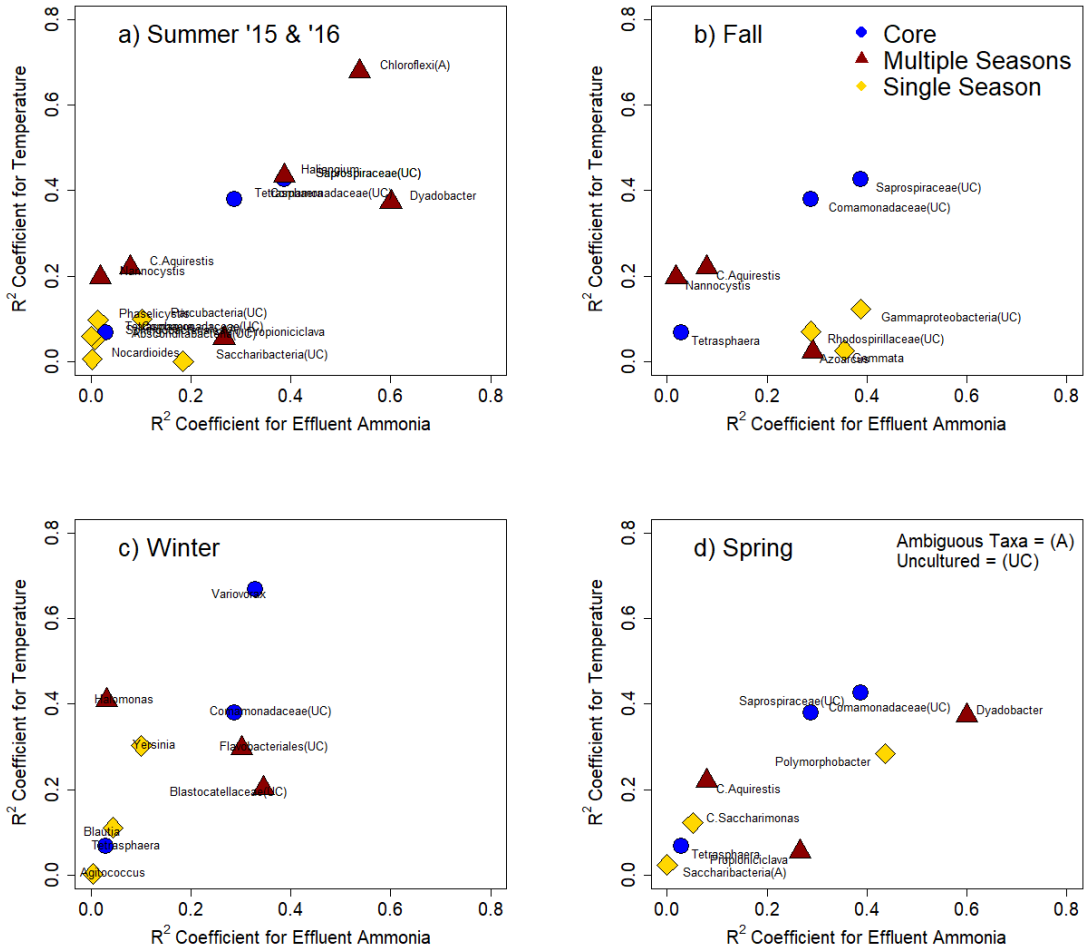

Figure S2.4. The correlation coefficients regressed against influent water temperature and effluent ammonia concentration are on the y and x-axis respectively for the top 3 highest abundance OTUs in the core (blue dots), multiple season (red triangles), and one season communities (yellow diamonds). These high abundance OTUs are often categorically seasonal as opposed to temperature dependent regressions.

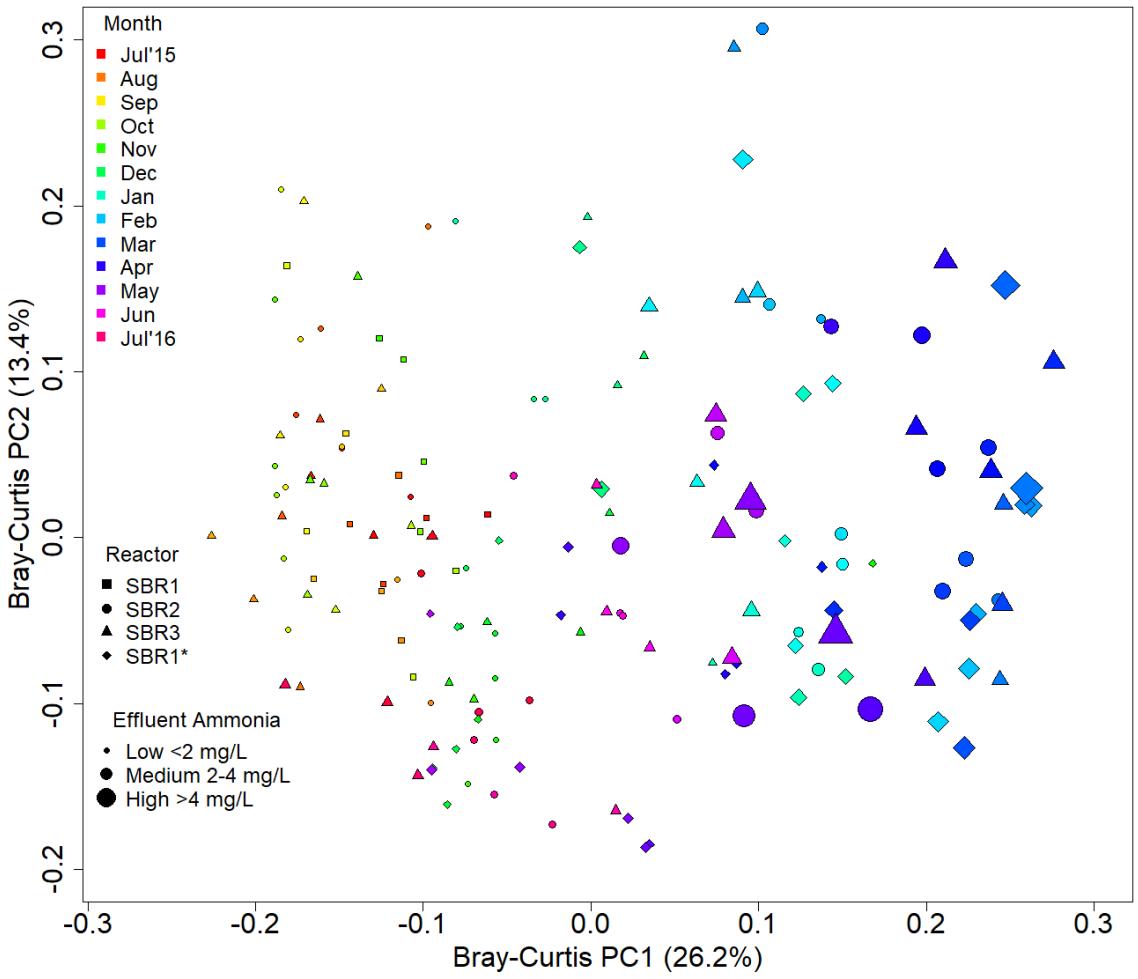

Figure S2.5. Principal Coordinates analysis was performed using Bray-Curtis dissimilarity. The rainbow color gradient denotes the changes in the months. Each reactor is plotted separately based on shape (Square-SBR1, Circle-SBR2, Triangle-SBR3, Diamond-SBR1*). The effluent ammonia concentration denotes the size of the data points. PC1 represents a separation based on the months and effluent ammonia concentration.

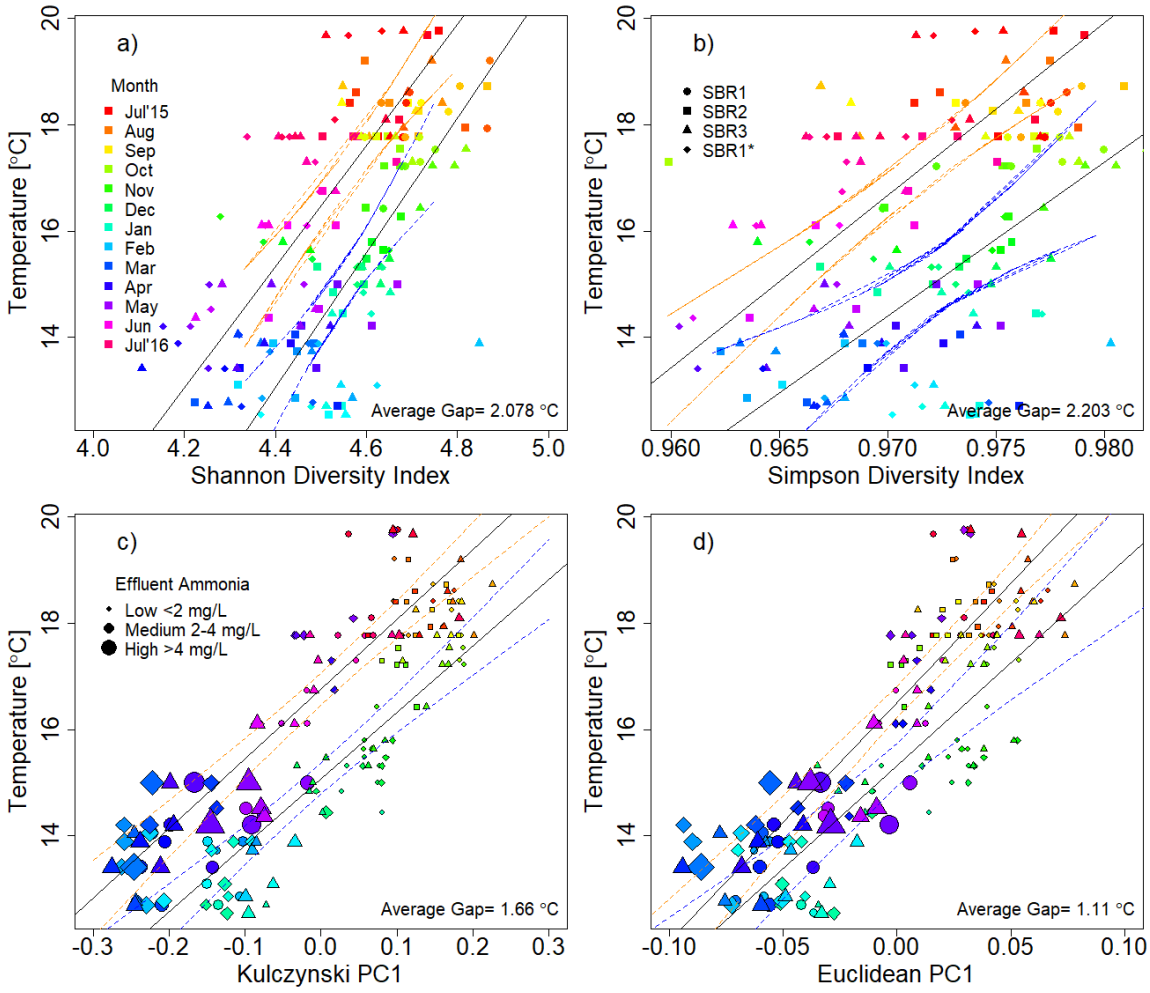

Figure S2.6. Several diversity metrics were regressed against the influent water temperature including a) Shannon diversity, b) Simpson diversity, c) Kulcynski, and d) Euclidean. The rainbow color gradient denotes the changes in the months. Each reactor is plotted separately based on shape (Square-SBR1, Circle-SBR2, Triangle-SBR3, Diamond-SBR1*). The linear regression is shown with the 95% confidence intervals as dashed lines for Spring and Summer in orange and Fall and Winter in blue. Each plot shows similar recovery lags ranging from 1.11°C up to 2.20°C. The first two figures represent this trend in a single dimension with alpha diversity while the other two represent this trend on the highest axis of variance in multi-dimensional, beta diversity dissimilarity matrices.

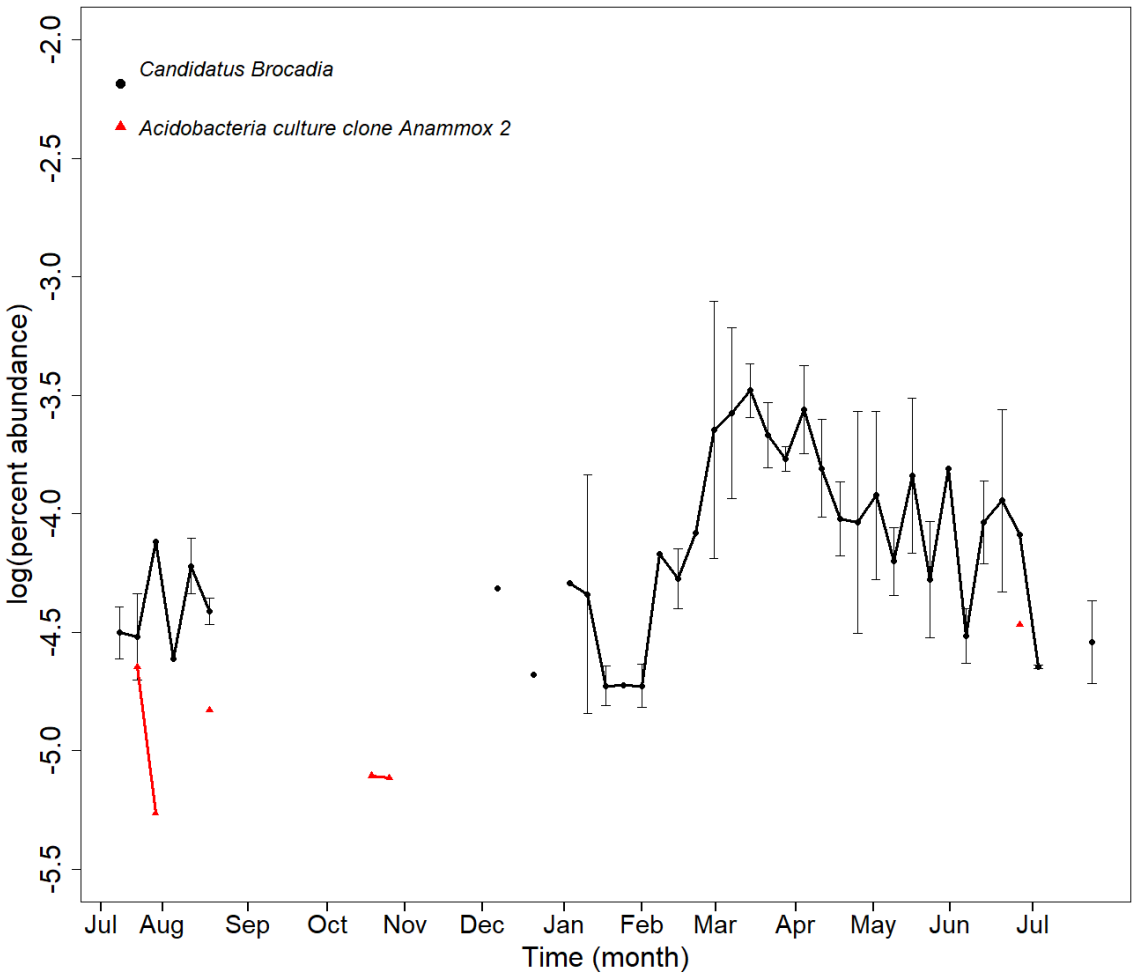

Figure S2.7. One OTU affiliated to a taxa comprising known anaerobic ammonia-oxidizing (anammox) bacterial was observed during the sample period, *Candidatus Broacadia* (black circles). A second OTU affiliated to an Acidobacteria clone from an Anammox enrichment is also included (red triangles). The relative sequence abundance of the *Candidatus Broacadia* OTU increases at the end of winter when nitrification performance decreased. During nitrification failure there is an abundance of both ammonia and nitrite in the reactors. The change in relative abundance of the *Candidatus Broacadia* OTU is probably not significant enough to be associated with nitrogen removal, however certain strains of *Candidatus Brocadia* thrive in colder temperatures (Hendrickx et al., 2014).

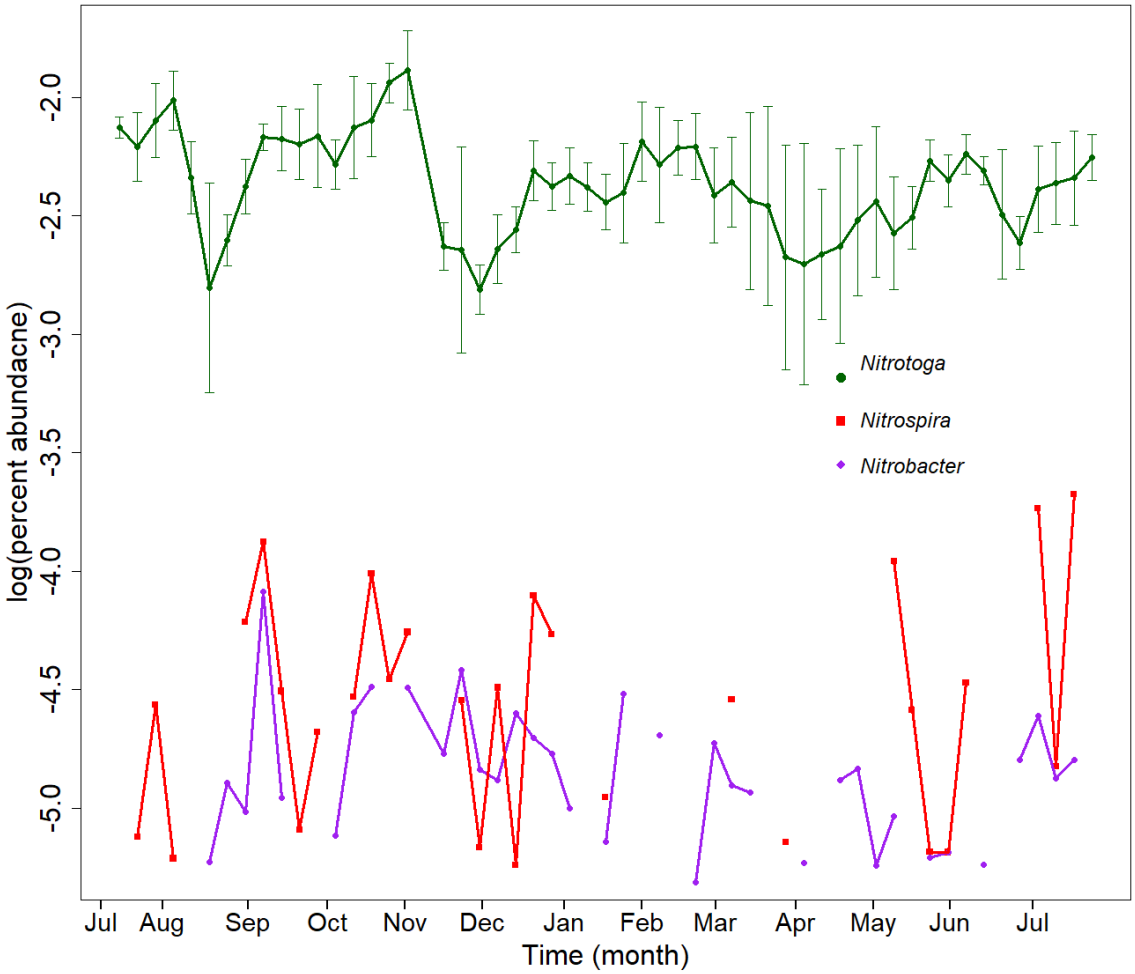

Figure S2.8. The known nitrite oxidizing community is highlighted over the months above. The dominance of *Nitrotoga* (green circles) over other nitrite oxidizing bacteria such as *Nitrospira* (red squares) and *Nitrobacter* (purple diamonds has been previously cultured from activated sludge and are ideal in temperatures between 10°C and 17°C (Alawi, Off, Kaya, & Spieck, 2009).

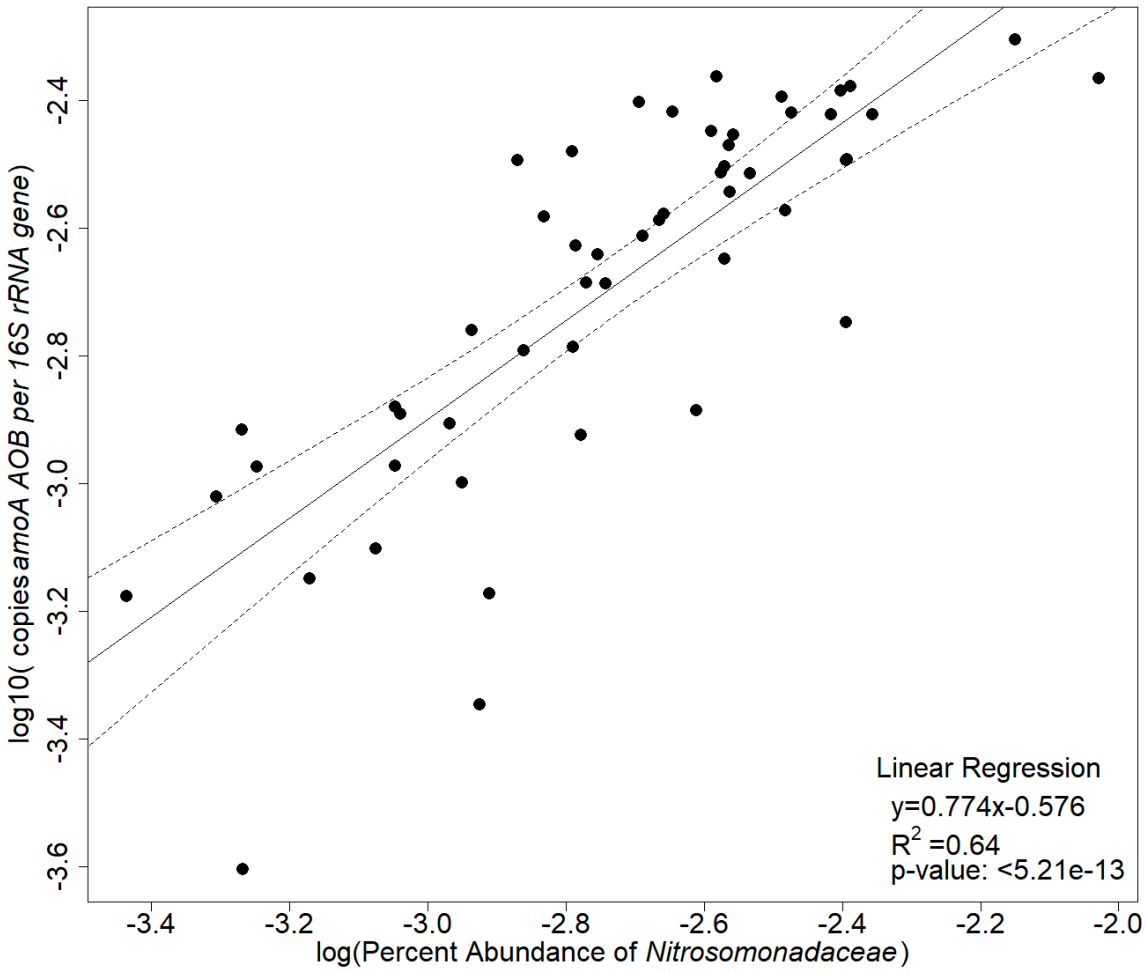

Figure S2.9. The percent abundance of *Nitrosomonadaceae* (x-axis) correlated to the copies of *amoA* (AOB) gene per *16S rRNA* gene (y-axis). The linear regression is shown in the solid line with the 95% confidence intervals denoted on the dashed line.

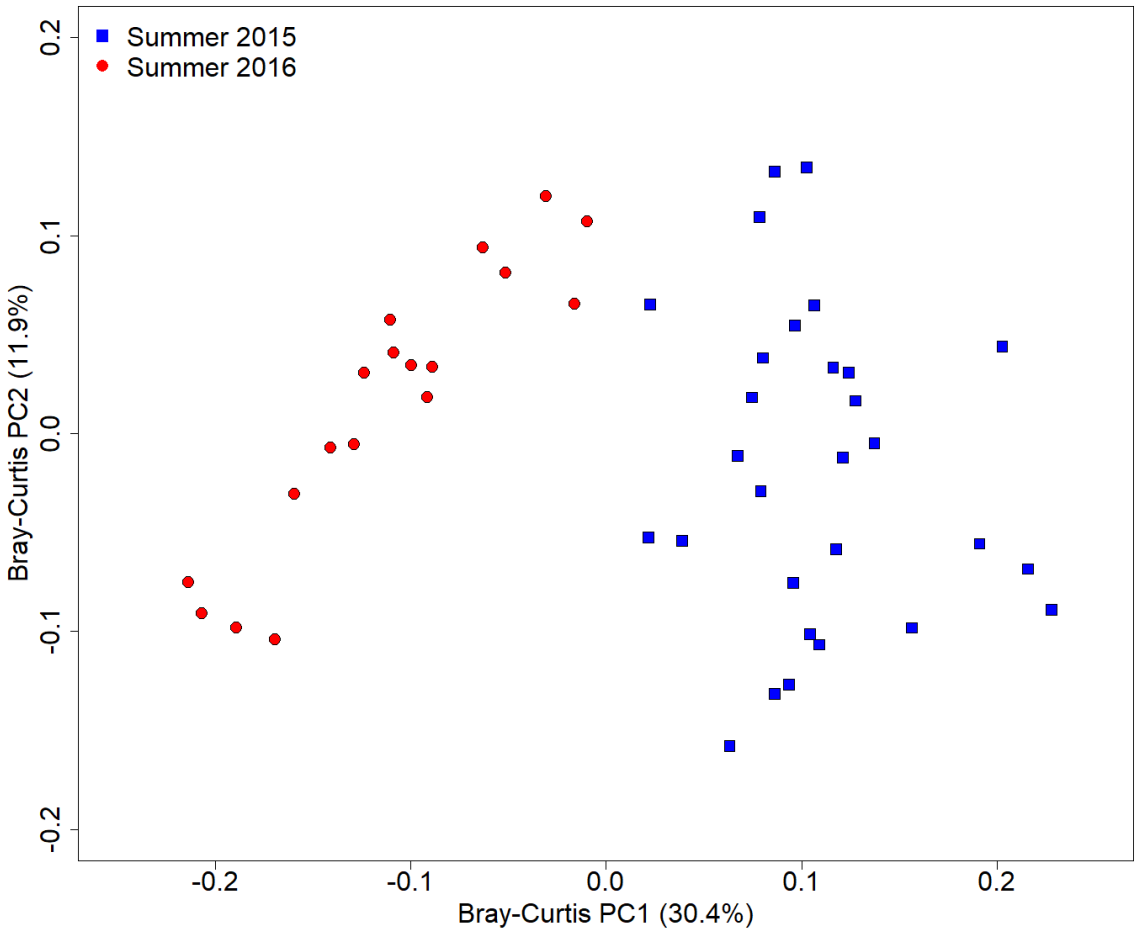

Figure S2.10. shows a principal coordinates analysis of only the two summers with July 2015 in blue, and July 2016 in red. The two separate and appear distinct, however they only overlap for three weeks. Summer 2015 started July 13th, 2015 until the end of summer. Summer 2016 started June 20th, 2016, and sampling finished July 30th with only three overlapping weeks.

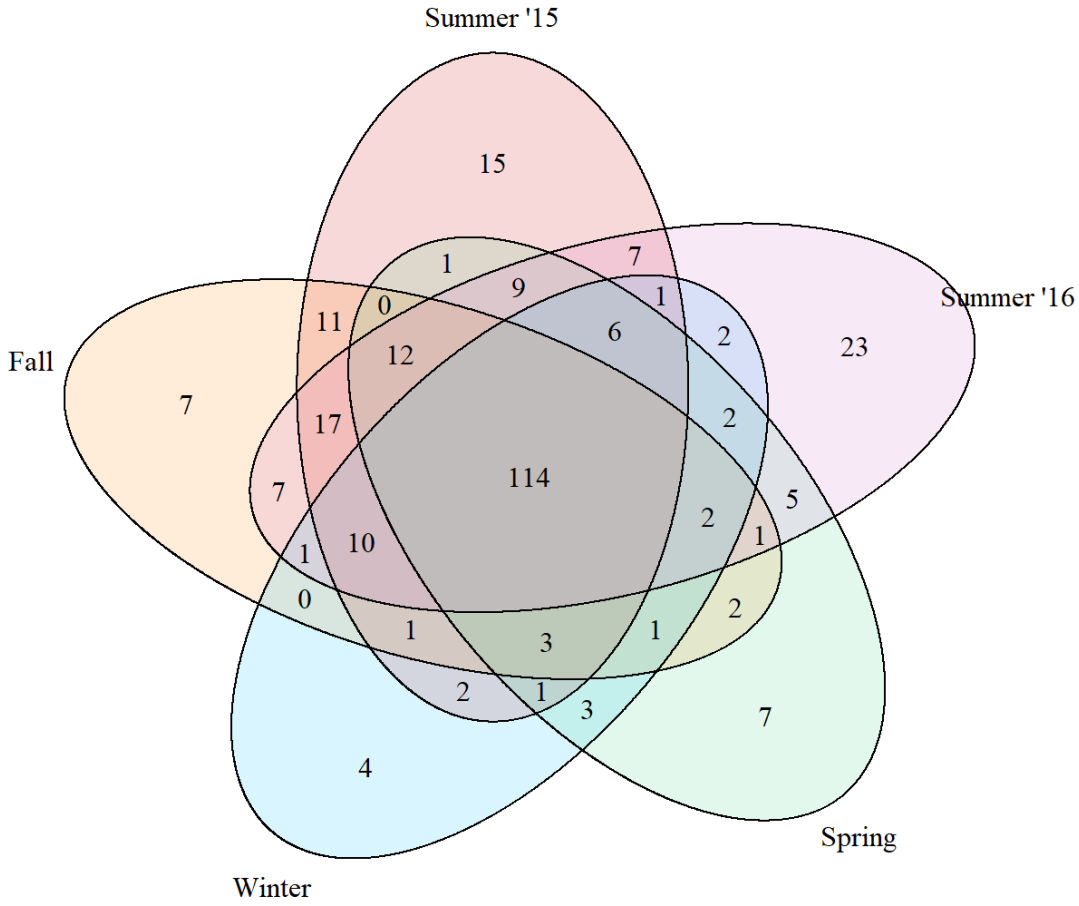

Figure S2.11. The quintuple venn diagram represents the core community, multiple season, and single season OTUs. Summer 2015 is represented in red, Fall in yellow, Winter in blue, Spring in green, and Summer 2016 in purple. The core 114 OTUs represent the shared space between all the seasons. Anything shared between two seasons is a multiple season OTU and listed only under each season is a single seasson OTU.

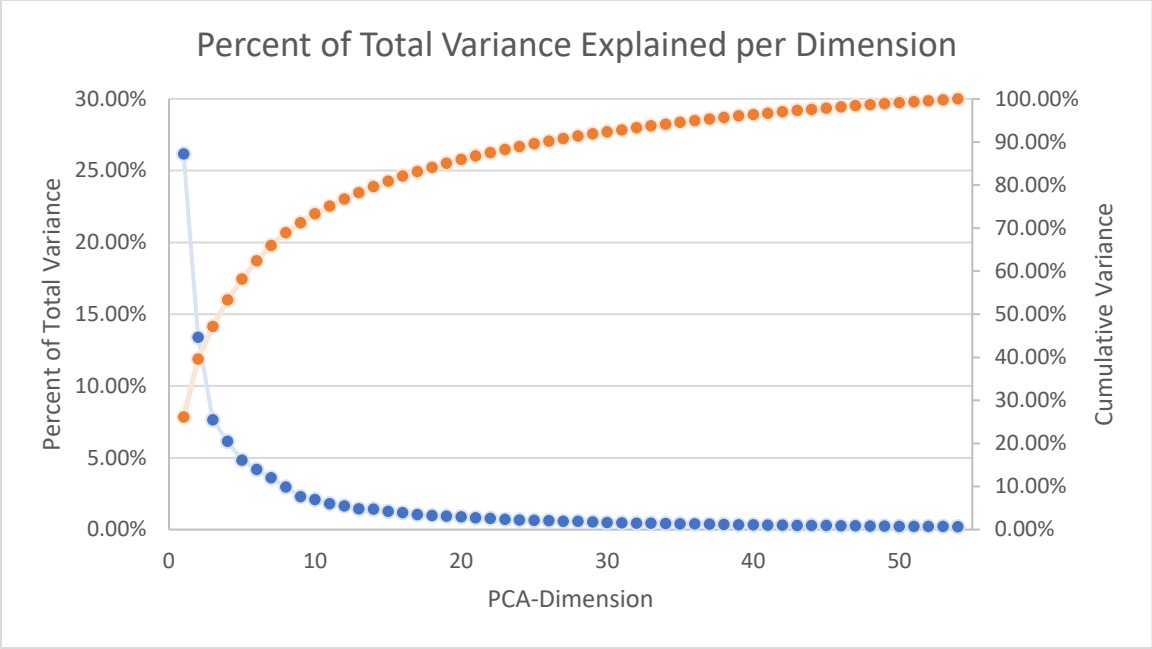

Figure S2.12. Bray-Curtis dissimilarity creates several dimensions where each dimension explains a portion of the total variance observed between samples. This plot highlights each individual dimension in the blue dots on the left y-axis. The orange dots are a cumulative total of the dimensions on the right y-axis.

Appendix B

Chapter 4 Supplemental Materials

Seasonal Activity and Community Composition Shifts in Full-Scale Activated Sludge Sequencing Batch Reactors

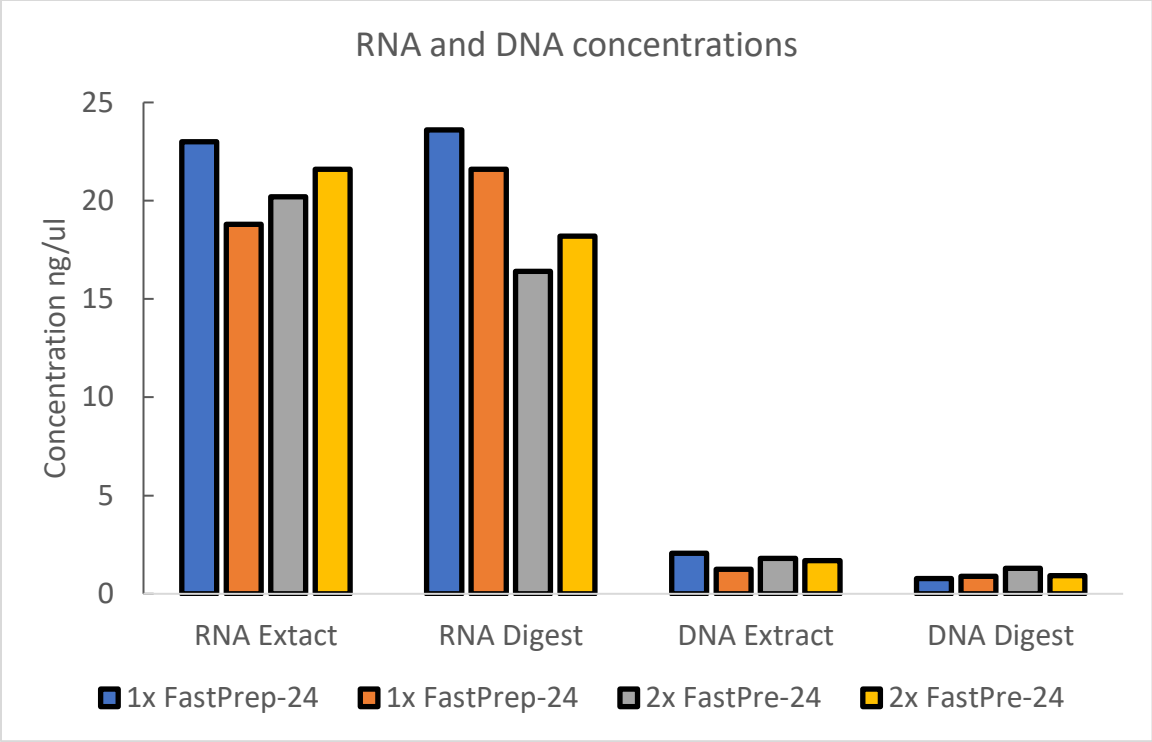

Figure S4.1 shows the concentrations of RNA and DNA immediately after RNA extraction ("Extract") and after DNA digestion ("Digest"). The blue and orange were run once on the FastPrep-24 homongenizer (40 seconds at 6m/s) while the gray and yellow samples were run twice. These were all performed using 50uL sample volumes.

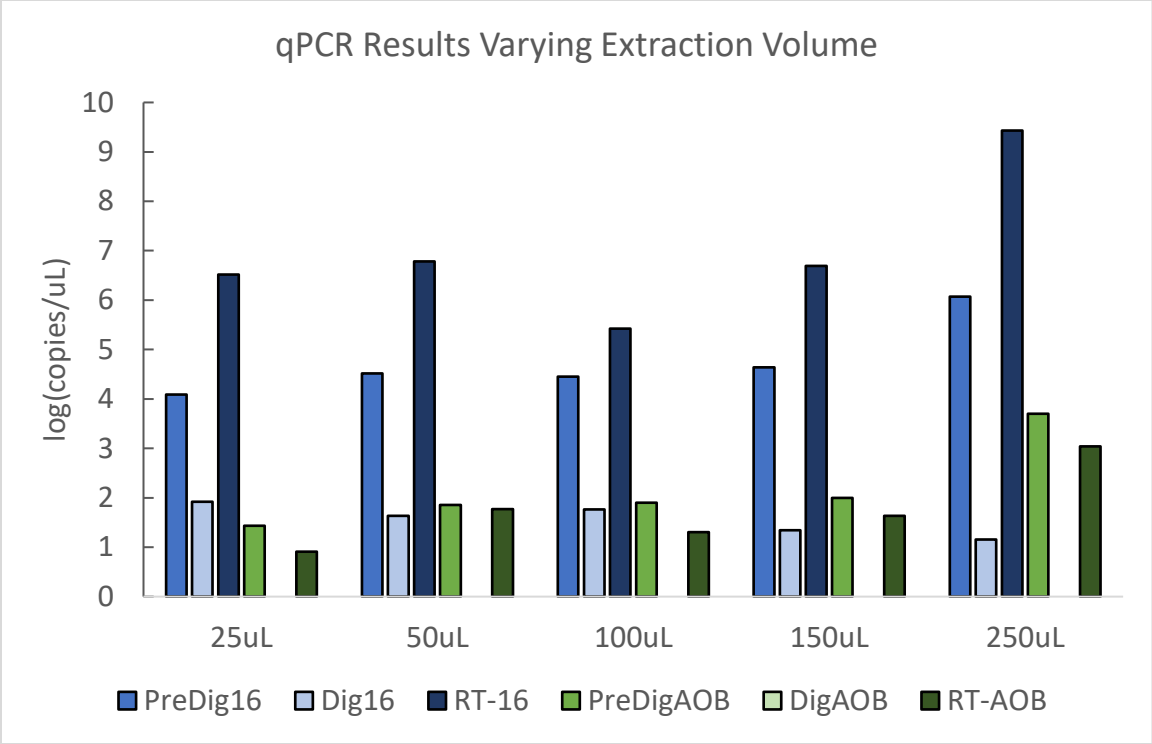

Figure S4.2 shows different sample volumes, ranging from 25ul, up to 250ul used for RNA extraction. The blue shades represent the samples quantified using RT-qPCR via 16S rRNA primers ('16'), while the green shades represent the same samples quantified using *amoA* primers for ammonia-oxidizing bacteria ('AOB'). The PreDig represents the raw extracted sample where only residual DNA is amplified. Dig represents the remaining DNA amplified after DNA digestion. RNA is not amplified in the PreDig or Dig samples, since the RNA still represents the reverse-compliment strand. After reverse transcription, the RT bars, the RNA is amplified as cDNA.

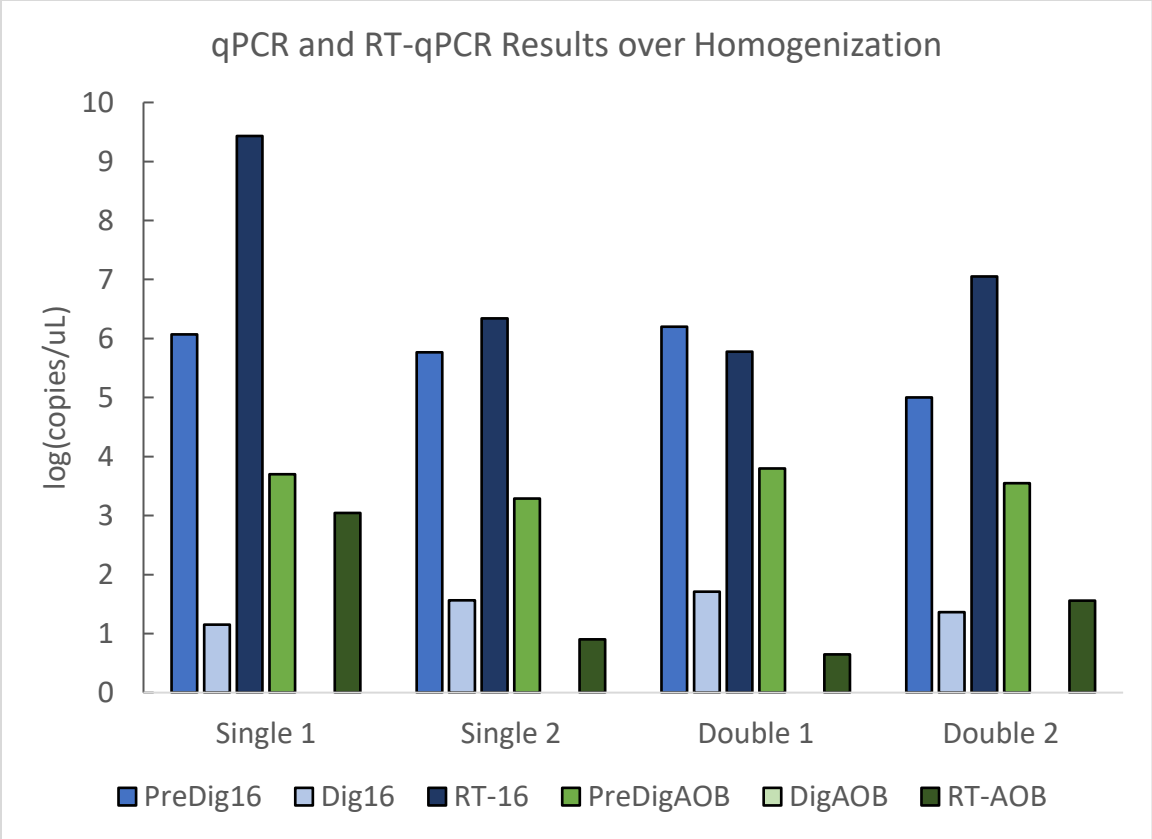

Figure S4.3 shows the effects of homogenizing samples one on a FastPrep-24, and twice (40sec, 6m/s). The blue shades represent the samples quantified using RT-qPCR via 16S rRNA primers ('16'), while the green shades represent the same samples quantified using *amoA* primers for ammonia-oxidizing bacteria ('AOB'). The PreDig represents the raw extracted sample where only residual DNA is amplified. Dig represents the remaining DNA amplified after DNA digestion. RNA is not amplified in the PreDig or Dig samples, since the RNA still represents the reverse-compliment strand. After reverse transcription, the RT bars, the RNA is amplified as cDNA. Performing the homogenization step twice appeared to disrupt the recovery of RNA reads. The recovery of RNA was successively worse with more homogenization steps (not shown). All samples started with 50uL volume.

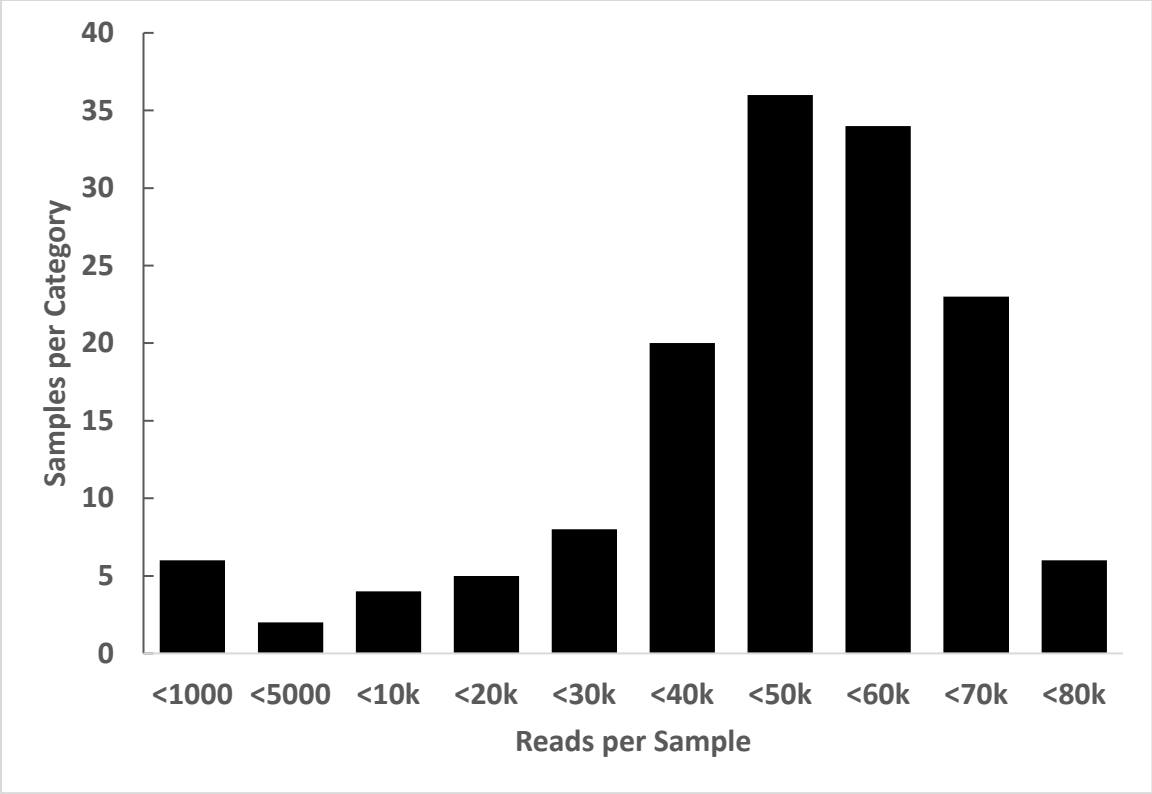

Figure S4.4 is a histogram of the reads per samples after processing in DADA2. Samples with less than 1000 reads were removed from the sample set.

Table S4.1 lists the samples with low reads which were removed from the dataset. All the samples were from Reactor 3 and were positioned similarly on the 96-well plate submitted for sequencing. Due to their position on the 96-well plate, and previously having been quantified for DNA, a handling issue may have arisen at the sequencing core.

Sample ID	Time	Season	Reactor	Reads
3spr16RNAy	Static Fill	Spring	Reactor 3	99
8spr16RNAy	Mixed Fill	Spring	Reactor 3	128
27bspr16RNAy	Settled Sludge	Spring	Reactor 3	462
14spr16RNAy	React 1	Spring	Reactor 3	530
27bfall16RNAy	Settled Sludge	Fall	Reactor 3	557
22spr16RNAy	React2	Spring	Reactor 3	718
14fall16RNAy	React 1	Fall	Reactor 3	787

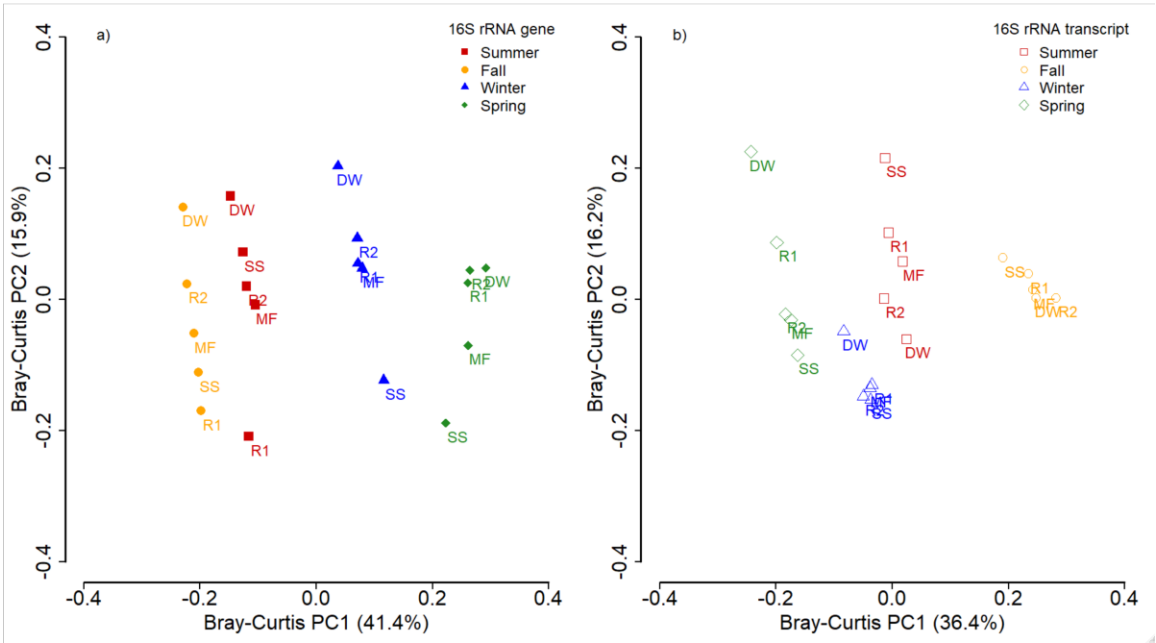

Figure S4.5 shows a principle coordinates analysis using the Bray-Curtis Dissimilarity Matrix on the 16S rRNA gene composition (Figure S4.5a) and the 16S rRNA transcript composition (Figure S4.5b). The composition in the summer is shown in red, the fall is shown in orange, the winter is shown in blue, and the spring is shown in green. The reactor cycles are denoted by their abbreviations (SF= static fill* not included, MF= Mixed Fill, R1= React 1, R2= React 2, DW = decanted water, SS= settled sludge).

Table S4.2 highlights the top three highest abundance OTUs (based on 16S rRNA gene abundance) which significantly fluctuate (either based on 16S rRNA genes or 16S rRNA transcripts) throughout the seasons in each subfigure of Figure3a-f.

	Top 3 Seasonally Trending OTUs when comparing seasons.	16S rRNA gene %	16S rRNA transcript %
Figure3a	Summer		
	Patescibacteria_Saccharimonadia_Saccharimonadales_NA_NA	1.37%	0.16%
	Actinobacteria_Actinobacteria_Propionibacteriales_Propionibacteriaceae_Propionicimonas	0.17%	0.26%
	Actinobacteria_Actinobacteria_Propionibacteriales_Nocardioidaceae_Nocardioides	0.17%	0.10%
	Fall		
	Chloroflexi_Anaerolineae_SBR1031_A4b_NA	2.73%	2.54%
	Bacteroidetes_Bacteroidia_Chitinophagales_Saprospiraceae_Phaeodactylibacter	0.51%	0.73%
	Proteobacteria_AlphaproteoRickettsiales_Mitochondria_NA	0.32%	0.07%
Figure3b	Fall		
	Proteobacteria_Deltaproteobacteria_Myxococcales_Haliangiaceae_Haliangium	2.34%	6.28%
	Actinobacteria_Actinobacteria_Corynebacteriales_Mycobacteriaceae_Mycobacterium	1.38%	0.60%
	Bacteroidetes_Bacteroidia_Bacteroidales_Bacteroidaceae_Bacteroides	0.86%	0.06%
	Winter		
	WPS-2_NA_NA_NA_NA	1.12%	1.31%
	Patescibacteria_GraciliNA_NA_NA	0.90%	0.30%
	Proteobacteria_Alphaproteobacteria_Rhizobiales_Beijerinckiaceae_NA	0.29%	0.24%
Figure3c	Winter		
	Chloroflexi_Chloroflexia_Chloroflexales_Roseiflexaceae_Kouleothrix	1.71%	3.14%
	Patescibacteria_Gracilibacteria_Absconditabacteriales_(SR1)_NA_NA	1.50%	0.37%
	Chloroflexi_Anaerolineae_SBR1031_A4b_NA	1.12%	0.68%
	Spring		
	Proteobacteria_Alphaproteobacteria_Rhodobacterales_Rhodobacteraceae_Pseudorhodobacter	2.07%	1.07%
	Bacteroidetes_Bacteroidia_Cytophagales_Spirosomaceae_Persicitalea	2.04%	1.01%
	Bacteroidetes_Bacteroidia_Chitinophagales_Chitinophagaceae_Ferruginibacter	1.21%	0.44%
Figure3d	Spring		
	Proteobacteria_Alphaproteobacteria_Rhodobacterales_Rhodobacteraceae_Pseudorhodobacter	2.07%	1.07%
	Actinobacteria_Actinobacteria_Propionibacteriales_Propionibacteriaceae_Propioniciclava	1.44%	0.15%
	Proteobacteria_Alphaproteobacteria_Sphingomonadales_Sphingomonadaceae_Novosphingobium	0.94%	0.16%
	Summer		
	Chloroflexi_Chloroflexia_Chloroflexales_Roseiflexaceae_Kouleothrix	1.54%	3.13%
	Bacteroidetes_Bacteroidia_Bacteroidales_Bacteroidaceae_Bacteroides	1.15%	0.03%
	Proteobacteria_Gammaproteobacteria_Pseudomonadales_Moraxellaceae_NA	0.76%	2.47%
Figure3e	Fall		
	Chloroflexi_Chloroflexia_Chloroflexales_Roseiflexaceae_Kouleothrix	3.37%	4.00%
	Chloroflexi_Anaerolineae_SBR1031_A4b_NA	2.73%	19.41%
	Proteobacteria_Deltaproteobacteria_Myxococcales_Haliangiaceae_Haliangium	2.34%	8.86%
	Spring		
	Proteobacteria_Alphaproteobacteria_Rhodobacterales_Rhodobacteraceae_Pseudorhodobacter	2.07%	43.65%
	Bacteroidetes_Bacteroidia_Cytophagales_Spirosomaceae_Persicitalea	2.04%	36.98%
	Actinobacteria_Actinobacteria_Propionibacteriales_Propionibacteriaceae_Propionicimonas	1.52%	54.27%
Figure3f	Summer		
	Patescibacteria_Saccharimonadia_Saccharimonadales_NA_NA	1.37%	0.16%
	Bacteroidetes_Bacteroidia_Bacteroidales_Bacteroidaceae_Bacteroides	1.15%	0.03%
	Actinobacteria_Actinobacteria_Corynebacteriales_Mycobacteriaceae_Mycobacterium	1.13%	0.96%
	Winter		
	Chloroflexi_Anaerolineae_SBR1031_A4b_NA	1.12%	0.68%
	Planctomycetes_Phycisphaerae_Tepidisphaerales_Tepidisphaeraceae_Tepidisphaera	0.28%	0.13%
	Proteobacteria_Gammaproteobacteria_Oceanospirillales_Nitrincolaceae_Balneatrix	0.15%	0.01%

Table S4.3 shows the top three highest abundance OTUs (based on 16S rRNA genes) which were unique to each season and were not visually represented in the subfigures of Figure 4.3a-f. These OTUs do not occur in the comparative season, yet still represent a high abundance of each season's activated sludge composition based on 16S rRNA gene abundance.

	Top 3 OTUs unique to each season when compared to another season.	16S rRNA gene %	16S rRNA transcript %
Figure3a	**Summer**		
	Actinobacteria_Actinobacteria_Corynebacteriales_Nocardiaceae_Gordonia	0.45%	1.58%
	Proteobacteria_Alphaproteobacteria_Rhodobacterales_Rhodobacteraceae_Rubellimicrobium	0.15%	0.03%
	Cyanobacteria_Sericytochromatia_NA_NA_NA	0.08%	0.22%
	Fall		
	Patescibacteria_Parcubacteria_Candidatus_Moranbacteria_NA_NA	0.37%	0.00%
	Planctomycetes_Planctomycetacia_Isosphaerales_Isosphaeraceae_NA	0.28%	0.20%
	Planctomycetes_Planctomycetacia_Gemmatales_Gemmataceae_NA	0.16%	0.12%
Figure3b	**Fall**		
	Bacteroidetes_Bacteroidia_Bacteroidales_NA_NA	0.21%	0.00%
	Bacteroidetes_Bacteroidia_Bacteroidales_Prevotellaceae_Prevotella_7	0.14%	0.00%
	Actinobacteria_Thermoleophilia_Solirubrobacterales_Solirubrobacteraceae_NA	0.12%	0.10%
	Winter		
	Actinobacteria_Actinobacteria_Corynebacteriales_Nocardiaceae_Gordonia	0.82%	1.05%
	Armatimonadetes_Armatimonadia_Armatimonadales_Armatimonadaceae_Armatimonas	0.13%	0.16%
	Proteobacteria_Alphaproteobacteria_Rhizobiales_Beijerinckiaceae_FukuN57	0.06%	0.02%
Figure3c	**Winter**		
	Chloroflexi_Anaerolineae_Anaerolineales_Anaerolineaceae_UTCFX1	0.19%	1.33%
	Proteobacteria_Gammaproteobacteria_Betaproteobacteriales_Burkholderiaceae_Sphaerotilus	0.19%	1.67%
	Bacteroidetes_Bacteroidia_Chitinophagales_Saprospiraceae_Phaeodactylibacter	0.19%	0.74%
	Spring		
	Actinobacteria_Actinobacteria_Propionibacteriales_Propionibacteriaceae_Aestuariimicrobium	0.21%	0.01%
	Proteobacteria_Gammaproteobacteria_Betaproteobacteriales_Burkholderiaceae_Pseudorhodo	0.20%	0.03%
	Actinobacteria_Actinobacteria_Micrococcales_Demequinaceae_Demequina	0.14%	0.40%
Figure3d	**Spring**		
	Proteobacteria_Alphaproteobacteria_Rhizobiales_Beijerinckiaceae_NA	0.48%	0.22%
	Actinobacteria_Actinobacteria_Propionibacteriales_Propionibacteriaceae_Aestuariimicrobium	0.21%	0.01%
	Proteobacteria_Gammaproteobacteria_Betaproteobacteriales_Burkholderiaceae_Pseudorhodo	0.20%	0.03%
	Summer		
	Chloroflexi_Anaerolineae_Anaerolineales_Anaerolineaceae_UTCFX1	1.38%	1.77%
	Fusobacteria_Fusobacteriia_Fusobacteriales_Leptotrichiaceae_Hypnocyclicus	0.54%	0.04%
	Proteobacteria_Gammaproteobacteria_Pseudomonadales_Moraxellaceae_Enhydrobacter	0.34%	0.06%
Figure3e	**Fall**		
	Chloroflexi_Anaerolineae_Anaerolineales_Anaerolineaceae_UTCFX1	1.00%	2.26%
	Bacteroidetes_Bacteroidia_Chitinophagales_Saprospiraceae_Phaeodactylibacter	0.51%	0.73%
	Proteobacteria_Gammaproteobacteria_Pseudomonadales_Moraxellaceae_Enhydrobacter	0.46%	0.18%
	Spring		
	Actinobacteria_Actinobacteria_Corynebacteriales_Nocardiaceae_Gordonia	1.26%	2.56%
	Actinobacteria_Actinobacteria_Propionibacteriales_Propionibacteriaceae_Aestuariimicrobium	0.21%	0.01%
	Bacteroidetes_Bacteroidia_Flavobacteriales_Weeksellaceae_Chryseobacterium	0.17%	0.00%
Figure3f	**Summer**		
	Bacteroidetes_Bacteroidia_Cytophagales_Microscillaceae_NA	0.16%	0.04%
	Proteobacteria_Gammaproteobacteria_Betaproteobacteriales_Burkholderiaceae_Ramlibacter	0.10%	0.22%
	Proteobacteria_Gammaproteobacteria_Enterobacteriales_Enterobacteriaceae_Enterobacter	0.08%	0.00%
	Winter		
	Proteobacteria_Alphaproteobacteria_Rhizobiales_Beijerinckiaceae_NA	0.29%	0.24%
	Armatimonadetes_Armatimonadia_Armatimonadales_Armatimonadaceae_Armatimonas	0.13%	0.16%
	Planctomycetes_Planctomycetacia_Isosphaerales_Isosphaeraceae_NA	0.11%	0.09%

C_{OTU} = (Concentration of 16S rRNA genes via qPCR) * (OTU relative abundance via sequencing)

V = Volume of the Reactor

H = Heights of the Reactor

A = Area of the Reactor

SF = Static Fill

AS = Activated Sludge

R = Reactor

$$C_{OTU_{SF}}V_{SF} + C_{OTU_{AS}}V_{AS} = C_{OTU_R}V_R$$

$$V_{SF} + V_{AS} = V_R$$

$$H_{SF}A_R = V_{SF}$$

$$H_{AS}A_R = V_{AS}$$

$$H_RA_R = V_R$$

$$H_{SF}A_R + H_{AS}A_R = H_RA_R$$

$$H_{SF} + H_{AS} = H_R$$

$$\frac{H_{SF}}{H_R} + \frac{H_{AS}}{H_R} = 1$$

$$\frac{H_R - H_{AS}}{H_R} + \frac{H_{AS}}{H_R} = 1$$

$$\frac{H_R - H_{AS}}{H_R} = \%V_{SF}$$

$$\frac{H_{AS}}{H_R} = \%V_{AS}$$

$$C_{OTU_{SF}}\%V_{SF} + C_{OTU_{AS}}\%V_{AS} = C_{OTU_R}$$

$$When\ C_{OTU_{AS}}\%V_{AS} << C_{OTU_{SF}}\%V_{SF}\ Then: C_{OTU_{SF}}\%V_{SF} = C_{OTU_R}$$

These OTUs only pass through the reactors from the Static Fill Cycle

When $When\ C_{OTU_{AS}}\%V_{AS} \gg C_{OTU_{SF}}\%V_{SF}\ Then: C_{OTU_{AS}}\%V_{AS} = C_{OTU_R}$

These OTUs proliferate due to the activated sludge cycle and remain in the system.

Equation S4.1 shows the step-by-step equation to discern whether an OTU was proliferating in the activated sludge system or passing through the system. In this equation, C_{OTU} represents the concentration of each OTU by multiplying the relative abundance based on 16S rRNA gene sequencing by the total 16S rRNA concentration based on qPCR amplification.

Appendix C

Chapter 5 Supplemental Materials

Seasonal Variations in the Ammonia Oxidizing Community in Triplicate Full-Scale Sequencing Batch Reactors

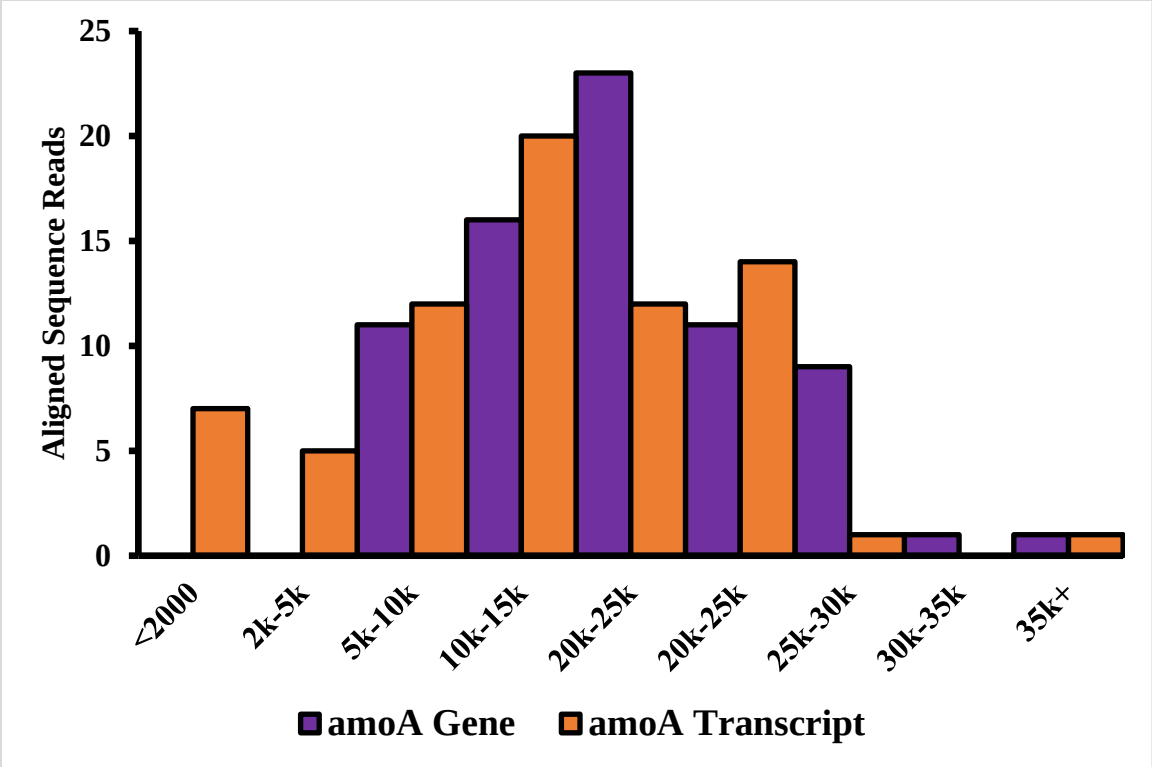

Figure S5.1 The histogram shows the average distribution of processed ASVs for the 72 *amoA* gene amplicon sequences and the 72 *amoA* transcript amplicon sequences. The *amoA* genes are shown in the purple while the *amoA* transcripts are in orange. The *amoA* gene samples had an average of 16,978±6763 merged pairs per sample while the *amoA* transcript samples averaged 13,106±7431 merged pairs per sample.

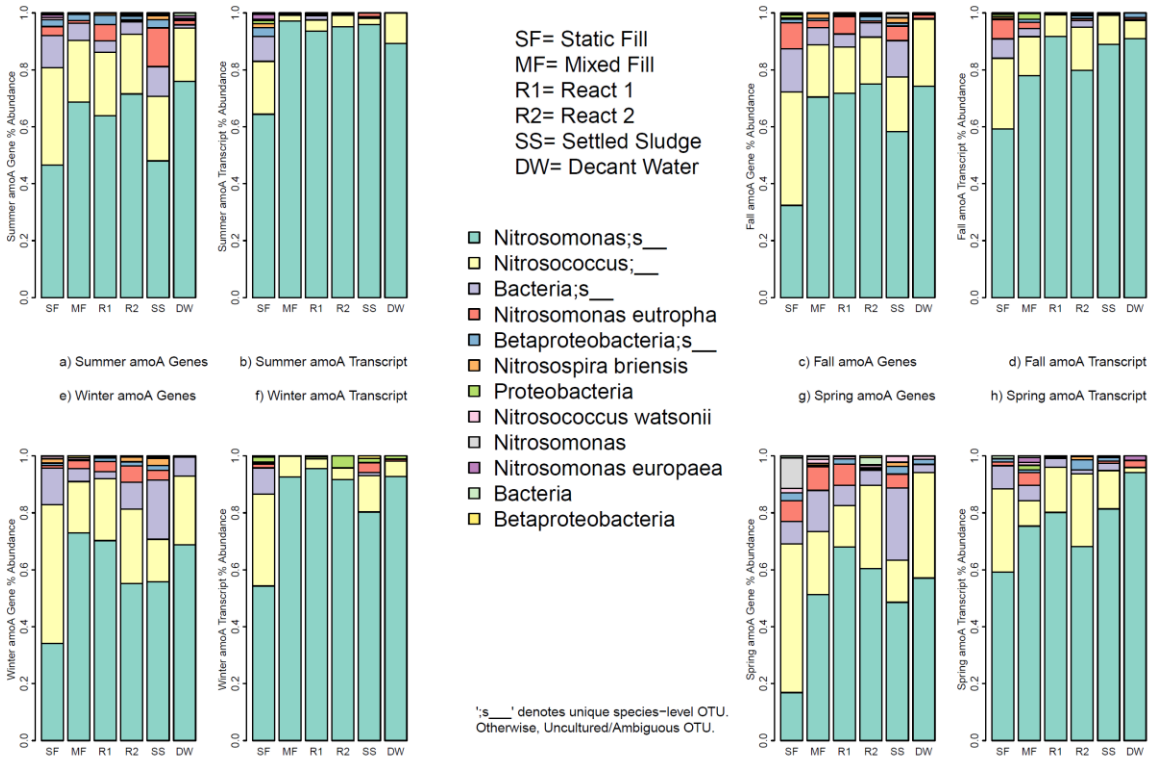

Figure S5.2 The average relative abundance of the triplicate sequencing batch reactors ASV clusters per season are represented above with summer in the upper left, fall in the upper right, winter in the lower left, and spring in the lower right. Each seasons quadrant has both the relative abundance of ASV clusters for *amoA* genes on the left, and *amoA* transcripts on the right. *Nitrosomonas* dominates the activated sludge system overall, while *Nitrosococcus* was the most abundant cluster in the influent wastewater during static fill (SF).

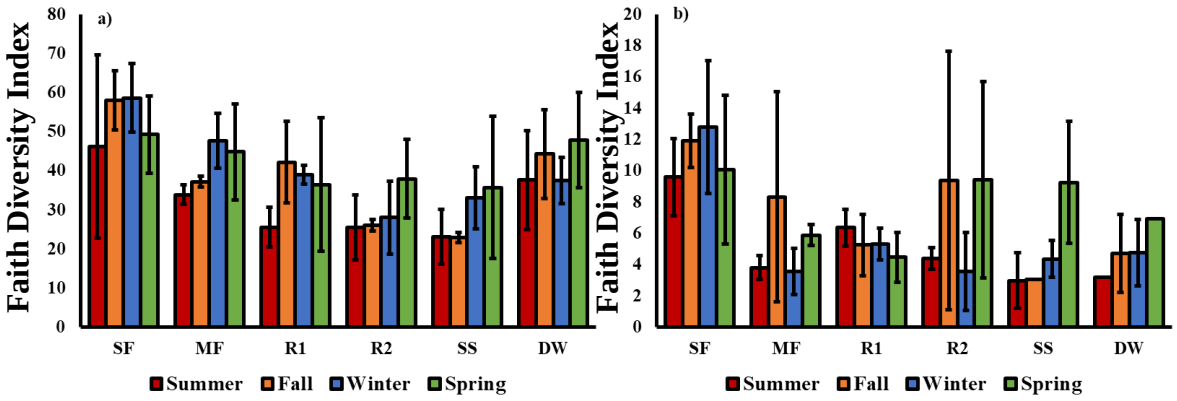

Figure S5.3 The Faith Phylogenetic Diversity Index was calculated for the *amoA* gene (Figure S5.3a) and the *amoA* transcript (Figure S5.3b) are rarified subsamples of 5000 reads and 2000 reads respectively. Each season is depicted throughout various points in the reactor sequence with summer in red, fall in orange, winter in blue, and spring in green. The triplicate sequencing batch reactors were averaged together after taking an individual reactors average over 1000-bootstrapped iterations. The standard deviations represent only the average between the three individual reactors, not the bootstrapped values. Even when the *amoA* gene was rarified to 2000 reads to be more comparable to *amoA* transcripts, the overall phylogenetic diversity of *amoA* genes is consistently higher than *amoA* transcripts. Additionally, when averaging the seasons together, the static fill (SF) is always statistically higher in diversity than the other reactor time points.

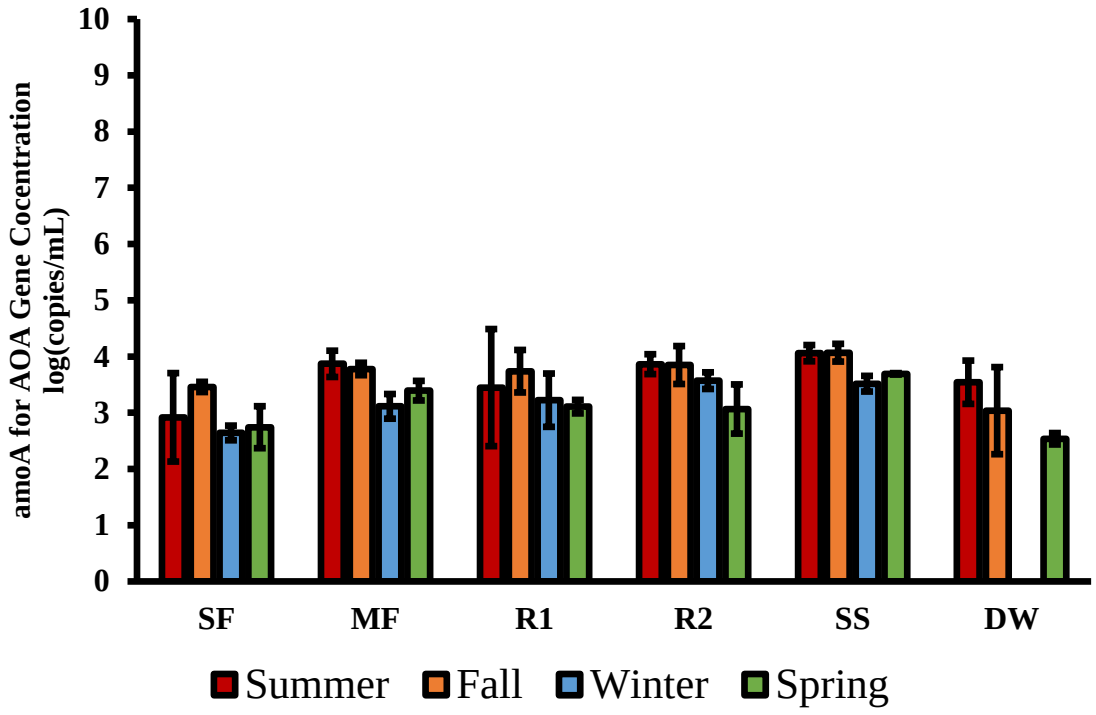

Figure S5.4 The average abundance of *amoA* genes for ammonia oxidizing archaea were quantified with the standard deviation of the triplicate sequencing batch reactors show. Each color represents a different season throughout the six-time points during the reactor cycle with summer in red, fall in orange, winter in blue, and spring in green. Throughout the reaction cycle, ammonia oxidizing archaea were about 2.5 orders of magnitude lower than the ammonia oxidizing bacteria. This low abundance of ammonia oxidizing archaea based on *amoA genes* in conjunction with most *amoA* transcript data falling below detection limits was determined to be insignificant overall to wastewater operations and not further analyzed. All *amoA* genes for ammonia oxidizing archaea in the decanted water (DW) for winter were below detection limits.

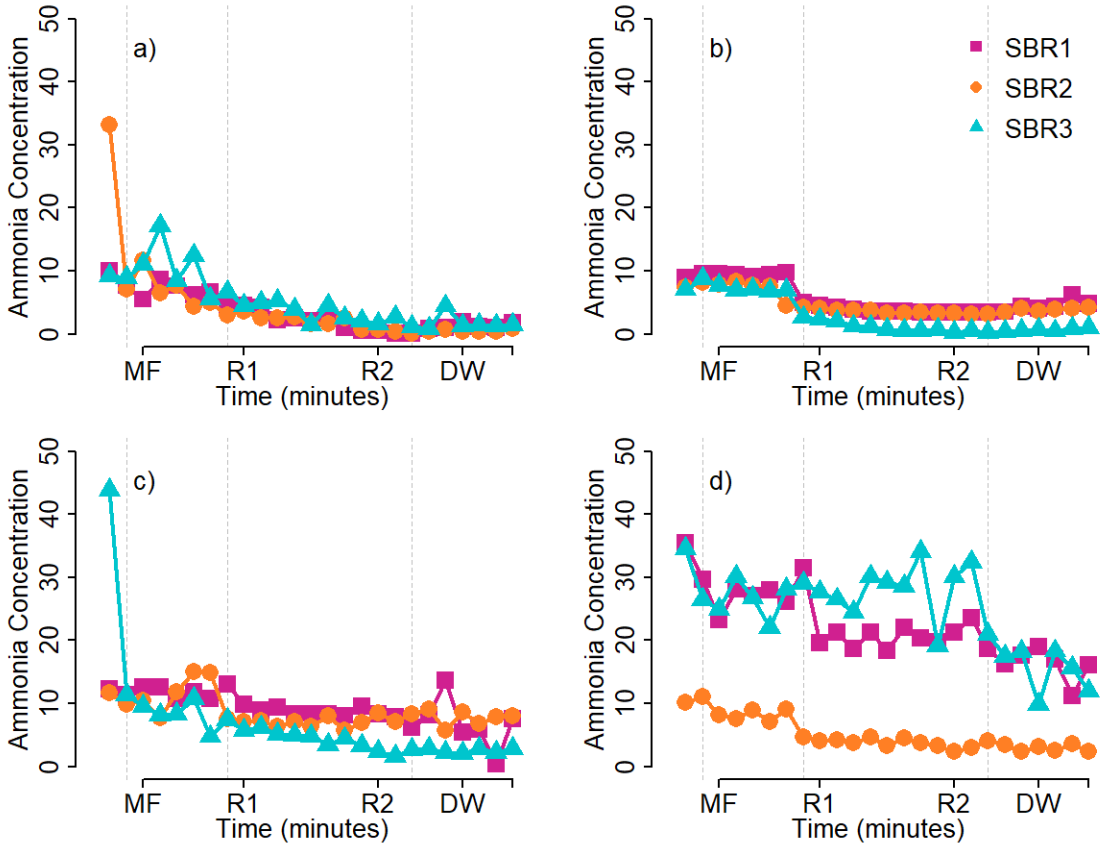

Figure S5.5 The ammonia concentration is shown throughout the triplicate sequencing batch reactors with each plot focusing on a different season. The plots are continuous from the end of static fill, through the hour-long mixed fill (MF), into the two-hour aerobic react cycle (R1 & R2), and through settling of the water about to be decanted from the reactor (DW). The reactors in summer are shown in the top left (a), fall is the top right (b), winter is the bottom left (c), and spring in the bottom right (d). Each reactor is color coded with sequencing batch reactor 1 (SBR1) in violet, reactor 2 in orange (SBR2), and reactor 3 (SBR3) in turquoise.